frontiers | Research Topics

Insights in veterinary regenerative medicine 2022

Edited by
Scott J. Roberts

Published in
Frontiers in Veterinary Science

ISSN 1664-8714
ISBN 978-2-8325-3622-3
DOI 10.3389/978-2-8325-3622-3

About Frontiers

Frontiers is more than just an open access publisher of scholarly articles: it is a pioneering approach to the world of academia, radically improving the way scholarly research is managed. The grand vision of Frontiers is a world where all people have an equal opportunity to seek, share and generate knowledge. Frontiers provides immediate and permanent online open access to all its publications, but this alone is not enough to realize our grand goals.

Frontiers journal series

The Frontiers journal series is a multi-tier and interdisciplinary set of open-access, online journals, promising a paradigm shift from the current review, selection and dissemination processes in academic publishing. All Frontiers journals are driven by researchers for researchers; therefore, they constitute a service to the scholarly community. At the same time, the *Frontiers journal series* operates on a revolutionary invention, the tiered publishing system, initially addressing specific communities of scholars, and gradually climbing up to broader public understanding, thus serving the interests of the lay society, too.

Dedication to quality

Each Frontiers article is a landmark of the highest quality, thanks to genuinely collaborative interactions between authors and review editors, who include some of the world's best academicians. Research must be certified by peers before entering a stream of knowledge that may eventually reach the public - and shape society; therefore, Frontiers only applies the most rigorous and unbiased reviews. Frontiers revolutionizes research publishing by freely delivering the most outstanding research, evaluated with no bias from both the academic and social point of view. By applying the most advanced information technologies, Frontiers is catapulting scholarly publishing into a new generation.

What are Frontiers Research Topics?

Frontiers Research Topics are very popular trademarks of the *Frontiers journals series*: they are collections of at least ten articles, all centered on a particular subject. With their unique mix of varied contributions from Original Research to Review Articles, Frontiers Research Topics unify the most influential researchers, the latest key findings and historical advances in a hot research area.

Find out more on how to host your own Frontiers Research Topic or contribute to one as an author by contacting the Frontiers editorial office: frontiersin.org/about/contact

Insights in veterinary regenerative medicine: 2022

Topic editor
Scott J. Roberts — Royal Veterinary College (RVC), United Kingdom

Citation
Roberts, S. J., ed. (2023). *Insights in veterinary regenerative medicine: 2022*. Lausanne: Frontiers Media SA. doi: 10.3389/978-2-8325-3622-3

Table of contents

frontiers | Frontiers in Veterinary Science

TYPE Editorial
PUBLISHED 20 September 2023
DOI 10.3389/fvets.2023.1285275

OPEN ACCESS

EDITED AND REVIEWED BY
Andres M. Perez,
University of Minnesota Twin Cities,
United States

*CORRESPONDENCE
Scott J. Roberts
✉ sjroberts@rvc.ac.uk

RECEIVED 29 August 2023
ACCEPTED 31 August 2023
PUBLISHED 20 September 2023

CITATION
Roberts SJ (2023) Editorial: Insights in veterinary regenerative medicine: 2022. *Front. Vet. Sci.* 10:1285275. doi: 10.3389/fvets.2023.1285275

Editorial: Insights in veterinary regenerative medicine: 2022

Scott J. Roberts*

Department of Comparative Biomedical Sciences, The Royal Veterinary College, London, United Kingdom

KEYWORDS

regenerative medicine, stromal cells, platelet rich plasma, extracellular vesicles, translational research

Editorial on the Research Topic
Insights in veterinary regenerative medicine: 2022

The progress of the veterinary regenerative medicine field over the first two decades of the twenty-first century has been considerable. Due to the similarities in many degenerative diseases (e.g., osteoarthritis; OA) between veterinary species and humans, this area of research is well suited to applying a "One Health" approach to innovations in veterinary regenerative medicine toward human medicine and *vice versa*.

In this Research Topic we aim to capture a snapshot of the research conducted, along with the questions, solutions and challenges in veterinary regenerative medicine over the preceding year. From the nine published articles in this Research Topic it is clear that current trends in veterinary regenerative medicine are synonymous with research in this area of human medicine, with a major research interest in mesenchymal stem/stromal cells (MSCs) and platelet rich plasma (PRP) for degenerative disease treatment. Interestingly, the review by Penning and van den Boom details the expanding field of organoid research and how this is contributing to new understanding. Herein, the authors pinpoint a lack of validated species-specific tools (such as antibodies and growth factors) as a major roadblock in extrapolation of human studies into that of veterinary species. The opportunities of companion animal organoid research are also thoroughly reviewed with respect to disease modeling, precision medicine and organ transplantation/replacement. The concept of standardization in MSC research and equivalence between human and veterinary research is also approached in the opinion article by Guest et al., whereby guidelines for reporting research involving the use of MSCs in veterinary settings are proposed. The minimal criteria suggested by the authors are closely aligned to the minimal criteria for defining human MSCs, set out by the ISCT (International Society for Cellular Therapy). However, the authors do propose further measures such as immunomodulatory analysis and the introduction of a Clinical Indications Prediction (CLIP) scale for veterinary MSCs, thus improving reproducibility and robustness.

The original research articles can be classified into those using MSCs or their derivatives toward regenerative applications, and those using PRP. Kearney et al. investigated whether the secretome of allogenic MSCs had anti-inflammatory effects in an equine model of joint inflammation when introduced intraarticularly. Interestingly, no differences were observed between the treatment effects of the MSC secretome and MSCs, thus if the effects are proved to be beneficial this may provide an effective off-the-shelf treatment for inflammatory joint disease in the horse. Clarke et al. took the innovative approach of investigating secreted extracellular vesicles (EVs) in the context of equine OA, where changes in the proteome of

the synovial fluid EVs following integrin α10-positive MSC administration were measured. The author's data suggest that MSC-derived EVs may play a role in mediating MSC efficacy and identify specific targets that warrant further investigation. Furthering the concept of the paracrine action of MSCs, Caruso et al. show that conditioned media from equine bone marrow MSCs promote wound healing *in vitro*. However, this effect was not translatable to equine cutaneous wound healing *in vivo* upon implantation of intact MSCs. Koch et al. attempted to understand changes in cytokine composition in a surgical model of equine tendon injury using an ultrafiltration technique. From this insight, the authors reported that MSC priming with the predominant cytokine (IL-1β) at similar concentrations found *in vivo* increased expression of IL-6, VEGF, and PGE2; which the authors predict may confer enhanced therapeutic potential. Armitage et al. investigated the efficacy of autologous MSCs for efficacy in chronic degenerative musculoskeletal conditions in dogs, with outcome measures spanning joint mobility through to pain. In this study, MSCs were introduced alone or in combination with PRP. The authors conclude that the treatments resulted in positive effects in the patient's status, indicating the utility of MSC treatment toward multiple degenerative musculoskeletal conditions. This study does highlight the potential of PRP as an adjuvant for MSC therapy, however, two other papers in this Research Topic detail the clinical application of PRP alone in canines. Matos Cruz and Mason report on their study where PRP was used following bilateral arthroscopic subtotal coronoidectomy of the fragmented medial coronoid process, with owner-reported outcomes recorded as a measure of efficacy. The authors conclude that when surgery was not successful, PRP appeared to reduce lameness long term. Successful outcome of PRP treatment was also reported in a case study of Flexor carpi ulnaris tendinopathy from Franini et al.. The authors report that their PRP-associated treatment programme resulted in the resolution of patient lameness and improvements in tendon parameters.

Although limitations exist with each of the studies detailed herein (discussed within each publication), this Research Topic showcases the advances the field is currently experiencing in the translation of basic research towards clinical application. Furthermore, it highlights the technological and reporting advances the field requires to ensure veterinary regenerative medicine can keep pace with advances in the human arena. Only through the creation of species-specific and validated reagents will we be able to realize this goal. Increased technological possibilities, such as single cell transcriptomics, epigenetic analysis and spatial technologies, frequently used in the investigation of human regenerative solutions, have a financial implication that is often challenging within the current funding landscape. As such, we need to make better use of comparative analysis and *in silico* tools to extrapolate data from all other fields and species.

Adoption of these concepts will contribute to achieving a successful "One Health" future for regenerative medicine.

Author contributions

SR: Writing—original draft, Writing—review and editing.

Conflict of interest

The author declares that the research was conducted in the absence of any commercial or financial relationships that could be construed as a potential conflict of interest.

The author(s) declared that they were an editorial board member of Frontiers, at the time of submission. This had no impact on the peer review process and the final decision.

Publisher's note

frontiers in Veterinary Science

OPINION
published: 07 March 2022
doi: 10.3389/fvets.2022.817041

Position Statement: Minimal Criteria for Reporting Veterinary and Animal Medicine Research for Mesenchymal Stromal/Stem Cells in Orthopedic Applications

Debbie J. Guest[1]*, *Jayesh Dudhia*[1], *Roger K. W. Smith*[1], *Scott J. Roberts*[1], *Michael Conzemius*[2], *John F. Innes*[3], *Lisa A. Fortier*[4] and *Richard L. Meeson*[1]

[1] Royal Veterinary College, London, United Kingdom, [2] College of Veterinary Medicine, University of Minnesota, Saint Paul, MN, United States, [3] CVS Group plc, ChesterGates Veterinary Specialists, Chester, United Kingdom, [4] Cornell University College of Veterinary Medicine, Ithaca, NY, United States

Keywords: mesenchymal, stem, stromal, cell, orthopedic, dog, horse

OPEN ACCESS

Edited by:
Cristina Esteves, University of Edinburgh, United Kingdom

Reviewed by:
Janina Burk, Justus-Liebig-University Giessen, Germany
Catharina De Schauwer, Ghent University, Belgium

***Correspondence:**
Debbie J. Guest
djguest@rvc.ac.uk

Specialty section:
This article was submitted to Veterinary Regenerative Medicine, a section of the journal Frontiers in Veterinary Science

Received: *17 November 2021*
Accepted: *08 February 2022*
Published: *07 March 2022*

Citation:
Guest DJ, Dudhia J, Smith RKW, Roberts SJ, Conzemius M, Innes JF, Fortier LA and Meeson RL (2022) Position Statement: Minimal Criteria for Reporting Veterinary and Animal Medicine Research for Mesenchymal Stromal/Stem Cells in Orthopedic Applications. Front. Vet. Sci. 9:817041. doi: 10.3389/fvets.2022.817041

INTRODUCTION

Mesenchymal stem/stromal cells (MSCs) have become a popular therapeutic strategy after their introduction into equine clinical practice for the treatment of tendon injuries in the early 2000's (1). They have since been used to treat other orthopedic diseases in the horse and, more recently, small companion animals where they have also been investigated for the treatment of neurological and cardiac abnormalities. Domestic mammals provide an ideal "proving ground" for this technology prior to its widespread use in human beings because of the aetiopathological similarities with equivalent human diseases. However, these investigations have involved the use of a wide range of cell products for both research and clinical use which are often poorly characterized and poorly described, with variable outcome descriptors, making objective assessment of safety and efficacy difficult, and comparison between studies impossible. While this was not unexpected when the technology was in early development, much evidence on the nature and function of MSCs has been obtained over the last 20 years. Despite this, there continues to be poorly standardized studies that lack scientific rigor and result in skepticism amongst clinicians regarding MSCs as a clinical therapy that impedes progress in this field. As such, there is an unmet need to standardize key parameters relating to clinical stem cell research in animals to improve the quality of the research reporting and provide greater confidence in the technology.

In this position statement, we aim to provide guidelines for reporting research involving the use of MSCs in veterinary settings of research and clinical therapy. We have focused on orthopedic conditions in horses and dogs, where the majority of research has been performed, and define MSCs according to the characteristics set out in **Figure 1A** and similar to the definition used in the human MSC arena (2).

DEFINING THE CELLS

We propose that there should be minimal definition criteria for the identity of the cells based on cell characteristics. However, we recognize that for autologous cells being used in clinical applications it is impractical to fully characterize cells from every case (patient). Even within the research field it is unlikely that laboratories will have the resources to characterize every population of cells which

A

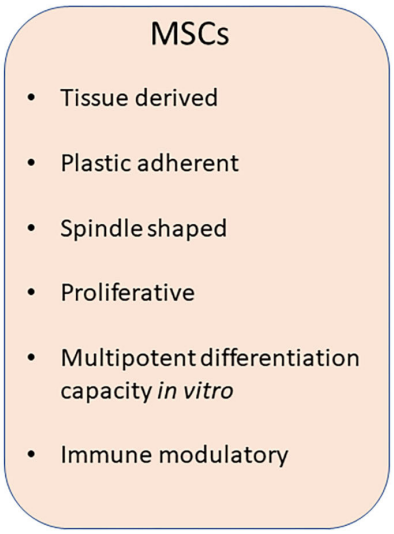

B

Defining Characteristics	Minimum	Optimal
Plastic adherence	✓	✓
Tri-lineage differentiation	✓	✓
Surface antigen expression: **Markers commonly positive:** CD90 CD73 CD105 CD29 CD44	Two positive markers.	All markers.
Markers commonly negative: CD79α/CD19 CD14/CD11b CD34 CD45	Two negative markers.	All markers.
MHC II expression (where used allogeneically)	✓	✓
***In vitro* immune suppression**		✓
Other analytical methods of potency[13]		✓

FIGURE 1 | (A) Characteristics of MSCs. **(B)** Suggested minimal and optimal definitions of equine and canine MSCs.

they derive, and there are practical limitations to performing every characterization descriptor while maintaining cells at a low passage number/population doublings for the experiment under investigation. We therefore propose that individual research laboratories or groups follow accepted (published) protocols for the production of MSCs which are described in sufficient detail so that they can be reproduced, or referred to such a description in an appropriate publication. In addition, batch testing of cells being used for research and for any use of allogeneic cells in clinical applications should then be performed to ensure consistency and quality control. As a minimum this should be performed the first time a protocol is applied or whenever a protocol is changed.

Minimal criteria for defining human MSCs, set out by the ISCT (International Society for Cellular Therapy), are in widespread use and include plastic adherence, specific protein surface antigen expression and multipotent differentiation potential (2). However, since these criteria were defined, our understanding of the *in vivo* mechanisms of action of adipose and bone marrow derived-MSCs, as commonly isolated and applied in veterinary protocols, have shifted away from the belief that they will undergo direct differentiation into tissue rebuilding cells, to the demonstration that these cells produce a multitude of factors that have immune suppression and trophic effects and confusion as to the identity of MSCs remains in all species (3–5).

In veterinary medicine, early publications struggled to report on all the criteria set out by the ISCT. This was mainly due to a lack of cross-reacting antibodies to the equivalent cell surface antigen. However, multiple markers for MSCs in dogs and horses have now been reported and species-specific antibodies are now more widely available commercially, although there are still conflicting reports on the exact expression profiles for many of these cell markers. We therefore propose that, a minimum number of species-specific positive and negative markers are used (**Figure 1B**) with the percentage of positive cells reported. However, we point out that the expression of these markers may vary between species. For example, CD73 is expressed by human (2) and canine MSCs (6, 7) but not equine MSCs (8–10). Furthermore, the culture method used (11) and origin of the cells (5, 12) may affect expression and so must be reported along with the heterogeneity of marker expression within the cell population and between donor animals. This will help to better understand the expression profiles in the horse and dog to build toward a stronger consensus on the most appropriate combination of surface markers to examine than is currently available. In all reports evidence of specific cross-reactivity of the antibodies to the species being investigated must be provided or referenced.

To date, no *in vitro* potency assay to predict MSC efficacy *in vivo* has been defined (13). Furthermore, different assays may be required to predict efficacy for different clinical contexts. No specific marker has been identified which accurately reflects the immunomodulatory abilities of MSCs and *in vitro* read outs commonly involve peripheral blood mononuclear cell proliferation suppression assays. We therefore suggest that, at

the present time, an optimal characterization of MSCs would involve the use of *in vitro* immune suppression assays in addition to a tri-lineage differentiation assay [to bone, cartilage and fat, assessed using staining of the cultured cells (2) with quantification performed through dye leaching]. Even though the mechanism of action of MSCs is no longer believed to be through direct differentiation of MSC into tissue cells, the tri-lineage differentiation assay provides a marker of stemness of the MSC.

In addition to these characteristics, and similar to guidelines proposed for human cell therapies (14) publications using veterinary MSCs should state:

- The tissue source for the recovery of the MSCs.
- Preparation method (e.g. enriched or minimally manipulated).
- Culture method (including passaging method, complete media formulation and type/source of serum).
- Passage number and cell seeding densities.
- Method for banking of research and clinically applied cells (15) (total cell number and concentration, passage, cryopreservation media, freezing conditions).

Furthermore, papers using MSCs for *in vivo* applications should state:

- Whether autologous or allogenic cells are used.
- ANTIGENICITY where allogenic cells are used (e.g., MHC expression).
- Cell dose.
- Dosing schedule.
- The vehicle used to suspend and deliver the cells into the animal.
- The method of delivery.
- Other medications delivered with the cells.

The vehicle itself may have independent or co-dependent effects on the impact of the MSCs. Given this, experimental studies should have a control group treated with the vehicle alone and studies based on clinical cases should have a robust comparison control group if possible. Furthermore, where biological products are used to deliver the cells the preparation methods must also be described in enough detail that the methodology can be accurately repeated. For example, platelet rich plasma (PRP) is commonly used as a delivery vehicle, but different preparation methods, as is common in the literature, can result in significant heterogeneity of the final product that is injected into the animal (16).

REPORTING OUTCOMES

We propose key inclusion and exclusion criteria combined with objective outcome measures that relate to specific mechanisms identified for MSCs in clinical orthopedic studies. Outcome measures have been highly variable between different veterinary studies. We propose obligatory usage of the now well established inclusion criteria and outcome definitions as proposed by Cook et al. (17) shown below. Although some aspects of definitions used here may be debated, the critical issue is that universal application of their definitions allows for an improved comparison between different studies.

Inclusion Criteria

Clinical research inherently has a variety of clinical variables, and highly specified and narrow inclusion criteria may prevent completion of a veterinary clinical study. It is however important that those variables should be presented in the paper to allow further interrogation of results, particularly for "outliers" as necessary. Minimum recording should include the patient signalment and disease characterization as follows:

- Details of treatment focus: which joint, tendon or ligament.
- Pre-treatment disease state (severity and duration prior to enrollment) and methods that were used to make the assessment.
- Medications/concurrent therapy.
- We recommend inclusion of a clinical summary table, documenting any change in medication/other unexpected events, against summary outcome result for each enrolled animal. This would allow readers to interrogate individual animal results or outliers.

Disease and Outcome Assessments Measures

Disease status assessment needs to be matched and aligned to treatment outcome assessments. We do not arbitrarily recommend specific assessment criteria as they need to be appropriately tailored to the disease in question, however, wherever possible an objective measure is preferred. They may include one or several of the following categories and ideally applied in combination, as no single assessment is fully comprehensive when evaluating the complex aspects of structural disease, functional limb usage and assessment of pain.

Imaging assessments: should involve the most relevant imaging modality and include lesion measurements, or disease grading such as osteoarthritis scoring systems. Wherever possible a recognized scoring system (18) or method of lesion measurement should be made.

Functional assessments: are ideally objective such as kinetic (force plate, or the more clinically accessible pressure mats), and kinematic (activity monitors/accelerometers), which can maximize objectivity and minimize care-giver placebo influence. Historically, assessment methods frequently include subjective clinician assessments of visual lameness scores, which have been proven to be unreliable. Goniometry and measures of muscle volume can also be considered if their methodology of measurement is accurately described and consistent.

Client reported outcome measure assessments (CROMS): patient assessments have become an integral part of human clinical outcome assessment and certain ones are recognized by the FDA and EMA and are included in some human phase III clinical trials. Although CROMs are semi-objective and there is wider variance compared to gait analysis, there are several studies in dogs now showing that gait analysis and CROMs show the same outcome in trials. Study design is important and care-giver placebo effect needs to be considered which is not an issue with

gait analysis, however they can provide measures of the "disease construct" which is not simply identified by gait/locomotion change. Examples include LOAD (Liverpool Osteoarthritis in Dogs) (18), CBPI (Canine Brief Pain Inventory) (19), COI (Canine Orthopedic index) (20), HCPI (Helsinki Chronic Pain Index) (21).

However, these assessment measures should be integrated to allow a global assessment of outcome as per Cook et al. (17) with modifications:

- Full function—restoration to, or maintenance of, full intended level and duration of activities and performance from preinjury or pre-disease status (without medication). This should equate to low scores on clinical metrology questionnaires, indicating negligible identification of pain or impact on quality of life.
- Acceptable function—restoration to, or maintenance of, intended activities and performance from preinjury. This should equate to intermediate scores on clinical metrology questionnaires, indicating presence of some pain and some impact on quality of life.
- Unacceptable function—all other outcomes (such as persistent lameness, reinjury, retirement, or euthanasia because of the disease), with high scores on clinical metrology questionnaires indicative of significant pain and poor quality of life.

When reporting clinical outcomes it is important to record:

- Whether the assessor was blinded to treatment.
- Who the assessors were (notional acknowledgment of their experience; veterinary graduate, new, experienced, advanced or specialist) and how many assessors took part.
- The pre-treatment state using an assessment measure which will also be used to assess response to treatment. i.e., how severely painful or lame, or size of tendon defect prior to treatment.

Reporting Time Frames

Most studies to-date have had varied follow up periods from 30 days through to two years for both dogs and horses. We endorse the study period terminology established by Cook et al. as follows:

- Perioperative (pre, intra, and postoperative)—0–3 months:
- Short term—>3–6 months.
- Mid term—>6–12 months.
- Long term—>12 months.

Currently many studies fall within the perioperative definition and we encourage more studies to extend into the short to mid-term, but acknowledge the difficulty and loss to follow-up seen in clinical studies as durations increase.

If studies have been carried out in accordance with the criteria we propose then the study outcomes will help to fill our knowledge gap irrespective of the duration of study. Nevertheless, longer periods of follow up clearly offer better scientific evidence of outcomes, particularly if the follow up is carried out periodically over time, as studies measuring the long term efficacy of the cells in improving clinical outcome are rare.

CONCLUDING REMARKS

We propose that the aforementioned framework be applied as our understanding and application of other technologies to this field develops. The markers commonly used to define MSCs do not readily differentiate them from fibroblasts (22), and over time, better combinations or more reliable surface antigens may present themselves. As an example, a Clinical Indications Prediction (CLIP) scale has been developed for human MSCs which uses TWIST1 expression levels to predict the therapeutic efficacy of MSC populations for different disease indications (23). To undertake a similar approach for MSCs in veterinary species would require comparisons of global gene and protein expression data between MSCs and other cell types and there are currently limited datasets available. Over time these approaches will become less cost prohibitive for the veterinary sector and adapting these new approaches does not preclude the continued application of the outlined principles; consistency in reporting, usage of recognized and standardized assessment criteria, and application of universally accepted study definitions.

To conclude, veterinarians and owners still rightly question if and how MSCs will help their pets. We propose that these guidelines should be utilized in publications and presentations to drive higher scientific standards and relevant regulation, and enable better comparison between studies to give greater confidence to the stakeholders of the veterinary field.

AUTHOR CONTRIBUTIONS

RM conceived the paper. DG and RM wrote the first draft of the manuscript. All authors contributed to manuscript revision and read and approved the submitted version.

REFERENCES

1. Smith RK, Korda M, Blunn GW, Goodship AE. Isolation and implantation of autologous equine mesenchymal stem cells from bone marrow into the superficial digital flexor tendon as a potential novel treatment. *Equine Vet J*. (2003) 35:99–102. doi: 10.2746/042516403775467388
2. Dominici M, Le Blanc K, Mueller I, Slaper-Cortenbach I, Marini F, Krause D, et al. Minimal criteria for defining multipotent mesenchymal stromal cells. The international society for cellular therapy position statement. *Cytotherapy*. (2006) 8:315–7. doi: 10.1080/14653240600855905
3. Caplan AI. Mesenchymal stem cells: time to change the name! *Stem Cells Transl Med*. (2017) 6:1445–51. doi: 10.1002/sctm.17-0051
4. Sipp D, Robey PG, Turner L. Clear up this stem-cell mess. *Nature*. (2018) 561:455–7. doi: 10.1038/d41586-018-06756-9
5. Viswanathan S, Shi Y, Galipeau J, Krampera M, Leblanc K, Martin I, et al. Mesenchymal stem versus stromal cells: international society for cell & gene therapy (ISCT®) mesenchymal stromal cell committee position statement on nomenclature. *Cytotherapy*. (2019) 21:1019–24. doi: 10.1016/j.jcyt.2019.08.002
6. Kafarnik C, McClellan A, Dziasko M, Daniels JT, Guest DJ. Canine corneal stromal cells have multipotent mesenchymal stromal cell properties *in vitro*. *Stem Cells Dev*. (2020) 29:425–39. doi: 10.1089/scd.2019.0163
7. Russell KA, Chow NHC, Dukoff D, Gibson TWG, LaMarre J, Betts DH, et al. Characterization and immunomodulatory effects of canine adipose tissue-

and bone marrow-derived mesenchymal stromal cells. *PLoS ONE*. (2016) 11:e0167442. doi: 10.1371/journal.pone.0167442
8. Harman RM, Patel RS, Fan JC, Park JE, Rosenberg BR, Van de Walle GR. Single-cell RNA sequencing of equine mesenchymal stromal cells from primary donor-matched tissue sources reveals functional heterogeneity in immune modulation and cell motility. *Stem Cell Res Ther*. (2020) 11:524. doi: 10.1186/s13287-020-02043-5
9. Ranera B, Lyahyai J, Romero A, Vázquez FJ, Remacha AR, Bernal ML, et al. Immunophenotype and gene expression profiles of cell surface markers of mesenchymal stem cells derived from equine bone marrow and adipose tissue. *Vet Immunol Immunopathol*. (2011) 144 147–54. doi: 10.1016/j.vetimm.2011.06.033
10. Paebst F, Piehler D, Brehm W, Heller S, Schroeck C, Tárnok A, et al. Comparative immunophenotyping of equine multipotent mesenchymal stromal cells: an approach toward a standardized definition. *Cytometry A*. (2014) 85:678–87. doi: 10.1002/cyto.a.22491
11. Radcliffe CH, Flaminio MJ, Fortier LA. Temporal analysis of equine bone marrow aspirate during establishment of putative mesenchymal progenitor cell populations. *Stem Cells Dev*. (2010) 19 269–82. doi: 10.1089/scd.2009.0091
12. Tryfonidou MA, Schumann S, Armeanu S, Harichandan A, Sivasubramaniyan K, Mollenhauer J, et al. Update on canine MSC markers. *Cytometry A*. (2014) 85:379–81. doi: 10.1002/cyto.a.22469
13. Galipeau J, Krampera M, Barrett J, Dazzi F, Deans RJ, DeBruijn J, et al. International society for cellular therapy perspective on immune functional assays for mesenchymal stromal cells as potency release criterion for advanced phase clinical trials. *Cytotherapy*. (2016) 18:151–9. doi: 10.1016/j.jcyt.2015.11.008
14. Murray IR, Chahla J, Safran MR, Krych AJ, Saris DBF, Caplan AI, et al. International expert consensus on a cell therapy communication tool: DOSES. *J Bone Joint Surg Am*. (2019) 101:904–11. doi: 10.2106/JBJS.18.00915
15. Bahsoun S, Coopman K, Akam EC. The impact of cryopreservation on bone marrow-derived mesenchymal stem cells: a systematic review. *J Transl Med*. (2019) 17:397. doi: 10.1186/s12967-019-02136-7
16. Chahla J, Cinque ME, Piuzzi NS, Mannava S, Geeslin AG, Murray IR, et al. A call for standardization in platelet-rich plasma preparation protocols and composition reporting: a systematic review of the clinical orthopaedic literature. *J Bone Joint Surg Am*. (2017) 99:1769–79. doi: 10.2106/JBJS.16.01374
17. Cook JL, Evans R, Conzemius MG, Lascelles BD, McIlwraith CW, Pozzi A, et al. Proposed definitions and criteria for reporting time frame, outcome, and complications for clinical orthopedic studies in veterinary medicine. *Vet Surg*. (2010) 39:905–8. doi: 10.1111/j.1532-950X.2010.00763.x
18. Walton MB, Cowderoy E, Lascelles D, Innes JF. Evaluation of construct and criterion validity for the 'Liverpool Osteoarthritis in Dogs' (LOAD) clinical metrology instrument and comparison to two other instruments. *PLoS ONE*. (2013) 8:e58125. doi: 10.1371/journal.pone.0058125
19. Brown DC, Boston R, Coyne JC, Farrar JT. A novel approach to the use of animals in studies of pain: validation of the canine brief pain inventory in canine bone cancer. *Pain Med*. (2009) 10:133–42. doi: 10.1111/j.1526-4637.2008.00513.x
20. Brown DC. The canine orthopedic index. Step 1: devising the items. *Vet Surg*. (2014) 43:232–40. doi: 10.1111/j.1532-950X.2014.12142.x
21. Hielm-Björkman AK, Rita H, Tulamo RM. Psychometric testing of the Helsinki chronic pain index by completion of a questionnaire in finnish by owners of dogs with chronic signs of pain caused by osteoarthritis. *Am J Vet Res*. (2009) 70:727–34. doi: 10.2460/ajvr.70.6.727
22. Halfon S, Abramov N, Grinblat B, Ginis I. Markers distinguishing mesenchymal stem cells from fibroblasts are downregulated with passaging. *Stem Cells Dev*. (2011) 20:53–66. doi: 10.1089/scd.2010.0040
23. Boregowda SV, Krishnappa V, Haga CL, Ortiz LA, Phinney DG. A clinical indications prediction scale based on twist1 for human mesenchymal stem cells. *EBioMedicine*. (2016) 4:62–73. doi: 10.1016/j.ebiom.2015.12.020

Conflict of Interest: JI is employed by CVS Group plc. With the University of Liverpool, JI is the joint license holder for the LOAD client-reported outcomes measure.

The remaining authors declare that the research was conducted in the absence of any commercial or financial relationships that could be construed as a potential conflict of interest.

Publisher's Note: All claims expressed in this article are solely those of the authors and do not necessarily represent those of their affiliated organizations, or those of the publisher, the editors and the reviewers. Any product that may be evaluated in this article, or claim that may be made by its manufacturer, is not guaranteed or endorsed by the publisher.

frontiers | Frontiers in Veterinary Science

ORIGINAL RESEARCH
published: 22 June 2022
doi: 10.3389/fvets.2022.907616

Treatment Effects of Intra-Articular Allogenic Mesenchymal Stem Cell Secretome in an Equine Model of Joint Inflammation

Clodagh M. Kearney[1], Sohrab Khatab[2], Gerben M. van Buul[2,3], Saskia G. M. Plomp[4], Nicoline M. Korthagen[4], Margot C. Labberté[1], Laurie R. Goodrich[5], John D. Kisiday[5], P. R. Van Weeren[4], Gerjo J. V. M. van Osch[2,6] and Pieter A. J. Brama[1]*

[1] School of Veterinary Medicine, University College Dublin, Dublin, Ireland, [2] Department of Orthopaedics and Sports Medicine, Erasmus MC, University Medical Center Rotterdam, Rotterdam, Netherlands, [3] Beacon Hospital, Dublin, Ireland, [4] Department of Clinical Sciences, Faculty of Veterinary Medicine, Utrecht University, Utrecht, Netherlands, [5] Equine Orthopaedic Research Center, Colorado State University, Fort Collins, CO, United States, [6] Department of Otorhinolaryngology, Erasmus MC, University Medical Center Rotterdam, Rotterdam, Netherlands

Background: Allogenic mesenchymal stem cell (MSC) secretome is a novel intra-articular therapeutic that has shown promise in *in vitro* and small animal models and warrants further investigation.

Objectives: To investigate if intra-articular allogenic MSC-secretome has anti-inflammatory effects using an equine model of joint inflammation.

Study Design: Randomized positively and negatively controlled experimental study.

Method: In phase 1, joint inflammation was induced bilaterally in radiocarpal joints of eight horses by injecting 0.25 ng lipopolysaccharide (LPS). After 2 h, the secretome of INFy and TNFα stimulated allogeneic equine MSCs was injected in one randomly assigned joint, while the contralateral joint was injected with medium (negative control). Clinical parameters (composite welfare scores, joint effusion, joint circumference) were recorded, and synovial fluid samples were analyzed for biomarkers (total protein, WBCC; eicosanoid mediators, CCL2; TNFα; MMP; GAGs; C2C; CPII) at fixed post-injection hours (PIH 0, 8, 24, 72, and 168 h). The effects of time and treatment on clinical and synovial fluid parameters and the presence of time-treatment interactions were evaluated. For phase 2, allogeneic MSC-secretome vs. allogeneic equine MSCs (positive control) was tested using a similar methodology.

Results: In phase 1, the joint circumference was significantly ($p < 0.05$) lower in the MSC-secretome treated group compared to the medium control group at PIH 24, and significantly higher peak synovial GAG values were noted at PIH 24 ($p < 0.001$). In phase 2, no significant differences were noted between the treatment effects of MSC-secretome and MSCs.

Main Limitations: This study is a controlled experimental study and therefore cannot fully reflect natural joint disease. In phase 2, two therapeutics are directly compared and there is no negative control.

Conclusions: In this model of joint inflammation, intra-articular MSC-secretome injection had some clinical anti-inflammatory effects. An effect on cartilage metabolism,

OPEN ACCESS

Edited by:
Jan H. Spaas,
Boehringer Ingelheim, Germany

Reviewed by:
Debbie Guest,
Royal Veterinary College (RVC), United Kingdom
Laura Barrachina,
National University of Ireland, Ireland

****Correspondence:***
Clodagh M. Kearney
clodagh.kearney@ucd.ie

Specialty section:
This article was submitted to Veterinary Regenerative Medicine, a section of the journal Frontiers in Veterinary Science

Received: *29 March 2022*
Accepted: *20 May 2022*
Published: *22 June 2022*

Citation:
Kearney CM, Khatab S, van Buul GM, Plomp SGM, Korthagen NM, Labberté MC, Goodrich LR, Kisiday JD, Van Weeren PR, van Osch GJVM and Brama PAJ (2022) Treatment Effects of Intra-Articular Allogenic Mesenchymal Stem Cell Secretome in an Equine Model of Joint Inflammation. Front. Vet. Sci. 9:907616. doi: 10.3389/fvets.2022.907616

evident as a rise in GAG levels was also noted, although it is unclear whether this could be considered a beneficial or detrimental effect. When directly comparing MSC-secretome to MSCs in this model results were comparable, indicating that MSC-secretome could be a viable off-the-shelf alternative to MSC treatment.

Keywords: mesenchymal stem cells, secretome, joint inflammation, equine model, lipopolysaccharide (LPS)

INTRODUCTION

Osteoarthritis (OA) is a common debilitating disease in horses and humans (1). Given the fact that chronic and intermittent inflammation plays a predominant role in the prolonged disruption of joint homeostasis characteristic of OA, inflammation appears to be a logical target for novel therapeutics.

Mesenchymal stem cells (MSCs) are increasingly considered to be a promising biological treatment option for OA in horses and humans, and recently much focus has been on the use of allogenic MSCs (2). While there is still some discussion regarding the safety and efficacy of allogenic MSCs, more recent studies have shown that allogenic MSCs show similar effects to autologous MSCs in normal and inflamed joints (3), and a recent review concluded from accumulating evidence in studies to date in horses that allogenic MSCs are safe (2). Recently an allogenic mesenchymal stem cell product became the first stem cell-based veterinary medicine approved by the European Medicine Agency (4).

There is mounting evidence that the anti-inflammatory effects of MSCs result from their capacity to influence their micro-environment through the secretion of trophic factors (5–10). These secreted factors, known as secretomes are a cocktail of mediators and extracellular vesicles involved in many processes including inflammation and regeneration. Beneficial therapeutic effects of stem cell secretome were first described in the cardiovascular field, where a group investigating the potential therapeutic effects of MSCs on cardiomyocytes after exposure to hypoxia demonstrated *in vivo* that myocardial protection could also be afforded by concentrations of paracrine factors secreted by MSCs (11). The potential of these secreted factors to exert paracrine effects was naturally of interest in orthopedic research. While early experimental work with MSCs focused on exploring their capacity for differentiation and repair or regeneration of damaged joint tissues, the ability of MSCs to locally embed and replace damaged tissue is now known to be low (12, 13). Similar to the work with cardiomyocytes it has now been hypothesized that much of the therapeutic effectiveness of MSCS in joint disease is due to their release of paracrine factors which could counteract inflammatory and catabolic processes and foment endogenous repair (9, 14, 15). This has led researchers to investigate these secreted factors themselves as novel therapeutics rather than the parent MSCs. Our group and others have previously shown beneficial effects of MSC-secretome in *in vitro* and small animal *in vivo* OA models where an earlier reduction in pain and protective effects on cartilage were noted (15–17). If it would be possible to use the secretome as a therapeutic treatment instead of the cells themselves, it would provide opportunities to optimize the composition and concentration of these components *in vitro*. This would allow for an off-the-shelf cell-free treatment option with the potential to be widely available and affordable.

To the best of our knowledge, intra-articular administration of MSC-secretome has not previously been studied *in vivo* in the horse, although reports of its use in other areas have recently emerged (18). A research group from Cornell University has investigated various applications with regard to wound healing and found that conditioned medium from equine mesenchymal stem cells had both positive effects in an equine *in vitro* wound healing model (19) and also that equine MSC-secretome inhibits biofilm formation and mature biofilms of various bacteria (20). Lange-Consigilio et al. investigated conditioned medium from amniotic membrane-derived MSCs (AMC-CM) as an intralesional treatment in horses and ponies with naturally occurring tendon or ligament injuries and reported no adverse effects and favorable clinical outcomes (21). Those promising findings further supported our aim of investigating MSC-secretome in an equine model of joint disease.

In the presented study, we use a bilateral low dose LPS-induced inflammatory joint model in horses to first investigate the potential anti-inflammatory effects of allogenic MSC-secretome on clinical parameters and various biological markers in synovial fluid related to inflammation and cartilage turnover, compared to a control consisting of carrier medium only (negative control). Next, we compared the efficacy of intra-articular MSC-secretome to allogenic MSCs from the same cell lines the secretome was derived from (positive control). We hypothesized that intra-articularly injected MSC-secretome would demonstrate anti-inflammatory effects in this equine model of joint inflammation, and that intra-articularly injected MSC-secretome would be as effective as MSCs in reducing inflammation.

MATERIALS AND METHODS

Study Design

A complete overview of the study design is shown in **Figure 1**. In preparation for the experimental phase of the study, bone marrow-derived MSCs previously collected and stored at the Colorado State University Veterinary Teaching Hospital under the approval of the Institutional Animal Care and Use Committee of Colorado State University (15-5810A) were transported to the Erasmus Medical Center in Rotterdam. Using these cells

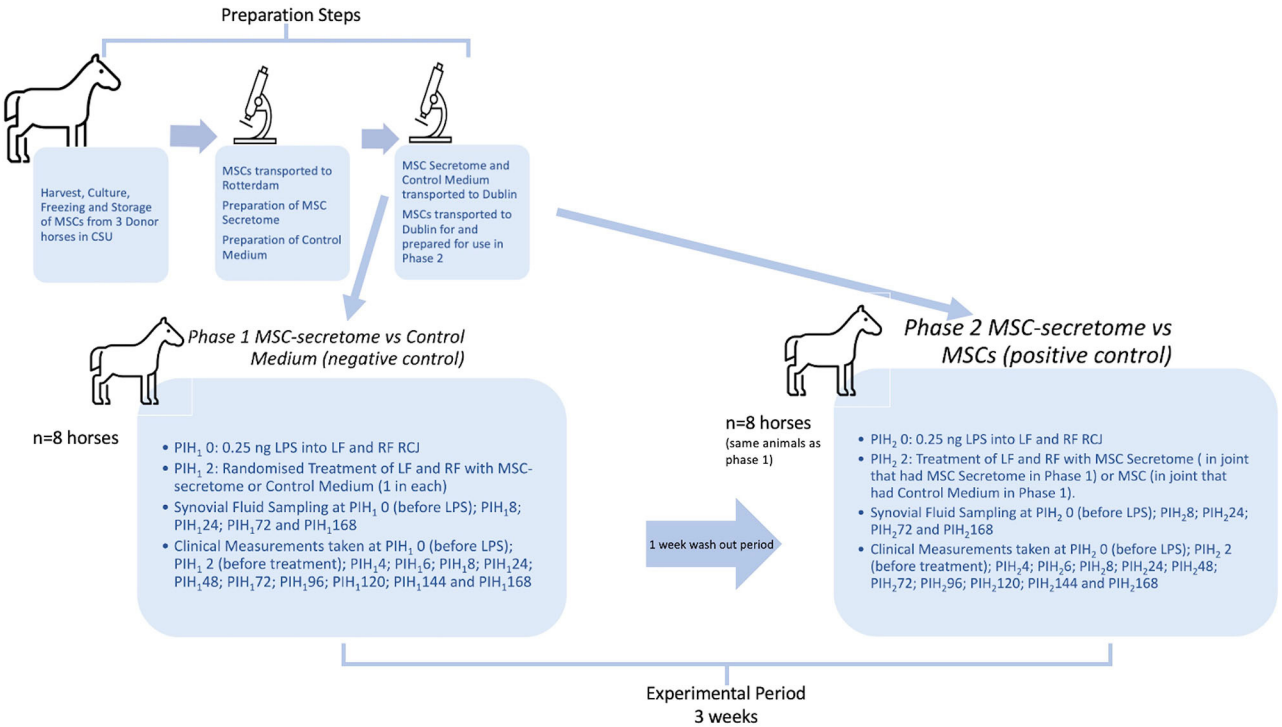

FIGURE 1 | Overview of study design. The preparation steps were carried out in advance of the experimental period. Bone marrow derived mesenchymal stem cells (MSCs) were harvested from donor horses in Colorado State University (CSU) Veterinary Teaching Hospital and cultured, frozen and stored according to their standard protocols. Later, MSCs were transported, still frozen, to Erasmus MC in Rotterdam, where they were thawed and cultured and then used to prepare Mesenchymal stem cell secretome (MSC-secretome) treatments. Cells from the same cell lines as used for the MSC preparation were also transported to Dublin, where the final preparatory steps and viability assessment were performed immediately prior to their use in Phase 2 of the experiment. The experimental period represents 3 weeks in total. PIH (Post Induction Hour) indicates time in hours after induction of inflammation with intra-articular injection of 0.25 ng of lipopolysaccharide (LPS) in each radiocarpal joint (RCJ) of 8 horses. At $PIH_1 2$, one randomly selected RCJ of each horse was injected with intra-articular mesenchymal stem cell secretome and the contralateral joint was injected with medium (negative control). Following $PIH_1 168$, horses had a washout period (7 days) during which they were on pasture rest. At $PIH_2 2$, the RCJ that had previously been treated with intra-articular mesenchymal stem cell secretome was again treated with intra-articular mesenchymal stem cell secretome and the contralateral joint was injected with mesenchymal stem cells (positive control).

MSC Secretome was prepared using techniques previously described for the production of secretome from Human bone marrow MSCs (17).Control medium was also prepared as a negative control, this product being the same formulation used to transport the MSC secretome but just not having been exposed to MSCs. Cells from the same cell lines as used for the MSC preparation were also transported to Dublin, where the final preparatory steps and viability assessment were performed immediately prior to their use in Phase 2 of the experiment.

For the experimental phase of the study 8 horses from the research herd of University College Dublin Lyons Research Farm were used following approval of the University College Dublin Animal Research Ethical Committee (AREC-16-29-Brama) and the Irish Health Products Regulatory Authority (AE18982-P105), in compliance with Irish legislation on experimental animal use. At the start of phase 1 both radiocarpal joints of each horse were injected with lipopolysaccharide (LPS) to induce joint inflammation. Two hours later one randomly selected radiocarpal joint of each horse was injected with intra-articular MSC secretome and the contralateral joint injected with control medium. Over the following week clinical parameters were measured and recorded, and serial synovial fluid samples were also taken during this period to determine the effect of each treatment on the joints involved. All investigators were unaware of the treatment assignment with the exception of the first author.

The same eight horses were used in both Phase 1 and Phase 2 of the study in an effort to reduce the numbers of experimental animals used so that each animal could act as its own control. Following a wash out period of 1 week after the last sampling, and 2 weeks after the first induction of inflammation with LPS Phase 2 of the study was initiated when inflammation was again induced in both radiocarpal joints of each horse with intra-articular injections of 0.25 ng of LPS. From previous work using the same dose of LPS intra-articularly, it was expected that all clinical and synovial markers of inflammation would be returned to baseline levels by this time (22). In this phase, the radiocarpal joint that had previously been treated with intra-articular MSC-secretome was again treated with

intra-articular MSC-secretome and the contralateral joint was injected with mesenchymal stem cells. Clinical measurements and synovial fluid samples were taken as before. Specific detail regarding each step of the study is documented in the following sections."

Collection and Expansion of MSCs

Equine bone marrow-derived MSCs from three donors were collected at the Colorado State University Veterinary Teaching Hospital. The procedure of harvesting and culturing MSCs is previously described (23). Specific characterization of these MSCs was not performed, however, previously published reports from this laboratory can give us some indication of the likely behavior of these cells. In respect of specific criteria set out in a recent position paper in this journal in this journal (24) these cells should demonstrate plastic adherence (23), chondrogenic and osteogenic potential (25–27), high CD 90, and low to negligible MHCII expression (26, 28). The MSCs were cryopreserved in a freeze media comprised of 95% fetal bovine serum (FBS) and 5% dimethyl sulfoxide (DMSO) and stored at −80°C prior to being shipped to Rotterdam. There the MSCs were cultured using previously described procedures (17). Briefly, MSCs were thawed, counted, and plated at 50,000 cells/cm^2 and, after 24 h, the flasks were rinsed to remove the non-adherent cells. When 70% confluency was achieved, MSC were trypsinized [0.25% trypsin/ethylenediaminetetraacetic acid (EDTA) solution (Life Technologies)] and seeded in cell culturing flasks at a density of 2,300 cells/cm^2 in expansion medium consisting of minimal essential medium alpha (αMEM; Gibco), 10% heat inactivated fetal calf serum (FCS; Gibco), 1.5 μg/ml fungizone (Invitrogen), 50 μg/ml gentamicin (Invitrogen), 25 μg/ml ascorbic acid-2-phosphate (Sigma-Aldrich) and 1 ng/mL fibroblast growth factor 2 (FGF2; AbD Serotec, Oxford, UK). Cells were cultured in an incubator at 37°C, 5% CO_2, and 90% humidity. The medium was refreshed 2 times a week. MSCs were passaged at ∼70% confluency. The cells were passaged three times in a monolayer prior to being used in the experimental protocols.

Preparation of MSC-Secretome and Control Medium

The dose of secretome per joint was planned to be the secretome equivalent of 10 × 10^6 MSCs. To produce the MSC-secretome, passage 3 MSCs were plated at a density of 3.5 × 10^4 cells/cm^2 and cultured for 24 h in an expansion medium. After 24 h, cells were activated to secrete immunomodulatory factors by culturing for 24 h in stimulating medium (15, 17). This stimulating medium consisted of αMEM supplemented with 1.5 μg/ml fungizone, 50 μg/ml gentamicin, 1% insulin–transferrin–selenium (ITS; Biosciences), 50 ng/ml equine interferon gamma (Recombinant Equine IFN-gamma Protein, R&D) and 50 ng/ml equine tumor necrosis factor alpha (Recombinant Equine TNF-alpha Protein, R&D). After 24 h of stimulation, MSCs were washed five times with phosphate-buffered saline (PBS; Gibco). To collect the paracrine factors, a collecting medium was added, consisting of only αMEM (MEM α, nucleosides, no phenol red, ThermoFisher) with 0.05% equine serum albumin (ESA; Rocky Mountain Biologicals Inc.)—to stabilize the secreted factors and as an adhesive for smaller molecules to bind to and to be retained after the concentration step—and without phenol red that can mimic estrogen and therefore influence cell behavior *in vivo*. About 1 ml of collecting medium was added per 2.0 × 10^5 MSCs. MSC-secretome was collected after 24 h and centrifuged at 700 × g for 8 min to remove cell debris. To achieve the desired concentration (secretome equivalent of 10 × 10^6 MSCs) in an end volume of 3 ml, suitable for intra-articular injection, the MSC-secretome was concentrated, according to a previously developed protocol by our lab (17). Briefly, this was done by loading MSC-secretome on a 3 kDa cut-off filter (Merck Millipore Centricon Plus-70 device, 3K) and spinning down for 20 min at 4,000 ×g. Molecules above 3 kDa were retained. The concentrated equine MSC-secretome was collected, aliquoted, and stored at −80°C for further use. For each injection concentrated MSC-secretome from each of the three donors was pooled to give aliquots of a final volume of 3 ml, representing the secretome of 10 × 10^6 MSC.

Control medium was prepared by subjecting the collecting medium used for the MSC-Secretome—αMEM (with no phenol red) and 0.05% equine serum albumin—to the same handling as the MSC-secretome, including 24 h incubation and concentration step, but not including exposure to the MSCs, and then stored at −80°C until required.

Both the MSC-secretome and the control medium were thawed on ice immediately prior to injection.

Preparation of MSC Injections

Circa 24 h prior to injection the culture flasks containing MSCs from the same cell lines as used for the production of MSC-secretome, were washed five times with phosphate-buffered saline (PBS; Gibco). Whereafter the same collecting medium as in the MSC-secretome preparation was added, consisting of only αMEM w/o phenol red with 0.05% equine serum albumin (ESA; Rocky Mountain Biologicals Inc.). Unlike the cells used for the MSC-secretome production, these MSCs were not stimulated with equine interferon gamma and equine tumor necrosis factor alpha as it was considered they would be exposed to an inflammatory environment in the LPS-inflamed joints. After 24 h, the MSCs were trypsinized and the MSCs were collected. The viability of the MSCs was evaluated after trypsinization: <5% of the cells were dead, as indicated by visual assessment following trypan blue positive staining. For each intra-articular injection, cells were pooled from each donor to give a total of 10 ×10^6 MSC collected in a volume of 3 ml of control medium. The cells were injected within 2–4 h of trypsinization and evaluation.

Experimental Animals

Eight horses (16 joints) were selected to participate in a randomized controlled experiment. The animals of various breeds (six mares and two geldings) (mean ± SD age 14.6 ± 2.4 years, bodyweight 370.4 ± 27.6 kg) were from the University research herd. There was no known history of forelimb lameness in any of the animals. Each animal was examined clinically by 2 ECVS boarded surgeons, and was found to have no sign of forelimb lameness. On clinical and radiographic examinations their carpal joints were found to be within normal limits. While individual animals were previously used in other experimental

studies the radiocarpal joints of these animals had not previously been injected or treated in any way. During the sampling phases of the experiment, the animals were stabled individually in single boxes (4 m × 4 m) on wood shavings. Horses received concentrates once daily, with regular hay and water provided *ad libitum*. Following the week of sampling and measurements during which the horses were stabled, they were then turned out to pasture in a familiar group for a week. They were brought back in on the morning of the second induction of LPS and were again stabled under the same conditions during this second week of sampling and measurements. Before commencement of Phase 2 of the study, each animal was again examined by two ECVS boarded surgeons and was found to be free of any forelimb lameness and of any clinical signs of inflammation of the radiocarpal joints (joint effusion, heat, or pain on palpation or flexion).

Experimental Protocol

Induction of Inflammation

At post induction time (PIH) 0, both carpi of each horse were clipped and prepared for dorsal arthrocentesis. Lipopolysaccharide from *Escherichia coli* O55:B5 (catalog number L5418; Sigma-Aldrich Ireland Ltd., Arklow, Co. Wicklow Ireland) was diluted to a final concentration of 0.25 ng/ml in sterile lactated Ringer's solution. Horses were sedated with xylazine (0.2–0.5 mg/kg intravenously, Chanazine 10%®; Chanelle, Ireland) and butorphanol (0.01–0.02 mg/kg intravenously; Alvegesic vet 10®, ALVETRA u. WERFFT GmbH, Vienna, Austria). Synoviocentesis was performed in each limb with a 20 G × 40 mm needle and 1 ml LPS solution (0.25 ng LPS) was delivered aseptically into each radiocarpal joint after withdrawal of the PIH 0 synovial fluid (SF) sample.

Treatments

Phase 1 MSC-Secretome vs. Medium (Negative Control)

In the first phase of the experiment, 2 h following induction of inflammation with LPS (PIH_12), following preparation of the regions as before, one randomly assigned radiocarpal joint of each horse was injected with 3 ml of allogeneic MSC-secretome (treatment), and the opposite radiocarpal joint was injected with the same volume of control medium (negative control).

Phase 2 MSC-Secretome vs. MSCs (Positive Control)

Following a wash-out period of 1 week after the last sampling, and 2 weeks after the first induction of inflammation with LPS, the same group of horses was used for Phase 2 of the study. From previous work using the same dose of LPS intra-articularly, it was expected that all clinical and synovial markers of inflammation would be returned to baseline levels by this time (22). In this second phase of the experiment, 2 h following induction of inflammation with LPS (PIH_22), following preparation of the regions as before, the same radiocarpal joint as had been treated with allogeneic MSC-secretome in the previous phase was injected with secretome (treatment), and the opposite radiocarpal joint was injected with allogeneic MSCs (positive control).

Clinical Evaluations

Welfare Monitoring

Before synoviocentesis and induction of inflammation and again every 2 h until PIH 8, and thereafter daily until PIH 168 a Composite Welfare Score (CWS) was assigned by an experienced vet. The CWS is the sum of scores for each of the following categories: food and water intake; clinical parameters (temperature, pulse, and respiratory rate); natural behavior; and provoked behavior. Each of the categories is scored on a scale of 0–4, so the total range of scores is 0–16. This scoring system has been designed by our group for this bilateral equine LPS model to monitor welfare and to fulfill institutional and national ethical regulatory requirements (scoresheet available in supporting information).

Clinical Measurements

In each induction, before synoviocentesis at PIH 0, every 2 h until PIH 8, and thereafter daily until PIH 168, radiocarpal joint effusion was graded on a subjective scale as previously described (29). An experienced clinician carefully palpated the joints and assigned a score ranging from 0 to 4; a score of 1, 2, or 3 denoting mild, moderate, or severe radiocarpal joint effusion, respectively, and 4 indicating severe swelling of the entire carpal region. In addition, joint circumference was measured at a fixed anatomical landmark at the level of the accessory carpal bone with a tape measure in mm. At the start of each phase, a mark was drawn on the skin over the accessory carpal bone to use as a reference point so that all measurements would be taken at the same level. All clinical measurements were performed by the first author and therefore cannot be considered to be blinded.

Synovial Fluid Analysis

At fixed time points (PIH 0, 8, 24, 72, and 168), synoviocentesis of each radiocarpal joint was performed under sedation as described above and a 4–5 ml sample of synovial fluid was collected. About 1.3 ml of this synovial fluid was placed in ethylenediamine tetra-acetic acid (EDTA) for manual white blood cell count (WBC) and total protein (TP) measurement (refractometer). The remainder was immediately centrifuged in plain tubes for 15 min at 4°C at 10,000 rpm and then aliquoted and stored at −80°C until further analysis.

Synovial Fluid Molecular Biomarker Analysis

Seven assays were performed on each synovial fluid sample.

Eicosanoid inflammatory mediators—Prostaglandin F2α (PGF2α), Prostaglandin E_2 (PGE_2), Prostaglandin E_1 (PGE_1), Leukotriene B_4 ($LTB_{4)}$, and 11-hydroxyeicosatetraenoic acid (11-HETE)—concentrations were determined by high-performance liquid chromatography (HPLC)–tandem mass spectrometry (MS/MS) analysis using previously validated methods (30). Briefly, measurements were made using a 4000 Q TRAP mass spectrometer with electrospray ionization (EPI) interface (Sciex, Toronto, ON), operated in multiple-reaction monitoring (MRM) mode at unit mass resolution. The mobile phases consisted of 10 mM ammonium acetate pH 3.5 in water, and 10 mM ammonium acetate pH 3.5 in methanol. Peaks were identified by comparison of retention time and mass spectra

of standards using Analyst software version 1.6.2 (Applied Biosystems, Nieuwerkerk a/d IJssel, The Netherlands).

General matrix metalloproteinase (MMP) activity was measured using cleavage of fluorogenic substrate FS-6i (Calbiochem, San Diego, CA, USA) as previously described (31, 32). Briefly, samples were first diluted 20-fold in MMP buffer [0.1 mol/L Tris, 0.1 mol/l NaCl, 10 mmol/L $CaCl_2$, 0.05% (w/v) Triton X-100, 0.1% (w/v) PEG6000, pH 7.5 and 5 mmol/L FS-6]. Samples were subsequently added in triplicate to a black 384-well microplate and the fluorescent signal was monitored continuously for 45 min at 37°C using a CLARIOstar microplate reader. The slope of the resultant linear curve [relative fluorescence units/s (RFU/s)] was then calculated as a measure of general MMP activity. A quantity of 5 mmol/L EDTA was used as a negative control.

Synovial fluid samples were evaluated for glycosaminoglycan (GAG) concentrations using a modified 1,9-dimethylmethyleneblue assay adapted for use in microtitre plates, as previously described (33).

C–C motif chemokine ligand 2 (CCL2) and tumor necrosis factor-α (TNF-α) concentrations were quantified using commercial equine-specific ELISA kits (DIY0694E-003 Kingfisher Biotech, Minnesota USA and #ESS0017, Thermo Fisher Scientific, Massachusetts, USA) using an adapted protocol as previously described (22). The coating buffer consisted of carbonate/bicarbonate buffer (pH 9.6) and the blocking/dilution buffer was PBS with 1% w/w bovine serum albumin (BSA) (Sigma Aldrich, Saint Louis, USA). Samples were diluted 1:1 in PBS/1% BSA/0.1% (v/v) Tween-20, and results were calculated to a standard curve plotted on four parameters logistic curve fit. Values equal to, or below the blank were set to zero.

Commercial ELISA kits were used to determine concentrations of collagen-cleavage neoepitope of type II collagen (C2C), and carboxypropeptide of type II collagen epitope (CPII) (IBEX Technologies, Quebec, Canada), following the manufacturer's recommendations. Samples for C2C were 1:1 diluted and for CPII were 1:10 diluted, both in buffer III, and results were calculated to a standard curve plotted on four parameter logistic curve fit. Values equal to, or below the blank were set to zero.

GAGs, CCL2, TNF-α, C2C, CPII, GAG were all quantified on a VersaMax™ ELISA microplate reader. GAGs were measured at 525 and 595 nm and all the ELISAs were measured according to the manufacturer's recommendations.

Statistical Analysis

An a priori power analysis was performed. The power calculation was based on previous similar studies using the LPS model with described differences in synovial fluid biomarkers indicating joint inflammation (31, 34, 35). The power calculation suggested that eight horses would give a power of 0.8 and an alpha error rate of 0.05. Data are presented as the mean ± standard deviation (SD).

For each phase, a linear mixed effects model for repeated measures was fitted, with the horse as a random effect and time, treatment, and their interaction as fixed effects. An Independent variance-covariance structure was used in the model. Planned univariate contrasts (Wald tests) were performed between marker concentrations in MSC-secretome (treatment) and medium (negative control) (Phase 1), or MSC-secretome (treatment) and MSC (positive control) (Phase 2) treated joints at specific time points following observation of an overall significant effect of treatment, using Bonferroni's correction for multiple comparisons, with each phase considered as a separate experiment. Normality was assessed by visual inspection of plots of standardized residuals. The suitability of the mixed effects model over a linear model was assessed by AIC, BIC, and Likelihood Ratio Test. Computer software was used (*Stata Statistical Software: Release 15*. StataCorp LLC, College Station, TX) and the level of significance was set at $p < 0.05$ for all statistical analyses ($p < 0.025$ with Bonferroni correction).

RESULTS

Phase 1: MSC-Secretome (Treatment) vs. Medium (Negative Control)

Validation of Inflammatory Response

In both control and treated limbs, clear inflammatory responses, in the form of the expected peaks and subsequent falls in total protein and synovial white blood cell counts were seen after administration of LPS (**Figures 2A,B**).

Welfare Monitoring

For those horses that had slight Composite Welfare Score (CWS) increases in the early stages of the period of inflammation, their scores had returned to the normal range by 24 h post induction (**Supplementary Table S2**).

Clinical Monitoring

For the primary research question investigating the effects of intra-articular administration of secretome on joint circumference a statistically significant treatment effect was seen with a reduction in joint circumference in the MSC-secretome treated group compared to the control treated group at PIH 24 (−0.33125 cm, $p = 0.0247$) and at PIH 168 (−0.45 cm, $p = 0.0012$) (**Figure 2C**). From the data in **Supplementary Table S3** it appears that joint circumference in both treatment groups remains above baseline levels at PIH 168, although it is not known whether these are significant differences as contrasts comparing each timepoint in each treatment group to baseline values were not performed. As joint effusion scores were on an ordinal scale, after consideration of the repeated measures design, in particular in conjunction with the small sample size ($n = 8$), formal statistical methods such as ordinal logistic regression were considered inappropriate. No appreciable differences were apparent from simple observation between treatment groups. Results are summarized in **Supplementary Table S3**.

Synovial Fluid Molecular Biomarker Monitoring

The results for all synovial fluid parameters are summarized in **Supplementary Table S4**, which also includes where available our laboratory's baseline ranges for each synovial fluid biomarker.

Regarding the effects of intra-articular administration of secretome on synovial concentrations of biomarkers, results indicate a difference in treatment effect with increases in GAG

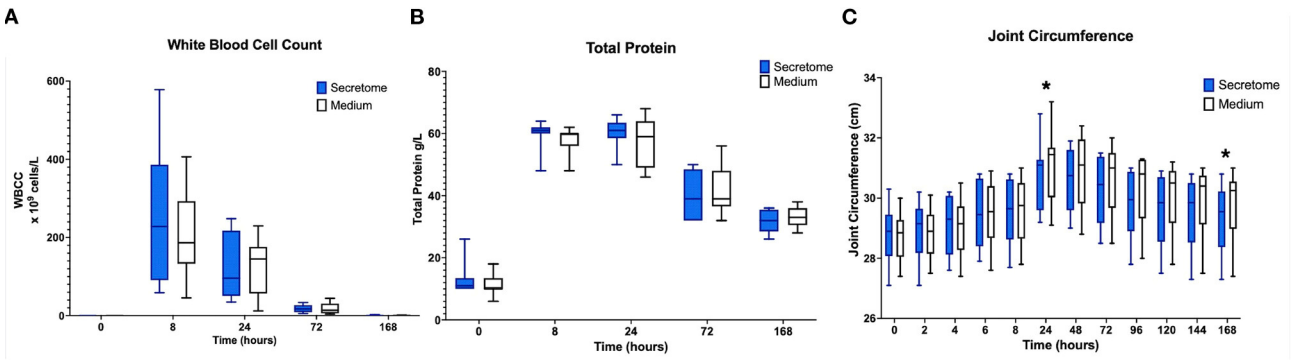

FIGURE 2 | Phase 1 synovial white blood cell counts, total protein, and joint circumference. **(A)** Synovial White Blood Cell Count, **(B)** Synovial Fluid Total Protein, and **(C)** Joint Circumference over time following induction of inflammation with intra-articular injection of 0.25 ng of LPS in the left and right radiocarpal joints of horses at PIH_1 0 ($n = 8$ horses). Joints were treated with either intra-articular mesenchymal stem cell (MSC) secretome or medium (negative control) at $PIH_1$2. Boxes depict median and interquartile ranges; whiskers denote minimum and maximum values. For the Synovial White Blood Cell Count, the box and whiskers for the first timepoint are not visible on the graph as the values for these were very low with each measurement recorded being $< 1 \times 10^9$ cells/L. *$p < 0.05$, indicating time points where there are significant treatment effects.

concentrations in the MSC-secretome treated group compared to the control treated group in the first phase at PIH 24 (+201.29 μ/ml, $p = 0.00067$) (**Figure 3A**). For the other biomarkers, treatment effects are not evident, as illustrated for selected markers in **Figures 3B,C**.

Summarizing the results of the comparison between MSC-secretome and medium indicated that MSC-secretome reduces joint circumference and influences GAG release, but not other synovial fluid cartilage turnover or inflammation markers.

Phase 2: MSC-Secretome (Treatment) vs. MSCs (Positive Control)

Validation of Inflammatory Response

In both groups (MSC and MSC-secretome treated joints) clear inflammatory responses in the form of the expected peaks and subsequent falls in synovial white blood cell counts and total protein were seen after administration of LPS (**Figures 4A,B**).

Welfare Monitoring

As in Phase 1 for horses that had slight CWS increases in the early stages of the period of inflammation, their scores had returned to the normal range by 24 h post induction (**Supplementary Table S2**).

Clinical Monitoring

A potentially confounding finding was that from **Supplementary Tables S3**, **S5** it can be seen that for both treatment groups the joint circumference was slightly higher at Timepoint 0 of Phase 2 than at Timepoint 168 of Phase 1. This was unexpected as the measurements had been decreasing toward the end of Phase 1 and the horses were carefully checked at the start of Phase 2 and no evidence of joint effusion was recorded at Timepoint 0. This apparent discrepancy would seem to be due to some inconsistency in the placement of the marks drawn on the skin over the accessory carpal bone meaning that measurements were taken at slightly different levels between groups.

For joint circumference, while from PIH 24 onwards the values of the MSC-secretome treated group appeared lower than those of the MSC treated group these differences were not found to be significant (**Figure 4C**). For joint effusion scores, as in Phase 1, no appreciable differences were observed between treatment groups. Results are summarized in **Supplementary Table S5**.

Synovial Fluid Molecular Biomarker Monitoring

The results for all synovial fluid parameters are summarized in **Supplementary Table S6**.

No significant differences between the MSC-secretome treated and MSC treated joints were noted for any clinical or synovial fluid biomarker as illustrated for selected markers in **Figure 5**. For synovial GAG, the peak value of the MSC-secretome treated group was higher than the peak value of the MSC treated group at PIH 24 but this did not reach significance ($p = 0.029$) (**Figure 5B**).

In summary, the comparison between MSC-secretome and MSCs revealed no significant difference in treatment effect.

DISCUSSION

In this study, we compared the effect of intra-articular allogenic MSC-secretome in an equine within-animal-controlled model of joint inflammation to negative control (medium) and positive control (allogenic MSCs). We report two main findings. First, when compared to negative control, intra-articular allogenic MSC-secretome reduces joint circumference and increases GAG release at the 24-h timepoint (PIH 24) in an equine model of LPS induced synovial inflammation. Second, when compared in the same equine LPS model of synovial inflammation, no significant differences in treatment effects of intra-articular allogenic MSC-secretome vs. allogeneic MSCs were detected.

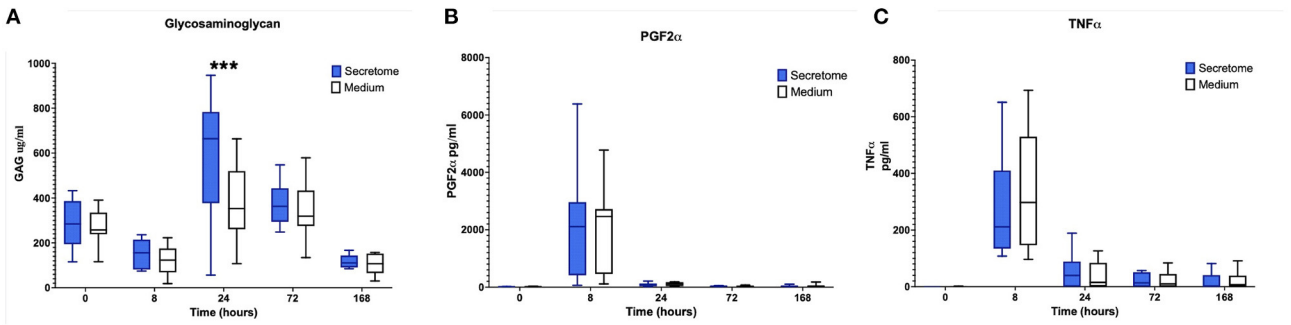

FIGURE 3 | Phase 1 synovial fluid glycosaminoglycan, prostaglandin F2α and tumor necrosis factor α. **(A)** Glycosaminoglycan, **(B)** Prostaglandin F2α, and **(C)** Tumor Necrosis Factor α concentrations in synovial fluid over time following induction of inflammation with intra-articular injection of 0.25 ng of LPS in the left and right radiocarpal joints of horses at PIH_1 0 ($n = 8$ horses). Joints were treated with either intra-articular mesenchymal stem cell (MSC)-secretome or medium (negative control) at $PIH_1$2. Boxes depict median and interquartile ranges; whiskers denote minimum and maximum values. ***$p < 0.001$, indicating timepoints where there are significant treatment effects.

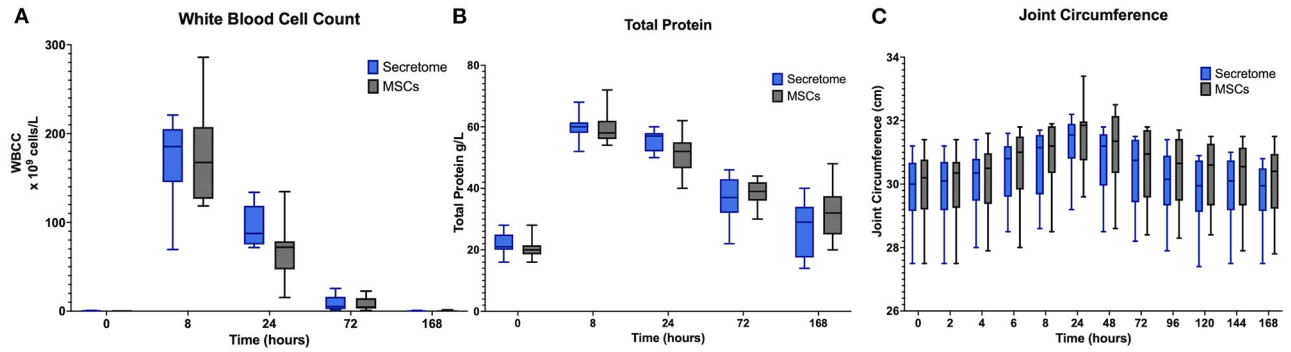

FIGURE 4 | Phase 2 synovial white blood cell counts, total protein and joint circumference. **(A)** Synovial White Blood Cell Count, **(B)** Synovial Fluid Total Protein, and **(C)** Joint Circumference over time following induction of inflammation with intra-articular injection of 0.25 ng of LPS in the left and right radiocarpal joints of horses at PIH_2 0 ($n = 8$ horses). Joints were treated with either intra-articular mesenchymal stem cell (MSC)-secretome of mesenchymal stem cells (MSCs) (positive control) at $PIH_2$2. Boxes depict median and interquartile ranges; whiskers denote minimum and maximum values. For the Synovial White Blood Cell Count the box and whiskers for the first timepoint are not visible on the graph as the values for these were very low with each measurement recorded is $<1 \times 10^9$ cells/L.

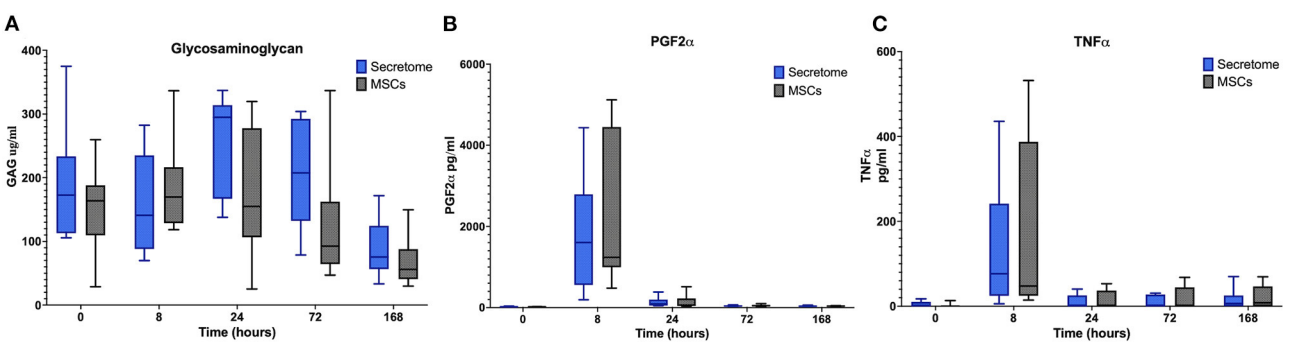

FIGURE 5 | Phase 2 synovial fluid glycosaminoglycan, prostaglandin f2α and tumor necrosis factor α. **(A)** Glycosaminoglycan, **(B)** Prostaglandin F2α, and **(C)** Tumor Necrosis Factor α concentrations in synovial fluid over time following induction of inflammation with intra-articular injection of 0.25 ng of LPS in the left and right radiocarpal joints of horses at PIH_2 0 ($n = 8$ horses). Joints were treated with either intra-articular mesenchymal stem cell (MSC)-secretome of mesenchymal stem cells (MSCs) (positive control) at $PIH_2$2. Boxes depict median and interquartile ranges; whiskers denote minimum and maximum values.

In our previous *in vivo* study assessing the effects of MSC-secretome injection in a murine OA model, clinical benefits such as an early reduction in pain as determined by increased weight bearing were seen (17). In the present study, clinical benefit seen

as a significant reduction in carpal circumference in the group of horses treated with MSC-secretome was noted, corroborating what was found in the earlier mouse model.

The previous *in vitro* work also demonstrated anti-inflammatory and matrix turnover altering effects of MSC secretome on human osteoarthritic cartilage and synovium (11). In addition, we found a reduction in cartilage damage after MSC-secretome injection in our murine OA model study (15, 17). Other groups have shown protective effects of MSC-secretome in an inflammatory *in vitro* chondrocyte model (16) and beneficial effects of MSC-derived extracellular vesicles in various pre-clinical OA models *in vivo* (36, 37). In the present study, we demonstrated a significant increase in levels of GAGs in the synovial fluid of secretome-treated joints compared to the control (medium treated) joints. In previous studies using GAG levels as outcome assessments when investigating intra-articular therapeutics increases in GAG levels (38, 39) have been varyingly explained as either a catabolic response due to an increased breakdown of GAGs already present in the cartilage, or as an anabolic response reflected by an increase in GAG production of the cartilage being exposed to an inflammatory environment. From our results, we cannot definitively assess whether the increased GAG concentration found in secretome treated joints was caused by a catabolic or an anabolic response, but the inclusion of further biomarkers such as the CS 846 epitope which has been found to be useful as a marker of aggregran synthesis (40) could help to clarify this in future studies.

MSCs have been studied as a potential form of cell therapy for equine joint disease in both experimental and clinical settings (41–44). Currently, in Europe, there are two approved veterinary stem cell-based products, namely allogenic blood or umbilical cord-derived mesenchymal stem cells, which lend credibility to their therapeutic potential. For this study, we chose allogenic bone marrow-derived MSCs as our positive control—given similar expected effects and based on the experience of our group with bone marrow-derived MSCs. In the second phase of this study, we report that there were no significant differences in treatment effects of intra-articular allogenic MSC-secretome and allogenic MSCs in this model of joint inflammation. We consider this to be a positive finding, considering that the allogenic MSCs are now generally accepted to be safe for use in equine joints (45), and safety and efficacy have been further validated by European Medicine Agency authorizations (4). We also observe in our study that a second dose of secretome did not result in increased inflammatory responses when compared to MSCs injection. However, it is challenging to compare our results to other studies investigating the effects of allogenic MSCs in equine joints, given the differences in MSC sources, experimental models, and outcome measures reported. As we did not directly test the efficacy of allogenic MSCs by comparing them to a negative control while we can conclude that in the second phase of our study the efficacy of MSCs and MSC-secretome are equivocal the possibility that neither are effective in this model of inflammation cannot be ruled out. It must be acknowledged that the effect on clinical measurements seen in the first phase of this study while significant is quite small, and it is unclear whether these would translate to clinical benefit. This finding is perhaps disappointing, particularly compared to the more positive results reported by Williams et al. for their umbilical derived MSCs (46). However, there are many differences between the models used, not least the source of MSCs, the dose of LPS and the timing of treatment. We believe that our results do support the overall conclusions from other studies (3, 46, 47), that allogenic MSCs but also allogenic MSC-secretome are safe for use and warrant further investigation.

A significant weakness in this study is the limited characterization of the therapeutic treatments investigated. While we have previously used the techniques described to produce MSC secretome from human MSCs (17), it would have been useful to further characterize the therapeutic produced here from equine MSCs. In the absence of further evaluation of the product, it is difficult to predict what therapeutic effects it could be expected to have, and it is clear that species differences can be expected. For example, in the study by Khatab et al. investigation of human MSC-derived secretome, indoleamine 2,3-dioxygenase (IDO) activity was measured to confirm the anti-inflammatory potential of donors but such assay was not even possible for the equine donors as equine MSCs do not produce IDO (48). Further evaluation of the equine MSC-secretome produced using the described techniques, which at the minimum should involve measurement of some expected inflammatory cytokines in the product should be included in any future studies. Similarly, we would consider it essential in future studies to include further characterization of the MSCs used. While previously published studies and other studies using MSCs isolated and cultured using these methods can give us some insight into the expected traits of these cells for this study (23, 25–28) specific characterization of the pooled MSCs used for the current study was regrettably not performed. Future work should include at least the suggested minimal definitions for equine MSCs as set out in a recent position study (24). This would not only allow for better standardization of the MSCs used and therefore of the secretome obtained, but also allow for easier comparison of these with MSCs and MSC-based products investigated by other research groups. The limited amount of characterization in the current study means that the previously mentioned disappointing comparison with other studies or reported success in clinical cases is perhaps then not surprising, as we cannot be sure that we are comparing similar products.

The horse is a particularly interesting experimental model for joint research, being both a target species for novel therapeutics and a suitable translational model (49, 50). Based on *in vitro* findings regarding differences in the behavior of MSCs in inflammatory environments it appears that testing the safety and potential efficacy of allogeneic MSCs using experimental models of inflammation may be particularly important (45). Previous studies examining the effects of MSCs in an *in vivo* inflammatory joint environment have each used different models of joint inflammation. Williams et al. reported a significant reduction in inflammation when allogenic umbilical cord blood-derived MSCs were administered into joints inflamed with a 0.5 ng dose of LPS (46). Using the more severe amphotericin-B model of joint inflammation, to examine the effects of allogenic bone marrow derived stem cells Barrachina et al. reported that

clinical and synovial inflammatory parameters were significantly reduced, and also that the second injection of allogeneic cells yielded no adverse reactions (47). A further study reported by Colbath et al. looking at the effects of allogenic and autogenous bone marrow-derived stem cells in an rIL-1β model of synovial inflammation did not find either type of MSCs to be effective in reducing inflammation (3). While no experimental model will exactly replicate naturally occurring disease, we have chosen to focus on the equine intra-articular LPS synovitis model as our group has extensive experience with this model and it has now been widely used for testing potential therapeutics (31, 32, 34, 35, 46). We have demonstrated that sub nano doses of LPS elicit marked, reliable yet transient effects on certain synovial fluid inflammatory biomarkers, MMP activity, and some markers of cartilage turnover (51). Additionally, synovial fluid biomarkers in horses have been extensively studied (40) and changes in synovial fluid concentrations of the same have been used as outcomes measures in studies investigating the effects of various interventions and therapeutics (35, 52).

One of the main limitations of large animal models, in general, is the inherent variability in biological responses between animals. Within animal controlled models are effective in counteracting this limitation. In addition, bilateral orthopedic models have been proven to significantly enhance statistical power (53). We recently refined our model to ethically allow for animal controlled testing of therapeutics in a bilateral low dose LPS induced inflammation model by using a lower dose of LPS (0.25 ng) (22, 32). A disadvantage of this low dose bilateral model is that it precludes the use of unilateral lameness measurements as an outcomes measure. Lameness assessment is inherently reliant on the ability to detect asymmetry of movement between limbs, which may be absent when bilateral lameness is present (54). We do not believe that any described lameness grading systems are suitable for application to bilateral lameness. Indeed, assigning grades in bilateral lameness is thought by some experts to be potentially misleading (54). Furthermore, while it does produce reliable intra-articular inflammation, it is accepted that doses of <0.5 ng LPS give variable, inconsistent levels of lameness (55). Hence lameness levels in our study, while monitored and recorded as part of the overall composite welfare scores, were not considered to be valid outcome measures in this study and therefore were not evaluated or reported as such.

We believe allogenic MSC-secretome as a treatment of joint inflammation could offer many clinical and logistical advantages over MSCs themselves. The use of allogenic stem cells has previously been acknowledged to have potential medical advantages over autologous cells (2). Allogenic cells may be screened and characterized prior to administration leading to a more consistent, higher quality end product. Ongoing production processes rather than the logistical restraints of multiplying cells from the target animal allow for wider availability and cost effectiveness, which is of particular importance in veterinary medicine (48). In addition to wider accessibility, the off-the-shelf nature of the potential end-product could also allow for more appropriate timing of treatment and repeated treatments where necessary. There is a further potential benefit to MSC-secretome being a cell-free product as it is known that MSCs maintain a certain degree of immunogenicity, particularly after stimulation which is performed to optimize their trophic effects (15, 56, 57). It is expected that the concentration of immune complexes in the secretome is lower than with cells, causing a weaker host inflammatory response (58). MSC-secretome could therefore also be a more attractive product due to the potential risk of immunological reactions to foreign MHC antigens expressed by MSCs (59).

Work outlining the importance of MSC extracellular vesicles and other secreted factors is ongoing (60). As these components become further characterized, we may be better able to direct toward the production of certain trophic factors with the use of specific priming techniques. In addition, optimal dosages and timings need to be determined. In the future we could have the ability to produce more targeted treatments for specific conditions, and stages of the disease. While this study is an important first step to establishing the safety and potential efficacy of MSC-secretome as an intra-articular therapeutic, clearly further investigations are needed. Equally, in the absence of an ideal experimental model for joint inflammation, and as we know different inflammatory environments can stimulate MSCs in different ways, it would be interesting to compare the effects of MSCs and MSC-secretome in different models of intra-articular disease, and even more relevantly in cases of naturally occurring disease.

LIMITATIONS

A number of limitations to this experimental model must be acknowledged. While this low dose intra-articular LPS model certainly produces a reliable intra-articular inflammation, the transient and self-limiting nature of this inflammation is of course not completely reflective of natural disease states, where recurrent episodes of inflammation play a crucial role in development and progression of OA.

A further limitation is that only markers of cartilage metabolism were investigated, and the cartilage in these joints was not directly examined either before (by means of direct arthroscopic visualization and/or biopsy) or after (arthroscopic visualization or post mortem examination) the experimental treatments were administered. It would have been interesting to compare the findings in our biomarkers to any changes in the structure of the cartilage or synovium. Histopathological evaluation of the cartilage for example have helped elucidate the reasons for the differences in GAG levels between treatment groups. However, such examinations were outside of the scope of this study.

The use of the same joints for both phases of the study could also be considered a limitation. Based on our previous work examining the effects of LPS induction and repeated inductions of LPS (22, 51) we know that outcomes measures return to baseline values around 7 days post LPS induction. Therefore, we were confident that leaving 14 days between LPS inductions would be a sufficient period. The return to within or close to baseline ranges seen for the majority of biomarkers by timepoint 168 in Phase 1 would appear to support this. While the minimal

effects seen in Phase 1 of the study suggest it is unlikely that there are sustained effects in this joint as we do not know what the duration of effect (if any) of MSC-secretome is, we cannot fully exclude the possibility that in Phase 2 we are seeing the cumulative effect of two doses of MSC-secretome. An Advantage from a safety point of view was that this approach provided the opportunity to evaluate a repeated dose of the MSC-secretome, to assess if there was any obvious evidence of sensitization.

A further limitation to consider with this model is that we have not isolated the potential inflammatory effect of repeated arthrocentesis, which has been previously reported (52, 61). Therefore, it is not possible to determine to what degree the physical insults of arthrocentesis and fluid aspiration may be contributing to the articular inflammatory reaction described, and how much of the reaction is a response to the LPS itself. While this was not addressed here, an earlier study where responses in saline injected control joints were studied showed that while increases in gross markers of inflammation such as total protein and white blood cell counts were seen in control joints (62), these responses were substantially less than the increases noted here. Further studies comparing the effects of absolute controls (saline) to the effects of LPS found that there were substantially greater responses in the LPS injected joints across a range of markers such as prostaglandin E2 and tumor necrosis factor-α (63, 64). Given this evidence and considering the principles of 3 R, we believe that using more animals as controls was not justified, particularly as in this bilateral model each joint undergoes the same degree of "insult" or inflammation induced from the LPS plus the physical effects of sampling across the same timeline and therefore it is the effects of the therapeutics being investigated on the sum of this inflammation that is of interest.

CONCLUSIONS

In conclusion, we have found indications for a small beneficial effect of allogenic MSC-secretome on clinically assessed inflammation as well as an effect on matrix turnover dynamics evaluated by biological markers. Additionally, while further investigations comparing the two both to each other and to negative controls are clearly needed our findings suggest that the treatment effects of allogenic MSC-secretome in this model are comparable to those of intra-articular allogenic MSCs. These results encourage further development of secretome-based strategies for therapeutic use as a durable and off-the-shelf disease modifying anti-osteoarthritic drug.

DATA AVAILABILITY STATEMENT

The original contributions presented in the study are included in the article/**Supplementary Material**, further inquiries can be directed to the corresponding author.

ETHICS STATEMENT

The animal study was reviewed and approved by University College Dublin Animal Research Ethics Subcommittee University College Dublin Ireland and Irish Health Products Regulatory Authority and Institutional Animal Care and Use Committee of Colorado State University (harvesting of donor cells).

AUTHOR CONTRIBUTIONS

CK participated in the study design, carried out the experimental procedures, performed the statistical analysis, and drafted the manuscript. SK prepared the MSC-secretome and MSCs. JK and LG harvested, characterized, and cultured the MSCs from donor animals. GB drafted the manuscript. NK and SP provided technical support with the synovial fluid analyses, performed the mediator and marker assays, and assisted in manuscript preparation. ML assisted with the experimental procedures, provided technical support with the synovial fluid processing and analyses, and assisted in manuscript preparation. PB, GO, and PV conceived of the study, participated in its design and coordination, and helped draft the manuscript. All authors read and approved the final manuscript.

FUNDING

The authors would like to indicate that the data presented in this manuscript are part of a larger study investigating the effects of several intra-articular therapeutics on synovial fluid inflammatory parameters and cartilage biomarkers in inflamed equine joints. That study was partly funded by the UCD Wellcome Institutional Strategic Support Fund Clinical Primer Scheme, UCD Foundation (R14799), Dutch Arthritis Association (LLP-22), and the Dutch Organization for Science, Division Applied and Engineering Sciences (Grant No. 12898).

ACKNOWLEDGMENTS

The authors would like to express their sincere gratitude to Prof. Kelly and his staff at Trinity College, Dublin, Ireland, for the use of their facilities for culturing the equine MSCs and preparing the injections. We also express our sincere gratitude to the staff and students at UCDVH and UCD Lyons Research farm for help with data collection.

SUPPLEMENTARY MATERIAL

The Supplementary Material for this article can be found online at: https://www.frontiersin.org/articles/10.3389/fvets.2022.907616/full#supplementary-material

REFERENCES

1. McIlwraith CW, Frisbie DD, Kawcak CE. The horse as a model of naturally occurring osteoarthritis. *Bone Joint Res.* (2012) 1:297–309. doi: 10.1302/2046-3758.111.2000132
2. Colbath AC, Dow SW, McIlwraith CW, Goodrich LR. Mesenchymal stem cells for treatment of musculoskeletal disease in horses: relative merits of allogeneic versus autologous stem cells. *Equine Vet J.* (2020) 52:654–63. doi: 10.1111/evj.13233
3. Colbath AC, Dow SW, Hopkins LS, Phillips JN, McIlwraith CW, Goodrich LR. Single and repeated intra-articular injections in the tarsocrural joint with allogeneic and autologous equine bone marrow-derived mesenchymal stem cells are safe, but did not reduce acute inflammation in an experimental interleukin-1beta model of synovitis. *Equine Vet J.* (2019) 52:601–12. doi: 10.1111/evj.13222
4. EMA. *First Stem Cell-Based Veterinary Medicine Recommended for Marketing Authorisation*. Available online at: https://www.ema.europa.eu/en/documents/press-release/first-stem-cell-based-veterinary-medicine-recommended-marketing-authorisation_en.pdf (accessed May 25, 2021).
5. Caplan AI, Dennis JE. Mesenchymal stem cells as trophic mediators. *J Cell Biochem.* (2006) 98:1076–84. doi: 10.1002/jcb.20886
6. Kinnaird T, Stabile E, Burnett MS, Shou M, Lee CW, Barr S, et al. Local delivery of marrow-derived stromal cells augments collateral perfusion through paracrine mechanisms. *Circulation.* (2004) 109:1543–9. doi: 10.1161/01.CIR.0000124062.31102.57
7. Ren G, Zhang L, Zhao X, Xu G, Zhang Y, Roberts AI, et al. Mesenchymal stem cell-mediated immunosuppression occurs via concerted action of chemokines and nitric oxide. *Cell Stem Cell.* (2008) 2:141–50. doi: 10.1016/j.stem.2007.11.014
8. Prockop DJ. Repair of tissues by adult stem/progenitor cells (MSCs): controversies, myths, and changing paradigms. *Mol Ther.* (2009) 17:939–46. doi: 10.1038/mt.2009.62
9. Timmers L, Lim SK, Hoefer IE, Arslan F, Lai RC, Oorschot AAM van, et al. Human mesenchymal stem cell-conditioned medium improves cardiac function following myocardial infarction. *Stem Cell Res.* (2011) 6:206–14. doi: 10.1016/j.scr.2011.01.001
10. Blanc KL, Mougiakakos D. Multipotent mesenchymal stromal cells and the innate immune system. *Nat Rev Immunol.* (2012) 12:383–96. doi: 10.1038/nri3209
11. Gnecchi M, He H, Liang OD, Melo LG, Morello F, Mu H, et al. Paracrine action accounts for marked protection of ischemic heart by Akt-modified mesenchymal stem cells. *Nat Med.* (2005) 11:367–8. doi: 10.1038/nm0405-367
12. Murphy JM, Fink DJ, Hunziker EB, Barry FP. Stem cell therapy in a caprine model of osteoarthritis. *Arthr Rheum.* (2003) 48:3464–74. doi: 10.1002/art.11365
13. Barry F, Murphy M. Mesenchymal stem cells in joint disease and repair. *Nat Rev Rheumatol.* (2013) 9:584–94. doi: 10.1038/nrrheum.2013.109
14. Prockop DJ, Oh JY. Mesenchymal stem/stromal cells (MSCs): role as guardians of inflammation. *Mol Ther.* (2012) 20:14–20. doi: 10.1038/mt.2011.211
15. Buul GM van, Villafuertes E, Bos PK, Waarsing JH, Kops N, Narcisi R, et al. Mesenchymal stem cells secrete factors that inhibit inflammatory processes in short-term osteoarthritic synovium and cartilage explant culture. *Osteoarthr Cartil.* (2012) 20:1186–96. doi: 10.1016/j.joca.2012.06.003
16. Platas J, Guillén MI, Caz MDP del, Gomar F, Mirabet V, Alcaraz MJ. Conditioned media from adipose-tissue-derived mesenchymal stem cells downregulate degradative mediators induced by interleukin-1β in osteoarthritic chondrocytes. *Mediat Inflam.* (2013) 2013:1–10. doi: 10.1155/2013/357014
17. Khatab S, van Osch G, Kops N, Bastiaansen-Jenniskens Y, Bos K, Verhaar JA, et al. Mesenchymal stem cell secretome reduces pain and prevents cartilage damage in a murine osteoarthritis model. *Eur Cells Mater.* (2018) 36:218–30. doi: 10.22203/eCM.v036a16
18. Mocchi M, Dotti S, Bue MD, Villa R, Bari E, Perteghella S, et al. Veterinary regenerative medicine for musculoskeletal disorders: can mesenchymal stem/stromal cells and their secretome be the new frontier? *Cells.* (2020) 9:1453. doi: 10.3390/cells9061453
19. Bussche L, Harman RM, Syracuse BA, Plante EL, Lu YC, Curtis TM, et al. Microencapsulated equine mesenchymal stromal cells promote cutaneous wound healing in vitro. *Stem Cell Res Ther.* (2015) 6:66. doi: 10.1186/s13287-015-0037-x
20. Marx C, Gardner S, Harman RM, de Walle GRV. The mesenchymal stromal cell secretome impairs methicillin-resistant Staphylococcus aureus biofilms via cysteine protease activity in the equine model. *Stem Cell Transl Med.* (2020) 9:746–57. doi: 10.1002/sctm.19-0333
21. Lange-Consiglio A, Rossi D, Tassan S, Perego R, Cremonesi F, Parolini O. Conditioned medium from horse amniotic membrane-derived multipotent progenitor cells: immunomodulatory activity in vitro and first clinical application in tendon and ligament injuries *in vivo*. *Stem Cells Dev.* (2013) 22:3015–24. doi: 10.1089/scd.2013.0214
22. Kearney CM, Korthagen NM, Plomp SGM, Labberté MC, Grauw JC, Weeren PR, et al. Treatment effects of intra-articular triamcinolone acetonide in an equine model of recurrent joint inflammation. *Equine Vet J.* (2021) 53:1277–86. doi: 10.1111/evj.13396
23. Kisiday JD, Hale BW, Almodovar JL, Lee CM, Kipper MJ, McIlwraith CW, et al. Expansion of mesenchymal stem cells on fibrinogen-rich protein surfaces derived from blood plasma. *J Tissue Eng Regen M.* (2011) 5:600–11. doi: 10.1002/term.352
24. Guest DJ, Dudhia J, Smith RKW, Roberts SJ, Conzemius M, Innes JF, et al. Position statement: minimal criteria for reporting veterinary and animal medicine research for mesenchymal stromal/stem cells in orthopedic applications. *Front Vet Sci.* (2022) 9:817041. doi: 10.3389/fvets.2022.817041
25. Kisiday JD, Goodrich LR, McIlwraith CW, Frisbie DD. Effects of equine bone marrow aspirate volume on isolation, proliferation, and differentiation potential of mesenchymal stem cells. *Am J Vet Res.* (2013) 74:801–7. doi: 10.2460/ajvr.74.5.801
26. Kisiday JD, Colbath AC, Tangtrongsup S. Effect of culture duration on chondrogenic preconditioning of equine bone marrow mesenchymal stem cells in self-assembling peptide hydrogel. *J Orthop Res.* (2019) 37:1368–75. doi: 10.1002/jor.24123
27. Kisiday JD, Kopesky PW, Evans CH, Grodzinsky AJ, McIlwraith CW, Frisbie DD. Evaluation of adult equine bone marrow- and adipose-derived progenitor cell chondrogenesis in hydrogel cultures. *J Orthopaed Res.* (2008) 26:322–31. doi: 10.1002/jor.20508
28. Colbath AC, Dow SW, Phillips JN, McIlwraith CW, Goodrich LR. Autologous and allogeneic equine mesenchymal stem cells exhibit equivalent immunomodulatory properties in vitro. *Stem Cells Dev.* (2017) 26:503–11. doi: 10.1089/scd.2016.0266
29. Owens JG, Kamerling SG, Stanton SR, Keowen ML, Prescott-Mathews JS. Effects of pretreatment with ketoprofen and phenylbutazone on experimentally induced synovitis in horses. *Am J Vet Res.* (1996) 57:866–74.
30. de Grauw JC, van de Lest CHA, van Weeren PR. A targeted lipidomics approach to the study of eicosanoid release in synovial joints. *Arthr Res Ther.* (2011) 13:R123. doi: 10.1186/ar3427
31. Grauw JC, Lest CHA, Brama PAJ, Rambags BPB, Weeren PR. *In vivo* effects of meloxicam on inflammatory mediators, MMP activity and cartilage biomarkers in equine joints with acute synovitis. *Equine Vet J.* (2010) 41:693–9. doi: 10.2746/042516409X436286
32. Cokelaere SM, Plomp SGM, Boef E de, Leeuw M de, Bool S, Lest CHA van de, et al. Sustained intra-articular release of celecoxib in an equine repeated LPS synovitis model. *Eur J Pharm Biopharm.* (2018) 128:327–36. doi: 10.1016/j.ejpb.2018.05.001
33. de Grauw JC, Brama PA, Wiemer P, Brommer H, van de Lest CH, van Weeren PR. Cartilage-derived biomarkers and lipid mediators of inflammation in horses with osteochondritis dissecans of the distal intermediate ridge of the tibia. *Am J Vet Res.* (2006) 67:1156–62. doi: 10.2460/ajvr.67.7.1156
34. de Grauw JC, van Loon JPAM, van de Lest CHA, Brunott A, Weeren PRV. *In vivo* effects of phenylbutazone on inflammation and cartilage-derived biomarkers in equine joints with acute synovitis. *Vet J.* (2014) 201:51–6. doi: 10.1016/j.tvjl.2014.03.030
35. Sladek S, Kearney C, Crean D, Brama PAJ, Tajber L, Fawcett K, et al. Intra-articular delivery of a nanocomplex comprising salmon calcitonin, hyaluronic acid, and chitosan using an equine model of joint inflammation. *Drug Deliv Trans Res.* (2018) 8:1421–35. doi: 10.1007/s13346-018-0557-x

36. Toh WS, Foldager CB, Pei M, Hui JHP. Advances in mesenchymal stem cell-based strategies for cartilage repair and regeneration. *Stem Cell Rev Rep.* (2014) 10:686–96. doi: 10.1007/s12015-014-9526-z
37. Zhang J, Huang X, Wang H, Liu X, Zhang T, Wang Y, et al. The challenges and promises of allogeneic mesenchymal stem cells for use as a cell-based therapy. *Stem Cell Res Ther.* (2015) 6:234. doi: 10.1186/s13287-015-0240-9
38. Frisbie DD, Kawcak CE, Trotter GW, Powers BE, Walton RM, McIlwraith CW. Effects of triamcinolone acetonide on an in vivo equine osteochondral fragment exercise model. *Equine Vet J.* (1997) 29:349–59. doi: 10.1111/j.2042-3306.1997.tb03138.x
39. Celeste C, Ionescu M, Poole AR, Laverty S. Repeated intraarticular injections of triamcinolone acetonide alter cartilage matrix metabolism measured by biomarkers in synovial fluid. *J Orthop Res.* (2005) 23:602–10. doi: 10.1016/j.orthres.2004.10.003
40. McIlwraith CW. Use of synovial fluid and serum biomarkers in equine bone and joint disease: a review. *Equine Vet J.* (2005) 37:473–82. doi: 10.2746/042516405774480102
41. Frisbie DD, Kisiday JD, Kawcak CE, Werpy NM, McIlwraith CW. Evaluation of adipose-derived stromal vascular fraction or bone marrow-derived mesenchymal stem cells for treatment of osteoarthritis. *J Orthop Res.* (2009) 27:1675–80. doi: 10.1002/jor.20933
42. Ferris DJ, Frisbie DD, Kisiday JD, McIlwraith CW, Hague BA, Major MD, et al. Clinical outcome after intra-articular administration of bone marrow derived mesenchymal stem cells in 33 horses with stifle injury. *Vet Surg.* (2014) 43:255–65. doi: 10.1111/j.1532-950X.2014.12100.x
43. Loon VJFV, Scheffer CJW, Genn HJ, Hoogendoorn AC, Greve JW. Clinical follow-up of horses treated with allogeneic equine mesenchymal stem cells derived from umbilical cord blood for different tendon and ligament disorders. *Vet Quart.* (2014) 34:92–7. doi: 10.1080/01652176.2014.949390
44. Broeckx SY, Seys B, Suls M, Vandenberghe A, Mariën T, Adriaensen E, et al. Equine allogeneic chondrogenic induced mesenchymal stem cells are an effective treatment for degenerative joint disease in horses. *Stem Cells Dev.* (2019) 28:410–22. doi: 10.1089/scd.2018.0061
45. Colbath AC, Dow SW, Hopkins LS, Phillips JN, McIlwraith CW, Goodrich LR. Allogeneic vs. autologous intra-articular mesenchymal stem cell injection within normal horses: clinical and cytological comparisons suggest safety. *Equine Vet J.* (2020) 52:144–51. doi: 10.1111/evj.13136
46. Williams LB, Koenig JB, Black B, Gibson TWG, Sharif S, Koch TG. Equine allogeneic umbilical cord blood derived mesenchymal stromal cells reduce synovial fluid nucleated cell count and induce mild self-limiting inflammation when evaluated in an LPS induced synovitis model. *Equine Vet J.* (2016) 48:619–25. doi: 10.1111/evj.12477
47. Barrachina L, Remacha AR, Romero A, Vitoria A, Albareda J, Prades M, et al. Assessment of effectiveness and safety of repeat administration of proinflammatory primed allogeneic mesenchymal stem cells in an equine model of chemically induced osteoarthritis. *BMC Vet Res.* (2018) 14:241. doi: 10.1186/s12917-018-1556-3
48. Carrade DD, Lame MW, Kent MS, Clark KC, Walker NJ, Borjesson DL. Comparative analysis of the immunomodulatory properties of equine adult-derived mesenchymal stem cells. *Cell Med.* (2012) 4:1–11. doi: 10.3727/215517912X647217
49. Moran CJ, Ramesh A, Brama PAJ, O'Byrne JM, O'Brien FJ, Levingstone TJ. The benefits and limitations of animal models for translational research in cartilage repair. *J Exp Orthop.* (2016) 3:1–12. doi: 10.1186/s40634-015-0037-x
50. Laverty S, Sandy JD, Celeste C, Vachon P, Marier JF, Plaas AHK. Synovial fluid levels and serum pharmacokinetics in a large animal model following treatment with oral glucosamine at clinically relevant doses. *Arthr Rheum.* (2005) 52:181–91. doi: 10.1002/art.20762
51. de Grauw JC, de Lest CHV. Inflammatory mediators and cartilage biomarkers in synovial fluid after a single inflammatory insult: a longitudinal experimental study. *Arthr Res Ther.* (2009) 11:R35. doi: 10.1186/ar2640
52. Boom RV den, Lest CHA van de, Bull S, Brama RAJ, Weeren PRV, Barneveld A. Influence of repeated arthrocentesis and exercise on synovial fluid concentrations of nitric oxide, prostaglandin E2 and glycosaminoglycans in healthy equine joints. *Equine Vet J.* (2005) 37:250–6. doi: 10.2746/0425164054530740
53. Orth P, Zurakowski D, Alini M, Cucchiarini M, Madry H. Reduction of sample size requirements by bilateral versus unilateral research designs in animal models for cartilage tissue engineering. *Tissue Eng Part C Methods.* (2013) 19:885–91. doi: 10.1089/ten.tec.2012.0699
54. Dyson S. Can lameness be graded reliably? *Equine Vet J.* (2011) 43:379–82. doi: 10.1111/j.2042-3306.2011.00391.x
55. Palmer JL, Bertone AL, Malemud CJ, Mansour J. Biochemical and biomechanical alterations in equine articular cartilage following an experimentally-induced synovitis. *Osteoarthr Cartil.* (1996) 4:127–37. doi: 10.1016/S1063-4584(05)80321-8
56. Schu S, Nosov M, O'Flynn L, Shaw G, Treacy O, Barry F, et al. Immunogenicity of allogeneic mesenchymal stem cells. *J Cell Mol Med.* (2012) 16:2094–103. doi: 10.1111/j.1582-4934.2011.01509.x
57. Barrachina L, Remacha AR, Romero A, Vázquez FJ, Albareda J, Prades M, et al. Priming equine bone marrow-derived mesenchymal stem cells with proinflammatory cytokines: implications in immunomodulation–immunogenicity balance, cell viability, and differentiation potential. *Stem Cells Dev.* (2017) 26:15–24. doi: 10.1089/scd.2016.0209
58. Rani S, Ryan AE, Griffin MD, Ritter T. Mesenchymal stem cell-derived extracellular vesicles: toward cell-free therapeutic applications. *Mol Ther.* (2015) 23:812–23. doi: 10.1038/mt.2015.44
59. Hill JA, Cassano JM, Goodale MB, Fortier LA. Antigenicity of mesenchymal stem cells in an inflamed joint environment. *Am J Vet Res.* (2017) 78:867–75. doi: 10.2460/ajvr.78.7.867
60. Ragni E, Orfei CP, Luca PD, Mondadori C, Viganò M, Colombini A, et al. Inflammatory priming enhances mesenchymal stromal cell secretome potential as a clinical product for regenerative medicine approaches through secreted factors and EV-miRNAs: the example of joint disease. *Stem Cell Res Ther.* (2020) 11:165. doi: 10.1186/s13287-020-01677-9
61. Boom R, Brama PAJ, Kiers GH, DeGroot J, Barneveld A, Weeren PR. The influence of repeated arthrocentesis and exercise on matrix metalloproteinase and tumour necrosis factor a activities in normal equine joints. *Equine Vet J.* (2004) 36:155–9. doi: 10.2746/0425164044868602
62. Tulamo RM, Bramlage LR, Gabel AA. Sequential clinical and synovial fluid changes associated with acute infectious arthritis in the horse. *Equine Vet J.* (1989) 21:325–31. doi: 10.1111/j.2042-3306.1989.tb02681.x
63. Lucia JL, Coverdale JA, Arnold CE, Winsco KN. Influence of an intra-articular lipopolysaccharide challenge on markers of inflammation and cartilage metabolism in young horses. *J Anim Sci.* (2013) 91:2693–9. doi: 10.2527/jas.2012-5981
64. Wang G, Li X, Jiang R, Li Y, Fan X, Zheng Y, et al. Changes in synovial fluid inflammatory mediators and cartilage biomarkers after experimental acute equine synovitis. *Bull Vet Inst Pulawy.* (2015) 59:129–34. doi: 10.1515/bvip-2015-0019

Conflict of Interest: The authors declare that the research was conducted in the absence of any commercial or financial relationships that could be construed as a potential conflict of interest.

frontiers | Frontiers in Veterinary Science

TYPE Original Research
PUBLISHED 02 August 2022
DOI 10.3389/fvets.2022.938706

OPEN ACCESS

EDITED BY
Scott J. Roberts,
Royal Veterinary College (RVC),
United Kingdom

REVIEWED BY
Evelien De Bakker,
Ghent University, Belgium
Matthew D. Johnson,
University of Florida, United States

*CORRESPONDENCE
Alyssa M. Matos Cruz
alyssamatos24@gmail.com

SPECIALTY SECTION
This article was submitted to Veterinary Regenerative Medicine, a section of the journal Frontiers in Veterinary Science

RECEIVED 07 May 2022
ACCEPTED 12 July 2022
PUBLISHED 02 August 2022

CITATION
Matos Cruz AM and Mason DR (2022) Owner assessed outcomes following elbow arthroscopy with or without platelet rich plasma for fragmented medial coronoid process. *Front. Vet. Sci.* 9:938706. doi: 10.3389/fvets.2022.938706

Owner assessed outcomes following elbow arthroscopy with or without platelet rich plasma for fragmented medial coronoid process

Alyssa M. Matos Cruz[1]* and David R. Mason[2]

[1]MedVet Columbus, Worthington, OH, United States, [2]Las Vegas Veterinary Specialty Center, Las Vegas, NV, United States

Objective: Document the outcomes of bilateral arthroscopic subtotal coronoidectomy for the fragmented medial coronoid process, quantify persistent lameness that required additional treatment (PRP), and document the outcomes of dogs that followed up with PRP injections.

Study design: Retrospective study.

Sample population: Overall, 115 dogs underwent arthroscopy alone and 31 received PRP at least 6 weeks after arthroscopy. The owner's response rate was ~50% (73 dogs).

Methods: Collected data included signalment, unilateral or bilateral clinical signs, intra-articular chondroprotective injection during the procedure, if PRP intra-articular injection was received postoperatively, and if it was received, the time from the initial surgery to administration was recorded. Outcomes were assessed *via* standardized owner questionnaires using the Liverpool Osteoarthritis in Dogs (LOAD) score, the Canine Brief Pain Inventory (CBPI) score, and the overall quality of life (QOL) assessment.

Results: Approximately 20% of the patients received PRP post-operatively due to persistent lameness following surgery. Similar pain scores were found between the two groups with an average of 11–13 LOAD score, 13–15 CBPI score, and good quality of life. Older animals at the time of surgery and those that received pain-relieving medications after the procedure were more painful and affected their functional outcome. PRP as an adjunctive therapy achieved a perceived good to excellent quality of life in ~90% of pets in this population.

Conclusion: Arthroscopy and subtotal coronoidectomy followed by PRP, if needed, seemed to decrease pain, and improve lameness in the long term.

Clinical significance: PRP should be considered as adjunctive therapy in dogs with the limited response to arthroscopy alone.

KEYWORDS

platelet rich plasma (PRP), elbow dysplasia, fragmented medial coronoid, arthroscopy, orthopedics, regenerative medicine

Introduction

Elbow dysplasia affects many large breed dogs worldwide and is considered an extremely debilitating disease due to its natural progression. The most common etiology of elbow arthrosis is the fragmented medial coronoid process (FMCP), after the cartilaginous process ossifies and the deeper layer of chondrocytes undergo malacia (1). One of the surgical treatments involve arthroscopic fragment removal and osteochondral debridement. However, this does not always eliminate the clinical signs related to pain and lameness, especially, in the older dogs (1). This is partly because cartilage has a poor-regenerative capacity. Platelet-rich plasma (PRP) is being used in human and veterinary medicine for many disease processes including joint disease, due to its growth factors and anti-inflammatory properties (2, 3). Intra-articular use of platelet-rich plasma has been a topic of investigation and debate due to its anabolic and anti-catabolic effects aiming to increase cartilage regenerative capacity and reduction of inflammatory mediators (2, 3). Fortier et al. reviewed *in vitro* laboratory investigations, preclinical animal model studies, and human clinical studies which collectively support the use of PRP for cartilage injuries and joint pain (4).

Platelet-rich plasma injections have been used in human medicine for osteoarthritis and treatment of inflammatory orthopedic conditions without a consensus of their efficacy (5–10). A meta-analysis of human studies did not find PRP intraarticular injections an effective treatment for osteoarthritis compared to hyaluronic acid (5). However, in another set of meta-analyses of the randomized controlled trials including over one thousand participants, intra-articular injections of PRP were reported to decrease pain and improve function levels up to 12 months when compared to placebo, hyaluronic acid, and corticosteroid injections (6–10).

In veterinary medicine, platelet-rich plasma has been used and reported as a treatment option for a variety of disease processes with favorable outcomes and no major complications (11–19). Platelet-rich plasma has been described as a treatment for supraspinatus tendinopathy (11), early partial cranial cruciate ligament tears (12), bilateral hip osteoarthritis (13), large cutaneous wounds (14), aural hematomas (15), lumbosacral stenosis (16), stifle osteoarthritis secondary to medically managed chronic cranial cruciate ligament tears (17), and for bone healing in traumatic fractures (18) and also high-tibial osteotomy (19). In these cases, all had favorable outcomes, except for use in high-tibial osteotomies in which there was no significant difference between control and experimental groups. Considering its low-complication risk and ease of collection and administration, PRP can have potential value as adjunctive therapy for cartilage defects and promoter of healing in medial compartment disease in dogs. To the author's knowledge, there have been no studies on the use of PRP for medial compartment disease after subtotal coronoidectomy and osteochondral debridement. Assessing the potential clinical benefits of PRP as adjunctive therapy for FMCP is paramount to improve the quality of life of pets and owner satisfaction after elbow arthroscopy in pets with this debilitating condition.

Our objectives were to document the outcome of bilateral arthroscopic subtotal coronoidectomy for the bilateral fragmented medial coronoid process and to quantify persistent lameness that required additional treatment. The second objective was to document the outcomes of the dogs that received platelet-rich plasma injection when refractory to surgical treatment alone. We hypothesized that overall dogs would have a good quality of life, good function, and low-pain levels with surgery alone or with adjunctive platelet-rich plasma when surgery alone did not achieve the desired clinical outcome.

Materials and methods

Inclusion criteria

The database of the Las Vegas Veterinary Specialty Center was reviewed for dogs that underwent elbow arthroscopy between 1 March 2013 and 30 March 2021, performed by the same board-certified surgeon (DM). Only dogs diagnosed with a bilateral fragmented medial coronoid process *via* arthroscopy that underwent a subtotal coronoidectomy were evaluated in this study. Dogs were excluded if they underwent arthroscopic surgery twice, received PRP during the procedure, or had other elbow or shoulder joint-related comorbidities (osteochondrosis dissecans, ununited anconeal process, and radio-ulnar incongruency). A minimum of 6 weeks past the surgery date was required to be included in the study.

Data collection

Collected data included breed, weight, sex, age at the time of surgery, unilateral or bilateral clinical signs, intra-articular chondroprotective injection during the procedure (hyaluronic acid, HA, and polyglutamic acid, PGA), and if platelet-rich plasma intra-articular (IA) injection was received postoperatively, and the time from the initial surgery to the administration of platelet-rich plasma injection. The PRP injections were offered to clients that were still showing lameness at least 6 weeks after the procedure or lack of improvement as perceived by the owners.

Outcome assessment

The outcomes were assessed *via* standardized owner questionnaires using the Liverpool Osteoarthritis in Dogs

(LOADs) score, the Canine Brief Pain Inventory (CBPI) score, and the overall quality of life (QOL) assessment. The medications the pets were receiving at the time of the questionnaire were also recorded. Medications were categorized as an anti-inflammatory (prednisone and non-steroidal anti-inflammatory, NSAID), joint supplements, and miscellaneous pain medications (gabapentin, amantadine, and tramadol).

Statistical methods

The response variables were the use of PRP (binary, 01), and the outcome of LOAD (continuous), CBPI (continuous), and QOL (ordinal). The factors that were described and tested for association with PRP were age, weight, number of sides clinically affected (unilateral vs. bilateral), and gender. Descriptive data were reported by the means of mean, SD, median, and 25th and 75th quartiles. Analysis was by multivariate logistic regression. The factors that were tested for association with the outcomes were PRP, gender, age, number of sides clinically affected, IA injection, and use of NSAID, supplements, or other pain medications. Analysis was by multiple linear regression. Multicollinearity was tested by means of variance inflation factor; <2.5 was considered acceptable. Linearity was tested by the means of residual plots. The *P*-values were reported.

Results

There were 182 dogs diagnosed with a bilateral fragmented medial coronoid process *via* arthroscopy that underwent a subtotal coronoidectomy. In total, thirty-six dogs were excluded from the data analysis: two underwent elbow arthroscopy twice, two passed away from unrelated causes prior to completing the recovery period, five had unilateral FMCP, eight received PRP during the procedure, and nineteen with elbow or shoulder joint-related comorbidities (osteochondrosis dissecans, ununited anconeal process, and radio-ulnar incongruency).

Of the 146 dogs that met the inclusion criteria, 115 underwent surgery alone (SXA group). In total, thirty-one patients received PRP (PRP group) based on the physical examination and owner assessment of surgery success past the recovery period. In total, 73 owners answered the questionnaires (50% response rate). From the SXA group, 53 answered the questionnaire (46%). From the PRP group, 20 answered the questionnaire (65%). The questionnaires were answered following a minimum of 6 weeks up to 5 years postoperatively, which is the time PRP treatment became available to our population. The mean follow-up time for SAX was 1,220 days, for PRP was 1,269 days, with a total mean follow-up time of 1,234 days (about 3 and a half years) from the initial arthroscopic procedure day to the date the questionnaire was received.

The mean and median weight was 34 kg, mean age was 26 months (SD, 22) with a median of 18 months (about 1 and a half years), and the mean number of days until PRP was administered was 247 days (SD 355) with a median of 106. Dog's ages ranged from 5 to 92 months (7.5 years old). There was a total of 61 females, 11 intact and 50 spayed, and 85 males, 22 intact and 63 neutered. Most dogs were presented with unilateral clinical signs (104) and the rest presented with bilateral lameness or pain (41). Most, 128 dogs, received an intraarticular injection with hyaluronic acid gel perioperatively. At the time of the survey, 10 dogs were receiving anti-inflammatories (non-steroidal anti-inflammatories or prednisone), 17 were receiving supplements (including glycosaminoglycans, chondroitin, fish oil, etc.), and 9 were receiving other types of pain medications (including gabapentin, amantadine, or/and tramadol).

The overall (both groups) median and mean LOAD and CBPI scores, and QOL obtained from the questionnaires are summarized in Table 1. When the SXA group was analyzed separately from the PRP group the data was the following: SXA median LOAD was 11 (4–19), CBPI 3 (0–13), and QOL good (3). The mean LOAD was 13 (SD 9), CBPI was 13 (SD 23), and QOL was good (3, SD 1) (Table 2). For the PRP group, the median LOAD was 11 (4–19), CBPI 3 (0–13), and QOL good (3). The mean LOAD was 13 (SD 9), CBPI was 13 (SD 23), and QOL was good (3, SD 1) (Table 3). A summary of results when the overall patient results were evaluated for a threshold of 20 for LOAD, 30 for CBPI and good or better quality of life is shown in Table 4, which was 81%, 85%, and 95% of patients, respectively.

The use of PRP on refractory cases was not associated with any factor (age, weight, if one or both elbows were clinical at the time of initial presentation, gender, or neuter status). LOAD scores were influenced by the use of anti-inflammatories and age. LOAD was 11 units higher for those using anti-inflammatories, and for each month increase in age, LOAD increased by 0.11. Similarly, CBPI was influenced by the use of pain medications and age. CBPI increased by 0.5 with each month of age and if miscellaneous pain medications were given, CBPI was 18.2 higher. The QOL decreased with age and if other pain medications were given (Table 5). Adjunctive treatment with PRP injections showed no statistical significance for outcomes of LOAD and QOL, but seemed to be significantly associated with CBPI, *P*-value of 0.03 (Table 6).

Discussion

Based on our data collection, ∼20% (31/146) of the owners whose pets underwent the arthroscopic procedures at our hospital were unhappy with surgery results (persistent lameness) and received PRP at least 6 weeks postoperatively but mostly after 3 months to a year postsurgery. The overall outcome of both groups when analyzed together and separately was favorable, with an average of 11–13 of a total of 52 LOAD score,

TABLE 1 Summary of all the cases.

All data $n = 146$	Kg	Age (months)	LOAD	CBPI	QOL
Mean	34.7	26.1	13.2	14.9	3.2
Median	34.0	18.0	11.0	4.0	3.0
SD	12.3	22.6	8.9	23.1	1.0
25th Percentile	27.0	10.0	6.5	0.0	3.0
75th Percentile	41.0	36.0	18.5	17.0	4.0

TABLE 2 Summary for arthroscopy alone (SXA).

PRP= 0	Kg	Age (months)_	LOAD	CBPI	QOL
Mean	34.0	26.9	12.6	13.0	3.2
Median	33.0	18.0	11.0	3.0	3.0
SD	10.9	22.9	9.4	23.4	1.0
25th Percentile	27.0	11.0	4.0	0.0	3.0
75th Percentile	40.0	36.0	18.5	13.5	4.0

and of 13–15 of a possible 100 total CBPI score, and good quality of life. No statistical difference in outcome was found between the two groups, except for CBPI. However, the significance is questionable given the strong selection bias for the patients receiving PRP.

As depicted in Table 4, a total of 95% of all the owners considered their dogs to have a good, very good, or excellent quality of life. Approximately 81% had a LOAD score <20 which is equivalent to mild-to-moderate osteoarthritic changes based on the LOAD guidelines, and 85% had a CBPI <30 which rates the severity of their dog's pain and the degree to which that pain interferes with function on a scale of 1–10 for 10 questions (maximum score of 100). With that in mind, ∼87% of our population benefited from surgery and PRP injections when needed.

Our results also showed that older animals at the time of surgery seemed to have worse outcomes and those that were maintained on pain-relieving medications for long term were also considered to be more painful and with negative effects on their functional long-term outcome. This is most likely due to the progression of joint arthrosis and arthritis seen with the medial compartment disease. It is possible that when left untreated these changes might occur more rapidly, suggesting that surgery should be pursued early on if FMCP is suspected as reported previously (20–22). The anti-inflammatory use factor is not surprising as it is widely preferred as the first line of treatment for pain in the orthopedic disease.

Our 20% unsatisfaction rate after arthroscopic evaluation and subtotal coronoidectomy, was similar to that previously reported by Fitzpatrick et al. (20). In their study, ∼45% of owners were satisfied with results at 5 weeks postoperatively, and 96% at 24 weeks (about 5 and a half months). In our study, the difference in lameness from 6 weeks postoperatively (initial recheck) vs. long term was not able to be accurately measured and evaluated because of the lack of complete clinical records or lack of in person rechecks. Owner phone updates were requested in many of our cases and only followed up with a minority if there was a lack of improvement. When long-term outcome (1–6 years postoperatively) was evaluated, the percentage of satisfaction and sound dogs was similar to our results at 80% (23).

Previous studies using owner-assessed outcomes after treatment of a fragmented medial coronoid process seemed to be in accordance with our results. In a small study of Bernese Mountain dogs, although there was decreased range of motion and increased radiographic evidence of osteoarthritis, all the owners reported improved lameness and function (24). In another prospective study, although only some of the dogs were completely sound, all the owners were satisfied with surgery outcomes at 6–24 months (about 2 years) postoperatively (25). When looking at the more objective measurements using kinematic analysis up to 180 days (about 6 months) post arthroscopy, a slight improvement was noted after surgery (26). It has been reported that function improves regardless of incongruency and cartilage erosion present, although the improvement was more significant in the latter, suggesting addressing incongruency might not be as beneficial long term which is beyond the scope of this study (27, 28).

Although arthroscopy and subtotal coronoidectomy generally is the treatment of choice for specialty care regarding medial compartment disease, there are multiple studies that did not find an appreciable long-term difference when compared

TABLE 3 Summary of patients who received PRP (PRP).

PRP= 1	Kg	Age (months)	Days from surgery to PRP treatment	LOAD	CBPI	QOL
Mean	37.5	23.4	246.7	14.8	19.8	3.0
Median	35.0	15.0	106.0	13.5	14.0	3.0
SD	16.4	21.6	355.7	7.4	22.0	0.8
25th Percentile	27.0	9.0	67.0	8.0	5.8	2.3
75th Percentile	45.0	33.0	168.0	21.0	20.8	3.8

with the medically managed patients at 12 months (1 year) and 56 months (4.6 years), respectively (29, 30). Moreover, recent studies have evaluated the elbow joint objectively and found that there are calcified bodies remaining or formed after arthroscopy. In one study looking at recurrent lameness with computed tomography (CT) or arthroscopic re-evaluation, it was reported that after a mean of 3 years progressive osteoarthritis and cartilage damage was seen in the form of loose scar tissue or calcified bodies (31). Of 29 dogs evaluated, 12 had calcified bodies, and 14 had scar tissue formation suspected secondary to the first arthroscopic procedure (31). In contrast, Renner et al. (32) evaluated immediate or short-term postoperative CT scans for bony remnants and found that 73% of cases had remaining lesions, mostly at the radial incisure. That study reported that only 5% of radial incisure lesions were removed and 72% of apical lesions were removed completely. Different surgeons, techniques, and different lesion locations could pose another variable for outcomes. Although the specific location of lesions was not specified, the technique and surgeon variability were controlled in this study. If there are secondary changes or loose fragments because of the surgical procedure as implied in the mentioned study, it might be worth considering anti-inflammatory and cartilage effects of PRP at the time of surgery instead of only in a selected number of cases.

Due to its retrospective nature and subjective measurements, this study has several limitations. The timeframe and follow-up period varied between the two groups, preventing direct comparisons. The PRP group lacks a baseline score or objective evaluation of joints to evaluate significant improvement before and after additional treatment, and the source of pain and recurrent lameness. There is also a financial burden with additional therapy that is not accounted for when evaluating and assuming success on those that did not follow-up or did not receive PRP. Although most owners were satisfied with arthroscopy regardless of PRP administration, the low-response rate (50%), prevents the ability to draw conclusions. Establishing accurate conclusions on surgical outcomes based on owner assessment of pain levels in dogs is difficult. Many subjective factors can influence owner satisfaction such as activity level, expense, and client–staff interactions. Objective data, such as force plate analysis and kinematic gait evaluations, and a prospective controlled study design could strengthen our conclusions.

TABLE 4 Overall outcomes summary.

	QOL good, very good, excellent	LOAD < 20	CBPI < 30
SXA (53)	50	44	46
PRP (20)	19	15	16
Total (73)	69	59	62
Total percentage	95%	81%	85%

TABLE 5 Regression analysis summary.

	LOAD	CBPI	QOL
Age (months)	0.11	0.53	−0.02
NSAID	11.06	N/A*	N/A*
Miscellaneous pain medications	N/A*	18.20	−0.69

*N/A when *P*-value was >0.1 or variance inflation factor >2.5.

Overall, our results showed long-term benefit to dogs with medial compartment disease due to FMCP with arthroscopic subtotal coronoidectomy, subchondral debridement, and PRP when used as an adjunctive therapy. Not all the dogs needed PRP for successful outcomes but it seems to help the 20% of the population where surgery alone is not as effective. When surgery was not successful according to owners, PRP seemed to improve the degree of lameness long term as dogs were improved at recheck and did not need further rounds of the PRP injections. Owners reported low pain levels as described by LOAD and CBPI scores, and good quality of life. To date, there are no clinical studies looking at PRP for elbow joint pain or disease. Approximately 81–95% of our population post surgery with or without PRP injections had a good function and low-pain levels.

This percentage might be different given the limitation of lack of owner response and recheck timeframe. For the minority of cases that received PRP after 6 weeks prior to a full recovery (∼3–4 months), an argument can be made that they might

TABLE 6 Significance of PRP on the outcome (univariate analysis).

Outcome	*P*-value
LOAD	0.20
CBPI	0.03
QOL	0.1

have had a full recovery without the need for PRP treatment. At the time of the study, further rounds of PRP were being offered to those patients that remained lame. It would have been helpful to ask the owners if they would have or would pursue PRP based on their pet's lameness as some owners might have several reasons unrelated to the clinical signs for not following up with additional therapy, including financial, lifestyle, or other personal reasons.

Platelet-rich plasma therapy should be considered as adjunctive therapy for those non-responsive or with a limited response to arthroscopy because of their growth factors and anti-inflammatory properties. However, further investigation on PRP therapy in dogs, and its effects on cartilage repair are necessary to make definitive treatment plans in the future.

Data availability statement

The original contributions presented in the study are included in the article/supplementary material, further inquiries can be directed to the corresponding author.

Author contributions

All authors listed have made a substantial, direct, and intellectual contribution to the work and approved it for publication.

Acknowledgments

We acknowledge the contributions of Hauptman J.G., for his work on the statistics and thank him for his efforts toward this work.

Conflict of interest

The authors declare that the research was conducted in the absence of any commercial or financial relationships that could be construed as a potential conflict of interest.

Publisher's note

References

1. Kirberger RM, Fourie SL. Elbow dysplasia in the dog: pathophysiology, diagnosis, and control: review article. *J S Afr Vet Assoc.* (1998) 69:43–54. doi: 10.4102/jsava.v69i2.814

2. Mascarenhas R, Saltzman B, Fortier L, Cole B. Role of platelet-rich plasma in articular cartilage injury and disease. *J Knee Surg.* (2014) 28:003–10. doi: 10.1055/s-0034-1384672

3. Kennedy MI, Whitney K, Evans T, LaPrade RF. Platelet-rich plasma and cartilage repair. *Curr Rev Musculoskelet Med.* (2018) 11:573–82. doi: 10.1007/s12178-018-9516-x

4. Fortier LA, Hackett CH, Cole BJ. The effects of platelet-rich plasma on cartilage: basic science and clinical application. *Oper Tech Sports Med.* (2011) 19:154–9. doi: 10.1053/j.otsm.2011.03.004

5. Zhang H, Wang C, Li H, Huang Y, Li Z. Intra-articular platelet-rich plasma versus hyaluronic acid in the treatment of knee osteoarthritis: a meta-analysis. *Drug Des Develop Therapy.* (2018) 12:445–53. doi: 10.2147/DDDT.S156724

6. Shen L, Yuan T, Chen S, Xie X, Zhang C. The temporal effect of platelet-rich plasma on pain and physical function in the treatment of knee osteoarthritis: systematic review and meta-analysis of randomized controlled trials. *J Orthopaed Surg Res.* (2017) 12:1–12. doi: 10.1186/s13018-017-0521-3

7. El-beltagy AM, Zakaria ZM, Ibrahim MA-S. Intra-articular injections of platelet-rich plasma versus hyaluronic acid in treatment of knee osteoarthritis (systematic review and meta-analysis). *QJM Int J Med.* (2021) 114:hcab104-014. doi: 10.1093/qjmed/hcab104.014

8. Belk JW, Kraeutler MJ, Houck DA, Goodrich JA, Dragoo JL, McCarty EC. Platelet-rich plasma versus hyaluronic acid for knee osteoarthritis: a systematic review and meta-analysis of randomized controlled trials. *Am J Sports Med.* (2021) 49:249–60. doi: 10.1177/0363546520909397

9. Niroomand Sadabad H, Behzadifar M, Arasteh F, Behzadifar M, Dehghan HR. Efficacy of platelet-rich plasma versus hyaluronic acid for treatment of knee osteoarthritis: a systematic review and meta-analysis. *Elect Phys.* (2016) 8:2115–22. doi: 10.19082/2115

10. Tang JZ, Nie MJ, Zhao JZ, Zhang GC, Zhang Q, Wang B. Platelet-rich plasma versus hyaluronic acid in the treatment of knee osteoarthritis: a meta-analysis. *J Orthopaed Surg Res.* (2020) 15:1–15. doi: 10.1186/s13018-020-01919-9

11. Ho LK, Baltzer WI, Nemanic S, Stieger-Vanegas SM. Single ultrasound-guided platelet-rich plasma injection for treatment of supraspinatus tendinopathy in dogs. *Can Vet J La Revue Veterinaire Canadienne.* (2015) 56:845-849.

12. Canapp SO, Leasure CS, Cox C, Ibrahim V, Carr BJ. Partial cranial cruciate ligament tears treated with stem cell and platelet-rich plasma combination therapy in 36 dogs: a retrospective study. *Front Vet Sci.* (2016) 3:112. doi: 10.3389/fvets.2016.00112

13. Alves JC, Santos A, Jorge P. Platelet-rich plasma therapy in dogs with bilateral hip osteoarthritis. *BMC Vet Res.* (2021) 17:1–11. doi: 10.1186/s12917-021-02913-x

14. Iacopetti I, Patruno M, Melotti L, Martinello T, Bedin S, Badon T, et al. Autologous platelet-rich plasma enhances the healing of large cutaneous wounds in dogs. *Front Vet Sci.* (2020) 7:575449. doi: 10.3389/fvets.2020.575449

15. Perego R, Spada E, Moneta E, Baggiani L, Proverbio D. Use of autologous leucocyte-and platelet-rich plasma (L-PRP) in the treatment of aural hematoma in dogs. *Vet Sci.* (2021) 8:172. doi: 10.3390/vetsci8090172

16. Hernández-Guerra ÁM, Carrillo JM, Sopena JJ, Vilar JM, Peláez P, Cuervo B, et al. Platelet-rich plasma for the treatment of degenerative lumbosacral stenosis: a study with retired working dogs. *Animals.* (2021) 11:2965. doi: 10.3390/ani11102965

17. Venator K, Frye CW, Gamble L-J, Wakshlag JJ. Assessment of a single intra-articular stifle injection of pure platelet rich plasma on symmetry indices in dogs with unilateral or bilateral stifle osteoarthritis from long-term medically managed cranial cruciate ligament disease. *Vet Med Res Rep.* (2020) 11:31–8. doi: 10.2147/VMRR.S238598

18. López S, Vilar JM, Sopena JJ, Giménez D, Chicharro Alcántara D, Carrillo Poveda JM, et al. Assessment of the efficacy of platelet-rich plasma in the treatment of traumatic canine fractures. *Int J Mol Sci.* (2019) 20:1075. doi: 10.3390/ijms20051075

19. Franklin SP, Burke EE, Holmes SP. The effect of platelet-rich plasma on osseous healing in dogs undergoing high tibial osteotomy. *PLoS ONE.* (2017) 12:e0177597. doi: 10.1371/journal.pone.0177597

20. Conzemius MG, Aper RL, Corti LB. Short-term outcome after total elbow arthroplasty in dogs with severe, naturally occurring osteoarthritis. *Vet Surg.* (2003) 32:545–52. doi: 10.1111/j.1532-950X.2003.00545.x

21. De Hann JJ, Roe RC, Lewis DD, Renberg WC, Kerwin SC, Bebchuk TN. Elbow arthrodesis in twelve dogs. *Vet Comp Orthop Traumatol.* (1995) 9:115–9. doi: 10.1055/s-0038-1632515

22. Cook JL, Payne JT. Surgical treatment of osteoarthritis. *Vet Clin North Am Small Anim Pract.* (1997) 27:931–44. doi: 10.1016/s0195-5616(97)50087-8

23. Fitpatrick N, Smith TJ, Evans RB, O'Riordan J, Yeadon R. Subtotal coronoid ostectomy for treatment of medial coronoid disease in 263 dogs. *Vet Surg.* (2009) 38:233–45. doi: 10.1111/j.1532-950X.2008.00491.x

24. de Bakker E, Van Vynckt D, Coppieters E, van Bree H, Van Ryssen B, Samoy YCA. Arthroscopic treatment of fragmented coronoid process with severe elbow incongruity. *Vet Comp Orthopaed Traumatol.* (2013) 26:27–33. doi: 10.3415/VCOT-11-06-0087

25. Cook JL, Cook CR. Bilateral shoulder, and elbow arthroscopy in dogs with forelimb lameness: diagnostic findings and treatment outcomes. *Vet Surg.* (2009) 38:224–32. doi: 10.1111/j.1532-950X.2008.00490.x

26. Galindo-Zamora V, Dziallas P, Wolf DC, Kramer S, Abdelhadi J, Lucas K, et al. Evaluation of thoracic limb loads, elbow movement, and morphology in dogs before and after arthroscopic management of unilateral medial coronoid process disease. *Vet Surg.* (2014) 43:819–28. doi: 10.1111/j.1532-950X.2014.12250.x

27. Barthélémy NP, Griffon DJ, Ragetly GR, Carrera I, Schaeffer DJ. Short- and long-term outcomes after arthroscopic treatment of young large breed dogs with medial compartment disease of the elbow. *Vet Surg.* (2014) 43:935–43. doi: 10.1111/j.1532-950X.2014.12255.x

28. Krotscheck U, Böttcher PB, Thompson MS, Todhunter RJ, Mohammed HO. Cubital subchondral joint space width and CT osteoabsorptiometry in dogs with and without fragmented medial coronoid process. *Vet Surg.* (2014) 43:330–338. doi: 10.1111/j.1532-950X.2014.12121.x

29. Burton NJ, Owen MR, Kirk LS, Toscano MJ, Colborne GR. Conservative versus arthroscopic management for medial coronoid process disease in dogs: a prospective gait evaluation. *Vet Surg.* (2011) 40:972–80. doi: 10.1111/j.1532-950X.2011.00900.x

30. Dempsey L, Maddox T, Comerford E, Pettitt R, Tomlinson A. A comparison of owner-assessed long-term outcome of arthroscopic intervention versus conservative management of dogs with medial coronoid process disease. *Vet Comp Orthopaed Traumatol.* (2019) 32:001–9. doi: 10.1055/s-0038-1676293

31. Coppieters E, Seghers H, Verhoeven G, Gielen I, Samoy Y, de Bakker E, et al. Arthroscopic, computed tomography, and radiographic findings in 25 dogs with lameness after arthroscopic treatment of medial coronoid disease. *Vet Surg.* (2016) 45:246–53. doi: 10.1111/vsu.12443

32. Renner C, Medl N. Computed tomographic assessment of the completeness of arthroscopic subtotal coronoidectomy in dogs with medial coronoid disease. *Vet Rec.* (2021) 190:e1069. doi: 10.1002/vetr.1069

frontiers | Frontiers in Veterinary Science

TYPE Original Research
PUBLISHED 11 August 2022
DOI 10.3389/fvets.2022.963759

OPEN ACCESS

EDITED BY
Chavaunne T. Thorpe,
Royal Veterinary College (RVC),
United Kingdom

REVIEWED BY
Sushmitha S. Durgam,
The Ohio State University,
United States
Danae Zamboulis,
Royal Veterinary College (RVC),
United Kingdom

*CORRESPONDENCE
Lauren V. Schnabel
lvschnab@ncsu.edu

SPECIALTY SECTION
This article was submitted to Veterinary Regenerative Medicine, a section of the journal Frontiers in Veterinary Science

RECEIVED 07 June 2022
ACCEPTED 18 July 2022
PUBLISHED 11 August 2022

CITATION
Koch DW, Berglund AK, Messenger KM, Gilbertie JM, Ellis IM and Schnabel LV (2022) Interleukin-1β in tendon injury enhances reparative gene and protein expression in mesenchymal stem cells. *Front. Vet. Sci.* 9:963759. doi: 10.3389/fvets.2022.963759

Interleukin-1β in tendon injury enhances reparative gene and protein expression in mesenchymal stem cells

Drew W. Koch[1,2], Alix K. Berglund[1,2], Kristen M. Messenger[2,3], Jessica M. Gilbertie[1,2], Ilene M. Ellis[1] and Lauren V. Schnabel[1,2]*

[1]Department of Clinical Sciences, College of Veterinary Medicine, North Carolina State University, Raleigh, NC, United States, [2]Comparative Medicine Institute, North Carolina State University, Raleigh, NC, United States, [3]Department of Molecular Biomedical Sciences, College of Veterinary Medicine, North Carolina State University, Raleigh, NC, United States

Tendon injury in the horse carries a high morbidity and monetary burden. Despite appropriate therapy, reinjury is estimated to occur in 50–65% of cases. Although intralesional mesenchymal stem cell (MSC) therapy has improved tissue architecture and reinjury rates, the mechanisms by which they promote repair are still being investigated. Additionally, reevaluating our application of MSCs in tendon injury is necessary given recent evidence that suggests MSCs exposed to inflammation (deemed MSC licensing) have an enhanced reparative effect. However, applying MSC therapy in this context is limited by the inadequate quantification of the temporal cytokine profile in tendon injury, which hinders our ability to administer MSCs into an environment that could potentiate their effect. Therefore, the objectives of this study were to define the temporal cytokine microenvironment in a surgically induced model of equine tendon injury using ultrafiltration probes and subsequently evaluate changes in MSC gene and protein expression following *in vitro* inflammatory licensing with cytokines of similar concentration as identified *in vivo*. In our *in vivo* surgically induced tendon injury model, IL-1β and IL-6 were the predominant pro-inflammatory cytokines present in tendon ultrafiltrate where a discrete peak in cytokine concentration occurred within 48 h following injury. Thereafter, MSCs were licensed *in vitro* with IL-1β and IL-6 at a concentration identified from the *in vivo* study; however, only IL-1β induced upregulation of multiple genes beneficial to tendon healing as identified by RNA-sequencing. Specifically, vascular development, ECM synthesis and remodeling, chemokine and growth factor function alteration, and immunomodulation and tissue reparative genes were significantly upregulated. A significant increase in the protein expression of IL-6, VEGF, and PGE2 was confirmed in IL-1β-licensed MSCs compared to naïve MSCs. This study improves our knowledge of the temporal tendon cytokine microenvironment following injury, which could be beneficial for the development and determining optimal timing of administration of regenerative therapies. Furthermore, these data support

the need to further study the benefit of MSCs administered within the inflamed tendon microenvironment or exogenously licensed with IL-1β *in vitro* prior to treatment as licensed MSCs could enhance their therapeutic benefit in the healing tendon.

KEYWORDS

tendon, cytokine, ultrafiltration probe, mesenchymal stem cell, licensing

Introduction

Tendon injury in the horse, most commonly affecting the superficial digital flexor tendon (SDFT), has a high morbidity and monetary burden associated with treatment, rehabilitation, and lost athletic performance (1, 2). Despite appropriate therapy, high reinjury rates are estimated to occur in 50–65% of cases (1–3). In the last 20 years, implementation of mesenchymal stem cell (MSC) therapy has secured a prominent position in treating a variety of musculoskeletal injuries. Specifically, intralesional administration of MSCs in horses has improved SDFT architecture in experimental settings and reduced reinjury rate in clinical cases (3, 4). Despite these improved outcomes following MSC therapy, new insights into MSC biology have created a paradigm shift. It is now believed that the effect of MSCs is not due to local engraftment and differentiation, but instead from secretion of bioactive paracrine factors commonly referred as the secretome (5, 6). Particularly, data have shown that inflammatory molecules stimulate, or license, MSCs to enhance their secretion of reparative and immunomodulatory factors to a greater degree than in their naïve, or unlicensed, state (7–10). While this has translated to increased research in licensed MSCs for other inflammatory diseases, minimal work has examined inflammatory licensed MSCs for the treatment of tendon injuries (11).

Understanding the tissue microenvironment during injury guides our ability to develop new therapies to combat detrimental molecular mechanisms and encourage local reparative factors to improve healing. However, as recently reviewed (12), our knowledge of the temporal cytokine profile following tendon injury is limited due, in part, to the difficulty in obtaining adequate antemortem samples without compromising tendon structure and function. Our current understanding of the tendon microenvironment following injury has relied upon simplified models of injury in cell culture, intermittent post-mortem analyses in terminal animal disease models, or evaluation of human clinical patients with naturally occurring, but non-standardized tendon injuries (13, 14). Therefore, more thoroughly determining the temporal change in the cytokine profile in a standardized tendon injury model would advance our knowledge of the molecular mechanisms that drive healing and disease, which could subsequently advance our ability to develop more effective therapies for tendon injury. Furthermore, examining how this inflammatory microenvironment affects MSCs and their secreted factors in the context of MSC licensing has the potential to advance MSC therapy for tendon injuries.

The objectives of this study were 2-fold: (1) define the *in vivo* temporal cytokine profile of the tendon microenvironment using a novel ultrafiltration probe implanted into a surgically induced tendon lesion in the horse; and (2) determine how the predominant inflammatory cytokines identified in **(author?)** (1) affect the MSC gene and protein expression *in vitro*. We hypothesized that the use of a novel ultrafiltration probe would allow us to define the temporal cytokine profile in a surgically induced model of tendon injury. Further, we hypothesized that licensing of MSCs separately with IL-1β or IL-6 at the concentration identified in the *in vivo* tendon microenvironment would enhance tendon-beneficial gene and protein expression.

Materials and methods

Animal use and welfare

Seven Thoroughbred horses (age median 5 years, range 4–13 years; median weight 490 kg, 405–513 kg), free of clinical lameness and palpable or ultrasonographically evident tendon injury were enrolled, and underwent surgical induction of a core lesion of both forelimb SDFTs in an experimental protocol approved by the Institutional Animal Care and Use Committee of North Carolina State University (Protocol #20-389). For the entire study period, horses were housed in an individual 12 × 12 foot concrete stall with rubber floor mats with bedding and provided water and grass hay *ad libitum* in a temperature-controlled facility. Preoperative complete blood count and serum chemistry were performed prior to surgery and weekly thereafter.

Ultrafiltration probe development and surgical technique

The ultrafiltration probes used were a modified version of a commercially available probe (BASi Research Products,

West Layfayette, IN, USA) used for pharmacokinetic and pharmacodynamic (PK/PD) modeling studies. These probes consist of three loops of membrane with a 30 kDa molecular weight cutoff, joined to a single, non-permeable conducting tube (15, 16). Our group, with assistance from BASi Research Products, performed both *ex vivo* and *in vivo* pilot studies to custom design a modified ultrafiltration probe with a slimmer profile consisting of a single loop of membrane with a 100 kDa molecular weight cutoff to ensure collection of larger cytokines like TNF-α (17).

Horses were anesthetized, moved to an operating theater, and maintained with general inhalant anesthesia. Core lesions were created in the extrasynovial portion of both forelimb SDFTs of seven horses using a previously published method shown to induce consistent injury with a similar ultrasonographic and histologic progression encountered in naturally occurring equine SDFT injury (18). Briefly, following aseptic preparation, local anesthesia with bupivacaine liposome injectable suspension (Nocita®, Elanco Animal Health, Inc., Greenfield, IN) of the medial and lateral palmar metacarpal nerves and medial and lateral metacarpal nerves was performed immediately distal to the head of the second and fourth metacarpal bones and tendon lesions induced under ultrasonographic guidance as previously described. Thereafter, a custom-designed 100 kDa ultrafiltration probe (BASi Research Products, West Lafayette, IN, USA) was threaded retrograde through a 12-gauge venous catheter (Zoetis, Inc., Kalamazoo, MI, USA) to seat the probe entirely within the lumen (Figures 1A,B). The probe-venous catheter was then inserted within the lumen of an ultrafiltration probe introducer needle (BASi Research Products, West Lafayette, IN, USA, Figure 1C). Using this method, the function of the introducer needle was placement of the ultrafiltration probe within the lesion while the venous catheter provided support at the probe base to ensure it was maintained within the tendon when the introducer needle was removed. Following placement of ultrafiltration probes in six horses, the catheter and introducer needle were removed, and probe location confirmed with ultrasonography (Figures 1D–G). A single horse underwent creation of bilateral SDFT lesions without placement of ultrafiltration probes to serve as control. Skin incisions of all horses were closed with 2-0 polypropylene in a simple interrupted pattern, the limbs bandaged standardly, and horses recovered from general inhalant anesthesia.

Horses received prophylactic gentamicin sulfate (6.6 mg/kg, q 24 h, IV) and penicillin G potassium (22,000 IU/kg, q 6 h, IV) prior to surgery and for 3 days after. Postoperative analgesia was provided by morphine sulfate (0.05–0.1 mg/kg, q 12–24 h, IM) for 2–3 days depending on comfort. Non-steroidal anti-inflammatory drugs (NSAIDs) were purposefully avoided to prevent alteration of the tendon cytokine profile. Following recovery from general anesthesia, each limb was unbandaged, a sterile evacuated tube containing protease inhibitors (BD, Franklin Lakes, NJ) attached to the needle and conducting tube system of the ultrafiltration probe, and the limb rebandaged. Tendon ultrafiltrate was collected from evacuated tubes within the first 3–5 h following surgery and a new tube replaced and changed every 12 h thereafter. Samples were aliquoted into cryovials immediately following collection and stored at −80°C until analysis within 4 months following collection. Ultrasound-guided percutaneous aspiration of lesions of the single control horse was attempted on day one, three, seven, and ten postoperatively and samples aliquoted and stored as with tendon ultrafiltrate. Horses were hand walked for five (week one), ten (week two), and fifteen (week three) minutes twice daily until the conclusion of the study. At 21 days following surgery, horses were sedated and euthanized with an intravenous overdose of sodium pentobarbital. Tendon from a representative limb was collected for histopathology in two horses.

Cytokine characterization

Cytokine concentration for equine-specific interleukin-1β (IL-1β),−6,−8,−10, fibroblast growth factor-2 (FGF-2), tumor necrosis factor-α (TNF-α), interferon-γ (IFN-γ), interferon inducible protein-10 (IP-10), transforming growth factor-β1 (TGF-β1),−2, and−3 were measured in tendon ultrafiltrate with a fluorescent bead-based multiplex assay (MILLIPLEX, Equine Multiplex Assay, MilleporeSigma, MA, USA) and performed according to manufacturer's instructions. For the multiplex assay, concentrations measured below the lower limit of quantification (LLoQ) were assigned a value of 0.1 of the LLoQ. Prostaglandin E2 (PGE2) was determined using a colorimetric competitive ELISA according to manufacturer's instructions (Enzo Life Sciences, Inc., Farmingdale, NY, USA). All samples were analyzed in duplicate. Tendon ultrafiltrate from later timepoints was pooled for TGF-β and PGE2 analysis due to small sample volume.

RNA sequencing of licensed MSCs

Banked equine bone marrow-derived MSCs ($n = 6$, donor horse age median 9 years, range 6–12 years) were utilized for this study and were isolated as previously described (19). MSCs were thawed and seeded in complete MSC media (19) containing 10% fetal bovine serum (FBS) and when cultures reached 80% confluency, MSCs were passaged with Accutase cell-dissociation solution (Innovative Cell Technologies) and 0.35×10^6 cells plated on 100 mm culture plates for RNA sequencing experiments. MSCs were passaged 2–3 times prior to use. Twenty-four hours following passage and adherence, cells were licensed by adding complete MSC media containing 2 ng/ml recombinant human IL-1β (R&D Systems) or 2 ng/ml recombinant human IL-6 (BioLegend) for 72 h with media

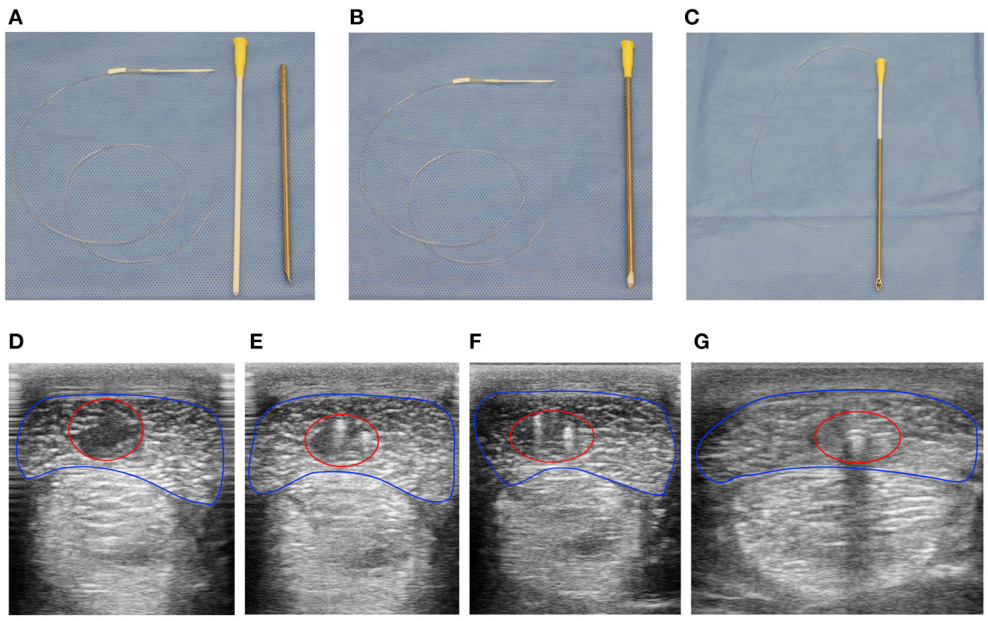

FIGURE 1
Ultrafiltration probes were easily placed under ultrasound guidance within the center of surgically induced equine SDFT lesions. Instruments required to place ultrafiltration probes within surgically induced lesions of the SDFT. **(A)** Ultrafiltration probe (left), venous catheter (middle), and Basi® introducer needle (right). The venous catheter was threaded normograde into the introducer needle **(B)**, followed by retrograde threading of the ultrafiltration probe into the venous catheter-introducer needle **(C)**. Using ultrasound guidance **(D–G)**, the device facilitated placement of the ultrafiltration probe within tendon lesions (red circle) of the SDFT (blue outline) following surgical induction. At the most proximal extent **(D)** a large hypoechoic lesion with loss of tendon fiber is visualized. Moving distally, the two fibers of the ultrafiltration probe loop can be visualized as hyperechoic foci within the hypoechoic lesion **(E,F)**. Finally, acoustic shadowing due to gas within the lumen of the conducting tubing **(G)** was observed at the most distal extent of the tendon lesion proximal to tube exit from the tendon and skin.

exchanged at 48 h. After 72 h, cells were washed and lifted in preparation for RNA-sequencing.

Total RNA was extracted from paired P3 or P4 naïve, IL-1β licensed, and IL-6 licensed MSCs from six donor horses using the RNeasy Mini kit (Qiagen). Libraries were generated and poly(A) enriched using 1 μg of RNA as input. Indexed samples were sequenced using a 150 base pair paired-end protocol on a HiSeq 2500 (Illumina) according to the manufacturer's protocol. Sequence reads were trimmed to remove possible adaptor sequences and nucleotides with poor quality using Trimmomatic v.0.36. The trimmed reads were mapped to the EquCab 3.0 reference genome available on ENSEMBL using the STAR aligner v2.5.2b. Unique gene hit counts were calculated using featureCounts from the Subread package v1.5.2. Using DESeq2, a comparison of gene expression between the naive and IL-1β or IL-6 licensed MSCs was performed. The Wald test was used to generate *p*-values and log2 fold changes. Genes with an adjusted *p*-value of <0.05 and log2 fold change >1 were determined to be differentially expressed for each comparison. The quantification and poly(A) selection of mRNA, library preparation, sequencing, and bioinformatics were outsourced to GENEWIZ, Inc.

MSC protein expression

Supernatants from paired naïve and licensed MSCs ($n = 4$, donor horse age median 17 years, range 12–23 years) were collected, spun at 500*xg* for 10 min to remove cellular debris, and stored at −80°C until analysis. Protein expression of IL-1β licensed MSCs were evaluated with ELISA assays for equine IL-6 (R&D Systems, Minneapolis, MN, USA), human PGE2 (Enzo Biochem, Inc., Farmingdale, NY, USA), and equine VEGF (Kingfisher Biotech, Saint Paul, MN, USA) and performed per manufacturer's instructions. For PGE2 analysis, supernatant from IL-1β licensed MSCs was diluted 1:100 in reagent diluent.

Statistical analysis

Tendon ultrafiltrate volumes were assessed for normal distribution by Shapiro-Wilk test. Descriptive analysis was performed for both tendon ultrafiltrate volume and cytokine concentration. Normally distributed data was reported as mean ± standard deviation while non-parametric data reported with median and interquartile range. A one-tailed paired *t*-test was

used to examine difference in protein expression for ELISA assays. All analysis and figure preparation were performed using GraphPad Prism (GraphPad Software Inc; La Jolla, CA, USA). The functional enrichment analysis of RNA-sequencing data was performed using g:Profiler (version e104_eg51_p15_3922dba) with g:SCS multiple testing correction method applying significance threshold of 0.05.

Results

Animals and surgical implantation

An ultrafiltration probe was implanted in each core lesion of six horses. A single horse did not have ultrafiltration probes implanted to serve as control. All horses recovered from general anesthesia without incident and remained comfortable through the entirety of the 21-day study. Complete blood count and serum chemistry for all horses were unremarkable for the duration of the study. Ultrafiltration probes were easy to place within surgically induced lesions; however, maintenance of ultrafiltrate flow following surgery was more difficult as early ultrafiltrate had the tendency to slow or fully obstruct flow at the lumen of the needle connecting the conducting tubing to the evacuated tubes. However, once a new needle was exchanged, collection of tendon ultrafiltrate into the evacuated tubes resumed.

Cytokines in tendon microenvironment

Tendon ultrafiltrate was collected from the majority of ultrafiltration probes throughout the 21-day period; however, volume and frequency of collection varied between horses and between limbs of the same horse throughout (Supplementary Table 1). No significant difference was found in total ultrafiltrate volume collected over the 21-day period between individual horses and was normally distributed (4.411 ± 2.325 ml; $p = 0.944$).

Overall, pro-inflammatory cytokines peaked within the first 24–48 h (Figure 2A). IL-1β at 48 h (median 2,097 pg/ml, 668–5,505 pg/ml), IL-6 at 24 h (median 1,971 pg/ml, 1,114–2,475 pg/ml), and IL-8 at 24 h (median 110 pg/ml, 96–120 pg/ml). Quantifiable levels of IFN-γ, TNF-α, IP-10, IL-10 were not detected. More acutely, the highest levels of FGF-2 were identified within the first sampling period before 12 h (median 1,315 pg/ml, 605–1,423 pg/ml, Figure 2B). TGF-β isoforms were detected at varying times throughout the 21-day period (Figure 2B). TGF-β1 was measured in tendon ultrafiltrate throughout with a biphasic peak at 24 h (median 285 pg/ml, 221–314 pg/ml) and days 11–14 (median 344 pg/ml, 23.0–885 pg/ml). TGF-β2 levels peaked at day 3 (194 pg/ml, 5.4–399 pg/ml) and remained similar through the first week before declining over the final 10 days of the study. Finally, TGF-β3 was below the lower limit of detection except for on days 8–10 and at its peak at days 11–14 (median 85.4 pg/ml, 3.60–249 pg/ml). The concentration of PGE2 was initially measured in two horses and was below quantifiable limits in samples prior to day 15–18. Due to concerns about volume remaining for other assays, further characterization of PGE2 was abandoned. Only small volumes of hemorrhagic sample were obtained during attempts at ultrasound-guided percutaneous aspiration of the control horse lesions. Most cytokines measured from samples were below quantifiable level. This along with concern regarding peripheral blood contamination prevented analysis of samples from the single control horse.

Postmortem histopathology (hematoxylin and eosin) of representative tendons revealed presence of mildly reactive fibroblasts with extracellular matrix deposition within the tendon and surrounding ultrafiltration probe fibers (Supplementary Figure 1). Due to lack of indicators of chronic inflammation such as adjacent leukocyte infiltration, ultrafiltration probe fibers were determined to be inert as consistent with previous literature on the use of ultrafiltration probes in other locations within the body (15, 20, 21).

IL-1β licensed MSCs, but not IL-6 licensed, have enhanced reparative gene expression

Following IL-1β licensing of MSCs, a total of 788 significant differentially expressed genes (DEGs) were identified with 575 genes upregulated and 213 genes downregulated (Figure 3A). Those genes with the largest increase in expression included: NOS2, a key regulator of nitric oxide production, a reactive free radical involved in a variety of biologic processes (22); CCL20, an inflammatory chemokine that binds exclusively to CCR6 receptors commonly found in cells of the immune system (23); IL6, a pleotropic cytokine associated with inflammation, tissue healing, metabolism, and lymphocyte development (24); and FOXN4, a member of the forkhead box/winged-helix transcription superfamily that determines cell fate in neural and non-neural tissues (25). Genes with the largest downregulation included LOC106780963, an uncharacterized gene from chromosome 9; LMCD1, a regulator of MSC osteogenic differentiation (26); PGFS, an enzyme responsible for prostaglandin F production which causes bronchial and arterial smooth muscle contraction (27); and MGP, a vitamin K-dependent protein associated with vascular calcification (28). Gene ontology (GO) enrichment analysis identified the top overrepresented terms in the entire DEG set. The top ten molecular functions (MF), biological processes (BP), and cellular components (CC) for these data are listed (Figure 3B). Overrepresented

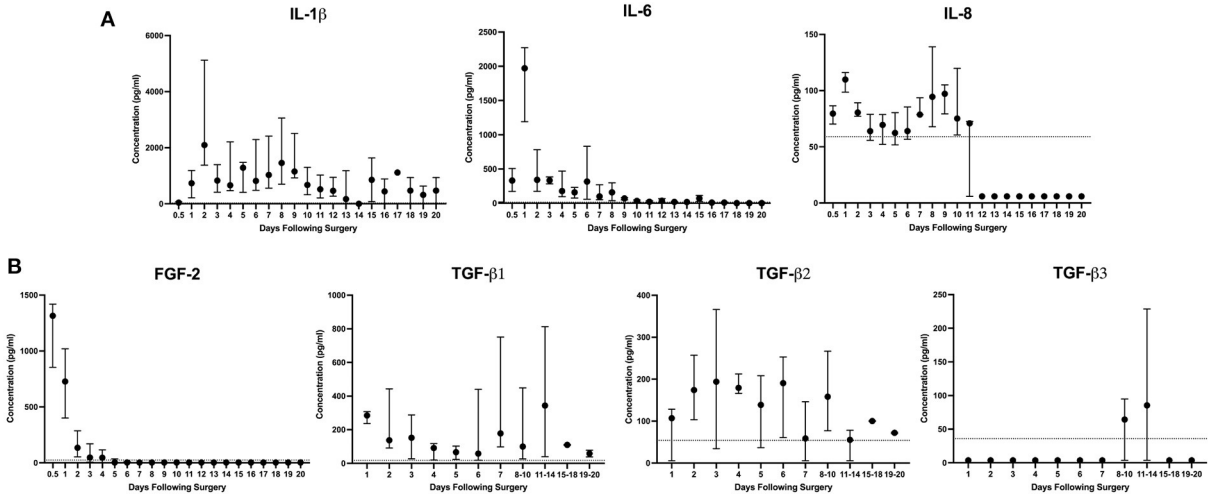

FIGURE 2
IL-1β and IL-6 are the predominant inflammatory cytokines present following surgically induced equine SDFT injury. Descriptive report of **(A)** inflammatory cytokines and **(B)** growth factors FGF-2 and TGF-β1,−2, and−3 in tendon ultrafiltrate were measured by ELISA following bilateral surgically induced SDFT injury of the forelimb over 21 days in 6 horses. Due to insufficient volume, samples from days 8 onward were grouped for TGF-β isoform analysis. When present, the dashed line at the y-axis represents the lower limit of quantification (LLoQ) for that cytokine or growth factor as determined by the assay manufacturer (MilliporeSigma, MA, USA). Concentrations measured below the LLoQ were assigned a value of 0.1 of the LLoQ.

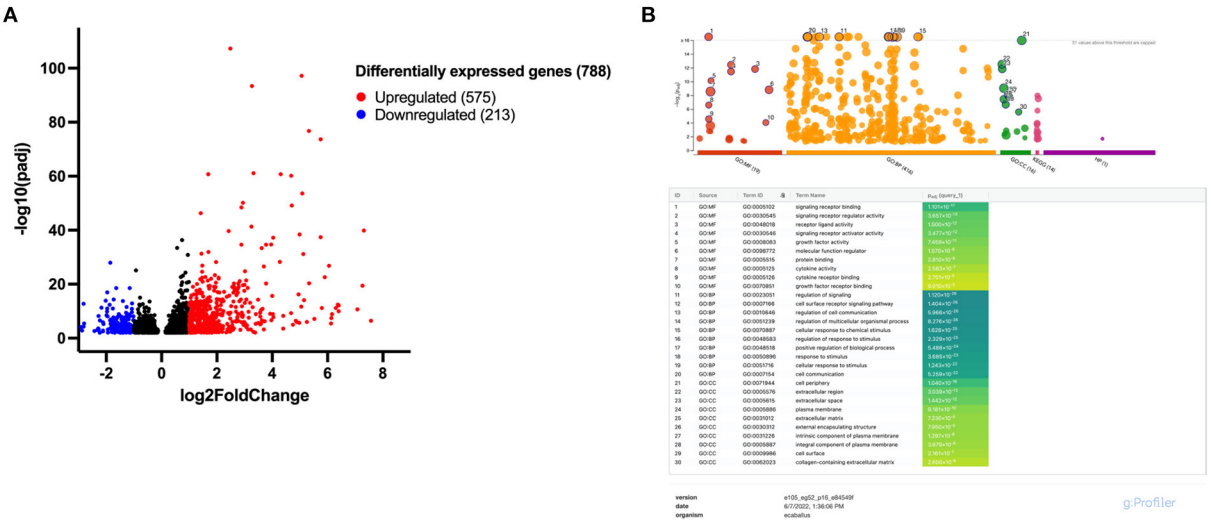

FIGURE 3
Approximately 788 differentially expressed genes (DEGs) were identified following IL-1β licensing of equine MSCs with overrepresented terms including growth factor and cytokine activity and extracellular matrix-associated functions. **(A)** Volcano plot for differential expression analysis depicting the $\log_2$ fold change and $-\log_{10}$ (adjusted *p* value) for gene transcripts in IL-1β licensed MSCs detected by RNA-sequencing. Significantly upregulated DEGs are presented in red and significantly downregulated DEGs in blue with absolute fold change >1.0 and a *p*-value < 0.01. **(B)** Manhattan plots from g:Profiler illustrating GO term enrichment analysis of DEGs of MSCs following IL-1β licensing. The top 10 enriched pathways for each GO term (MF, molecular function; BP, biological process; CC, cellular component) are presented.

terms identified by GO analysis included growth factor activity, cytokine activity, cell communication, extracellular matrix, and collagen-containing extracellular matrix among others (Figure 3B). For the top 100 upregulated genes, all significant GO terms for MF, BP, CC, KEGG pathways, and human phenotype ontology (HP) are shown in Supplementary Figure 2.

Of the 788 DEGs, multiple genes were identified that could be relevant—whether beneficial or detrimental—to the healing tendon (Figure 4; Table 1). Multiple differentially

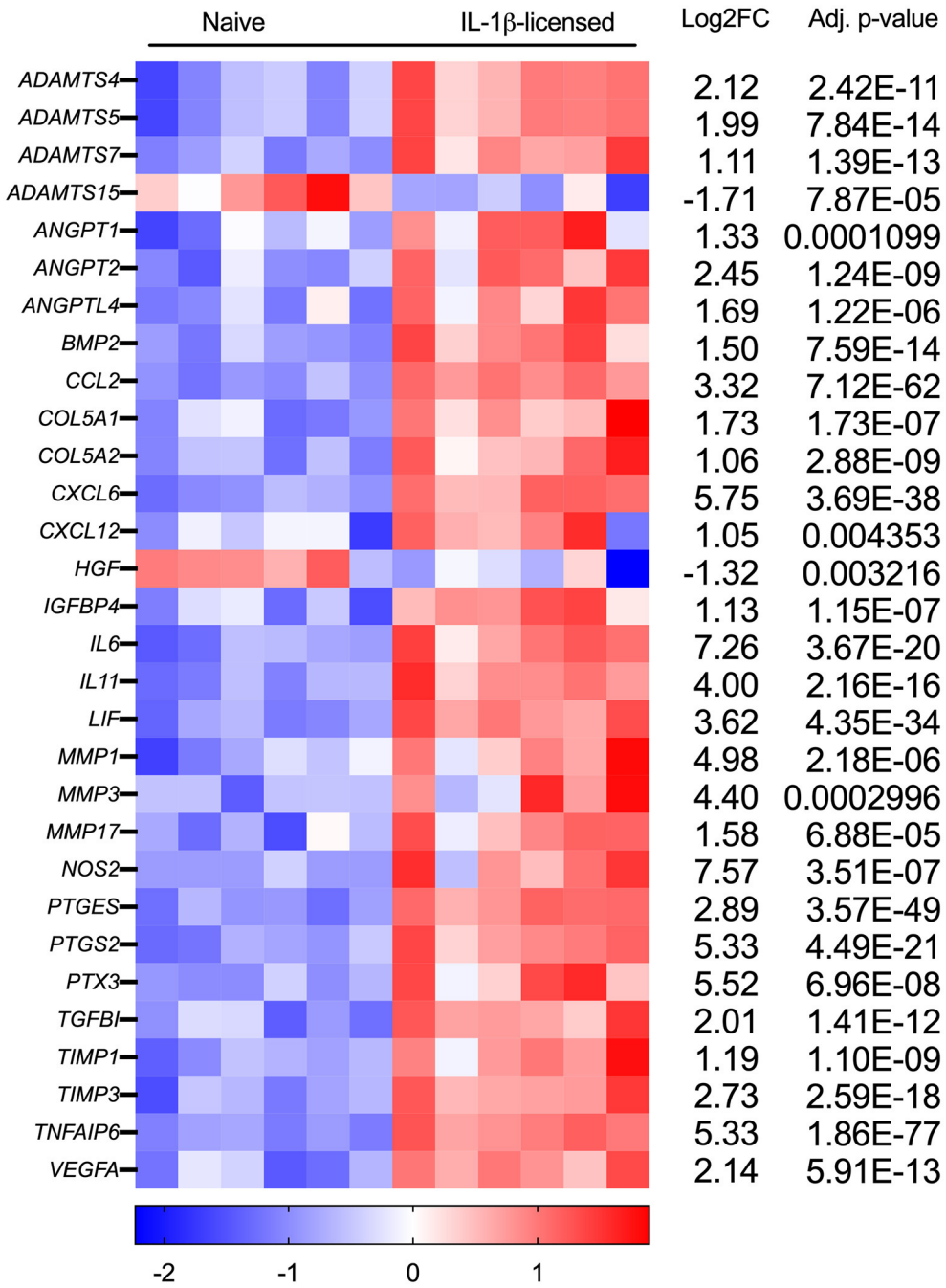

FIGURE 4
Tendon-relevant genes are significantly differentially regulated in equine MSCs following IL-1β licensing. Heat map representation using log2fold change of select significantly differentially expressed genes (DEGs) from RNA sequencing analysis following IL-1β licensing ($n = 6$ horses). Compared to naïve MSCs, gene downregulation is noted in blue and gene upregulation in red.

regulated genes were identified, that if translated to their downstream proteins, could have tendon-relevant effects (Table 1) through tendon or MSC-specific function including those associated with vascular development (ANGPT1/2, ANGTPL4, CXCL6, VEGF-A, VEGF-C), synthesis and remodeling of the tendon ECM (ADAMTS4/5, COL5A1/A2, IL6, MMP1/3/17, NOS2, TIMP1/3), chemokine and growth factor function alteration (MMP1/3), and immunomodulation and tissue reparative effects (IL6, NOS2, PTGES, PTGS2). Following MSC licensing with IL-6, EGR3 and FOSB were

the lone DEGs identified. Neither was considered relevant to MSC function in the context of tendon development or healing.

IL-1β licensed MSCs secrete significantly more IL-6, PGE2, and VEGF than naïve MSCs

Three DEGs in IL-1β-licensed MSCs identified in RNA-seq data were chosen due to their known relevance to tendon healing, to confirm downstream protein expression. Cell culture supernatant obtained from IL-1β licensed MSCs produced significantly more IL-6 ($p = 0.0126$), PGE2 ($p = 0.0193$), and VEGF ($p = 0.0162$) compared to their paired naïve controls (Figure 5). IL-6 is a pleotropic cytokine present following tendon injury and regulates leukocyte infiltration and controls duration of pro-inflammatory mediator release (12, 66). Prostaglandin E2 is a primary mediator of equine MSC immunomodulation, is present following tendon injury, and likely plays a critical, concentration-dependent role in both the reparative response as well as the development of chronic injury (67, 68). VEGF, present following tendon loading and tenocyte mechanical stimulation, appears to improve strength of healing tendon when administered exogenously (69). These data support that IL-1β licensing is inducing changes in gene and protein expression in MSCs and this phenotype could provide tendon-relevant effects.

Discussion

This is the first study of its kind to define the temporal cytokine profile following surgically induced tendon injury. A novel method of implantation of an ultrafiltration probe within the center of the equine SDFT was implemented where it was determined that inflammation was predominated by IL-1β and IL-6. Additionally, concentrations of both cytokines peaked at ∼2,000 pg/ml (2 ng/ml) within 48 h following injury. When MSCs were subsequently licensed with a similar concentration of exogenous recombinant human IL-1β, licensed MSCs upregulated expression of multiple genes that could impart benefit to the healing tendon. Further, downstream expression for three select genes were supported by significantly higher protein concentrations measured in culture supernatant compared to naïve MSCs. These data further improve our understanding of the tendon microenvironment following injury and provide evidence that IL-1β licensed MSCs could provide enhanced therapeutic benefit compared to their naïve counterparts.

Elucidating the temporal cytokine profile in tendon following injury is critical to guide development of novel therapies that aim to return the biochemical composition and biomechanical strength of healing tendon to its native state. Attempts to characterize the interplay of cytokines in the tendon microenvironment in both health and disease have employed cell culture, tissue biopsy, and subcutaneous microdialysis as recently review by Ellis et al. (12). However, the inability to repeatedly sample the injured tendon microenvironment in conjunction with inconsistent standardization of samples from naturally occurring disease limit our understanding of the temporal change that occurs following injury (13, 14). To rectify this, our group was able to sample the tendon microenvironment twice daily for 21 days in a surgically induced model using a novel method that employed ultrafiltration probes. The distinct advantages of this technique include standardization of tendon lesions, implementation of a relevant large animal model of tendon injury, and daily temporal characterization of the tendon microenvironment that would otherwise require large numbers of terminal animal studies (18, 70–72). We demonstrate that ultrafiltration probes were effective in facilitating characterization of the cytokine milieu in tendon injury. Additionally, lack of histopathologic evidence of foreign body reaction (73) within examined tendons indicate the cytokines at their measured concentration were an accurate reflection of the tendon microenvironment following injury. While we did not attempt to elucidate the cell-specific source of these cytokines, *in vitro* studies support this milieu is likely secreted by a combination of local and infiltrating cells including tendon fibroblasts, tendon stem/progenitor cells, and immune cells (14, 74, 75). The authors recognize that although the cytokine quantification herein is limited to the analytes present in the commercial kits and does not represent all analytes involved in the molecular cascade, the novel method employed to characterize the tendon microenvironment is an essential first step and establishes a new technique to collect further data on the microenvironment following injury and in response to therapy. Despite the associated bias when selecting cytokines to analyze tendon ultrafiltrate, published literature of the injured tendon microenvironment (12, 13, 76) was used to support selection of the most relevant cytokines in our custom multiplex within species-specific assay constraints.

While the therapeutic effect of MSCs was previously attributed to local engraftment and cell differentiation, it is now understood that MSC functions include their ability to stimulate angiogenesis, apoptosis, immunomodulation, and recruitment and stimulation of systemic and endogenous progenitor cells through secretion of paracrine mediators (77, 78). Interestingly, these functions can be dramatically altered when naive MSCs are administered within an injured tissue microenvironment or following exogenous exposure to pro-inflammatory cytokines, deemed MSC licensing (5, 77). In experimental settings, administration of MCSs licensed with inflammatory cytokines or molecules such as bacterial lipopolysaccharide (LPS) can ameliorate pathologic change in

TABLE 1 Function of downstream proteins produced from DEGs identified from IL-1β licensed MSCs that could impart tendon-relevant effects.

Gene	Log2 fold change	*p*-value	Function of downstream protein
ADAMTS4	2.119087765	3.89E-13	Inhibited by TIMP3 (29), cleave Glu-X bond of aggrecan core protein (30)
ADAMTS5	1.986039748	8.24E-16	Cleave Glu-X bond of aggrecan core protein (30)
ADAMTS7	1.112947643	1.53E-15	Smooth muscle cell migration and COMP digestion (30)
ADAMTS15	−1.705114295	5.43E-06	Cleave Glu-X bond of aggrecan core protein (30)
ANGPT1	1.331215264	7.98E-06	Support vascular maintenance and homeostasis, promotes self-renewal of adult muscle stem cells (31)
ANGPT2	2.450315564	2.59E-11	Can agonize or antagonize angiopoietin-1 and dependent on concurrent presence of VEGF (31, 32)
ANGPTL4	1.694800283	4.99E-08	Enhances *in vitro* tenocyte migration, regulates tenocyte cell cycle genes (33), angiogenesis (34)
BMP2	1.504661232	7.84E-16	Exogenous administration induces expression of collagen type I in human tenocytes (35) and in equine tenocytes overexpressing BMP2 (36), but can induce mineralization in both equine tenocytes/MSCs overexpressing BMP2 (36)
CCL2	3.321170222	2.92E-65	Associated with GDF5-induced human MSC tenogenic differentiation (37), in conjunction with CXCL12, induces MO polarization and secretion of IL-10 (38)
COL5A1	1.729683994	5.68E-09	Encodes one of the three alpha chain to assemble collagen type V; forms heterofibrils with collagen type I and II (39)
COL5A2	1.056264925	6.59E-11	Encodes one of the three alpha chain to assemble collagen type V; forms heterofibrils with collagen type I and II (39)
CXCL6	5.752098101	4.79E-41	Ability to indue angiogenesis (40), induces MSC secretion of pro-angiogenic genes (41)
CXCL12	1.051902676	0.000612448	In conjunction with CCL2, induces MO polarization and secretion of IL-10 (38)
HGF	−1.324646103	0.000422508	Inhibits TGFβ-1-induced myofibroblast differentiation of rat tendon fibroblasts (42)
IGFBP4	1.133446579	3.67E-09	Secreted by senescent MSCs and induces senescence in previously unaffected MSCs (43)
IL6	7.262226972	1.68E-22	Increased peritendinous COL1 terminal telopeptide concentrations (44), induced through *in vitro* mechanical stretching of healthy human tendon fibroblasts (45), increased gene expression in chronic human tendinopathy (46)
IL11	4.001668021	1.62E-18	Driver of tissue fibrosis (47), induces TIMP production in articular chondrocytes/synovial fibroblasts (48)
LIF	3.615225809	7.72E-37	IL-6 cytokine family member responsible for induction of JAK-STAT signaling pathway
MMP1	4.975771726	9.42E-08	Secreted-type collagenase with ability to bind native, triple helical collagen type I-III and CTGF (30), selectively degrades CTGF from the CTGF-VEGF complex and restores VEGF angiogenic activity (49), chemokine (CCL2, CXCL12 others) inhibition (50)
MMP3	4.400692659	2.56E-05	Secreted-type stromelysin that selectively degrades CTGF from the CTGF-VEGF complex and restores VEGF angiogenic activity (49), chemokine (CCL2, CXCL12 others) inhibition (50)
MMP17	1.579842693	4.66E-06	Membrane-anchored MMP associated with pericellular proteolysis (30)
NOS2*	7.569179419	1.24E-08	Increased tenocyte collagen synthesis (51), reduction in tendon CSA and load-to-failure when inhibited (52, 53)
PTGES	2.88704628	3.17E-52	Enzyme responsible for terminal step of transformation of COX-derived PGH2 into PGE2 (54)
PTGS2*	5.3337729	1.81E-23	Primary enzyme responsible for controlling PGE2 synthesis in response to inflammation (55)
PTX3	5.521333296	2.16E-09	Anti-inflammatory effects when bound to hyaluronic acid-heavy chain complex induced by TSG-6 (56)
TGFBI	2.011919175	1.82E-14	Negative regulator of TLR-induced inflammation (57), chondroprotective (58)
TIMP1	1.190793601	2.28E-11	Variable ability to inhibit various MMPs and ADAMs (30), regulation of cell migration (59)
TIMP3	2.726335861	1.56E-20	Inhibit ADAMTS-4,−5, various ADAMs (including ADAM17/TACE), and pro-MMP-9 (cleaves denatured collagen) (30), regulate cytokine signaling and inflammatory cell adhesion (50), inhibits angiogenesis through VEGFR2 binding (60)

(Continued)

TABLE 1 Continued

Gene	Log2 fold change	*p*-value	Function of downstream protein
TNFAIP6	5.325227457	5.08E-81	Results in TSG-6 responsible for anti-inflammatory and tissue protective/reparative effects mediated through TSG-6 binding of matrix proteins and chemokines, essential for TGF-β1-induced fibroblast to myofibroblast differentiation, and inhibits BMP-2 driven osteoblast differentiation of MSCs (56)
VEGFA	2.144734795	7.27E-15	Induce hemangiogenesis (61); variable effects identified based on model, VEGF isoform, and timing of exogenous delivery (62, 63); stimulation of MMPs and inhibition of TIMPs (64, 65)

Gene name, log2fold change, and *p*-value from RNA sequencing data of MSCs following IL-1β licensing with literature to support tendon-relevant function through tendon or MSC-specific function.

ADAMTS, a disintegrin and metalloproteinase with thrombospondin motif; ANGPT, angiopoietin; ANGPTL, angiopoietin like; BMP, bone morphogenetic protein; CCL, C-C motif chemokine ligand; COL, collagen; COMP, cartilage oligomeric matrix protein; COX, cyclooxygenase; CSA, cross sectional area; CTGF, connective tissue growth factor; CXCL, C-X-C motif chemokine ligand; HGF, hepatocyte growth factor; IGFBP, insulin like growth factor binding protein; IL, interleukin; LIF, leukemia inhibitory factor; MMP, matrix metalloproteinase; MO, macrophage; MSC, mesenchymal stem cell; NOS, nitric oxide synthase; PGE2, prostaglandin E2; PGH2, prostaglandin H2; PTGES, prostaglandin E synthase; PTGS, prostaglandin-endoperoxide synthase; PTX, pentraxin; TGFβ, transforming growth factor beta; TGFBI, transforming growth factor beta induced; TIMP, tissue inhibitor of metalloproteinase; TACE, TNF-α converting enzyme; TNFAIP, TNF alpha induced protein; TSG-6, TNF-stimulated gene-6; VEGFA, vascular endothelial growth factor A.

*Also known as: NOS2 = iNOS, inducible NOS; PTGS2 = COX-2 (cyclooxygenase-2).

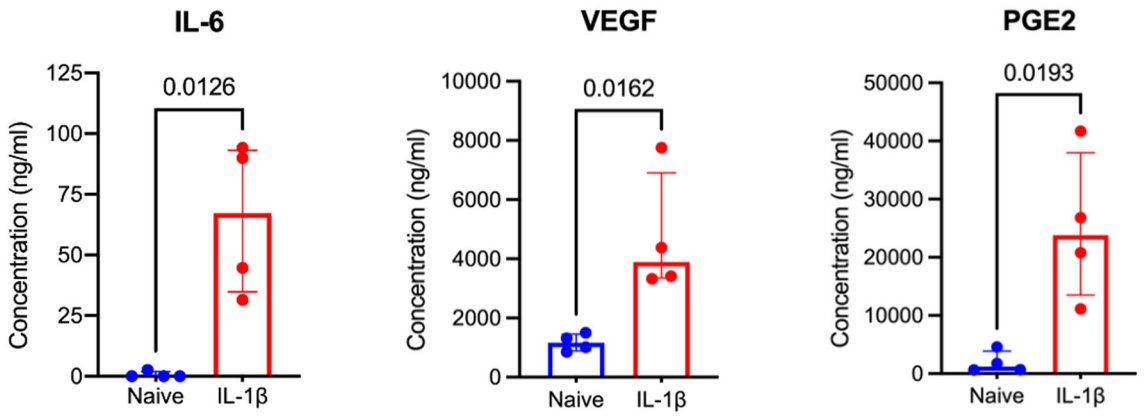

FIGURE 5
IL-1β licensed equine MSCs produce significantly more IL-6, VEGF, and PGE2 than naïve MSCs. From RNA sequencing data, three proteins known to have tendon-relevant effects were selected to confirm downstream protein expression. Analysis of MSC cell culture supernatants by ELISA assay confirmed increased protein expression of IL-6, VEGF, and PGE2 following IL-1β licensing compared to naïve MSC controls. A one-tailed paired *t*-test was used to examine difference in protein expression between groups.

the colon (79), improve corneal allograft survival (8), and improve cardiac fibrosis following cardiac ischemia (80). Despite these benefits in various body systems, only two studies have been published that implement MSC licensing and their effect on tendon tissue. Positive outcomes were noted, respectively, in tenocyte gene expression and tendon healing in projects that examined the *in vitro* effect of licensing MSCs with pioglitazone, a hypoglycemic agent, on tenocytes (81) and TNF-α licensed MSCs in a PLG scaffold in a rat Achilles tendon defect (11). From the *in vivo* tendon microenvironment cytokine data, IL-1β and IL-6 were chosen to license MSCs to evaluate effects on gene and protein expression while IL-8 was avoided where it was present at low levels in the tendon microenvironment. Further, from RNA-seq data, naïve equine MSCs were not determined to express IL-8 receptors CXCR1 and−2. Although we understand the effect of IL-1β on MCS gene and protein expression, the influence of IL-6 is less understood (82, 83). Additionally, even less is understood of equine MSCs response following exposure to inflammation with what we do know based on proteomic analysis after IL-1β treatment during chondrogenic differentiation (84). As this is the first report of transcriptome-wide changes in equine MSCs following exposure to inflammatory cytokines, these data presented advance our understanding of MSC biology and will serve as a foundation for future work studying the therapeutic benefit of licensed MSCs.

While increased expression of many genes following IL-1β licensing of MSCs could be beneficial to the healing tendon, it would be remiss to ignore others that conversely could be detrimental. It plausible that IL-1β licensed MCS secretion of IL-11 (tissue fibrosis), reduction in HGF (inhibitor of myofibroblast differentiation), or excessive PGE2 production could be unwanted side effects of treatment. What is poorly understood at this time is how this IL-1β licensed MSC secretome would affect the tendon microenvironment and whether certain molecules impart benefit and trump detrimental effects of others. Assessing the effect of the IL-1β licensed MSC secretome on tenocytes is a critical next step and a current focus of our laboratory. Finally, while genes expanded upon herein were discussed due to their known association with tenocyte and/or MSC function or their role in tendon healing, the authors recognize that many of the other differentially regulated genes could greatly impact the tendon microenvironment if IL-1β licensed MSCs were administered *in vivo*. However, discussion of these genes was omitted as they lack experimental evidence for their role in tendon development and healing.

Our interest is in improving therapy for equine tendon injuries, however, the utility of the horse as a comparative and preclinical model for developing translational therapies for human tendon injury is promising. Human tendon injuries account for more than 32 million musculoskeletal injuries a year in the United States with an increasing incidence and health care-associated cost due to an aging population pursuing more athletic activity (85–87). Despite appropriate therapy, continued high postoperative reinjury rates have shifted focus toward regenerative medicine approaches to improve outcomes (88, 89). However, the lack of randomized, blinded clinical trials combined with tepid results in case series have prevented support for their continued use (90, 91). While no animal model perfectly recapitulates human tendon injury, equine SDFT injury is an accepted comparative model for exercise-induced Achilles injury in humans (72). Additionally, a recent report suggests equine tenocytes have a tendon marker, collagen expression, and ECM gene repertoire most similar to humans (92). With this in mind, data presented herein could be the first step in enhancing MSC therapy for equine tendon injuries while providing the foundation for future translational studies.

Limitations of this study include inconsistent ultrafiltrate collection between limbs of the same horse and between individual horses along with wide individual horse variation in tendon ultrafiltrate cytokine concentration. It is also likely that the cytokine profile described in the context of this acute injury model does not represent the cytokine profile of chronic tendon injury. Characterization of the later and chronic stages of tendon injury are still warranted and may shed light on the potential therapeutic benefit of licensed MSCs for such injury stages. Despite significant upregulation of multiple MSC genes and downstream proteins that could be beneficial to the healing tendon, it is unknown whether greater expression or these bioactive factors all in combination would truly enhance repair and requires further examination. Finally, the authors recognize that while licensing of cells with a single cytokine does appear to improve the reparative gene and protein expression of MSCs, this does not represent all the cytokines, chemokines, and growth factors they would experience in an *in vivo* system and could therefore drastically alter their transcriptome compared to *in vitro* assays.

In conclusion, this is the first study to quantify the temporal cytokine profile over 21 days in an equine model of surgically induced tendon injury. Our results indicate that the tendon microenvironment within the first 48 h following injury contains a concentration of IL-1β that beneficially modulates MSC gene and protein expression and then rapidly resolves. Because current culture expansion techniques require weeks to prepare both newly isolated and banked MSCs, a situation would rarely arise allowing a veterinarian to administer cells into an actively inflamed tendon as a method to improve MSC therapeutic potential. Therefore, an alternative approach could include *in vitro* licensing of MSCs prior to treatment to mimic exposure to this environment. However, before it can be recommended to implement IL-1β licensed MSCs in clinical cases of equine tendon injury, further studies are required examining both their effect on tenocytes in culture as well as in preclinical *in vivo* equine studies if *in vitro* experiments support their use. Overall, data generated in this study greatly expand our knowledge of the cytokine microenvironment during tendon injury and support the continued investigation of IL-1β licensed MSCs as a potential therapeutic.

Data availability statement

The data presented in the study are deposited in the NCBI GEO repository, accession number GSE208569, and can be found at https://www.ncbi.nlm.nih.gov/geo/query/acc.cgi?acc=GSE208569.

Ethics statement

The animal study was reviewed and approved by North Carolina State University Institutional Animal Care and Use Committee.

Author contributions

DK, AB, KM, JG, and LS contributed to study conception and design. DK and AB performed statistical analyses. DK drafted the manuscript with all authors contributing edits. All

authors contributed to acquisition of data and interpretation of data. All authors read and approved the final manuscript.

Funding

This work was supported by the Grayson-Jockey Club Research Foundation (LS) and the Fund for Orthopedic Research in honor of Gus and Equine athletes (F.O.R.G.E; LS) with stipend support from the National Institutes of Health grants T32OD011130 (DK), K01OD027037 (AB), and T35OD011070 (IE).

Acknowledgments

The authors would like to thank Ms. Julie Long for laboratory technical assistance and NCSU Laboratory Animal Resources staff for their help with animal care and handling. The authors would also like to thank the team at Basi Research Products, and especially Dr. Lauren Elolf, for the extensive assistance provided in the development of the custom 100 kDa ultrafiltration probes used in this study.

Conflict of interest

The authors declare that the research was conducted in the absence of any commercial or financial relationships that could be construed as a potential conflict of interest.

Publisher's note

Supplementary material

The Supplementary Material for this article can be found online at: https://www.frontiersin.org/articles/10.3389/fvets.2022.963759/full#supplementary-material

References

1. Patterson-Kane JC, Firth EC. The pathobiology of exercise-induced superficial digital flexor tendon injury in Thoroughbred racehorses. *Vet J.* (2009) 181:79–89. doi: 10.1016/j.tvjl.2008.02.009

2. O'meara B, Bladon B, Parkin TDH, Fraser B, Lischer CJ. An investigation of the relationship between race performance and superficial digital flexor tendonitis in the Thoroughbred racehorse. *Eq Vet J.* (2010) 42:322–26. doi: 10.1111/j.2042-3306.2009.00021.x

3. Godwin EE, Young NJ, Dudhia J, Beamish IC, Smith RKW. Implantation of bone marrow-derived mesenchymal stem cells demonstrates improved outcome in horses with overstrain injury of the superficial digital flexor tendon. *Equine Vet J.* (2012) 44:25–32. doi: 10.1111/j.2042-3306.2011.00363.x

4. Schnabel LV, Lynch ME, van der Meulen MCH, Yeager AE, Kornatowski MA, Nixon AJ. Mesenchymal stem cells and insulin-like growth factor-I gene-enhanced mesenchymal stem cells improve structural aspects of healing in equine flexor digitorum superficialis tendons. *J Orthopaed Res.* (2009) 27:1392–98. doi: 10.1002/jor.20887

5. Shi Y, Wang Y, Li Q, Liu K, Hou J, Shao C, et al. Immunoregulatory mechanisms of mesenchymal stem and stromal cells in inflammatory diseases. *Nat Rev Nephrol.* (2018) 14:493–507. doi: 10.1038/s41581-018-0023-5

6. Krampera M, Galipeau J, Shi Y, Tarte K, Sensebe L. Immunological characterization of multipotent mesenchymal stromal cells-The international society for cellular therapy (ISCT) working proposal. *Cytotherapy.* (2013) 15:1054–61. doi: 10.1016/j.jcyt.2013.02.010

7. Broekman W, Amatngalim GD, de Mooij-Eijk Y, Oostendorp J, Roelofs H, Taube C, et al. TNF-aα and IL-1β-activated human mesenchymal stromal cells increase airway epithelial wound healing *in vitro* via activation of the epidermal growth factor receptor. *Respirat. Res.* (2016) 17:1–12. doi: 10.1186/s12931-015-0316-1

8. Murphy N, Treacy O, Lynch K, Morcos M, Lohan P, Howard L, et al. TNF-α/IL-1β–licensed mesenchymal stromal cells promote corneal allograft survival via myeloid cell-mediated induction of Foxp3+ regulatory T cells in the lung. *FASEB J.* (2019) 33:9404–21. doi: 10.1096/fj.201900047R

9. Cassano JM, Schnabel LV, Goodale MB, Fortier LA. Inflammatory licensed equine MSCs are chondroprotective and exhibit enhanced immunomodulation in an inflammatory environment. *Stem Cell Res Therapy.* (2018) 9:1–13. doi: 10.1186/s13287-018-0840-2

10. Planat-Benard V, Varin A, Casteilla L. MSCs and inflammatory cells crosstalk in regenerative medicine: concerted actions for optimized resolution driven by energy metabolism. *Front Immunol.* (2021) 12:626755. doi: 10.3389/fimmu.2021.626755

11. Aktas E, Chamberlain CS, Saether EE, Duenwald-Kuehl SE, Kondratko-Mittnacht J, Stitgen M, et al. Immune modulation with primed mesenchymal stem cells delivered via biodegradable scaffold to repair an Achilles tendon segmental defect. *J Orthopaed Res.* (2017) 35:269–80. doi: 10.1002/jor.23258

12. Ellis IM, Schnabel LV, Berglund AK. Defining the profile: characterizing cytokines in tendon injury to improve clinical therapy. *J Immunol Regener Med.* (2022) 16:100059. doi: 10.1016/j.regen.2022.100059

13. Morita W, Dakin SG, Snelling SJB, Carr AJ. Cytokines in tendon disease: a systematic review. *Bone Joint Res.* (2017) 6:656–64. doi: 10.1302/2046-3758.612.BJR-2017-0112.R1

14. Schulze-Tanzil G, Al-Sadi O, Wiegand E, Ertel W, Busch C, Kohl B, et al. The role of pro-inflammatory and immunoregulatory cytokines in tendon healing and rupture: new insights. *Scand J Med Sci Sports.* (2011) 21:337–51. doi: 10.1111/j.1600-0838.2010.01265.x

15. Messenger KM, Wofford JA, Papich MG. Carprofen pharmacokinetics in plasma and in control and inflamed canine tissue fluid using *in vivo* ultrafiltration. *J Vet Pharmacol Ther.* (2016) 39:32–9. doi: 10.1111/jvp.12233

16. Messenger KM, Papich MG, Blikslager AT. Distribution of enrofloxacin and its active metabolite, using an in vivo ultrafiltration sampling technique after the injection of enrofloxacin to pigs. *J Vet Pharmacol Ther.* (2012) 35:452–59. doi: 10.1111/j.1365-2885.2011.01338.x

17. Rossard TP. *Tumor Necrosis Factor* New York, NY: Nova Biomedical Books (2009).

18. Schramme M, Hunter S, Campbell N, Blikslager A, Smith R. A surgical tendonitis model in horses: technique, clinical, ultrasonographic and histological characterisation. *Vet Comp Orthopaed Traumatol.* (2010) 23:231–9. doi: 10.3415/VCOT-09-10-0106

19. Schnabel LV, Pezzanite LM, Antczak DF, Felippe MJB, Fortier LA. Equine bone marrow-derived mesenchymal stromal cells are heterogeneous in MHC class II expression and capable of inciting an immune response *in vitro*. *Stem Cell Res Therapy.* (2014) 5:13. doi: 10.1186/scrt402

20. Mzyk DA, Bublitz CM, Sylvester H, Mullen KAE, Hobgood GD, Baynes RE, et al. Short communication: use of an ultrafiltration device in gland cistern for continuous sampling of healthy and mastitic quarters of lactating cattle for pharmacokinetic modeling. *J Dairy Sci.* (2018) 101:10414–20. doi: 10.3168/jds.2018-14849

21. Underwood C, Collins SN, van Eps AW, Allavena RE, Medina-Torres CE, Pollitt CC. Ultrafiltration of equine digital lamellar tissue. *Vet J.* (2014) 202:314–22. doi: 10.1016/j.tvjl.2014.05.007

22. Förstermann U, Sessa WC. Nitric oxide synthases: regulation and function. *Eur Heart J.* (2012) 33:829-37. doi: 10.1093/eurheartj/ehr304

23. Lee AYS, Eri R, Lyons AB, Grimm MC, Korner H. CC chemokine ligand 20 and its cognate receptor CCR6 in mucosal T cell immunology and inflammatory bowel disease: odd couple or axis of evil? *Front Immunol.* (2013) 4:194. doi: 10.3389/fimmu.2013.00194

24. Tanaka T, Narazaki M, Kishimoto T. Il-6 in inflammation, immunity, and disease. *Cold Spring Harbor Perspect Biol.* (2014) 6:1–16. doi: 10.1101/cshperspect.a016295

25. Xiang MQ Li SG. Foxn4: a multi-faceted transcriptional regulator of cell fates in vertebrate development. *Sci China Life Sci.* (2013) 56:985–93. doi: 10.1007/s11427-013-4543-8

26. Zhu B, Xue F, Zhang C, Li G. LMCD1 promotes osteogenic differentiation of human bone marrow stem cells by regulating BMP signaling. *Cell Death Dis.* (2019) 10:1–11. doi: 10.1038/s41419-019-1876-7

27. Watanabe K. Prostaglandin F synthase. *Prostagland Other Lipid Mediat.* (2002) 68–9:401–7. doi: 10.1016/S0090-6980(02)00044-8

28. Bjørklund G, Svanberg E, Dadar M, Card DJ, Chirumbolo S, Harrington DJ, et al. The role of matrix Gla protein (MGP) in vascular calcification. *Curr Med Chem.* (2019) 27:1647–60. doi: 10.2174/0929867325666180716104159

29. Porter S, Clark IM, Kevorkian L, Edwards DR. The ADMTS metalloproteinases. *Biochem J.* (2005) 386:15–27. doi: 10.1042/BJ20040424

30. Shiomi T, Lemaître V, D'Armiento J, Okada Y. Matrix metalloproteinases, a disintegrin and metalloproteinases, and a disintegrin and metalloproteinases with thrombospondin motifs in non-neoplastic diseases: review article. *Pathol Int.* (2010) 60:477–96. doi: 10.1111/j.1440-1827.2010.02547.x

31. Koh GY. Orchestral actions of angiopoietin-1 in vascular regeneration. *Trends Mol Med.* (2013) 19:31–9. doi: 10.1016/j.molmed.2012.10.010

32. Nowicki M, Wierzbowska A, Małachowski R, Robak T, Grzybowska-Izydorczyk O, Pluta A, et al. ANGPT1, ANGPT2, and MMP-9 expression in the autologous hematopoietic stem cell transplantation and its impact on the time to engraftment. *Ann Hematol.* (2017) 96:2103–12. doi: 10.1007/s00277-017-3133-4

33. Jamil S, Mousavizadeh R, Roshan-Moniri M, Tebbutt SJ, McCormack RG, Duronio V, et al. Angiopoietin-like 4 enhances the proliferation and migration of tendon fibroblasts. *Med Sci Sports Exerc.* (2017) 49:1769–77. doi: 10.1249/MSS.0000000000001294

34. la Paglia L, Listì A, Caruso S, Amodeo V, Passiglia F, Bazan V, et al. Potential role of ANGPTL4 in the cross talk between metabolism and cancer through PPAR signaling pathway. *PPAR Res.* (2017) 2017:1–15. doi: 10.1155/2017/8187235

35. Pauly S, Klatte F, Strobel C, Schmidmaier G, Greiner S, Scheibel M, et al. BMP-2 and BMP-7 affect human rotator cuff tendon cells *in vitro*. *J Shoulder Elbow Surg.* (2012) 21:464–73. doi: 10.1016/j.jse.2011.01.015

36. Murray SJ, Santangelo KS, Bertone AL. Evaluation of early cellular influences of bone morphogenetic proteins 12 and 2 on equine superficial digital flexor tenocytes and bone marrow-derived mesenchymal stem cells in vitro. *Am J Vet Res.* (2010) 71:103–14. doi: 10.2460/ajvr.71.1.103

37. Tan SL, Ahmad TS, Ng WM, Azlina AA, Azhar MM, Selvaratnam L, et al. Identification of pathways mediating growth differentiation factor5-induced tenogenic differentiation in human bone marrow stromal cells. *PLoS ONE.* (2015) 10:e0140869. doi: 10.1371/journal.pone.0140869

38. Galipeau J. Macrophages at the nexus of mesenchymal stromal cell potency: the emerging role of chemokine cooperativity. *Stem Cells.* (2021) 39:1145–54. doi: 10.1002/stem.3380

39. Gelse K, Pöschl E, Aigner T. Collagens - structure, function, and biosynthesis. *Adv Drug Deliv Rev.* (2003) 55:1531–46. doi: 10.1016/j.addr.2003.08.002

40. Strieter RM, Polverini PJ, Kunkel SL, Arenberg DA, Burdick MD, Kasper J, et al. The functional role of the ELR motif in CXC chemokine-mediated angiogenesis. *J Biol Chem.* (1995) 270:27348–57. doi: 10.1074/jbc.270.45.27348

41. Kim SW, Lee DW Yu LH, Zhang HZ, Kim CE, Kim JM, Park TH, et al. Mesenchymal stem cells overexpressing GCP-2 improve heart function through enhanced angiogenic properties in a myocardial infarction model. *Cardiovasc Res.* (2012) 95:495–506. doi: 10.1093/cvr/cvs224

42. Cui Q, Fu S, Li Z. Hepatocyte growth factor inhibits TGF-β1-induced myofibroblast differentiation in tendon fibroblasts: Role of AMPK signaling pathway. *J Physiol Sci.* (2013) 63:163–70. doi: 10.1007/s12576-013-0251-1

43. Severino V, Alessio N, Farina A, Sandomenico A, Cipollaro M, Peluso G, et al. Insulin-like growth factor binding proteins 4 and 7 released by senescent cells promote premature senescence in mesenchymal stem cells. *Cell Death Dis.* (2013) 4:e911. doi: 10.1038/cddis.2013.445

44. Andersen MB, Pingel J, Kjær M, Langberg H. Interleukin-6: A growth factor stimulating collagen synthesis in human tendon. *J Appl Physiol.* (2011) 110:1549–54. doi: 10.1152/japplphysiol.00037.2010

45. Skutek M, van Griensven M, Zeichen J, Brauer N, Bosch U. Cyclic mechanical stretching enhances secretion of Interleukin 6 in human tendon fibroblasts. *Knee Surg Sports Traumatol Arthrosc.* (2001) 9:322–26. doi: 10.1007/s001670100217

46. Legerlotz K, Jones ER, Screen HRC, Riley GP. Increased expression of IL-6 family members in tendon pathology. *Rheumatology.* (2012) 51:1161–65. doi: 10.1093/rheumatology/kes002

47. Cook SA, Schafer S. Hiding in plain sight: interleukin-11 emerges as a master regulator of fibrosis, tissue integrity, and stromal inflammation. *Annu Rev Med.* (2020) 71:263–76. doi: 10.1146/annurev-med-041818-011649

48. Maier R, Ganu V, Lotz M. Interleukin-11, an inducible cytokine in human articular chondrocytes and synoviocytes, stimulates the production of the tissue inhibitor of metalloproteinases. *J Biol Chem.* (1993) 268:21527–32. doi: 10.1016/S0021-9258(20)80573-0

49. Hashimoto G, Inoki I, Fujii Y, Aoki T, Ikeda E, Okada Y. Matrix metalloproteinases cleave connective tissue growth factor and reactivate angiogenic activity of vascular endothelial growth factor 165. *J Biol Chem.* (2002) 277:36288–95. doi: 10.1074/jbc.M201674200

50. Gill SE, Parks WC. Metalloproteinases and their inhibitors: regulators of wound healing. *Int J Biochem Cell Biol.* (2008) 40:1334–47. doi: 10.1016/j.biocel.2007.10.024

51. Xia W, Szomor Z, Wang Y, Murrell GAC. Nitric oxide enhances collagen synthesis in cultured human tendon cells. *J Orthopaed Res.* (2006) 24:159–72. doi: 10.1002/jor.20060

52. Xia W, Wang Y, Appleyard RC, Smythe GA, Murrell GAC. Spontaneous recovery of injured Achilles tendon in inducible nitric oxide synthase gene knockout mice. *Inflamm Res.* (2006) 55:40–5. doi: 10.1007/s00011-005-0006-4

53. Murrell GAC, Szabo C, Hannafin JA, Jang D, Dolan MM, Deng XH, et al. Modulation of tendon healing by nitric oxide. *Inflamm Res.* (1997) 46:19–27. doi: 10.1007/s000110050027

54. Murakami M, Nakatani Y, Tanioka T, Kudo I. Prostaglandin E synthase. *Prostagland Other Lipid Mediat.* (2002) 68–9:383–99. doi: 10.1016/S0090-6980(02)00043-6

55. Park JY, Pillinger MH, Abramson SB. Prostaglandin E2 synthesis and secretion: the role of PGE2 synthases. *Clin Immunol.* (2006) 119:229–40. doi: 10.1016/j.clim.2006.01.016

56. Day AJ, Milner CM. TSG-6: a multifunctional protein with anti-inflammatory and tissue-protective properties. *Matrix Biol.* (2019) 78–9:60–83. doi: 10.1016/j.matbio.2018.01.011

57. Yang Y, Sun H, Li X, Ding Q, Wei P, Zhou J. Transforming growth factor beta-induced is essential for endotoxin tolerance induced by a low dose of lipopolysaccharide in human peripheral blood mononuclear cells. *Iran J Allergy Asthma Immunol.* (2015) 14:321–30.

58. Ruiz M, Toupet K, Maumus M, Rozier P, Jorgensen C, Noël D, et al. secreted by mesenchymal stromal cells ameliorates osteoarthritis and is detected in extracellular vesicles. *Biomaterials.* (2020) 226:119544. doi: 10.1016/j.biomaterials.2019.119544

59. Chen P, Farivar AS, Mulligan MS, Madtes DK. Tissue inhibitor of metalloproteinase-1 deficiency abrogates obliterative airway disease after heterotopic tracheal transplantation. *Am J Respir Cell Mol Biol.* (2006) 34:464–72. doi: 10.1165/rcmb.2005-0344OC

60. Qi JH, Ebrahem Q, Moore N, Murphy G, Claesson-Welsh L, Bond M, et al. novel function for tissue inhibitor of metalloproteinases-3 (TIMP3): Inhibition of angiogenesis by blockage of VEGF binding to VEGF receptor-2. *Nat Med.* (2003) 9:407–15. doi: 10.1038/nm846

61. Rauniyar K, Jha SK, Jeltsch M. Biology of vascular endothelial growth factor C in the morphogenesis of lymphatic vessels. *Front Bioeng Biotechnol.* (2018) 6:7. doi: 10.3389/fbioe.2018.00007

62. Zhang F, Liu H, Stile F, Lei MP, Pang Y, Oswald TM, et al. Effect of vascular endothelial growth factor on rat achilles tendon healing. *Plast Reconstr Surg.* (2003) 112:1613–19. doi: 10.1097/01.PRS.0000086772.72535.A4

63. Liu X, Zhu B, Li Y, Liu X, Guo S, Wang C, et al. The role of vascular endothelial growth factor in tendon healing. *Front Physiol.* (2021) 12:766080. doi: 10.3389/fphys.2021.766080

64. Pufe T, Petersen WJ, Mentlein R, Tillmann BN. The role of vasculature and angiogenesis for the pathogenesis of degenerative tendons disease. *Scand J Med Sci Sports*. (2005) 15:211–22. doi: 10.1111/j.1600-0838.2005.00465.x

65. Halper J. Advances in the use of growth factors for treatment of disorders of soft tissues. In: Halper J, editor. *Progress in Heritable Soft Connective Tissue Disorders*. Dordrecht: Springer (2013). p. 69–76.

66. Millar NL, Murrell GAC, Mcinnes IB. Inflammatory mechanisms in tendinopathy - towards translation. *Nat Rev Rheumatol.* (2017) 13:110–22. doi: 10.1038/nrrheum.2016.213

67. Carrade Holt DD, Wood JA, Granick JL, Walker NJ, Clark KC, Borjesson DL. Equine mesenchymal stem cells inhibit T cell proliferation through different mechanisms depending on tissue source. *Stem Cells Dev.* (2014) 23:1258–65. doi: 10.1089/scd.2013.0537

68. Zhang J, Wang JHC. Prostaglandin E2 (PGE2) exerts biphasic effects on human tendon stem cells. *PLoS ONE.* (2014) 9:e87706. doi: 10.1371/journal.pone.0087706

69. Vasta S, di Martino A, Zampogna B, Torre G, Papalia R, Denaro V. Role of VEGF, nitric oxide, and sympathetic neurotransmitters in the pathogenesis of tendinopathy: a review of the current evidences. *Front Aging Neurosci.* (2016) 8:186. doi: 10.3389/fnagi.2016.00186

70. Cadby JA, David F, van de Lest C, Bosch G, van Weeren PR, Snedeker JG, et al. Further characterisation of an experimental model of tendinopathy in the horse. *Equine Vet J.* (2013) 45:642–8. doi: 10.1111/evj.12035

71. Patterson-Kane JC, Rich T. Achilles tendon injuries in elite athletes: Lessons in pathophysiology from their equine Counterparts. *ILAR J.* (2014) 55:86–99. doi: 10.1093/ilar/ilu004

72. Patterson-Kane JC, Becker DL, Rich T. The pathogenesis of tendon microdamage in athletes: the horse as a natural model for basic cellular research. *J Comp Pathol.* (2012) 147:227–47. doi: 10.1016/j.jcpa.2012.05.010

73. Kumar V, Abbas AK, Aster JC. Inflammation and repair. In: Kumar V, Abbas AK, Aster JC, editors. *Robbins and Cotran Pathologic Basis of Disease*. Philadelphia, PA: Elsevier Saunders (2015). p. 69–111.

74. Tarafder S, Chen E, Jun Y, Kao K, Sim KH, Back J, et al. Tendon stem/progenitor cells regulate inflammation in tendon healing via JNK and STAT3 signaling. *FASEB J.* (2017) 31:3991–8. doi: 10.1096/fj.201700071R

75. Stolk M, Klatte-Schulz F, Schmock A, Minkwitz S, Wildemann B, Seifert M. New insights into tenocyte-immune cell interplay in an *in vitro* model of inflammation. *Sci Rep.* (2017) 7:9801. doi: 10.1038/s41598-017-09875-x

76. Müller SA, Todorov A, Heisterbach PE, Martin I, Majewski M. Tendon healing: an overview of physiology, biology, and pathology of tendon healing and systematic review of state of the art in tendon bioengineering. *Knee Surg Sports Traumatol Arthrosc.* (2015) 23:2097–105. doi: 10.1007/s00167-013-2680-z

77. Ma S, Xie N, Li W, Yuan B, Shi Y, Wang Y. Immunobiology of mesenchymal stem cells. *Cell Death Differ.* (2014) 21:216–25. doi: 10.1038/cdd.2013.158

78. da Silva Meirelles L, Fontes AM, Covas DT, Caplan AI. Mechanisms involved in the therapeutic properties of mesenchymal stem cells. *Cytok Growth Factor Rev.* (2009) 20:419–27. doi: 10.1016/j.cytogfr.2009.10.002

79. Fan H, Zhao G, Liu L, Liu F, Gong W, Liu X, et al. Pre-treatment with IL-1β enhances the efficacy of MSC transplantation in DSS-induced colitis. *Cell Mol Immunol.* (2012) 9:473–81. doi: 10.1038/cmi.2012.40

80. Yao Y, Zhang F, Wang L, Zhang G, Wang Z, Chen J, et al. Lipopolysaccharide preconditioning enhances the efficacy of mesenchymal stem cells transplantation in a rat model of acute myocardial infarction. *J Biomed Sci.* (2009) 16:74. doi: 10.1186/1423-0127-16-74

81. Kim W, Lee SK, Kwon YW, Chung SG, Kim S. Pioglitazone-primed mesenchymal stem cells stimulate cell proliferation, collagen synthesis and matrix gene expression in tenocytes. *Int J Mol Sci.* (2019) 20:472. doi: 10.3390/ijms20030472

82. Ren G, Zhao X, Zhang L, Zhang J, L'Huillier A, Ling W, et al. Inflammatory cytokine-induced intercellular adhesion molecule-1 and vascular cell adhesion molecule-1 in mesenchymal stem cells are critical for immunosuppression. *J Immunol.* (2010) 184:2321–28. doi: 10.4049/jimmunol.0902023

83. Ren G, Zhang L, Zhao X, Xu G, Zhang Y, Roberts AI, et al. Mesenchymal stem cell-mediated immunosuppression occurs via concerted action of chemokines and nitric oxide. *Cell Stem Cell.* (2008) 2:141–50. doi: 10.1016/j.stem.2007.11.014

84. Bundgaard L, Stensballe A, Elbæk KJ, Berg LC. Mass spectrometric analysis of the in vitro secretome from equine bone marrow-derived mesenchymal stromal cells to assess the effect of chondrogenic differentiation on response to interleukin-1β treatment. *Stem Cell Res Therapy.* (2020) 11:187. doi: 10.1186/s13287-020-01706-7

85. Raikin SM, Garras DN, Krapchev PV. Achilles tendon injuries in a United States population. *Foot Ankle Int.* (2013) 34:475–80. doi: 10.1177/1071100713477621

86. Rajpar I, Barrett JG. Multi-differentiation potential is necessary for optimal tenogenesis of tendon stem cells. *Stem Cell Res Therapy.* (2020) 11:152. doi: 10.1186/s13287-020-01640-8

87. Lipman K, Wang C, Ting K, Soo C, Zheng Z. Tendinopathy: injury, repair, and current exploration. *Drug Des Devel Ther.* (2018) 12:591–603. doi: 10.2147/DDDT.S154660

88. Park SH, Lee HS, Young KW, Seo SG. Treatment of acute achilles tendon rupture. *Clin Orthoped Surg.* (2020) 12:1–8. doi: 10.4055/cios.2020.12.1.1

89. Tsekes D, Konstantopoulos G, Khan WS, Rossouw D, Elvey M, Singh J. Use of stem cells and growth factors in rotator cuff tendon repair. *Eur J Orthopaed Surg Traumatol.* (2019) 29:747–57. doi: 10.1007/s00590-019-02366-x

90. Cho WS, Chung SG, Kim W, Jo CH, Lee SU, Lee SY. Mesenchymal stem cells use in the treatment of tendon disorders: a systematic review and meta-analysis of prospective clinical studies. *Ann Rehabil Med.* (2021) 45:274–83. doi: 10.5535/arm.21078

91. van den Boom NAC, Winters M, Haisma HJ, Moen MH. Efficacy of stem cell therapy for tendon disorders: a systematic review. *Orthopaed J Sports Med.* (2020) 8:1–10. doi: 10.1177/2325967120915857

92. Oreff GL, Fenu M, Vogl C, Ribitsch I, Jenner F. Species variations in tenocytes' response to inflammation require careful selection of animal models for tendon research. *Sci Rep*. (2021) 11:12451. doi: 10.1038/s41598-021-91914-9

frontiers | Frontiers in Veterinary Science

TYPE Original Research
PUBLISHED 14 November 2022
DOI 10.3389/fvets.2022.1011905

OPEN ACCESS

EDITED BY
Eleonora Iacono,
University of Bologna, Italy

REVIEWED BY
Hesam Dehghani,
Ferdowsi University of Mashhad, Iran
Mudasir Bashir Gugjoo,
Sher-e-Kashmir University of Agricultural Sciences and Technology of Kashmir, India

*CORRESPONDENCE
Madhu S. Dhar
mdhar@utk.edu

†PRESENT ADDRESSES
Michael Caruso,
Reedsdale Equine Specialists, Tullahoma, TN, United States
James Schumacher,
2026 Via Tesoro, Las Cruces, NM, United States

SPECIALTY SECTION
This article was submitted to Veterinary Regenerative Medicine, a section of the journal Frontiers in Veterinary Science

RECEIVED 04 August 2022
ACCEPTED 18 October 2022
PUBLISHED 14 November 2022

CITATION
Caruso M, Shuttle S, Amelse L, Elkhenany H, Schumacher J and Dhar MS (2022) A pilot study to demonstrate the paracrine effect of equine, adult allogenic mesenchymal stem cells *in vitro*, with a potential for healing of experimentally-created, equine thoracic wounds *in vivo*. *Front. Vet. Sci.* 9:1011905. doi: 10.3389/fvets.2022.1011905

A pilot study to demonstrate the paracrine effect of equine, adult allogenic mesenchymal stem cells *in vitro*, with a potential for healing of experimentally-created, equine thoracic wounds *in vivo*

Michael Caruso[1†], Shannon Shuttle[1], Lisa Amelse[1], Hoda Elkhenany[1,2], James Schumacher[1†] and Madhu S. Dhar[1,2*]

[1]Department of Large Animal Clinical Sciences, College of Veterinary Medicine, University of Tennessee, Knoxville, Knoxville, TN, United States, [2]Department of Surgery, Faculty of Veterinary Medicine, Alexandria University, Alexandria, Egypt

Regenerative biological therapies using mesenchymal stem cells (MSCs) are being studied and used extensively in equine veterinary medicine. One of the important properties of MSCs is the cells' reparative effect, which is brought about by paracrine signaling, which results in the release of biologically active molecules, which in turn, can affect cellular migration and proliferation, thus a huge potential in wound healing. The objective of the current study was to demonstrate the *in vitro* and *in vivo* potentials of equine allogenic bone marrow-derived MSCs for wound healing. Equine bone marrow-derived MSCs from one allogenic donor horse were used. Equine MSCs were previously characterized for their *in vitro* proliferation, expression of cluster-of-differentiation markers, and trilineage differentiation. MSCs were first evaluated for their migration using an *in vitro* wound healing scratch assay, and subsequently, the conditioned medium was evaluated for their effect on human fibroblast proliferation. Subsequently, allogenic cells were intradermally injected into full-thickness, cutaneous thoracic wounds of 4 horses. Wound healing was assessed by using 3-D digital imaging and by measuring mRNA expression of pro-and anti-inflammatory markers for 30 days. Using human fibroblasts in an *in vitro* wound healing assay, we demonstrate a significantly higher healing in the presence of conditioned medium collected from proliferating MSCs than in the presence of medium containing fetal bovine serum. The *in vitro* effect of MSCs did not translate into a detectable effect *in vivo*. Nonetheless, we proved that molecularly characterized equine allogenic MSCs do not illicit an immunologic response. Investigations using MSCs derived from other sources (adipose tissue, umbilical cord), or a higher number of MSCs or a compromised animal model may be required to prove the efficacy of equine MSCs in wound healing *in vivo*.

KEYWORDS

horse, mesenchymal stem cells, wound healing, bone marrow, allogenic cells, thoracic wounds

Introduction

Regenerative biological therapies using mesenchymal stem cells are being used extensively to treat horses for injuries. Bone marrow-derived mesenchymal stem cells or mesenchymal stromal cells (BM-MSCs) are self-renewing, expandable *in vitro*, and able to differentiate into cellular lineages, each capable of producing various types of cells, including adipocytes, osteoblasts, chondrocytes, and skin cells (1–5).

Wound healing is a dynamic process involving complex interactions between many cellular and biochemical events. Paracrine signaling results in the release of soluble factors, including growth factors, cytokines, and chemokines that promote the many biological events required for healing, such as cellular migration and proliferation, deposition of extracellular matrix, angiogenesis, and remodeling (5–8). The release of these factors from fibroblasts, inflammatory cells, skin progenitor cells, and fat- and bone marrow-derived MSCs, are crucial to these biological events (4, 6, 8–11). Several mechanisms by which MSCs exert a positive effect on wound healing have been identified. These include the enhancement of angiogenesis by secretion of pro-angiogenic factors and the differentiation into endothelial cells and/or pericytes, M2 macrophages polarization, the recruitment of endogenous stem/progenitor cells, extracellular matrix production and remodeling, and immunosuppressive effects. (12).

Studies of the effects of MSCs transplanted into wounds of human patients and experimentally created wounds of other species, including rodents, rabbits, goats, and dogs, have demonstrated the therapeutic effects of MSCs in improving dermal regeneration and healing (4, 6, 8, 9, 13–16). The reparative effect of MSCs is brought about by paracrine signaling, which results in release of biologically active molecules that affect cellular migration and proliferation, and in survival of cells surrounding the injured area (8, 11). Javazon et al. demonstrated that directly applying BM-MSCs to cutaneous wounds of diabetic mice resulted in significantly improved epithelialization, angiogenesis, and formation of granulation tissue (10). Kim et al. documented that MSC-treated wounds of dogs healed more rapidly with increased cellular proliferation, collagen synthesis, and angiogenesis than did control wounds (15). Arno et al. showed that MSCs derived from human Warton's Jelly promoted wound healing in mice by up-regulating the expression of genes involved in neovascularization, re-epithelialization, and fibroproliferation in MSC-treated fibroblasts (8).

Even though the pathophysiological mechanisms of equine wound repair, and the effects of platelet-rich plasma on equine wound healing have been reported (17, 18), reports demonstrating the effect of equine BM-MSCs on experimentally created wounds of horses are lacking. We hypothesized that eBM-MSCs have the potential to speed healing of wounds of horses, and that we could demonstrate this potential *in vitro* and *in vivo*. We hypothesized that injecting molecularly-tested, allogenic, eBM-MSCs into the periphery of a cutaneous wound would not trigger an adverse effect and would enhance epithelialization and wound contraction primarily through paracrine signaling. To prove our hypotheses, eBM-MSCs cultured from a 4-year-old, mixed-breed gelding and previously characterized with respect to their proliferation, expression of stem-cell markers, and *in vitro* capacity for tri-lineage differentiation were used (19, 20). *In vitro* scratch assays were performed to assess the effect of conditioned medium (CM) collected from eBM-MSCs on the migration and proliferation of human skin primary fibroblasts. Finally, eBM-MSCs were applied to experimentally-created, full-thickness, cutaneous thoracic wounds of 4 adult horses to evaluate the wound healing response *in vivo*.

Materials and methods

Animals

All experiments were carried out using institution approved protocols. Three female American Quarter horses and one, mixed-breed female horse, 12–23 years old, were used as recipients of the eBM-MSCs. All had no current or past health problems. All were housed and maintained under the same conditions, and each was confined to an individual stall.

Allogenic eBM-MSCs

All procedures were performed as described previously (19, 20). Allogenic eBM-MSCs from one 4-year-old, mixed breed horse, which was negative for Equine infectious anemia, equine parvovirus, equine pegivirus, non-primate hepacivirus, and Theiler's diseases associated virus, were used. Cryobanked MSCs, previously characterized by their proliferation, expression of mesenchymal stem cell surface markers and *in vitro* trilineage differentiation potential were used. Cryopreserved cells were thawed rapidly in a 37°C water bath and were washed with prewarmed phenol red-free, antibiotic - free, and FBS-free media. Cells were collected by centrifugation at 200 g at room temperature for 10 min. Cells were suspended in Dulbecco's Modified Eagle Medium (DMEM F12), and incubated at 37°C in presence of DMEM F12 + 10% fetal bovine serum + 1% penicillin/streptomycin mixture. The incubator was maintained at 5% CO_2 and 95% atmospheric air.

Equine BM-MSCs were expanded and cells from passages 4–5 were used in the *in vitro* scratch assays and for implantation into the wounds *in vivo*.

Total RNA was extracted from biopsy samples from each horse at 3, 7, 15, and 30 days after treatment. using an RNeasy

Mini RNA kit[1] according to the manufacturer's instructions and as described earlier (19). Messenger RNA expressions of pro- and anti-inflammatory targets, including, TGFβ, IGF, IL1β, TNFα, and IL8, were measured using quantitative PCR. SYBR green-based absolute blue qPCR mix[2] with100-pM concentrations of commercially synthesized, forward and reverse primers[2] were used. PCR conditions and the primer sequences were as described earlier (21, 22).

All qPCRs were run on the Agilent Mx3005P, and data were analyzed using MxPro analysis software[3]. Delta Ct was calculated for each sample after it was normalized with the Ct value of equine 18S RNA. Using a cDNA blank, samples with a Ct value of $\geq$30 were given an arbitrary expression of zero.

Preparation of conditioned medium (cm)

Equine BM-MSCs from the allogenic donor were seeded at a cellular density of about 5000 cells/cm^2, and the CM was collected after 48 h.

Human foreskin fibroblasts (HFF-1)

Commercially obtained, normal human fibroblasts (HFF-1)[4] were grown in DMEM high glucose medium[5] containing 10% fetal bovine serum and 1% penicillin/streptomycin at 37°C, with 5% CO_2. Passage 7–8 HFF cells were seeded at a cellular density of about 5000 cells/cm^2, and the CM was collected after 48 h.

Proliferation and migration of HFF

Migration of HFFs was demonstrated *in vitro* using a wound healing assay. Human fibroblasts were seeded at density of 20,000 cells/cm^2 to form a monolayer of cells of about 80% confluency. One scratch/sample/well was made with a 200 μL pipette tip, to ensure that a gap of 400–500 μM was created in each well. Cellular debris was washed with Hank's Balanced Salt Solution[2]. Cells were then maintained in the presence of eBMMSC-CM, HFF-CM, or FBS-containing growth medium. Cells incubated in the presence of 0% eBMMSC-CM (100% FBS), 10, 25, 50, and 75% eBMMSC-CM (90–25% FBS), and 100% eBMMSC-CM (0% FBS), and HFF-CM were tested.

In vitro migration in the presence of freshly collected CM was also compared to the migration in the presence of a thawed sample that had been frozen at −80°C. Each assay was repeated in triplicate in two independent experiments.

For gap/wound closure or healing, two randomly selected points along each wound were identified, and the horizontal distance between the two wound edges was measured using black and white phase-contrast microscopy. Measurements were made at 16, 20, 24, 40, and 44 h, post-wounding.

The HFF proliferation rate in presence of eBMMSC-CM was assessed at 2, 4, and 7 days using the CellTiter 96® Aqueous Non-Radioactive (MTS) assay[6] according to the manufacturer's instructions. The optical density of the complex formed between cells and the MTS reagent was measured on a microplate fluorescence reader[7] at 490 nm. Medium without cells was used as a blank. A graph of sample absorbance corrected with the blank vs. days of proliferation was generated, and data were analyzed. HFF growth medium and 100% FBS-containing MSC growth medium were used as controls.

In vivo equine cutaneous wound healing model

Under sedation, two, 4-cm diameter and two, 2-cm diameter wounds were created aseptically on each side of the thorax of each recipient horse. The 4-cm diameter wounds were created at the 14th and 10th intercostal spaces on a line parallel to the ground at the level of the ventral aspect of the tuber coxae. The 2-cm diameter wounds were created at the 14th and 10th intercostal spaces, 4–6 cm ventral to the 4-cm diameter wounds. Skin at the site of wounding was desensitized with 2% mepivacaine HCl[2]. A shallow, circular cutaneous skin incision was created using a stainless steel, 4-cm or 2-cm punch. The incision was extended to subcutaneous tissue with a scalpel blade, and skin within each incision was sharply excised and designated as the day 0 sample. Sterile gauze pads were applied to each wound, and the wounds were covered with a sterile, combine bandage, which was secured to the thorax with a commercially available abdominal bandage[8].

Subcutaneous implantation of allogenic eBM-MSCs

Two days post-wounding, 2 × 10^6 eBM-MSCs suspended in 1 mL sterile, isotonic saline solution were injected subcutaneously at 4 equidistant sites on each wound. The untreated wounds served as controls and were injected with

1 Qiagen, Valencia, California, USA.

2 Fisher Scientific, Pittsburgh, Pennsylvania, USA.

3 Agilent Technologies, Santa Clara, California, USA.

4 ATCC, Manassas, VA, USA.

5 Carl Zeiss Inc., Thornwood, New York, New York, USA microscope.

6 Promega Inc., Madison, Wisconsin, USA.

7 BioTeck, Winooski, Vermont, USA.

8 Wire 2 Wire Vet Products, LLC, Lexington, KY, USA.

the vehicle only. Wounds were dressed and bandaged as described above.

3-D imaging for wound measurements

All 4-cm diameter wounds were photographed immediately after wound creation (time 0), and at each bandage change. Images were imported into a computer software program linked to the 3-D camera[9], and data were analyzed as described earlier (23). The percentage wound healing was calculated by measuring the wound area at days 3, 7, 15 and 30 post treatment. Changes in areas at each time point were compared to the areas measured at day 0, and are finally reported as the % change.

Skin biopsies

The 2-cm diameter wounds were biopsied to collect samples for RNA isolation and qPCR. Each biopsy was obtained from a different site on each wound.

Statistical analyses

All qPCR data were analyzed using mixed model analysis, with the gene expression ratios as the dependent variables, treatment as the between-subject fixed independent factor, time as the within-subject independent factor, and horse nested within treatment as the random factor. SAS procedure, PROC MIXED in SAS/STAT[10] was used to conduct the analyses. Similarly, all measurements for the *in vitro* wound healing assays and the *in vivo* wound images were compared using 2-way ANOVA. Statistical significance was set to $P < 0.05$. All graphs are generated using GraphPad Prism 9.

Results

Equine BMMSC-CM promotes wound healing *in vitro*

To assess the effect of eBM-MSCs on wound healing, an *in vitro* wound healing assay was performed, wherein the HFF migration was assessed in the presence of eBMMSC-CM for 16–44 h. In the first experiment, the effect of wound closure was evaluated using a range of concentrations of the conditioned media, and wound healing was assessed in presence of 0, 10, 25, 50, 75, and 100% eBMMSC-CM (Figures 1A,B). Significant HFF migration treated with 100% eBMMSC-CM resulted in gap closure as early as 16 h ($P < 0.05$), whereas no gap closure was observed in HFFs treated with growth medium containing 10% FBS even after 44 h post-wounding (Figure 1A).

Even though all doses of eBMMSC-CM showed healing, significant effects were consistently observed at all time-points with 100% eBMMSC-CM. Figure 1B represents microscopic images comparing the wound healing in presence of medium containing 10% FBS with 100% eBMMSC-CM. All measurements were compared to measurements at time 0 and then expressed as percentage healing relative to the wound's original size.

Next, wound healing in presence of 100% freshly isolated eBMMSC-CM was compared with that in the presence of eBMMSC-CM stored in −80°C. This experiment was carried out to mimic a clinical condition in which freshly expanded or cryopreserved allogenic MSCs could be provided for immediate use. As demonstrated in Figure 1C, significant gap closure was observed at all time-points in presence of both fresh and frozen CM. Note that freshly collected CM provided a relatively higher healing percentage, which was not statistically significant.

Equine BMMSC-CM promote the proliferation of HFF *in vitro*

Because proliferation of fibroblasts is an important aspect of wound healing, we next determined whether the increased incidence of wound closure in HFFs is also accompanied by an increase in enhanced proliferation of fibroblasts treated with eBMMSC-CM. As illustrated in Figure 2, HFFs were cultured for 7 days in presence of freshly isolated 100% eBMMSCs-CM, and the HFF proliferation was measured using the MTS assay. Cell proliferation linearly increased 3-fold within 7 days. No cell death was observed during this time.

Lack of immunologic response to allogenic eBM-MSCs

As determined by visible and subjective clinical analyses, all horses remained clinically normal throughout the study period. Appetite, body weight, activity, body temperature, and heart and respiratory rates were always within normal limits. Healing in all wounds progressed without visible signs of infection or immunogenic reaction suggesting that the allogenic MSCs could be used safely *in vivo*.

Effect of equine BMMSC-CM on wound healing *in vivo*

Next, we assessed if the *in vitro* effects observed with eBMMSC-CM could be translated to an *in vivo* wound model. All 4-cm diameter wound images were analyzed using a

9 Eykona Technologies Ltd., Fuel3D Inc., Greenville, NC, USA.

10 SAS Institute Inc., Cary, NC, USA.

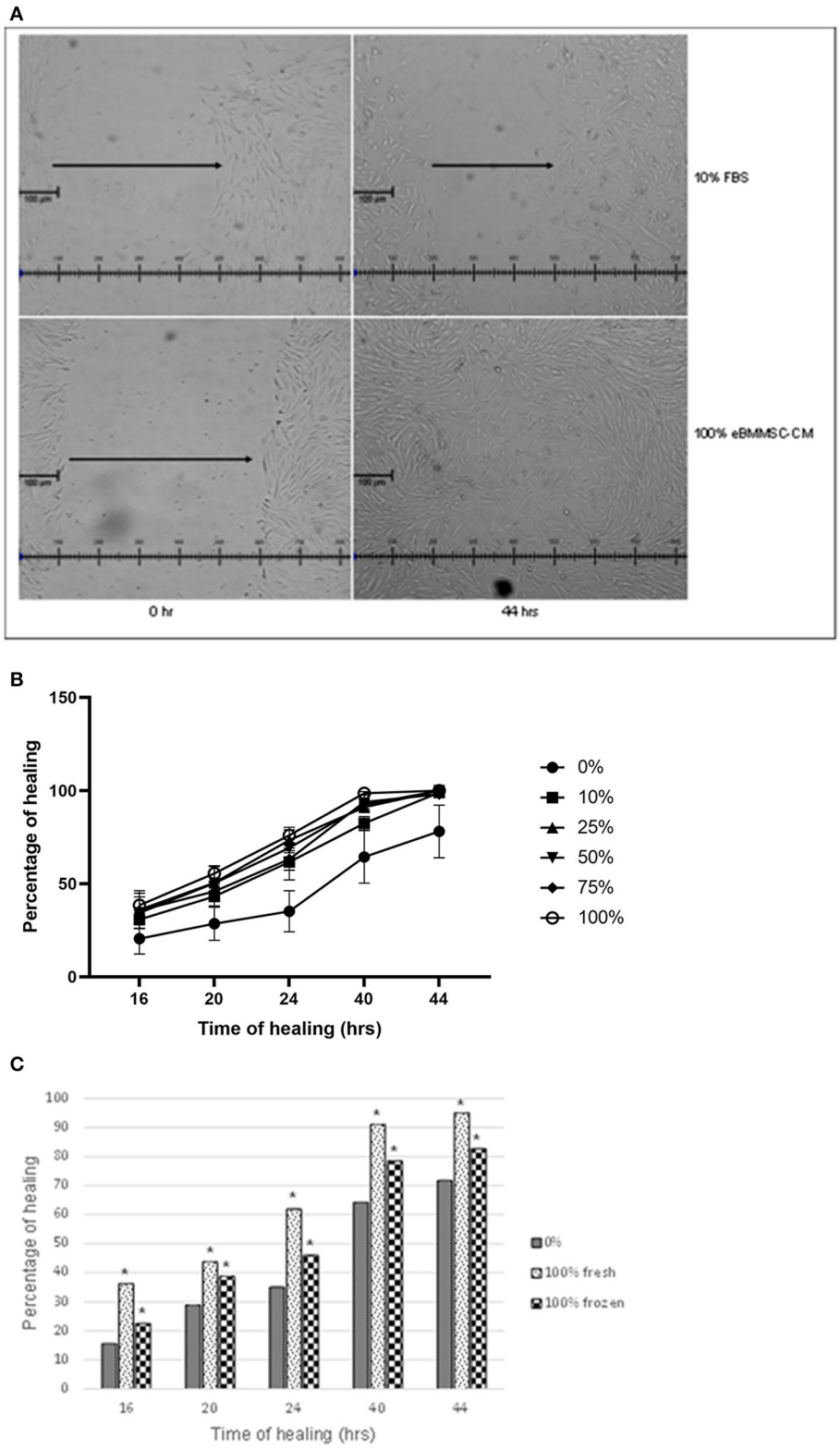

FIGURE 1
(A) Effect of varying eBMMSC-CM concentrations. 400–500 μm gaps were created in a monolayer of HFFs, and were treated with varying concentrations of eBMMSC-CM for 16–44 h. Gap closure was measured at each time point and data is reported as the percentage healing at a

(Continued)

FIGURE 1 (Continued)
specific point relative to time 0. Results are shown as the mean ± SD of quadruplicates within a representative of two independent experiments. *$P < 0.05$ is considered significant. **(B)** Effect of eBMMSC-CM on HFF migration. 400–500 μm gaps were created in a monolayer of HFFs, and were treated with growth medium containing 10% FBS (Top) or 100% eBMMSC-CM (Bottom), and gap closure was evaluated using phase contrast microscopy. Representative images of quadruplicates within a representative of two independent experiments are shown. **(C)** *In vitro* wound healing assay to compare frozen and freshly isolated eBMMSC-CM. 400–500 μm gaps were created in a monolayer of HFFs, and were treated with either freshly isolated 100% eBMMSC-CM or 100% eBMMSC-CM stored in -80^0C. Wound Gap closure was measured at each time point and data is reported as the percentage healing at a specific point relative to time 0. Results are shown as the mean ± SD of quadruplicates within a representative of two independent experiments. *$P < 0.05$ is considered significant.

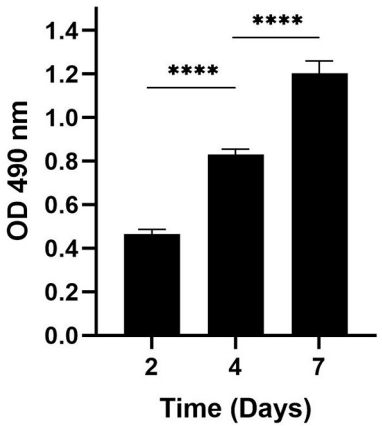

FIGURE 2
Measurement of proliferation rate of HFFs. MTS assay was used to demonstrate the proliferation of HFFs in presence of 100% eBMMSC-CM over a period of 7 days. The results represent the mean ± SD with $n = 3$ for each bar. ****$p < 0.0001$.

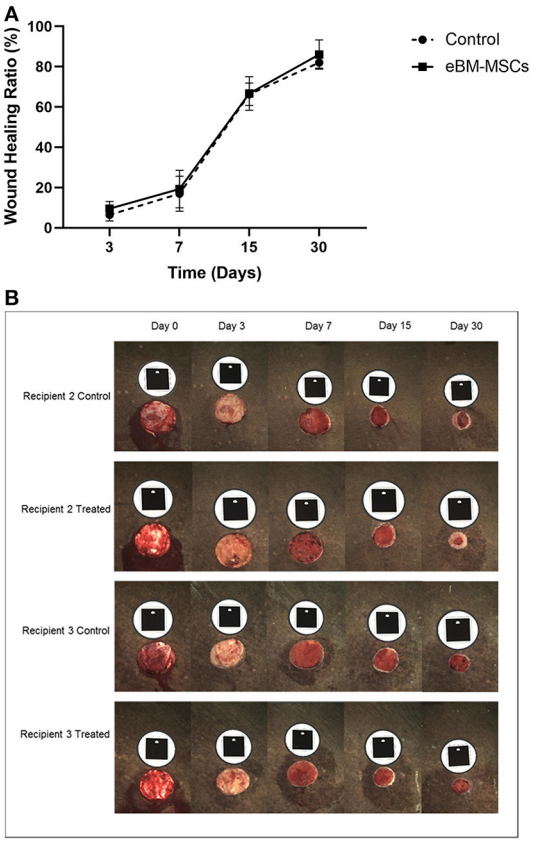

FIGURE 3
Wound healing in recipient horses. **(A)** Graph showing percentage changes in wound healing in all horses as a function of time. The wound area is measured in mm^2 at time 0, and subsequently at days 3, 7, 15 and 30. The area at each time point is then compared to the area at time 0. Finally, the % wound healing is expressed and plotted graphically. **(B)** Representative digital images of the 4 cm diameter wounds in the recipients 2 and 3 at various time points are shown. The black tag above each wound is the marker and is recognized by the camera to ensure a consistent and reproducible angle when the image is taken. Note the significant amount of epithelialized region of the wound in the Recipient 2 treated panel.

trace-area function in the software. All measurements were recorded in mm^2 (23). Using the digital images, we measured the Healing rate (mm^2/day) = (previous total area – subsequent inner area) ÷ number of days between the two time-points (Figure 3A). The healing rate was used to assess the combined effect of epithelialization and contraction because these two processes occur simultaneously and could not be segregated. Epithelialization was observed subjectively in all groups only after day 15.

As seen in the representative pictures from one recipient horse, subjectively, eBMMSC-treated wounds appeared to show a faster healing rate with increased epithelialization compared to controls (Figure 3B). These changes were observed in 2 out of 4 recipients indicating horse-to-horse variation. As a result, when data from all the horses were taken together, none of the measurements obtained above were significantly different between control and stem cell-treated wounds.

In vivo mRNA expression of pro– and anti–inflammatory markers

Different phases of wound healing are accompanied by changes in cytokines, and therefore, we assessed whether there were any eBM-MSC-mediated modulations of mRNA expression of TGFβ, IGF, IL1β, TNFα, and IL8, pre- and post-treatment. Real-time PCR profiles of each of the markers were assessed at days 3, 7, 15, and 30 post-treatment. Samples of

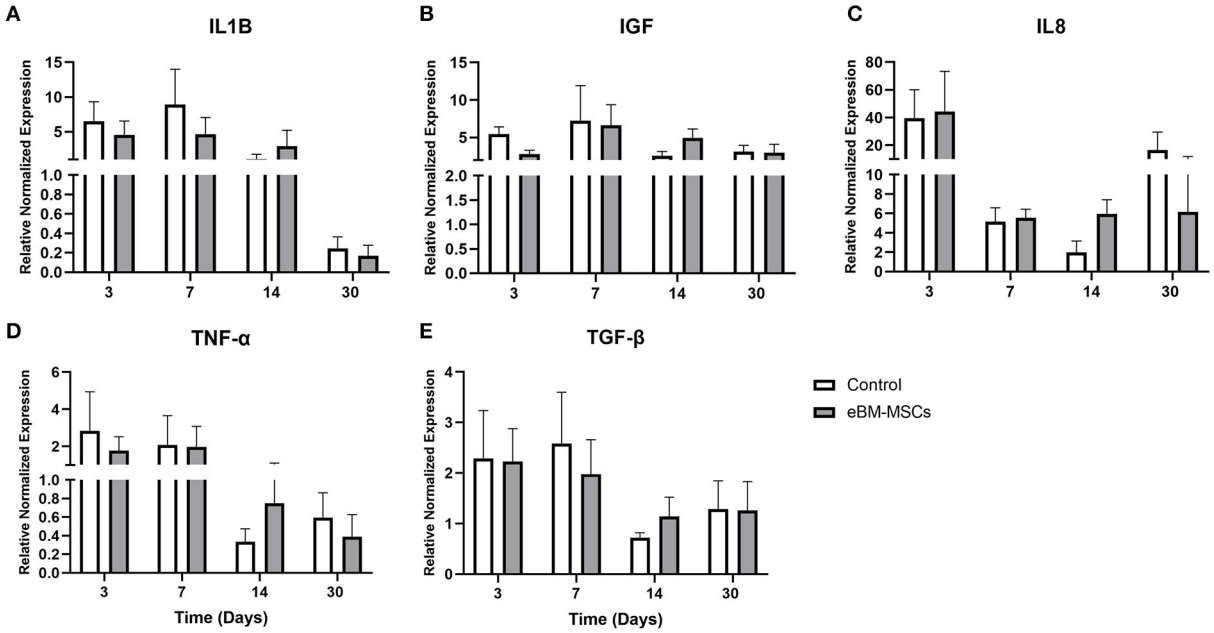

FIGURE 4
Real time PCR of the pro- and anti-inflammatory markers. The expression profiles of ILβ **(A)**, IGF **(B)**, IL8 **(C)**, TNFα **(D)** and TGFβ **(E)** were generated at days 3, 7, 15 and 30 post therapy. Changes in expression for each mRNA was normalized with the Ct values obtained for 18S RNA and are plotted as Delta Ct in arbitrary units (AU). $P < 0.05$ was set as significant.

skin collected when the wounds were created (day 0) were used as pretreated samples. Normalized delta Ct values of each mRNA obtained at days 3,7,15, and 30 were compared day 0 to assess these changes (Figure 4). Results demonstrated no significant changes in expression between control and treated groups during the entire study.

Discussion

Bone-marrow-derived MSCs are multipotent cells that have the potential to differentiate into multiple lineages, including lineages capable of producing adipocytes, osteocytes, chondrocytes, neurons, skeletal muscle, and endothelial cells (1–5). Adult MSCs are ideal to use in cellular-based therapies because of the relative ease of techniques for isolation and expansion and because of their low immunogenicity.

Using the minimal set of standard criteria (24, 25), we have identified an allogenic donor from which MSCs were generated and cryopreserved and used in this study. Because BM-MSCs obtained from different organisms, including horses, are immunomodulatory and lack the MHC II, they should not illicit an immunologic response when implanted into the tissues of another animal. With this knowledge, we were confident that we could safely implant eBM-MSCs from the allogenic donor into the experimentally created wounds of the 4 horses used in this study. As expected, none of the recipient horses showed signs of immunological response to the allogenic cells.

Cutaneous wound healing is a complex process primarily involving the migration and proliferation of fibroblalsts. We used an immortalized, commercially available HFF-cell line, and fibroblasts cultured served to assess dermal fibroblastic response to injury *in vitro*. We assessed the effect of CM derived from healthy, proliferating eBM-MSCs on proliferation of HFFs and subsequently cultured the human HFFs and created a "wound" on the monolayer and assessed the paracrine effect that the eBM-MSCs had on closure of that wound.

The *in vitro* analyses revealed that eBMMSC-CM enhances both the migration and proliferation of human fibroblasts, suggesting that eBM-MSCs may secrete a factor or factors necessary for healing, thus supporting their paracrine function. This agrees with other studies (26, 27). For instance, *in vitro* studies have shown that conditioned medium from fat-derived MSCs alone accelerates wound healing in mice due to the paracrine effect of the medium. Pro-angiogenic factors, such as vascular endothelial growth factor (VEGF), are secreted from MSCs, and these factors have been suggested to be one of the pro-angiogenic mechanisms by which fat-derived MSCs accelerate healing *in vivo* (26, 27). Similarly, promotion of proliferation and migration of mouse keratinocytes *in vivo* by conditioned medium of BM-MSCs has been demonstrated (28).

In our study, the significant effect of eBM-MSCs on wound healing observed *in vitro* did not translate consistently *in vivo*,

even though digital imaging showed an increased healing in the BMMSC-treated wounds in 2 out of 4 recipients. We have several hypotheses to explain this discrepancy. One important factor to consider is the source of MSCs. Fat-derived equine MSCs might prove to be better than eBM-MSCs at healing of equine wounds. Liu et al. demonstrated that human, fat-derived MSCs had a more substantial effect on the cutaneous wound healing of mice than did MSCs derived from the amnion and bone marrow. Histological evaluation showed enhanced epithelialization only in the group treated with fat-derived MSCs (29).

Secondly, using MSCs to speed wound healing may be beneficial only when healing is impaired or compromised. Mesenchymal stem cells might prove beneficial when applied to non-healing and chronic wounds, such as those of elderly human patients, diabetic patients, patients with large injuries, and patients receiving glucocorticosteroid therapy. Wounds of these patients have impaired production of cytokines and reduced angiogenesis (30–33). The experimentally created wounds on the horses' thorax in this study were acute, and the horses were systemically normal. Furthermore, in this model, since the wounds were not chronic, the paracrine effect of the eBM-MSCs may have been inconsequential, because the growth factors involved in wound healing may have been abundant and functional, making those supplied by the MSCs redundant. MSCs might prove useful when applied to chronic wounds depleted of functional or containing non-functional growth factors. Because wounds on the distal portion of the limb of horses heal more slowly than those on the thorax (34), a limb wound model might be considered compromised and may be more likely to demonstrate positive effects of exogenous MSCs. The disadvantage of using an equine limb wound model, however, is exuberant granulation tissue formation which may confound the results. In a pilot study using 2 horses, we found that control wounds and eBMMSC-treated wounds on the distal portion of the limb filled with exuberant granulation tissue. The results were difficult to interpret when measures to control exuberant granulation tissue formation were instituted (data not shown).

Finally, the viability and the sustained presence of eBM-MSCs at the site of implantation also raise some doubt about the efficacy of MSCs in wound healing in this model.

Latest tissue engineering approaches emphasize the application of scaffolds in wound healing (35–37). Even though a variety of natural and synthetic material-based scaffolds are being fabricated, appropriate knowledge of the physicochemical properties of the biomaterials and scaffolds is needed. At the same time, one has to evaluate the interaction between endogenous progenitor and exogenously delivered stem cells with the scaffolds and hence, even though there is potential, practical skin scaffold materials remain to be developed. Challenges exist that we have to circumvent before translating this technology to skin tissue engineering.

The *in vivo* portion of this study was a pilot experiment to assess whether the paracrine effect of eBM-MSCs observed *in vitro* could be translated in a relatively simple wound model, and hence, a small sample number of horses were used. As demonstrated in Figure 3, objective measurements showed that the wounds of 2 of the 4 treated horses had improved healing, but, this positive effect was not significant when data from all 4 horses was analyzed collectively. Nonetheless, our data clearly supports the use of molecularly–tested equine allogenic eBM-MSCs to be a potential source of cells for the treatment of cutaneous wounds without any adverse effects. Even though there are published reports that demonstrate that mesenchymal stem cells do have the potential to heal equine cutaneous wounds (38–40), finding an optimal source of MSCs, finding an optimal number of cells to use, time and the route at which the therapy should be applied, and priming MSCs by exposing them to bioactive scaffolds are some of the aspects of regenerative medicine, which should be considered for a consistent and reproducible response.

In summary, we present data showing that eBM-MSCs enhance the proliferation and paracrine function of cutaneous fibroblasts. This *in vitro* effect induced by BM-MSCs, however, could not be replicated consistently, *in vivo* using our model. The influence of the source of equine MSCs for *in vivo* application to wounds requires more investigation, and the model used for *in vivo* assessment and delivery of MSCs may need to be improved.

The concentration and the quality of RNA was evaluated using the RNA 6000 Nano Kit and the 2100 Bioanalyzer system as per the manufacturer's recommendations (Agilent Technologies, Santa Clara, CA). An electropherogram showed intact 28S and 18S RNA bands and confirmed high quality RNA with RIN values > 9.0.

Data availability statement

The original contributions presented in the study are included in the article/supplementary materials, further inquiries can be directed to the corresponding authors.

Ethics statement

The animal study was reviewed and approved by University of Tennessee, Institutional Animal and Care Committee.

Author contributions

JS and MD were responsible for all *in vivo* and *in vitro* experimental planning, execution, data analysis and interpretation, respectively. MC carried out all *in vivo* experiments and data analysis. SS carried out *in vitro* wound assays and assisted MC in the animal studies. HE and LA

carried out the fibroblast proliferation and real time PCR assays. All authors proof read the manuscript and gave their consent for publication.

Funding

This work was supported by the Center of Excellence in Livestock Diseases and Human Health, University of Tennessee, Knoxville.

Acknowledgments

The authors thank Dr. Xiaocun Sun for assistance with statistical analysis and Drs. D. Geiser and A. Anderson for reviewing this manuscript.

Conflict of interest

The authors declare that the research was conducted in the absence of any commercial or financial relationships that could be construed as a potential conflict of interest.

Publisher's note

References

1. Fu X, Liu G, Halim A, Ju Y, Luo Q, Song G. Mesenchymal stem cell migration and tissue repair. *Cells.* (2019) 8:784. doi: 10.3390/cells8080784

2. Caplan AI. Mesenchymal stem cells: Time to change the name. *Stem Cells Transl Med.* (2017) 6:1445–51. doi: 10.1002/sctm.17-0051

3. Prockop DJ. Marrow stromal cells as stem cells for nonhematopoietic tissues. *Science.* (1997) 276:71–4. doi: 10.1126/science.276.5309.71

4. Fathke C, Wilson L, Hutter J, Kapoor V, Smith A, Hocking A, et al. Contribution of bone marrow-derived cells to skin: collagen deposition and wound repair. *Stem Cells.* (2004) 22:812–22. doi: 10.1634/stemcells.22-5-812

5. Sorrell JM, Caplan AI. Topical delivery of mesenchymal stem cells and their function in wounds. *Stem Cell Res Ther.* (2010) 1:6. doi: 10.1186/scrt30

6. Singer AJ, Clark RA. Cutaneous wound healing. *N Engl J Med.* (1999) 341:738–46. doi: 10.1056/NEJM199909023411006

7. Wu Y, Chen L, Scott PG, Tredget EE. Mesenchymal stem cells enhance wound healing through differentiation and angiogenesis. *Stem Cells.* (2007) 25:2648–59. doi: 10.1634/stemcells.2007-0226

8. Arno AI, Amini-Nik S, Blit PH, Al-Shehab M, Belo C, Herer E, et al. Human Wharton's jelly-mesenchymal stem cells promote skin wound healing through paracrine signaling. *Stem Cell Res Therapy.* (2014) 5:13. doi: 10.1186/scrt417

9. Nakagawa H, Akita S, Fukui M, Akino K. Human mesenchymal stem cells successfully improve skin-substitute wound healing. *Br J Dermatol.* (2005) 153:29–36. doi: 10.1111/j.1365-2133.2005.06554.x

10. Javazon EH, Keswani SG, Badillo AT, Crombleholme TM, Zoltick PW, Radu AP, et al. Enhanced epithelial gap closure and increased angiogenesis in wounds of diabetic mice treated with adult murine bone marrow stromal progenitor cells. *Wound Rep Reg.* (2007) 15:350–9. doi: 10.1111/j.1524-475X.2007.00237.x

11. Hocking AM, Gibran NS. Mesenchymal stem cells: paracrine signaling and differentiation during cutaneous wound repair. *Exp Cell Res.* (2010) 316:2213–9. doi: 10.1016/j.yexcr.2010.05.009

12. Motegi SI, Ishikawa O. Mesenchymal stem cells: the roles and functions in cutaneous wound healing and tumor growth. *J Dermatol Sci.* (2017) 86:83–9. doi: 10.1016/j.jdermsci.2016.11.005

13. Herdrich BJ, Lind RC, Liechty KW. Multipotent adult progenitor cells: their role in wound healing and the treatment of dermal wounds. *Cytotherapy.* (2008)10:543–550. doi: 10.1080/14653240802345820

14. Azari O, Babaei H, Derakhshanfar A, Nematollahi-Mahani SN, Poursahebi R, Moshrefi M. Effects of transplanted mesenchymal stem cells isolated from Wharton's jelly of caprine umbilical cord on cutaneous wound healing; histopathological evaluation. *Vet Res Commun.* (2011) 35:211–22. doi: 10.1007/s11259-011-9464-z

15. Kim JW, Lee JH, Lyoo YS, Jung DI, Park HM. The effects of topical mesenchymal stem cell transplantation in canine experimental cutaneous wounds. *Vet Dermatol.* (2013) 24:242–e53. doi: 10.1111/vde.12011

16. Maxson S, Lopez EA, Yoo D, Danilkovitch-Miagkova A, LeRoux MA. Role of mesenchymal stem cells in wound repair. *Stem Cells Transl Med.* (2012) 1:142–9. doi: 10.5966/sctm.2011-0018

17. Monteiro SO, Lepage OM, Theoret CL. Effects of platelet-rich plasma on the repair of wounds on the distal aspect of the forelimb in horses. *Am J Vet Res.* (2009) 70:277–82. doi: 10.2460/ajvr.70.2.277

18. Theoret CL, Wilmink JM. Aberrant wound healing in the horse: naturally occurring conditions reminiscent of those observed in man. *Wound Repair Regen.* (2013) 21:365–71. doi: 10.1111/wrr.12018

19. Carter-Arnold JL, Neilsen NL, Amelse LL, Odoi A, Dhar MS. *In vitro* analysis of equine, bone marrow-derived mesenchymal stem cells demonstrates differences within age- and gender-matched horses. *Equine Vet J.* (2014) 46:589–95. doi: 10.1111/evj.12142

20. Ursini TL, Amelse LL, Elkhenany HA, Odoi A, Carter-Arnold JL, Adair HS, et al. Retrospective analysis of local injection site adverse reactions associated with 230 allogenic administrations of bone marrow-derived mesenchymal stem cells in 164 horses. *Equine Vet J.* (2019) 51:198–205. doi: 10.1111/evj.12992

21. Dahlgren LA, Mohammed HO, Nixon AJ. Temporal expression of growth factors and matrix molecules in healing tendon lesions. *J Orthop Res.* (2005) 23:84–92. doi: 10.1016/j.orthres.2004.05.007

22. Audette RV, Lavoie-Lamoureux A, Lavoie J-P, Laverty S. Inflammatory stimuli differentially modulate the transcription of paracrine signaling molecules of equine bone marrow multipotent mesenchymal stromal cells. *Osteoarthritis Cartilage.* (2013) 21:1116–24. doi: 10.1016/j.joca.2013.05.004

23. Bowling FL, King L, Fadavi H, Paterson JA, Preece K, Daniel RW, et al. An assessment of the accuracy and usability of a novel optical wound measurement system. *Diabet Med.* (2009) 26:93–6. doi: 10.1111/j.1464-5491.2008.02611.x

24. De Schauwer C, Meyer E, Van de Walle GR, Van Soom A. Markers of stemness in equine mesenchymal stem cells: a plea for uniformitiy. *Theriogenology.* (2011) 75:1431–43. doi: 10.1016/j.theriogenology.2010.11.008

25. Dominici ML, Le Blanc K, Mueller I, Slaper-Cortenbach I, Marini FC, Krause DS, et al. Minimal criteria for defining multipotent mesenchymal stromal cells. The international society for cellular therapy position statement. *Cytotherapy.* (2006) 8:315–7. doi: 10.1080/14653240600855905

26. Moon MH, Kim SY, Kim YJ, Kim SJ, Lee JB, Bae YC, et al. Human adipose tissue-derived mesenchymal stem cells improve postnatal neovascularization in a mouse model of hindlimb ischemia. *Cell Physiol Biochem.* (2006) 17:279–90. doi: 10.1159/000094140

27. Lee EY, Xia Y, Kim WS, Kim MH, Kim TH, Kim KJ, et al. Hypoxia-enhanced wound healing function of adipose-derived stem cells: increase in stem cell proliferation and up-regulation of VEGF and bFGF. *Wound Repair Regen.* (2009) 17:540–7. doi: 10.1111/j.1524-475X.2009.00499.x

28. Chen L, Tredget EE, Wu PY, Wu Y. Paracrine factors of mesenchymal stem cells recruit macrophages and endothelial lineage cells and enhance wound healing. *PLoS ONE.* (2008) 3:e1886. doi: 10.1371/journal.pone.0001886

29. Liu X, Wang Z, Wang R, Zhao F, Shi P, Jiang Y, et al. Direct comparison of the potency of human mesenchymal stem cells derived from amnion tissue, bone marrow and adipose tissue at inducing dermal fibroblast responses to cutaneous wounds. *Int J Mol Med.* (2013) 31:407–15. doi: 10.3892/ijmm.2012.1199

30. Kim BC, Kim HT, Park SH, Cha JS, Yufit T, Kim SJ, et al. Fibroblasts from chronic wounds show altered TGF-beta-signaling and decreased TGF-beta Type II receptor expression. *J Cell Physiol.* (2003) 195:331–6. doi: 10.1002/jcp.10301

31. Caspersen CJ, Thomas GD, Boseman LA, Beckles GL, Albright AL. Aging, diabetes, and the public health system in the United States. *Am J Public Health.* (2012) 102:1482–97. doi: 10.2105/AJPH.2011.300616

32. Rumalla VK, Borah GL. Cytokines. Growth factors, and plastic surgery. *Plast Reconstr Surg.* (2001) 108:719–33. doi: 10.1097/00006534-200109010-00019

33. Asahara T, Masuda H, Takahashi T, Kalka C, Pastore C, Silver M, et al. Bone marrow origin of endothelial progenitor cells responsible for postnatal vasculogenesis in physiological and pathological neovascularization. *Circ Res.* (1999) 85:221–8. doi: 10.1161/01.RES.85.3.221

34. Wilmink JM, van Herten J, van Weeren PR, Barneveld A. Retrospective study of primary intention healing and sequestrum formation in horses compared to ponies under clinical circumstances. *Equine Vet J.* (2002) 34:270–3. doi: 10.2746/042516402776186047

35. Chaudhary C, Garg T. Scaffolds: a novel carrier and potential wound healer. *Crit Rev Ther Drug Carrier Syst.* (2015) 32:277–321. doi: 10.1615/CritRevTherDrugCarrierSyst.2015011246

36. Chaudhari AA, Vig K, Baganizi DR, Sahu R, Dixit S, Dennis V, et al. Future prospects for scaffolding methods and biomaterials in skin tissue engineering: a review. *Int J Mol Sci.* (2016) 17:1974. doi: 10.3390/ijms17121974

37. Rahmani Del Bakhshayesh A, Annabi N, Khalilov R, Akbarzadeh A, Samiei M, et al. Recent advances on biomedical applications of scaffolds in wound healing and dermal tissue engineering. *Artif Cells Nanomed Biotechnol.* (2018) 46:691–705. doi: 10.1080/21691401.2017.1349778

38. Mund SJ, Kawamura E, Awang-Junaidi AH, Campbell J, Wobeser B, MacPhee DJ, et al. Homing and engraftment of intravenously administered equine cord blood-derived multipotent mesenchymal stromal cells to surgically created cutaneous wound in horses: a pilot project. *Cells.* (2020) 9:1162. doi: 10.3390/cells9051162

39. Textor JA, Clark KC, Walker NJ, Aristizobal FA, Kol A, LeJeune SS, et al. Allogeneic stem cells alter gene expression and improve healing of distal limb wounds in horses. *Stem Cells Transl Med.* (2017) 7:98–108. doi: 10.1002/sctm.17-0071

40. Khashjoori B, Ghamsari SM, Dehghan MM, Farzad Mohajei S, Gholami H, Golshahi H, et al. Evaluation of the effects of adipose derived mesenchymal stem cells cultured on decellularized amniotic membrane in wound healing of distal part of the limbs in horse. *Iran J Vet Med.* (2019) 13:11–25. doi: 10.22059/IJVM.2019.244278.1004854

frontiers | Frontiers in Veterinary Science

TYPE Original Research
PUBLISHED 24 November 2022
DOI 10.3389/fvets.2022.1057667

OPEN ACCESS

EDITED BY
Scott J. Roberts,
Royal Veterinary College (RVC),
United Kingdom

REVIEWED BY
Jayesh Dudhia,
Royal Veterinary College (RVC),
United Kingdom
Luca Melotti,
University of Padua, Italy

*CORRESPONDENCE
Emily J. Clarke
eclarke@liverpool.ac.uk

SPECIALTY SECTION
This article was submitted to Veterinary Regenerative Medicine, a section of the journal Frontiers in Veterinary Science

RECEIVED 29 September 2022
ACCEPTED 10 November 2022
PUBLISHED 24 November 2022

CITATION
Clarke EJ, Johnson E, Caamaño Gutierrez E, Andersen C, Berg LC, Jenkins RE, Lindegaard C, Uvebrant K, Lundgren-Åkerlund E, Turlo A, James V, Jacobsen S and Peffers MJ (2022) Temporal extracellular vesicle protein changes following intraarticular treatment with integrin α10β1-selected mesenchymal stem cells in equine osteoarthritis. *Front. Vet. Sci.* 9:1057667. doi: 10.3389/fvets.2022.1057667

Temporal extracellular vesicle protein changes following intraarticular treatment with integrin α10β1-selected mesenchymal stem cells in equine osteoarthritis

Emily J. Clarke[1]*, Emily Johnson[2], Eva Caamaño Gutierrez[2], Camilla Andersen[3], Lise C. Berg[3], Rosalind E. Jenkins[4], Casper Lindegaard[3], Kristina Uvebrant[5], Evy Lundgren-Åkerlund[5], Agnieszka Turlo[1], Victoria James[6], Stine Jacobsen[3] and Mandy J. Peffers[1]

[1]Institute of Life Course and Medical Sciences, University of Liverpool, Liverpool, United Kingdom, [2]Computational Biology Facility, Liverpool Shared Research Facilities, Faculty of Health and Life Sciences, University of Liverpool, Liverpool, United Kingdom, [3]Department of Veterinary Clinical Sciences, University of Copenhagen, Copenhagen, Denmark, [4]Department of Pharmacology and Therapeutics, Institute of Systems, Molecular and Integrative Biology, Centre for Drug Safety Science Bioanalytical Facility, Liverpool Shared Research Facilities, University of Liverpool, Liverpool, United Kingdom, [5]Xintela AB, Lund, Sweden, [6]School of Veterinary Medicine and Science, University of Nottingham, Nottingham, United Kingdom

Introduction: Equine osteoarthritis (OA) is a heterogeneous, degenerative disease of the musculoskeletal system with multifactorial causation, characterized by a joint metabolic imbalance. Extracellular vesicles are nanoparticles involved in intracellular communication. Mesenchymal stem cell (MSC) therapy is a form of regenerative medicine that utilizes their properties to repair damaged tissues. Despite its wide use in veterinary practice, the exact mechanism of action of MSCs is not fully understood. The aim of this study was to determine the synovial fluid extracellular vesicle protein cargo following integrin α10β1-selected mesenchymal stem cell (integrin α10-MSC) treatment in an experimental model of equine osteoarthritis with longitudinal sampling.

Methods: Adipose tissue derived, integrin α10-MSCs were injected intraarticularly in six horses 18 days after experimental induction of OA. Synovial fluid samples were collected at day 0, 18, 21, 28, 35, and 70. Synovial fluid was processed and extracellular vesicles were isolated and characterized. Extracellular vesicle cargo was then analyzed using data independent acquisition mass spectrometry proteomics.

Results: A total of 442 proteins were identified across all samples, with 48 proteins differentially expressed (FDR $\leq$ 0.05) between sham-operated control joint without MSC treatment and OA joint treated with MSCs. The most significant pathways following functional enrichment analysis of the differentially abundant protein dataset were serine endopeptidase activity (p = 0.023), complement activation (classical pathway) (p = 0.023), and collagen containing extracellular matrix (p = 0.034). Due to the lack of an OA group without MSC treatment, findings cannot be directly correlated to only MSCs.

Discussion: To date this is the first study to quantify the global extracellular vesicle proteome in synovial fluid following MSC treatment of osteoarthritis. Changes in the proteome of the synovial fluid-derived EVs following MSC injection suggest EVs may play a role in mediating the effect of cell therapy through altered joint homeostasis. This is an important step toward understanding the potential therapeutic mechanisms of MSC therapy, ultimately enabling the improvement of therapeutic efficacy.

KEYWORDS

equine, osteoarthritis, extracellular vesicles, biologics, MSC therapy

Introduction

Osteoarthritis (OA) is a common disease of the joint, and is the cause of up to 60% of all lameness cases in horses (1). It is a progressive degenerative musculoskeletal pathology of synovial joints and results from an imbalance of catabolic and anabolic processes affecting cartilage and bone remodeling (2). This is associated with pain, reduced mobility and impaired welfare. OA is a complex heterogeneous condition with multiple causative factors, including mechanical, genetic, metabolic and inflammatory pathway activation, with a non-functional joint as the shared endpoint (3). In the disease there is a loss of articular cartilage, reduced elastoviscosity of synovial fluid, thickening of subchondral bone, joint space narrowing and osteophyte formation (4). Currently, OA is predominantly diagnosed based on clinical signs and radiographic imaging, capturing changes that are typical of the later disease stages. Treatment is symptomatic, with no current cure available to rescue the joint environment. Biological cell-based therapies include autologous conditioned serum, platelet-rich plasma, and expanded or non-expanded mesenchymal stem cells (MSCs). These regenerative therapies have the potential to enhance repair of damaged tissues or organs (5). Mesenchymal stem cell (MSC) therapy most commonly uses cells derived from bone marrow or adipose tissue (6). They are highly proliferative, plastic-adherent, fibroblast-like cells that express CD44, CD90, CD105 and do not express MHC class II or CD45 (7). MSCs are able to modulate and down-regulate immune system activity, reducing inflammatory cytokines associated with acute inflammation (8). However, MSC preparations display substantial heterogeneity of cell types that varies between donors and between tissue sources, which has led to varying results in tissue regeneration studies (9). Selection of MSCs to generate homogenous MSC preparations thus has the potential to improve the therapeutic outcome of MSC therapies (10, 11). Integrin α10β1, a collagen-binding receptor originally discovered on chondrocytes (12) is also expressed by MSCs (13) and can distinguish MSCs from other cell types in MSC preparations. MSCs selected for the expression of integrin α10β1 (integrin α10-MSCs) have shown improved adhesion to chondral and subchondral lesions in explant studies, improved chondrogenic differentiation ability as well as improved secretion of the immunomodulatory factor prostaglandin E2 (PGE2) *in vitro,* compared to unselected cells (14). It has been demonstrated that to mitigate the progression of osteoarthritis in an equine talar impact model such MSCs reduce cartilage fibrillation and subchondral bone sclerosis (15). In addition, labeled integrin α10-MSCs have been shown to home to cartilage defects in rabbit model after intraarticular administration and to directly participate in the regeneration of the cartilage (16).

MSC secreted factors are believed to have a critical role in the therapeutic efficacy. Thus, there is a drive to investigate and potentially develop cell-free therapeutics including Extracellular Vesicles (EVs) that reflect the biophysical characteristic of "parent" cells (17). EVs are nanoparticles enveloped in a phospholipid bilayer membrane and are secreted by most mammalian cells. EVs facilitate intercellular communication through the paracrine action of protein, lipid and nucleic acid cargo. EV subtypes, namely microvesicles and exosomes have been demonstrated to act in a protective manner, but also pathologically, dependent on the "parent" cell phenotype and subsequent *in vivo* environment (18, 19). Previous evidence has shown that EVs may at least partially drive the therapeutic effect of MSC treatment, by increasing cellular proliferation and infiltration in exosome-mediated cartilage repair by promoting a regenerative immune phenotype, characterized by higher infiltration of CD163 + macrophages and a reduction in proinflammatory cytokines such as interleukin 1β (IL-1β) (20), tumor necrosis factor- α (TNF-α) and interleukin 6 (IL-6) (21).

In *in vitro* equine models of OA, it has been found that chondrocytes stimulated with inflammatory cytokines had a reduced inflammatory phenotype following treatment with MSC -EVs. MSC-EVs also have an anti-catabolic effect evidenced by decreased expression of matrix metalloproteinase 13 (MMP-13) (22, 23). These observations were conserved across different species. In mice it was demonstrated that MSC-EVs reinduced the expression of chondrocyte markers (type II collagen, aggrecan) but inhibited catabolic (MMP-13) and

inflammatory (nitric oxide synthase; iNOS) markers. Thus the authors suggested that MSC-EVs act in a chondroprotective manner by inhibiting apoptosis and macrophage activation (24).

It is paramount to determine the mechanism of therapeutic action of MSCs and determine the contribution of secreted factors such as EVs in rescuing the OA phenotype, with the aim of producing a more targeted treatment. We demonstrate that intraarticular injection of MSCs affects protein cargo of synovial fluid EVs in an equine model of OA, decreasing the expression of proteins associated with pathways related to OA pathogenesis.

Materials and methods

Equine carpal osteochondral fragment model induction

The study was approved by the Danish Animal Experiments Inspectorate (#2020-15-0201-00602) as well as the Ethical Committee of the University of Copenhagen (project no 2020-016). OA was induced using a carpal osteochondral fragment-exercise model in a total of 6 Standardbred trotters (mares, 4 to 7 years of age). The model was previously described by McIlwraith et al. (1). OA was induced in the left carpus of all horses and the right carpus was sham operated on to serve as control. Horses were premedicated with a combination of romifidine 6 mg/100 kg (Sedivet®Vet, Boehringer Ingelheim Vetmedica, Missouri, United States), acepromazine 3 mg/100 kg (Plegicil Vet, Boehringer Ingelheim Vetmedica, Missouri, United States), atropine sulfate 0.5 mg/100 kg (Atropin, Aguettant Ltd, Bristol, United Kingdom), and butorphanol 3 mg/100 kg (Dolorex®, Ag Marin Pharmaceuticals, United States). Anesthesia was induced with ketamine 2.5 mg/kg (Ketador Vet, Richter Pharma AG, Oberosterreich, Austria) and midazolam 4 mg/100 kg (Midazolam "Accord", Accord-UK Ltd, Barnstaple, United Kingdom). The horses were placed in dorsal recumbency and anesthesia maintained with isoflourane (Vetflurane, Virbac, Carros, France). Perioperatively the horses received flunixin meglumine 1.1 mg/kg (Finadyne, MSD Animal Health, New Jersey, United States), penicillin 22.000 IU/kg (Benzylpenicillin PanPharma, Brancaster Pharma, Surrey, United Kingdom), and gentamicin 6.6 mg/kg (Genta-Equine, Dechra Veterinary Products, Shrewsbury, United Kingdom). Arthroscopic portals were made in the right carpus and the carpal joint was inspected for abnormalities. In the left carpus an osteochondral "chip" fragment was made with an 8 mm curved osteotome in the dorsal margin of the third facet of the distal surface of the radial carpal bone at the level of the medial plica. The fragment remained attached to the plica. The debris was not flushed from the joint. The horses were stall rested for 14 days after surgery. From day 2 following surgery horses were walked by hand every day. Treadmill exercise was initiated on day 14 after surgery. The horses were exercised 5 days a week for 8 weeks through the following program: 2 min slow trot 16–19 km/h (4.4–5.3 m/s), 2 min fast trot 32 km/h (9 m/s), 2 min slow trot 16-19 km/h (4.4–5.3 m/s). From day 14 the horses were allowed free pasture exercise every day. At day 18 MSCs were injected intraarticularly into the left joint with the osteochondral fragment only. Horses were humanely euthanized at the end of the study and both joints underwent both gross and histological examination. This data is not included.

TABLE 1 An overview of experimental groups and the longitudinal time points for SF collection.

		Day					
		0 (prior to surgery)	*18*	*21*	*28*	*35*	*70*
Group	*Sham*	→	No treatment	→			
	Control						
	OA		MSC administration	OA + MSCs	→		

OA + MSCs, Osteoarthritis and mesenchymal stem cells; OA, Osteoarthritis.

Aseptic arthrocentesis was conducted on osteochondral chip joints and sham control joints at specific time points: day 0, 18, 21, 28, 35, and 70, as shown in Table 1. The synovial fluid (SF) was centrifuged at 2,540 *g* at 4°C for 5 mins and then aliquoted into Eppendorf tubes, and snap frozen. After completion of collection, samples were transported on dry ice to the University of Liverpool, and stored at −80°C. For clarity, experimental groups were control (day 0-day 70), OA (day 0-day 18) and OA + MSCs (day 21–70) following MSC treatment of the OA group post sampling at day 18, as shown in Table 1.

Mesenchymal stem cell therapy

Equine MSCs were isolated from adipose tissue from a 7-year-old healthy gelding. Briefly, the adipose tissue was digested with collagenase, adipose cells were removed, and the stromal vascular fraction was isolated and expanded in culture. Cells were cultured to passage 3, and MSCs were then selected for high expression of integrin α10β1 (integrin α10-MSCs) by magnetic-activated cell sorting using a specific biotinylated integrin α10 monoclonal antibody (Xintela, Sweden) and anti-biotin microbeads (Miltenyi, North Rhine Westphalia, Germany). MSCs were subsequently washed in culture medium, reseeded and expanded for a further passage (passage 4), then frozen in 10% dimethyl sulfoxide (DMSO) cryopreservation medium (Cryostor, BioLife Solutions, Washington, United States) in liquid nitrogen until use. The frequency of MSCs expressing integrin α10β1 measured by flow cytometry, was 92.7% before cryopreservation.

On day 18 all six horses were treated with 20×10^6 integrin α10-MSCs (4 ml, in 10% DMSO in cryopreservation medium)

immediately after synovial sampling. Cryopreservation medium was not injected into the control joint. Day 18 was selected for MSC treatment to be administered to ensure an OA phenotype had developed within the joint as a response to surgical intervention. This was based on our previous study (25). The integrin α10-MSCs were thawed in a sterile water bath at 37°C, aspirated into a syringe through a 14G canula at a slow pace, and injected into the carpal joint of the OA-induced limb through a 20G canula over a minimum of 10 secs. The horses were stall rested for 2 days following treatment.

Sample preparation

The 1 ml of SF per sample was spun in a benchtop centrifuge (Eppendorf non-refrigerated centrifuge 5420) at 241 *g* for 10 min. The supernatant was removed and treated with hyaluronidase (1 μg/ml) by incubation at 37°C for 1 h. SF samples were then spun at 1,000 *g* for 5 min, and the supernatant was collected.

EV isolation—differential ultracentrifugation

Equine SF samples (200 μl) underwent differential ultracentrifugation (dUC) in order to isolate EVs. Samples were subjected to a 300 *g* spin for 10 min, 2,000 *g* spin for 10 min, 10,000 *g* spin for 30 min in a bench top centrifuge at room temperature. Samples were then transferred to Beckman Coulter thick wall polycarbonate 4 ml ultracentrifugation tubes, and centrifuged at 100,000 *g* for 70 min at 4°C (Optima XPN-80 Ultracentrifuge, Beckman Coulter, California, USA) in a 45ti fixed angle rotor, with the use of a 13 mm diameter Delrin adaptor. Supernatant was removed and sample pellets were resuspended in 50 μl of filtered phosphate buffered saline (PBS) (Gibco™ PBS, pH 7.4—Fisher Scientific, Massachusetts, USA).

Nanoparticle tracking analysis

Nanoparticle tracking analysis (NTA) was used to quantify EV concentration and size in all samples, using a NanoSight NS300 (Malvern Panalytical, Malvern, UK). Samples were prepared as previously described (26).

EV characterization

The ExoView platform (NanoView Biosciences, Malvern Hills Science Park, Malvern) was used to determine EV concentration, surface marker identification (CD9, CD81 and CD63) and to perform fluorescent microscopy and tetraspanin colocalisation analysis on selected samples. We had previously tested equine samples on both the human and murine chips and demonstrated the human chips were more compatible (data not shown). The ExoView analyzes EVs using visible light interference for size measurements and fluorescence for surface protein profiling. Samples were analyzed as previously described (25).

EV protein extraction

EV pellets were suspended in 200 μl of urea lysis buffer (6M Urea (Sigma-Aldrich, Dorset, United Kingdom), 1M ammonium bicarbonate (Fluka Chemicals Ltd., Gillingham, UK) and 0.5% sodium deoxycholate (Sigma-Aldrich, Dorset, United Kingdom)). Samples were sonicated at 5 μm for 3 × 10 secs per sample, with 1-min rest on ice between each sonication round.

SDS-PAGE and protein staining

Sodium dodecyl sulfate–polyacrylamide gel electrophoresis (SDS-PAGE) was used to separate proteins from EV protein extract. 7.5 ul of 2x Novex™ Tris-Glycine SDS Sample Buffer (ThermoFisher Scientific, Paisley, UK), supplemented with 8% of 2-Mercaptoethanol (Sigma-Aldrich, Dorset, UK), was added to 7.5 μl of sample SF-EV protein lysate. Samples were mixed and heated at 100°C for 10 min to denature proteins, then placed on ice. A NuPAGE™ 4 to 12%, Bis-Tris gel (ThermoFisher Scientific, Paisley, UK) was placed in the electrophoretic tank and the tank was filled with 1x NuPAGE® MES Running Buffer (ThermoFisher Scientific, Paisley, UK) (diluted from the 20x stock in ultrapure water). Samples were loaded onto the gel alongside the Novex™ Sharp Pre-stained Protein Standard ladder (ThermoFisher Scientific, Paisley, UK). Gels were run at 100V until completion of electrophoresis and visualized using colloidal coomassie blue (Thermofisher Scientific, Paisley, UK) according to manufacturer's guidelines.

In-solution digestion

95 μl of lysed and sonicated equine SF-EV were treated with 5 mM dithiothreitol (DTT) (Sigma-Aldrich, Dorset, UK) 100 mM at 60°C and 123 *g* for 30 mins. Iodoacetamide (Sigma-Aldrich, Dorset, UK) was then added to a final concentration of 20 mM and the samples were incubated at room temperature in the dark for 30 min. Following this 5 mM DTT was added to each sample, and incubated at room temperature for 15 min. 12 μl hydrophilic and hydrophobic magnetic carboxylate SpeedBeads (SP3 beads, total of 12 μl) (Cytiva, Massachusetts, United States) were added to each sample, followed by 120 μl ethanol (Sigma-

Aldrich, Dorset, UK). Samples were then incubated at 24°C and 123 *g* for 1 h. The beads were separated from samples using a magnetic stand and were washed three times with 180 µl 80% ethanol. They were resuspended in 100 mM ammonium bicarbonate (Fluka Chemicals Ltd., Gillingham, UK4 µg). Trypsin/LysC (2.4 µg) (Promega) was added to each sample. Samples were placed in a sonicator bath and sonicated for 30 secs to disaggregate the beads before being incubated overnight at 37°C and 123 *g*. Beads were removed from the samples using the magnetic stand and the supernatants were acidified by the addition of 1 µl trifluoroacetic acid (Sigma- Aldrich, Dorset, UK). Samples were then desalted using an Agilent mRP-C18 column, dried in a SpeedVac and resuspended in 0.1% formic acid. The UV absorbance measured during desalting was used to normalize the loading for mass spectrometry analysis with a final volume of 5 µl being loaded on the nano-LC column.

Data-dependent acquisition for generation of an equine SF EV spectral library

Equine SF was pooled using samples from the metacarpophalangeal joint from our equine musculoskeletal biobank (VREC561), and samples collected in this study from carpal joint of control group as well as OA, and OA + MSC group, resulting in a total of 11 ml SF. This was hyaluronidase treated (1 µg /ml) for 1 h at 37°C, as outlined in section 2.2. EVs were isolated using dUC, as outlined in section 2.4. The EV pellet was then reconstituted in 200 µl of urea lysis buffer. The samples were digested with trypsin/LysC for 3 h at 37°C, the concentration of urea was reduced to 1 M, and incubation was continued overnight at 37°C. Samples were fractionated on a PolySULFOETHYL, a strong cation exchange column, and 20 fractions were desalted, dried and resuspended in 0.1% formic acid. Aliquots were loaded onto an Eksigent nanoLC 415 (Sciex, Macclesfield, United Kingdom) equipped with a nanoAcquity UPLC Symmetry C18 trap column (Waters, Massachusetts, United States of America) and a bioZEN 2.6 µm Peptide XB-C18 (FS) nanocolumn (250 mm × 75 µm, Phenomenex, Macclesfield, United Kingdom). A gradient from 2–50% acetonitrile /0.1% formic acid (v/v) over 120 min at a flow rate of 300 nL/min was applied. Data-dependent acquisition was performed using nano liquid chromatography-tandem mass spectrometry on a Triple TOF 6600 (Sciex, Macclesfield, United Kingdom) in positive ion mode using 25 MS/MS per cycle (2.8 s cycle time), and the data were searched using ProteinPilot 5.0 (Sciex, Macclesfield, United Kingdom) and the Paragon algorithm (SCIEX) against the horse proteome (UniProt *Equus cabullus* reference proteome, 9,796, May 2021, 20,865 entries). Carbamidomethyl was set as a fixed modification of cysteine residues. The data were also searched against a reversed decoy database and proteins lying within a 1 or 5% global false discovery rate (FDR) were included in the library. Proteins were analyzed using FunRich.

Data-independent acquisition proteomics

A data-independent proteomic approach was utilized in the form of Sequential Windowed Acquisition of all theoretical fragments (SWATH) (27). Aliquots of 5 µl containing equal quantities of peptides were made up to a volume of 5 µl with 0.1% formic acid and data were acquired using the same 2 h gradient as the library fractions. SWATH acquisitions were performed using 100 windows of variable effective isolation width to cover a precursor m/z range of 400-1500 and a product ion m/z range of 100-1650. Scan times were 50 ms for TOF-MS and 36 ms for each SWATH window, gave a total cycle time of 3.7 secs. Retention time alignment and peptide/protein quantification were performed by Data-Independent Acquisition by Neural Networks (DIA-NN) (28), using the same reference horse proteome as above to reannotate the library. A precursor FDR of 1%, with match between runs and unrelated runs was selected. The mass spectrometry proteomics data were deposited to the ProteomeXchange Consortium via PRIDE (29) (reference PXD035303).

Statistical analysis

All statistical results were corrected for false discovery rate (FDR) using the Benjamini-Hochberg (BH) method unless stated otherwise. Results were considered significant at 5% FDR. Nanoparticle tracking analysis data was analyzed using non-parametric tests. A Kruskal-Wallis test was performed for concentration and size, followed by a Mann–Whitney U test per time point. Exoview data was analyzed using T-tests following parametric evaluation in GraphPad Prism 9.0. Statistical analysis of proteomics data was carried out using the R statistical programming environment (30), unless stated otherwise. The data was quality controlled; proteins with complete observations were normalized and log2 transformed for downstream analysis. Batch effect was detected and corrected via ComBat (31) prior to Principal Component Analysis (PCA) and further visualizations. The lmerTest implementation of lme4 (32) was used to fit linear mixed models (LMMs) to the log-transformed data for each protein to determine the effects of treatment, time, and treatment over time on horse joints. For the fitted models pairwise comparisons between the treatment and control were carried out at each time point using the emmeans package with the Kenward-Roger method (33). All graphical representations were undertaken using the package ggplot2 (34). Functional classification and enrichment analyses were performed using the clusterProfiler package (35). The proteins were annotated with

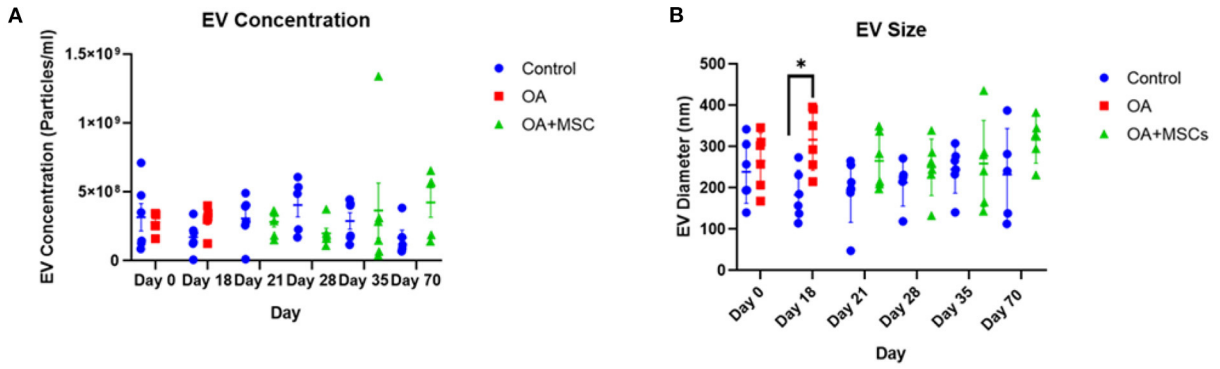

FIGURE 1
Size and concentration of synovial fluid-derived nanoparticles. Nanoparticle tracking analysis was undertaken using a Nanosight NS3000. All error bars are standard error of the mean (SEM). Statistical analysis undertaken in GraphPad Prism 9.0 using Kruskal Wallis tests with FDR correction and Mann Whitney tests within time points ($p < 0.05$, *; $p < 0.01$ **: $p < 0.001$, ***, $p < 0.0001$, ****). **(A)** EV concentration and **(B)** EV size.

GeneOntology (GO) terms using the UniProtKB ID Mapping tool. Over-representation analysis (ORA) was carried out for GO terms using the enricher function from the clusterProfiler package. The foreground was all the proteins that passed FDR, the background was all the processed proteins after missing values had been removed, i.e., all the proteins that were subjected to statistical analysis. Each term was required to have a minimum of three observed proteins annotated to it and an adjusted p-value <0.05.

Results

Equine carpal osteochondral fragment model

The carpal osteochondral fragment-exercise model used in this experiment has been shown to result in an OA phenotype with respect to clinical parameters, (1, 36–38) and this model has been used determine the response to to integrin α10-MSC treatment, lameness and joint degradation were assessed but are not shown (Anderson et al. unpublished data).

Nanoparticle tracking analysis to quantify EV size and concentration

Total particle concentration and size characterization was performed using NTA. NTA determined the average SF-EV sample concentration between control, OA and OA + MSCs across specific time points, specifically quantifying all nanoparticles within the sample (Figure 1A). No significant difference was observed in EV concentration between experimental groups, however a significant difference in EV size was found irrespective of time when comparing control and OA ($p = 0.02$) and control compared to OA + MSCs ($p = 0.02$). Specifically, EV size was significantly different between control and OA at day 18 before MSC treatment ($p = 0.02$) (Figure 1B). Results were suggestive of a heterogeneous population of nanoparticles.

Exoview assay characterizes equine synovial fluid extracellular vesicles, including morphology, and surface tetraspanins

In addition to NTA, representative EV samples were characterized using the human exoview tetraspanin chip assay. This assay specializes in characterizing the exosome subpopulations of EVs. Control at day 0, OA and control at day 18 and OA + MSCs and control at day 70 were compared. OA and OA + MSCs groups had a significantly higher concentration of EVs when compared with controls. For CD9 expression, control had 4.63×10^3 particles, OA had 21.91×10^3 particles, and OA with MSCs had 15.97×10^3 particles. Similarly, for CD81, control had 3.41×10^3 particles, OA had 17.23×10^3 particles and OA with MSCs had 12.48×10^3 particles (Figure 2). CD63 was not reported due to low particle counts for this tetraspanin; this has been attributed to poor protein homology between equine and human CD63 tetraspanins. EVs were visualized between groups with fluorescent microscopy, highlighting tetraspanin expression and EV morphology (Figure 3).

Spectral library for equine synovial fluid extracellular vesicles

Mass spectrometric analysis of the SF-EV pooled sample identified 2271 proteins, mapping at least one unique peptide. Of these proteins 2047 were identified and mapped to GO Cellular

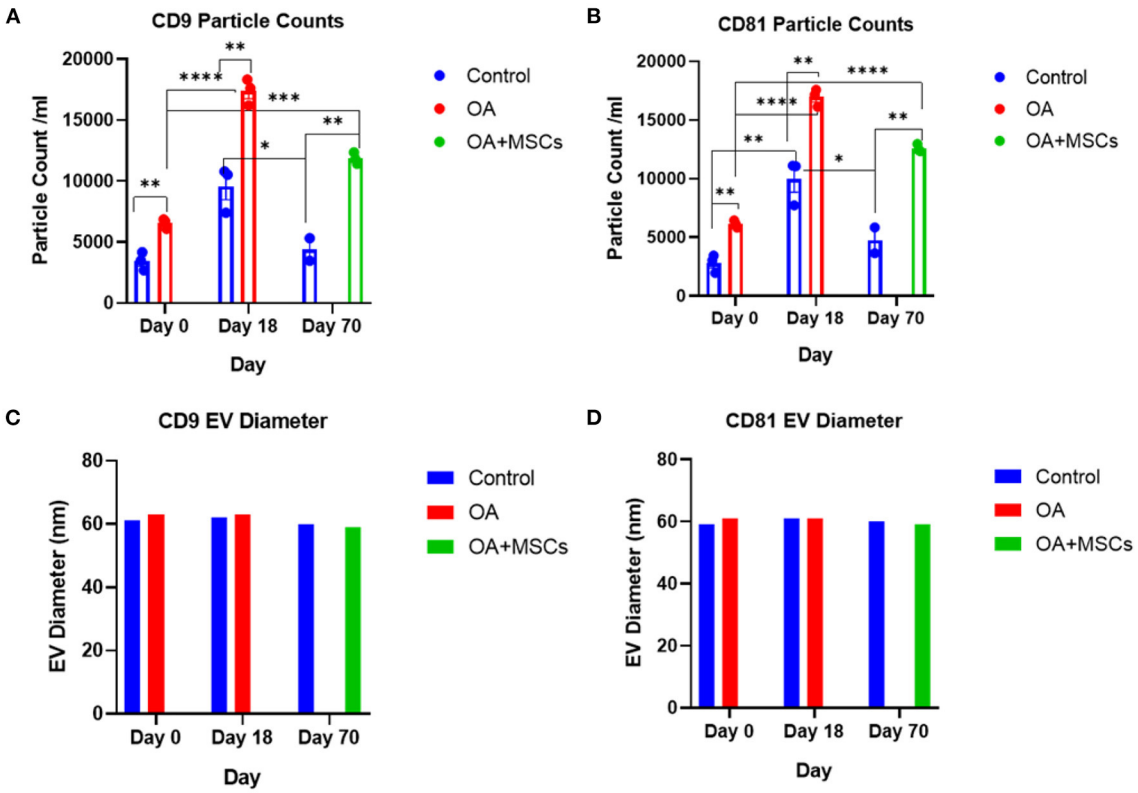

FIGURE 2
Sizing and enumeration of synovial fluid-derived EVs. All data was adjusted for dilution of the sample onto the chip. Shown is the average representing mean of three technical replicates that were run for each sample. Particle numbers were quantified by the number of particles in a defined area on the antibody capture spot. All bars are mean and standard error mean. **(A)** CD9 and **(B)** CD81-positive particles following probing with fluorescent tetraspanin antibodies. **(C)** Sizing of CD9 and **(D)** CD81 labeled EVs, normalized to MIgG control. Limit of detection was 50–200 nm. Statistical analysis undertaken in GraphPad Prism 9.0 using T-tests following parametric evaluation ($p < 0.05$, *; $p < 0.01$ **: $p < 0.001$, ***, $p < 0.0001$, ****).

Component terms using FunRich. Proteins were attributed to various cellular components, including extracellular space and exosomes, both $p \leq 0.001$, as shown in Figure 4. This library was then used to identify the proteins present within the individual samples.

A multivariate approach identified a time-dependent difference between disease stages pre- and post-treatment

A total of 442 proteins were identified across all samples submitted for SWATH-MS analysis. Multi-level PCA (mPCA) was carried out using the MixOmics R package principal component analysis (mPCA). PCA normally assumes the variables are not correlated. However, this study employed a repeat-measures design on the same horses. To account for the intraclass correlation between horses mPCA was employed. The first two principal components accounting for 54% of the variance were associated with the biological effect and demonstrated that the control and OA + MSC samples clustered by treatment (Figure 5). The later OA + MSC time points (day 70) appeared to cluster together with the control samples, reflecting a return to protein expression levels comparable to the healthy controls.

Longitudinal differential expression highlights 6 key pathways related to disease progression and treatment

Differentially expressed (DE) proteins were identified with the application of a linear mixed model with regressed factors comparing protein expression between experimental groups across time. Statistical significance was attributed to any protein with an FDR corrected p-value (BH) of $p \leq 0.05$ meeting a minimal 95% confidence interval. Of the 442 proteins identified,

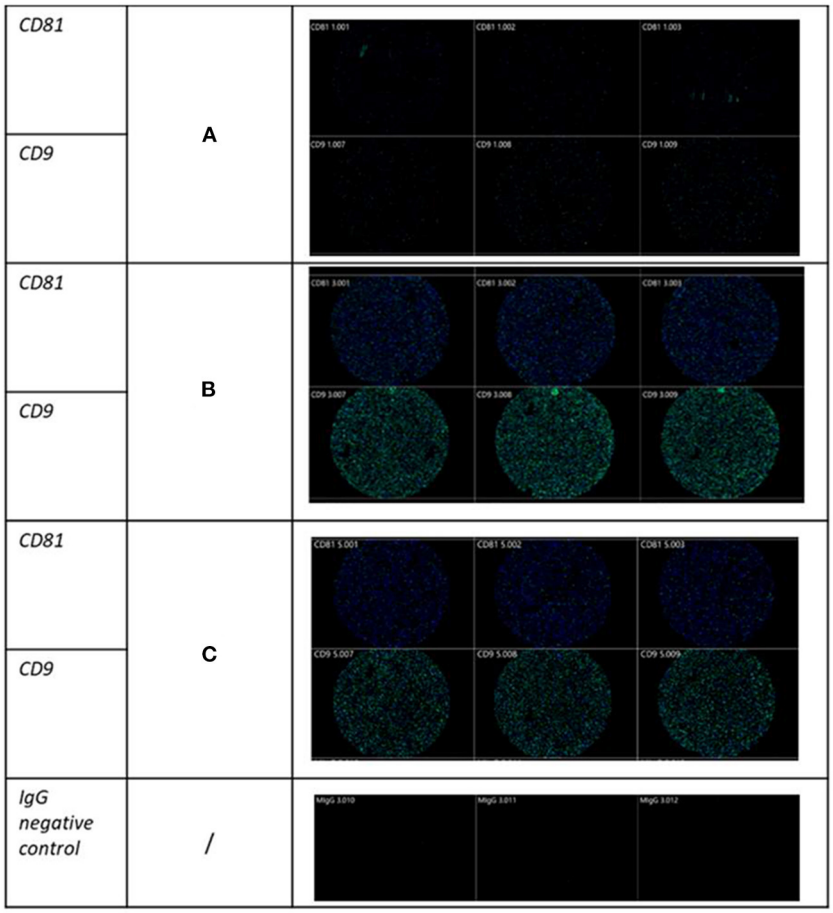

FIGURE 3
Visualization of SF-derived EVs from control, osteoarthritic (OA) and OA + MSCs joints using Exoview at selected time points. A fluorescent image of a representative spot is shown for each sample comparing **(A)** control, **(B)** OA, and **(C)** OA + MSCs with color denoting surface tetraspanin positive identification (blue-CD9, and green-CD81).

48 were present at significantly different levels ($p \leq 0.05$) between control and OA + MSCs regardless of time. Interestingly, there were no proteins DE after FDR correction in SF-EVs between control and OA at baseline and day 18 after OA induction, or between day 18 sham control and OA. The 10 proteins with the most statistically significant altered levels are shown in Table 2, including the time points at which pairwise comparisons show significant differences between control and OA + MSCs, and all 48 can be found in Supplementary Table 1. Figure 6 shows proteins attributed to the serine endopeptidase ($p = 0.02$) and complement pathways ($p = 0.03$), included hyaluronan binding protein 2 ($p = 0.04$) (Figure 6A), complement subcomponent C1r ($p = 0.03$) (Figure 6B), CD5 ($p = 0.01$) (Figure 6C), complement factor D ($p = 0.03$) (Figure 6D), C2 ($p = 0.04$) (Figure 6E), and C1 ($p = 0.04$) (Figure 6F). Other proteins attributed to the serine endopeptidase pathway include haptoglobin ($p = 0.03$), HtrA1 serine peptidase ($p = 0.03$) and complement factor B ($p = 0.04$). Proteins mapped to the collagen containing extracellular matrix ($p = 0.02$) included cartilage oligomeric matrix protein ($p = 0.001$), microfibril associated protein 4 ($p = 0.001$), thrombospondin 4 ($p = 0.003$), retinoic acid receptor responder protein 2 ($p = 0.03$), periostin ($p = 0.03$), EGF containing fibulin extracellular matrix protein 1 ($p = 0.03$), and cartilage intermediate layer protein ($p = 0.04$) (Supplementary Figure 1). The third most significant pathway was identified as complement activation classical pathway, with the following proteins attributed to it; two uncharacterized proteins, C9 ($p = 0.01$), C8A ($p = 0.02$), C1r ($p = 0.03$), C7 ($p = 0.03$), C2 ($p = 0.04$), and C1 ($p = 0.04$) (Supplementary Figure 1). Across all figures (Figures 6A, 4F) protein expression was significantly different at day 21, 28 and 35 when compared to control. All protein expressions returned to baseline control by day 70.

The lists of significant proteins were used to calculate functional enrichment with the aim of identifying relevant biological processes representative of the signature. Using an

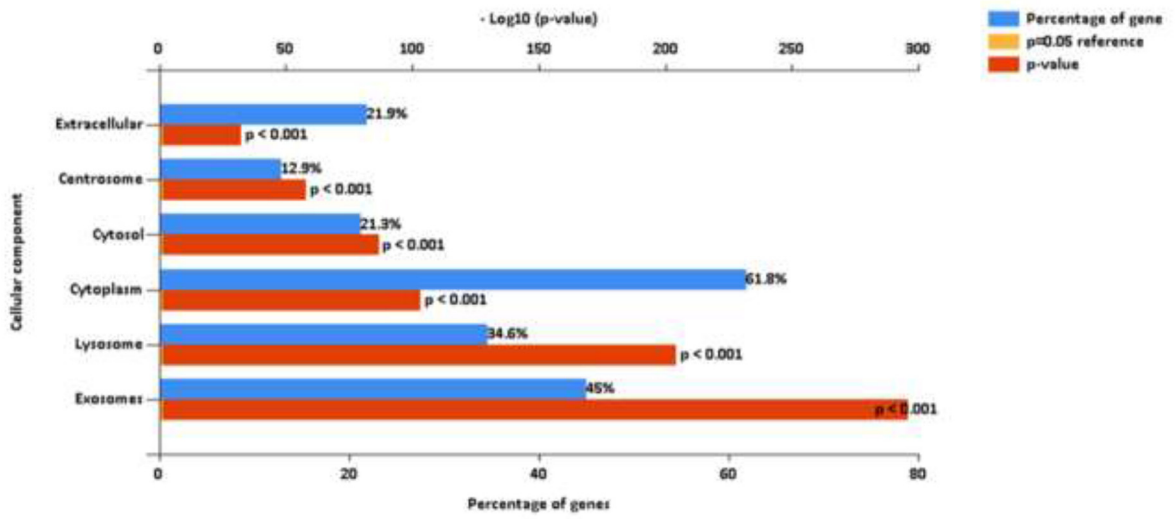

FIGURE 4
FunRich analysis output, after mapping 2,047 proteins to GO Cellular Component terms. These proteins were identified from a pooled sample of equine synovial fluid (11 ml) used to generate the SF-EV spectral library for this study. SF was sourced from healthy, OA and OA + MSC treated joints in order to encapsulate all potential proteins that may be present across all experimental groups.

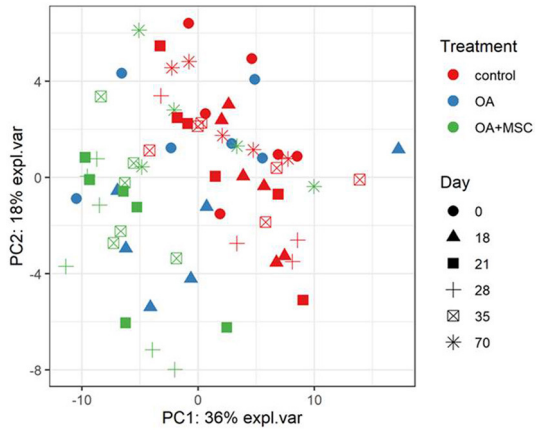

FIGURE 5
Multi-level PCA (mPCA). The first two principal components are plotted, accounting for ~54% of variance. Samples based on SWATH-MS. Each plotted point represents a horse, which are colored by their treatment and shaped by the day of the study.

overrepresentation analysis (ORA) approach on gene ontology (GO) annotations yielded six enriched pathways: serine endopeptidase activity ($p = 0.023$), complement activation (classical pathway) ($p = 0.023$), collagen containing extracellular matrix ($p = 0.034$), protein polymerization ($p = 0.039$), platelet aggregation ($p = 0.039$), elastic fiber ($p = 0.039$) (Figure 7).

Discussion

This study aimed to determine the EV protein cargo following integrin α10β1-selected mesenchymal stem cell (integrin α10-MSC) treatment in an experimental model of equine OA. To our knowledge this is the first study of its kind to quantify the global EV proteome *in vivo* after MSC treatment.

The osteochondral fragment model used in this study has been shown to produce reliable post-traumatic OA in the middle carpal joint of horses (1, 36–38). The mitigating effect of MSC treatment on the development of post-traumatic OA has been shown in a number of equine studies, although in different models, such as an osteochondral fragment model of the fetlock (39, 40) a blunt impact model of the tarsus (15) and injection of the irritant amphotericin B (41). In these studies, the MSC-treated horses developed significantly less severe OA over time compared to the untreated control horses in terms of decreased synovial effusion and a higher SF viscosity and glycosaminoglycan content, decreasing lameness over time, less severe macroscopic cartilage erosions, less radiographic signs of OA, and less histologic cartilage fibrillation and subchondral sclerosis. It should be highlighted that in the carpal osteochondral fragment model used by Frisbie et al. (37) a significant change was observed in response to surgical induction of OA. Both adipose derived MSCs and bone marrow derived MSCs were used as treatment. Despite improvement being seen with treatment compared with placebo with respect

TABLE 2 The top 10 differentially expressed ($p < 0.05$) proteins following the application of the linear mixed model, accounting for treatment and time point.

Protein	Accession number	*P*-Value (FDR adjusted)	Time point (Day)	Expression direction in OA + MSC group compared to control
Fibrinogen beta chain	F6PH38	0.0001	21,28,35	Increase
Fibrinogen gamma chain	A0A5F5PPB8	0.0001	21,28,35	Increase
Joining chain of multimeric IgA and IgM	A0A3Q2HW24	0.0003	21,28,35	Increase
Dynein heavy chain domain 1	A0A3Q2HE28	0.0005	21,28,35	Increase
Fibrinogen alpha chain	A0A3Q2HTG2	0.0005	21,28,35	Increase
Gelsolin (Actin-depolymerizing factor, ADF) (Brevin)	Q28372	0.0006	21,28,35	Decrease
Cartilage oligomeric matrix protein	A0A3Q2HRL2	0.001	21,28,35	Decrease
Microfibril associated protein 4	A0A3Q2HNH0	0.001	21,28,35	Increase
Glutathione peroxidase	A0A5F5PST7	0.003	21,28,35	Decrease
Insulin like growth factor binding protein 6	F7DEB1	0.003	21,28,35	Decrease

OA + MSCs, Osteoarthritis and mesenchymal stem cells; IgA, Immunoglobulin A; IgM, Immunoglobulin M.
Treatment and time were included as main effects, along with a treatment-by-time interaction term. Time point denoting significant pairwise comparisons between control and OA + MSCs is also shown.

to clinical parameters, in agreement with previous studies, no significant difference was determined.

The model induced a significant change in all but two parameters, no significant treatment effects were demonstrated, with the exception of improvement in synovial fluid effusion PGE2 levels with bone marrow-derived mesenchymal stem cells when compared to placebo. A greater improvement was seen with bone marrow-derived mesenchymal stem cells when compared to adipose-derived stromal vascular fraction and placebo treatment.

In our study, we identified a global change in the EV proteome, and identified a possible mechanism of MSC therapy. A time-dependent change in the EV protein cargo was also observed, suggestive of a time associated therapeutic effect, which is in line with previous reports of the effects of MSC-treatment.

We used dUC to isolate EVs following hyaluronidase treatment of SF. Hyaluronidase was used in order to break down hyaluronic acid as its presence in SF increases viscosity making the biofluid difficult to handle. This pretreatment is known to increase EV yield (35). In addition, it has also been suggested that SF-derived EVs should be sedimented at a speed of at least 100,000 *g* for optimal EV recovery, hence the decision to use this step within our isolation protocol (35). There are many EV isolation protocols with no standardized protocol agreed upon. Each isolation method results in different sample concentrations, purity, and EV profiles/ heterogeneity.

EVs were isolated from SF obtained from OA joints that were treated with MSCs and from untreated control joints. The EVs isolated were a heterogenous population that may have been derived from cells found in the intraarticular environment, such as synoviocytes and chondrocytes, and possibly from the MSCs injected into the joint. Nanoparticle tracking analysis conducted on all samples across all time points found no changes in EV concentration with time. It should be noted that NTA quantifies all nanoparticles within a sample and includes lipoproteins, proteins, viruses, nanovectors and drug delivery systems (42). This accounts for the difference in EV concentration between our NTA analysis and exoview analysis. We had limited resources to enable Exoview of all samples, and so used the platform for a subset of samples. Exoview analysis specifically focuses on the exosomal population of EVs by using antibodies for surface tetraspanins such as CD9, CD81 and CD63. In this study and our previous study, we were able to show species cross reactivity with the CD9 and CD81 tetraspanins, but not CD63 (25). Exoview analysis demonstrated an increase in the number of exosomes after OA-induction surgery prior to MSC injection. However, this may be due to immune cell infiltration within the first 18 days contributing to the difference. This is in contrast to a human study by Mustonen et al. which identified no change in EV concentration between SF-EVs from healthy and human late stage OA patients (43). Of course, differences could be due to the stage of disease post-traumatic model used in our model (early) versus the end-stage nature of the human study. Our results tentatively suggest that the OA-induction surgery

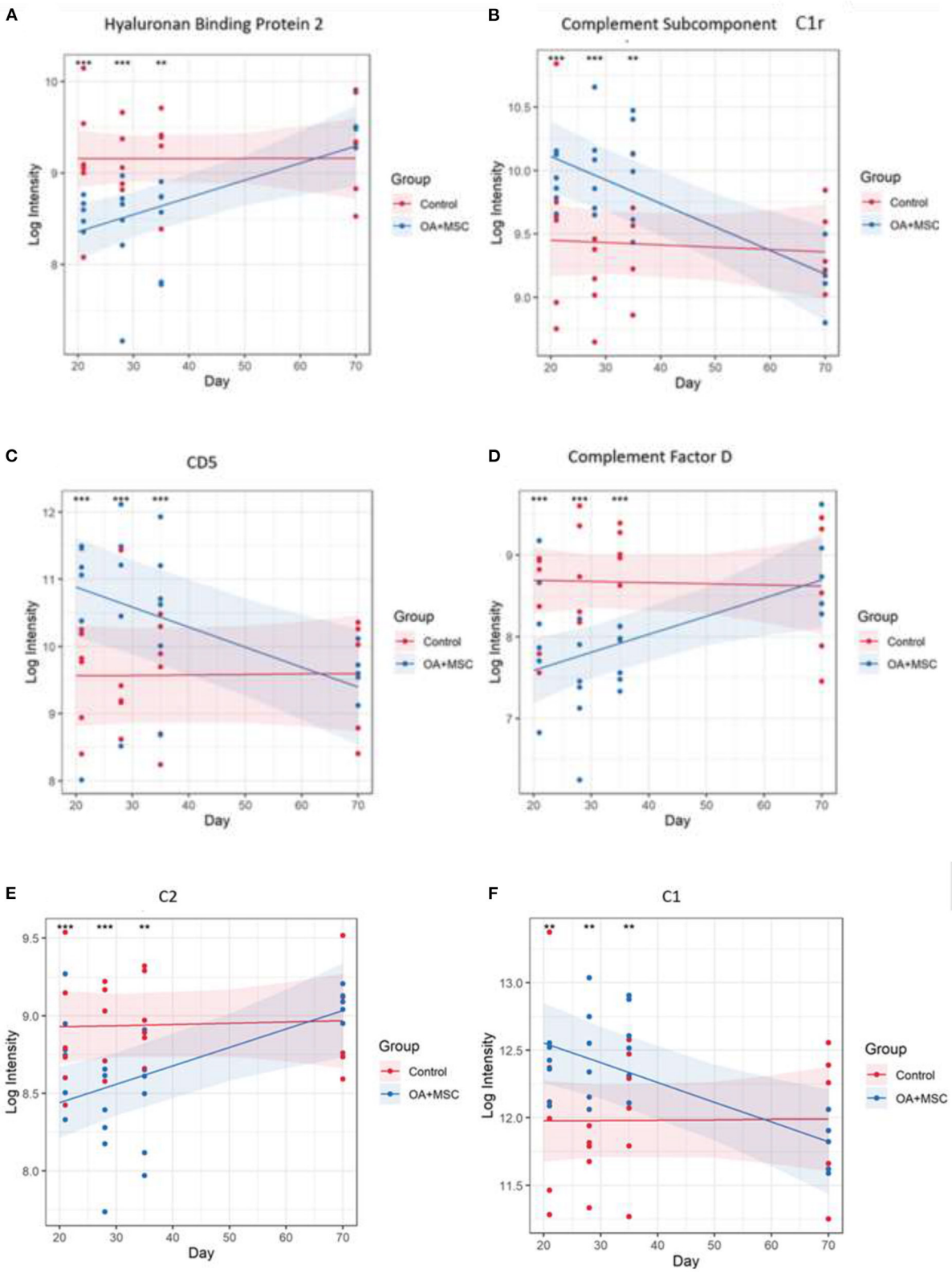

FIGURE 6
Protein expression changes in response to MSC treatment in OA joints vs control. **(A)** Hyaluronan binding protein 2, **(B)** Complement subcomponent C1r, **(C)** CD5, **(D)** Complement factor D, **(E)** C2, and **(F)** C1. The models were fitted using the lmerTest implementation of lme4. 48
(Continued)

FIGURE 6 (Continued)
proteins had a significant group, time, or group:time effect after FDR correction. For each protein with a significant effect the model was plotted using the effects and ggplot2 packages. The fitted model is shown as a line for the OA + MSC (blue) and control (red). The 95% confidence intervals for each group are shown as a shaded area. The raw data is included as points. At each time point pairwise comparisons were carried out between the treatment and control using the emmeans package. Significance thresholds were as follows: ($p < 0.05$, *; $p < 0.01$ **: $p < 0.001$, ***, $p < 0.0001$, ****).

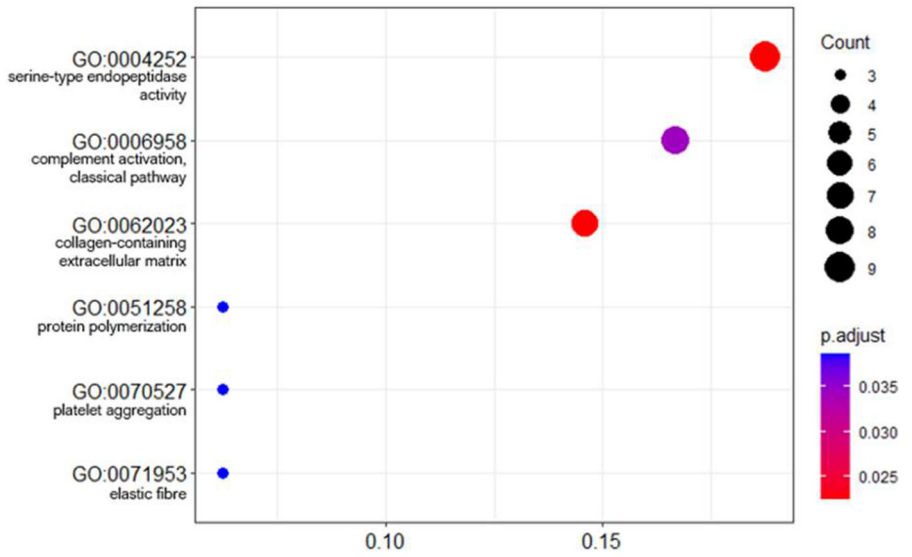

FIGURE 7
Dot plot of GO term enrichment analysis of differentially abundant proteins. The size of the dots indicates the number of proteins that mapped to that term. The x-axis is the protein ratio (number of proteins that map to the term divided by the total number of significant proteins). The dots are shaded by adjusted *p*-values (BH method).

actively increases the number of exosomes as a result of the acute trauma. This could be due to the access of subchondral bone to the SF environment following production of an osteochondral fragment or from tissues within the joint as a response to the formation of the fragment or both. However, our experimental design does not enable us to decipher this. A greater number of CD9 + and CD81 + EVs were identified across all experimental groups using the exoview assay. CD9 + exosomes have been postulated to be a target for inflammatory regulation in specific pathologies (31). In addition, the increase count observed in OA + MSC groups compared with control could be attributed to its presence on hematopoietic cells, and the role of CD9 in regulating hematopoietic stem cells differentiation (44). With respect to CD81, there is limited literature available postulating the role of specifically CD81 + EVs. However, the tetraspanin CD81 is involved in providing a scaffold enabling the recruitment of complementary proteins, enabling the function of many cellular processes. CD81 expression has been strongly associated with cancerous pathologies, and has been shown to promote tumor growth and metastasis in human melanoma, while its knockdown in osteosarcoma models has reduced tumor progression (45). Across all experimental groups the sham control remained significantly lower than the experimental group at all time points, suggestive of a minimal effect from the arthroscopy in the sham control groups. In addition, highlighting that there was a limited systemic effect from the surgical induction of OA.

In this study, SF samples following OA induction and then following the addition of MSCs to the joint were available up to day 70 of treatment post-induction. Unfortunately, SF samples from OA joints without MSC treatment were not available for this study. This makes it difficult to be definitive about the source of the EVs in the SF following addition of MSCs. We believe these will be a combination of tissue-derived and MSC-derived EVs, resulting from MSC-to-cell interactions, cell-to-MSC interactions, and cell-to-cell interactions. Allogeneic MSCs have been traced in the joint of an ovine OA model up to 14 weeks after injection (46) and up to 12 weeks after injection in an OA model in rats (47). Therefore, it is possible that MSCs were present in the joint at study termination 52 days (7½ weeks) after MSC-injection.

Post intraarticular injection of MSCs an increase in EV COMP expression was observed returning to baseline control by day 70. COMP is a key protein present in cartilage extracellular

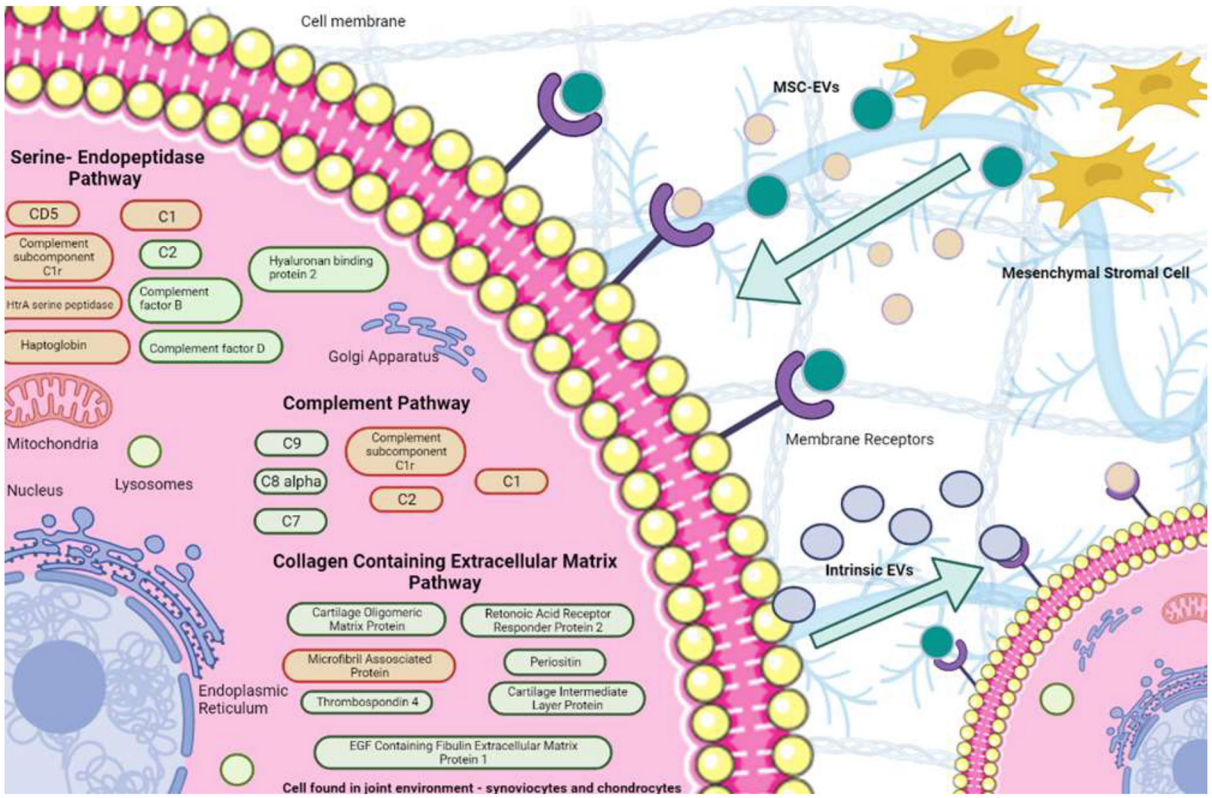

FIGURE 8
Potential mechanisms of action of SF-EVs following MSC treatment. EVs were sourced from both MSCs and the intraarticular environment. We hypothesized that MSC-EVs affect the intraarticular cells through their differential protein cargo, resulting in altered EV secretion from intrinsic cells. DE proteins attributed to given pathways are red (decreased expression to meet baseline or surpass it by day 70) or green (increased expression to reach baseline at day 70).

matrix and is a target of degradation in early OA (48). In addition, proteins such as gelsolin, which had increased expression during the OA + MSC group, has previously been attributed to chondrocyte migration. It could be postulated that proteins highly associated with the joint may be sourced from EVs secreted by joint cells, raising the question of how EVs interact in their *in vivo* environment in response to stimuli.

The most significant GO term associated with DE EV-proteins was serine endopeptidase activity following MSC treatment. Serine type endopeptidases, or serine proteinases have been attributed to proteolytic cartilage destruction. In addition, serine proteinases perform vital functions such as cytokine regulation and receptor activation (49). Degradomic studies have demonstrated that an increase in proteases activity in OA, such as in HtrA1 was responsible for cartilage proteolysis (50). HtrA1 decreased across time following MSC injection. In a murine model the genetic removal of HtrA1 delayed the degradation of articular or condylar cartilage in mice (51). Moreover, a previous study profiling the synovial fluid-derived EV proteome cargo in OA patients of both sexes identified sex-specific differences in cargo, with enriched pathways including proteins involved in endopeptidase activity, specifically in women (52). This is of note as all horses included in this study were mares. With respect to serine endopeptidase activity in MSCs it has previously been reported that interactions between BM-MSCs and natural killer cells are fundamental to improving MSC therapeutic efficacy. It has been stated that serpin B9 has a cytoprotective function in MSCs (53). In other diseases such as colorectal cancer, the use of MSCs identified serpins as having immunomodulatory effects, acting on immune cells in order to induce a wound healing phenotype, as well as angiogenesis and epithelial to mesenchymal transition (54). Therefore, we hypothesize that the change in SF-EV proteome post MSC injection has the capacity to affect the serine endopeptidase pathway that is known for its detrimental effect on cartilage degradation and further animal studies are required to elucidate this.

A further altered GO term included collagen containing extracellular matrix, often linked with joint homeostasis. Exosomes from embryonic MSCs were found to balance synthesis and degradation of the cartilage extracellular matrix in an *in vitro* murine model (55). In our study, we observe

a significant change in the expression of proteins associated with cartilage structure, such as COMP, hyaluronan binding protein 2, cartilage intermediate layer protein, chondroadherin and gelsolin. These proteins return to baseline control level by the end of our study. This suggests a restorative effect and return toward a healthy cartilage phenotype. It may be that such increased expression is more likely to be attributed to EVs secreted by native tissues than MSCs, which contribute to collagen extracellular matrix homeostatic function which could be beneficial in OA treatment. In addition, MSCs could be upstream regulators of these effects from native tissues. Hence it is possible that EVs from the native environment and MSCs are acting in concert with additional secreted factors to result in a therapeutic benefit.

In this study, the level of complement proteins in SF EVs decreased with time and returned to baseline in horses treated with MSCs, potentially affecting disease progression. The complement cascade was also a significantly enriched pathway. This pathway is activated in the early stages of OA, with C3a and C5a attributed to OA progression (56). In addition, it has been linked to extracellular cartilage matrix degradation, chondrocyte and synoviocyte inflammatory responses, cell lysis, synovitis, disbalanced bone remodeling, and osteophyte formation (57). Several complement components have previously been identified as upregulated in OA SF. It was reported that C3a and C5a promoted chemotaxis of neutrophils and monocytes, and increased leukotriene synthesis (58). In our study multiple complement factors were identified, including C7, C8, C9 and C2 (C3/C5 convertase) when comparing control to OA + MSCs across time. As such emphasizing that MSC therapy may act through the complement pathway in alleviating OA symptoms, or initiate a change in intrinsic tissues, altering the subsequent SF-EV proteome, reducing the effect of such pathway.

There are a number of limitations to our study. The duration of the study only enabled the quantification of the effect of MSCs *in vivo* on the global EV proteome in the short term. MSC viability following treatment could not be quantified. Thus, there is an inability to determine the number of EVs contributing to the SF-EV proteome derived from injected MSCs and those from joint tissues themselves.

The purpose of this study was to characterize EVs in the SF after MSC administration in equine joints with OA. The specific role of EVs secreted by the MSCs only still need to be elucidated through comparisons to untreated OA joints. One way to study MSC-derived EVs specifically could be to identify MSC-derived EVs based on surface markers.

The severity of OA phenotype is also a limitation, as the model has been shown to produce a post-traumatic OA phenotype with respect to clinical parameters, but molecularly there were no significant proteins identified between control and OA. Previous studies using the same OA model have shown an increase in the SF concentration of PGE2 and glycosaminoglycans in the OA joints shortly after OA induction (within the first two weeks) and an increase in the matrix degradation products CPII, CS846 and C1,2C only toward the end of the 70-day study period (59). Prior to FDR correction ANOVA identified 39 DE proteins with respect to group (control and OA), including: Spondin-1 ($p = 0.005$), HtrA1 serine endopeptidase ($p = 0.02$), and serotransferrin ($p = 0.01$), all of which have been previously implicated in OA pathogenesis (60–62). Thus, whilst we cannot be certain there appears to be an effect on the EV proteome following OA induction that would require further exploration with additional animal studies.

It needs to be determined if the MSC-EVs were acting in a causative or reactionary manner to the *in vivo* environment. There is a significant degree of variability with respect to MSC properties dependent on the donor or tissue source. Our study used integrin α10β1-selected adipose-derived MSCs and different results may have been achieved with an alternative source of MSCs or different MSC preparation methods. A study by Roelefs et al. found that synovium-derived adult GDF5-lineage MSCs had a significant role in response to joint injury (63). Thus, it is likely that the EV cargo will be MSC source dependent, potentially for the MSC-derived EVs as well as the joint tissue-EV response to MSCs. Another study by Broeckx et al. have shown reduced signs of OA following injection of chondrogenically induced peripheral blood-derived MSCs (64) in horses with induced OA. Barrachina et al. showed that proinflammatory primed MSCs have improved immunomodulatory abilities in the equine joint compared to naïve MSCs (41). A recent study showed that integrin α10-MSCs were able to home to a cartilage defect in rabbits and to directly participate in cartilage regeneration through chondrogenic differentiation *in vivo* (16), which has not previously been demonstrated with other MSC preparations. Therefore, we acknowledge that results of this study could have been different if another cell type was used.

With the caveat that we did not have a group of horses with OA but no MSC treatment and that we were unable to confirm the MSC survival time, we have postulated a potential mechanism of action of MSCs in our model. We hypothesize that after the introduction of MSCs into the joint, MSC-EVs deliver proteinous cargo into recipient cells found within the intra-articular environment, while also promoting intrinsic cellular changes altering the cargo of EVs secreted from native cells. We suggest they act partially through effects on the serine endopeptidase pathway, subsequently reducing its activity and OA pathogenic effect. In addition, altered EV proteins are implicated in the complement system and collagen containing extracellular matrix pathway, as shown in Figure 8. These altered pathways may provide potential targets

for therapeutic intervention and require further exploration in the context of MSC therapy and the use of MSC-EVs in OA. As such additional animal studies to assess if changes identified are due to the addition of MSCs to a joint in which OA has been induced or due to response of the joint to OA induction.

Conclusion

We characterized for the first time using an unbiased approach the SF-EV protein cargo in a model of OA after MSC administration. Changes in the proteome of the synovial fluid-derived EVs following allogeneic integrin α10-MSC administration are suggestive of EVs playing a role in mediating the effect of cell therapy. A time-dependent change in potential therapeutic efficacy of the injected MSCs was also observed. Potential targets were identified that warrant further investigation in order to determine their significance in pathophysiology and management of equine OA.

Data availability statement

The datasets presented in this study can be found in online repositories. The names of the repository/repositories and accession number(s) can be found below: The mass spectrometry proteomics data were deposited to the ProteomeXchange Consortium via PRIDE (21) (Reference: PXD035303).

Ethics statement

The animal study was reviewed and approved by Danish Animal Experiments Inspectorate (#2020-15-0201-00602) and the Ethical Committee of the University of Copenhagen (Project No: 2020-016).

Author contributions

MP, VJ, and SJ: conceptualization. EC, MP, SJ, CA, LB, EJ, ECG, RJ, and AT: methodology. EC, EJ, ECG, and RJ: formal analysis and visualization. EC, EJ, and RJ: investigation and data curation. EC: writing—original draft preparation. EC, MP, SJ, CA, LB, EJ, ECG, RJ, AT, CL, KU, and EL-Å: writing—review and editing. All authors have read and agreed to the published version of the manuscript.

Funding

EC is a self-funded Ph.D. student. MP is funded through a Wellcome Trust Intermediate Clinical Fellowship (107471/Z/15/Z). This work was supported by the Horserace Betting Levy Board in conjunction with the racing foundation (SPrj048). Our work is also supported by the Medical Research Council (MRC), Xintela AB, and Versus Arthritis as part of the MRC Versus Arthritis Center for Integrated research into Musculoskeletal Aging (CIMA). This work was funded by the Horserace Betting Levy Board (HBLB), project code SPrj048.

Acknowledgments

The authors acknowledge use of the CDSS Bioanalytical Facility and the Computational Biology Facility, services funded partially by the Liverpool Shared Research Facility Voucher Scheme (Liverpool Shared Research Facilities, Faculty of Health and Life Sciences, University of Liverpool).

Conflict of interest

Authors EL-Å and KU were employed by Xintela AB and have shares in the company.

The remaining authors declare that the research was conducted in the absence of any commercial or financial relationships that could be construed as a potential conflict of interest.

Publisher's note

Supplementary material

The Supplementary Material for this article can be found online at: https://www.frontiersin.org/articles/10.3389/fvets.2022.1057667/full#supplementary-material

References

1. McIlwraith CW, Frisbie DD, Kawcak CE. The horse as a model of naturally occurring osteoarthritis. *Bone Joint Res.* (2012) 1:297–309. doi: 10.1302/2046-3758.111.2000132

2. Ratneswaran A. Understanding osteoarthritis pathogenesis: a multiomics system-based approach. *Curr Opin Rheumatol.* (2020) 11:80–91. doi: 10.1097/BOR.0000000000000680

3. Thysen S, Luyten F, & RL-D models, 2015 undefined. Targets, models and challenges in osteoarthritis research. *dmm.biologists.org.* (2015) 5:16881. doi: 10.1242/dmm.016881

4. Smith AD, Morton AJ, Winter MD, Colahan PT, Ghivizzani S, Brown MP, et al. Magnetic resonance imaging scoring of an experimental model of osteoarthritis in the equine carpus. *Osteoarthr Res Soci-ety Int Proc.* (2014) 57:502–14. doi: 10.1016/j.joca.2014.02.528

5. Bogers SH. Cell-based therapies for joint disease in veterinary medicine: what we have learned and what we need to know. *Front Vet Sci.* (2018) 5:70. doi: 10.3389/fvets.2018.00070

6. Al Naem M, Bourebaba L, Kucharczyk K, Röcken M, Marycz K. Therapeutic mesenchymal stromal stem cells: Isolation, characterization and role in equine regenerative medicine and metabolic disorders. *Stem Cell Rev Reports.* (2020) 16:301–22. doi: 10.1007/s12015-019-09932-0

7. Barberini DJ, Freitas NPP, Magnoni MS, Maia L, Listoni AJ, Heckler MC, et al. Equine mesenchymal stem cells from bone marrow, adipose tissue and umbilical cord: Immunophenotypic characterization and differentiation potential. *Stem Cell Res Ther.* (2014) 5:1–11. doi: 10.1186/scrt414

8. Carrade DD, Lame MW, Kent MS, Clark KC, Walker NJ, Borjesson DL. Comparative analysis of the immunomodulatory properties of equine adult-derived mesenchymal stem cells 1. *Cell Med.* (2012) 4:1–11. doi: 10.3727/215517912X647217

9. Mcleod CM, Mauck RL, Orthopaedic M, Musculoskeletal T. On the origin and impact of mesenchymal stem cell heterogeneity : new insights and emerging tools for single. *Cell Anal.* (2017) 7:217–31. doi: 10.22203/eCM.v034a14

10. Johal KS, Lees VC, Reid AJ. Europe PMC Funders Group Adipose-derived stem cells : selecting for translational success. *Jama.* (2016) 10:79–96. doi: 10.2217/rme.14.72

11. Nielsen FM, Riis SE, Andersen JI, Lesage R, Fink T, Pennisi CP, Zachar V. Discrete adipose-derived stem cell subpopulations may display differential functionality after in vitro expansion despite convergence to a common phenotype distribution. *Stem Cell Res Ther.* (2016) 6:1–13. doi: 10.1186/s13287-016-0435-8

12. Camper L, Hellman U, Lundgren-åkerlund E. Isolation, cloning, and sequence analysis of the integrin subunit □ 10, a □ 1-associated collagen binding integrin expressed on chondrocytes *. *Jama.* (1998) 273:20383–9. doi: 10.1074/jbc.273.32.20383

13. Varas L, Ohlsson LB, Honeth G, Olsson A, Bengtsson T, Wiberg C, et al. et al. Growth Factor-2-Treated Mesenchymal Stem Cells with. *Stem Cells Devolop.* (2007) 978:965–78. doi: 10.1089/scd.2007.0049

14. Kristina Uvebrant, Linda Reimer Rasmusson, Jan F. Talts, Paolo Alberton AA and, Lundgren-Åkerlund E. Integrin α10β1-selected equine MSCs have improved chondrogenic differentiation, immunomodulatory and cartilage adhesion capacity. *Ann Stem Cell Res Res.* (2019) 9:153.

15. Delco ML, Goodale M, Talts JF, Pownder SL, Koff MF, Miller AD, et al. Integrin α10β1-selected mesenchymal stem cells mitigate the progression of osteoarthritis in an equine talar impact model. *Am J Sports Med.* (2020) 48:612–23. doi: 10.1177/0363546519899087

16. Andersen C, Uvebrant K, Mori Y, Aarsvold S, Jacobsen S, Berg LC, et al. Human integrin α10β1-selected mesenchymal stem cells home to cartilage defects in the rabbit knee and assume a chondrocyte-like phenotype. *Stem Cell Res Ther.* (2022) 13:1–15. doi: 10.1186/s13287-022-02884-2

17. Mocchi M, Dotti S, Bue MD, Villa R, Bari E, Perteghella S, et al. *Cells Veterinary Regenerative Medicine for Musculoskeletal Disorders: Can Mesenchymal Stem/Stromal Cells and Their Secretome Be the New Frontier? mdpi.com* (2018).

18. Cvjetkovic A, Jang S, Konečná B, reports JH-S, 2016 undefined. Detailed analysis of protein topology of extracellular vesicles–Evidence of unconventional membrane protein orientation. *nature.com* 16:338. doi: 10.1038/srep36338

19. Latifkar A, Hur YH, Sanchez JC, Cerione RA, Antonyak MA. New insights into extracellular vesicle biogenesis and function. *J Cell Sci.* (2019) 132:1–9. doi: 10.1242/jcs.222406

20. Zhang S, Chuah SJ, Lai RC, Hoi J, Hui P, Lim SK, et al. exosomes mediate cartilage repair by enhancing proliferation, attenuating apoptosis and modulating immune reactivity. *Biomaterials.* (2018) 156:16–27. doi: 10.1016/j.biomaterials.2017.11.028

21. Tofiño-Vian M, Guillén MI, Pérez Del Caz MD, Silvestre A, Alcaraz MJ. Microvesicles from human adipose tissue-derived mesenchymal stem cells as a new protective strategy in osteoarthritic chondrocytes. *Cell Physiol Biochem.* (2018) 47:11–25. doi: 10.1159/000489739

22. Hotham WE, Thompson C, Margaret F, Henson D, Szu-ting L. *The Anti-Inflammatory Effects of Equine Bone Marrow Stem Cell-Derived Extracellular Vesicles on Autologous Chondrocytes* (2021).

23. Arévalo-Turrubiarte M, Baratta M, Ponti G, Chiaradia E, Martignani E. Extracellular vesicles from equine mesenchymal stem cells decrease inflammation markers in chondrocytes in vitro. *Equine Vet J.* (2021) 21:21–11. doi: 10.1111/evj.13537

24. Cosenza S, Ruiz M, Toupet K, Jorgensen C, Noël D. Mesenchymal stem cells derived exosomes and microparticles protect cartilage and bone from degradation in osteoarthritis. *Sci Rep.* (2017) 7:1–12. doi: 10.1038/s41598-017-15376-8

25. Anderson JR, Jacobsen S, Walters M, Bundgaard L, Diendorfer A, Hackl M, et al. Small non-coding RNA landscape of extracellular vesicles from a post-traumatic model of equine osteoarthritis. *bioRxiv.* (2022) 03:483752. doi: 10.3389/fvets.2022.901269

26. Clarke EJ, Lima C, Anderson JR, Castanheira C, Beckett A, James V, et al. Optical photothermal infrared spectroscopy can differentiate equine osteoarthritic plasma extracellular vesicles from healthy controls. *bioRxiv.* (2022) 3:483922. doi: 10.1039/D2AY00779G

27. Gillet LC, Navarro P, Tate S, Röst H, Selevsek N, Reiter L, et al. Targeted data extraction of the MS/MS spectra generated by data-independent acquisition: A new concept for consistent and accurate proteome analysis. *Mol Cell Proteomics.* (2012) 11:1–17. doi: 10.1074/mcp.O111.016717

28. Demichev V, Messner CB, Vernardis SI, Lilley KS, Ralser M, DIA-NN. neural networks and interference correction enable deep proteome coverage in high throughput. *Nat Methods.* (2020) 17:41–4. doi: 10.1038/s41592-019-0638-x

29. Perez-Riverol Y, Csordas JB. The PRIDE database and related tools and resources in 2019: improving support for quantification data. *Nucleic Acid Res.* (2019) 5:1106. doi: 10.1093/nar/gky1106

30. Team Rs. Integrated Development for R. R Studio. (2015).

31. Leek JT, Johnson WE, Parker HS, Jaffe AE, Storey JD. The SVA package for removing batch effects and other unwanted variation in high-throughput experiments. *Bioinformatics.* (2012) 28:882–3. doi: 10.1093/bioinformatics/bts034

32. Kuznetsova A, Brockhoff PB, Christensen RHB. lmertest package: tests in linear mixed effects models. *J Stat Softw.* (2017) 82:1–26. doi: 10.18637/jss.v082.i13

33. Halekoh U, Højsgaard S, A. kenward-Roger approximation and parametric bootstrap methods for tests in linear mixed models-the R package pbkrtest. *J Stat Softw.* (2014) 59:1–32. doi: 10.18637/jss.v059.i09

34. Villanueva RAM, Chen ZJ. ggplot2: elegant graphics for data analysis (2nd ed). *Meas Interdiscip Res Perspect.* (2019) 17:160–7. doi: 10.1080/15366367.2019.1565254

35. Wu T, Hu E, Xu S, Chen M, Guo P, Dai Z, et al. et al. clusterprofiler 40: A universal enrichment tool for interpreting omics. *Data Innov.* (2021) 2:100141. doi: 10.1016/j.xinn.2021.100141

36. DD Frisbie SG,, PD Robbins CE and CM. Treatment of experimental equine osteoarthritis by in vivo delivery of the equine interleukin-1 receptor antagonist gene. *Gene Ther.* (2002) 2:12–20. doi: 10.1038/sj.gt.3301608

37. Frisbie DD, Kisiday JD, Kawcak CE, Werpy NM, Mcilwraith CW. Evaluation of adipose-derived stromal vascular fraction or bone marrow-derived mesenchymal stem cells for treatment of osteoarthritis. *J Orthop Res.* (2009) 9:1675–1680. doi: 10.1002/jor.20933

38. Frisbie DD, Kawcak CE, Trotter GW, Powers BE, Walton RM, Mcllwraltht CW. Effects of triamcinolone acetonide on an in vivo equine osteochondral fragment exercise model. *EQUINE Vet J.* (1997) 29:349–59. doi: 10.1111/j.2042-3306.1997.tb03138.x

39. Bertoni L, Jacquet-Guibon S, Branly T, Desancé M, Legendre F, Melin M, et al. Article evaluation of allogeneic bone-marrow-derived and umbilical cord blood-derived mesenchymal stem cells to prevent the development of osteoarthritis in an equine model. *Int J Mol Sci.* (2021) 22:1–18. doi: 10.3390/ijms22052499

40. Broeckx SY, Martens AM, Bertone AL, Brantegem LVAN, Duchateau L. The use of equine chondrogenic-induced mesenchymal stem cells as a treatment for osteoarthritis : A randomised, double-blinded, placebo-controlled proof-of-concept study. *Equine Vet J.* (2019) 51:787–94. doi: 10.1111/evj.13089

41. Barrachina L, Remacha AR, Romero A, Vitoria A, Albareda J, Prades M, et al. Assessment of effectiveness and safety of repeat administration of proinflammatory primed allogeneic mesenchymal stem cells in an equine model of chemically induced osteoarthritis. *Jama.* (2018) 8:1–17. doi: 10.1186/s12917-018-1556-3

42. Pellequer Y, Zanetta G, Rebibou JM, Severin I, Chagnon MC, Zissel G, et al. Development of a new methodology to determine size differences of nanoparticles with nanoparticle tracking analysis. *Appl Nanosci.* (2021) 11:2129–41. doi: 10.1007/s13204-021-01932-2

43. Mustonen AM, Capra J, Rilla K, Lehenkari P, Oikari S, Kääriäinen T, et al. Characterization of hyaluronan-coated extracellular vesicles in synovial fluid of patients with osteoarthritis and rheumatoid arthritis. *BMC Musculoskelet Disord.* (2021) 22:1–11. doi: 10.1186/s12891-021-04115-w

44. Brosseau C, Colas L, Magnan A, Brouard S. CD9 tetraspanin: A new pathway for the regulation of inflammation? *Front Immunol.* (2018) 9:1–12. doi: 10.3389/fimmu.2018.02316

45. Vences-Catalán F, Rajapaksa R, Kuo C-C, Miller CL, Lee A, Ramani VC, et al. Levy S. Targeting the tetraspanin CD81 reduces cancer invasion and metastasis. *Procced Nat Sci.* (2021) 118:e2018961118. doi: 10.1073/pnas.2018961118

46. Feng C, Luo X, He N, Xia H, Lv X, Zhang X, et al. Efficacy and persistence of allogeneic adipose-derived mesenchymal stem cells combined with hyaluronic acid in osteoarthritis after intra-articular. *Injection.* (2018) 24:219–33. doi: 10.1089/ten.tea.2017.0039

47. Horie M, Sekiya I, Muneta T, Ichinose S, Matsumoto K. Intra-articular injected synovial stem cells differentiate into meniscal cells directly and promote meniscal regeneration without mobilization to distant organs in rat massive meniscal defect. *Stem Cells* 27:878–887. doi: 10.1634/stemcells.2008-0616

48. Maly K, Sastre EA, Farrell E, Meurer A, Zaucke F. Comp and tsp-4: Functional roles in articular cartilage and relevance in osteoarthritis. *Int J Mol Sci.* (2021) 22:1–23. doi: 10.3390/ijms22052242

49. Wilkinson DJ, Arques M. del C, Huesa C, Rowan AD. Serine proteinases in the turnover of the cartilage extracellular matrix in the joint: implications for therapeutics. *Br J Pharmacol.* (2019) 176:38–51. doi: 10.1111/bph.14173

50. Bhutada S, Li L, Willard B, Muschler G, Piuzzi N, Apte SS. Forward and reverse degradomics defines the proteolytic landscape of human knee osteoarthritic cartilage and the role of the serine protease HtrA1. *Osteoarthr Cartil.* (2022) 30:1091–102. doi: 10.1016/j.joca.2022.02.622

51. Chen PH, Tang T, Liu C, Wang B, Mian M, Oka C, et al. High-temperature requirement a1 protease as a rate-limiting factor in the development of osteoarthritis. *Am J Pathol.* (2019) 189:1423–34. doi: 10.1016/j.ajpath.2019.03.013

52. Kolhe R, Owens V, Sharma A, Lee TJ, Zhi W, Ghilzai U, et al. Sex-specific differences in extracellular vesicle protein cargo in synovial fluid of patients with osteoarthritis. *Life.* (2020) 10:337. doi: 10.3390/life10120337

53. Najar M, Fayyad-Kazan M, Meuleman N, Bron D, Fayyad-Kazan H, Lagneaux L. Mesenchymal stromal cells of the bone marrow and natural killer cells: cell interactions and cross modulation. *J Cell Commun Signal.* (2018) 12:673–88. doi: 10.1007/s12079-018-0448-4

54. Leonard NA, Reidy E, Thompson K, McDermott E, Peerani E, Bort ET, et al. Stromal cells promote matrix deposition, remodelling and an immunosuppressive tumour microenvironment in a 3d model of colon cancer. *Cancers (Basel).* (2021) 13:5998. doi: 10.3390/cancers13235998

55. Wang Y, Yu D, Liu Z, Zhou F, Dai J, Wu B, et al. Exosomes from embryonic mesenchymal stem cells alleviate osteoarthritis through balancing synthesis and degradation of cartilage extracellular matrix. *Stem Cell Res Ther.* (2017) 8:1–13. doi: 10.1186/s13287-017-0632-0

56. Schäfer N, Grässel S. Involvement of complement peptides C3a and C5a in osteoarthritis pathology. *Peptides.* (2022) 154:170815. doi: 10.1016/j.peptides.2022.170815

57. Silawal S, Triebel J, Bertsch T, Schulze-Tanzil G. Osteoarthritis and the complement cascade. *Clin Med Insights Arthritis Musculoskelet Disord.* (2018) 11:1179544117751430. doi: 10.1177/1179544117751430

58. Woodell-May JE, Sommerfeld SD. Role of Inflammation and the Immune System in the Progression of Osteoarthritis. *J Orthop Res.* (2020) 38:253–7. doi: 10.1002/jor.24457

59. Frisbie DD, Al-Sobayil F, Billinghurst RC, Kawcak CE, McIlwraith CW. Changes in synovial fluid and serum biomarkers with exercise and early osteoarthritis in horses. *Osteoarthr Cartil.* (2008) 16:1196–204. doi: 10.1016/j.joca.2008.03.008

60. Sulaiman SS, Lau S, Tan W, Rahmad N, Ajat MM, Radzi R, et al. Comparison of synovial fluid proteome profiles between chemically induced rabbit model and surgically induced rabbit model in mimicking early osteoarthritis. *Osteoarthr Cartil.* (2020) 28:S349. doi: 10.1016/j.joca.2020.02.546

61. Tossetta G, Fantone S, Licini C, Marzioni D, Mattioli-Belmonte M. The multifaced role of HtrA1 in the development of joint and skeletal disorders. *Bone.* (2022) 157:116350. doi: 10.1016/j.bone.2022.116350

62. Aspden RM, Saunders FR. Osteoarthritis as an organ disease: From the cradle to the grave. *Eur Cells Mater.* (2019) 37:74–87. doi: 10.22203/eCM.v037a06

63. Roelofs AJ, Zupan J, Riemen AHK, Kania K, Ansboro S, White N, et al. Joint morphogenetic cells in the adult mammalian synovium. *Nat Commun.* (2017) 8:1–14. doi: 10.1038/ncomms15040

64. Beerts C, Suls M, Broeckx SY, Seys B, Vandenberghe A, Declercq J, et al. Tenogenically induced allogeneic peripheral blood mesenchymal stem cells in allogeneic platelet-rich plasma: 2-year follow-up after tendon or ligament treatment in horses. *Front Vet Sci.* (2017) 4:158. doi: 10.3389/fvets.2017.00158

frontiers | Frontiers in Veterinary Science

TYPE Original Research
PUBLISHED 13 January 2023
DOI 10.3389/fvets.2022.1014687

OPEN ACCESS

EDITED BY
Natalia Vapniarsky,
University of California, Davis,
United States

REVIEWED BY
Denis J. Marcellin-Little,
University of California, Davis,
United States
Mudasir Bashir Gugjoo,
Sher-e-Kashmir University of
Agricultural Sciences and Technology
of Kashmir, India

*CORRESPONDENCE
Andrew J. Armitage
✉ Andrew.armitage@
Greensidevetpractice.co.uk

SPECIALTY SECTION
This article was submitted to
Veterinary Regenerative Medicine,
a section of the journal
Frontiers in Veterinary Science

RECEIVED 08 August 2022
ACCEPTED 27 December 2022
PUBLISHED 13 January 2023

CITATION
Armitage AJ, Miller JM, Sparks TH,
Georgiou AE and Reid J (2023) Efficacy
of autologous mesenchymal stromal
cell treatment for chronic
degenerative musculoskeletal
conditions in dogs: A retrospective
study. *Front. Vet. Sci.* 9:1014687.
doi: 10.3389/fvets.2022.1014687

Efficacy of autologous mesenchymal stromal cell treatment for chronic degenerative musculoskeletal conditions in dogs: A retrospective study

Andrew J. Armitage[1]*, Joanna M. Miller[2], Tim H. Sparks[3], Alex E. Georgiou[2,4] and Jacqueline Reid[5,6]

[1]Greenside Veterinary Practice, Part of Linnaeus Veterinary Limited, Melrose, United Kingdom, [2]Cell Therapy Sciences Ltd., Coventry, United Kingdom, [3]Waltham Petcare Science Institute, Melton Mowbray, United Kingdom, [4]Coventry University, Coventry, United Kingdom, [5]University of Glasgow, Glasgow, United Kingdom, [6]NewMetrica Research Ltd., Glasgow, United Kingdom

Introduction: The objective of this study was to retrospectively analyze clinical data from a referral regenerative medicine practice, to investigate the efficacy of autologous mesenchymal stromal cells (MSC) in 245 dogs deemed unresponsive to conventional treatment by their referring vet.

Methods: Diagnostic imaging [radiology and musculoskeletal ultrasound (MSK-US)] identified musculoskeletal pathology holistically. MSCs, produced according to current guidelines, were initially administered with PRP by targeted injection to joints and/or tendons, with a second MSC monotherapy administered 12 weeks later to dogs with severe pathology and/or previous elbow arthroscopic interventions. Dogs with lumbosacral disease received epidural MSCs with additional intravenous MSCs administered to dogs with spondylosis of the cervical, thoracic and lumbar spine. All dogs received laser therapy at 10 J/cm^2 at the time of treatment and for 5 sessions thereafter. Objective outcome measures (stance analysis, range of joint motion, pressure algometry) and validated subjective outcome measures (owner reported VetMetrica HRQL^{TM} and veterinary pain and quality of life impact scores) were used to investigate short and long-term (6–104 weeks) efficacy. Outcome data were collected at predetermined time windows (0–6, 7–12, 13–18, 19–24, 25–48, 49–78, 79–104) weeks after initial treatment.

Results: There were statistically significant improvements in post compared with pre-treatment measures at all time windows in stance analysis, shoulder and hip range of motion, lumbosacral pressure algometry, and to 49–78 weeks in carpus and elbow range of motion. Improvements in 4 domains of quality of life as measured by VetMetricaTM were statistically significant, as were scores in vet-assessed pain and quality of life impact. In dogs receiving one initial treatment the mean time before a second treatment was required to maintain improvements in objective measures was 451 days. Diagnostic imaging confirmed the regenerative effects of MSCs in tendinopathies by demonstrating resolution of abnormal mineralization and restoration of normal fiber patterns.

Discussion: This represents the first study using "real-world" data to show that cell-based therapies, injected into multiple areas of musculoskeletal pathology in a targeted holistic approach, resulted in rapid and profound positive effects on the patient's pain state and quality of life which was maintained with repeat treatment for up to 2 years.

KEYWORDS

canine, tendinopathies, regenerative medicine, osteoarthritis, platelet rich plasma (PRP), laser therapy, lumbosacral disease, stem cells

1. Introduction

Chronic degenerative musculoskeletal (MSK) conditions such as osteoarthritis (OA) cause significant morbidity in working and pet dogs in the UK (1, 2). Osteoarthritis, which affects 2.5% of the UK dog population is one of the most common causes of chronic pain in dogs (3). Although OA is predominately a disease of the joint, it frequently results in associated soft tissue pathology in the joint capsule and support structures as the disease progresses (4). Joint changes lead to pain and debility causing offloading of the affected joint with compensatory overloading in other areas of the locomotor apparatus and spine (5–10). There is, however, surprisingly little published evidence linking altered biomechanics to concurrent musculoskeletal diseases (MSD), but the prevalence of multiple MSD in a patient is common (11). Although there are many primary degenerative conditions that affect the MSK system, secondary changes frequently complicate the clinical picture. Many patients present with multifactorial pathologies involving various tissue types, which makes these cases challenging to treat, requiring a multimodal approach, and can lead to treatment failures when management of one condition does not apply to another. Appropriate management of MSD requires accurate diagnosis to fully evaluate the condition and a holistic approach to treatment and, as such, a single therapeutic option for multiple MSD would be beneficial in human and veterinary medicine.

The aims of treatment are to reduce pain, decrease lameness and significantly improve the patient's quality of life (QOL). Surgical options, including full or partial joint replacements, joint arthrodesis, arthroscopic interventions, and tenotomies, aimed at improving limb function and reducing pain, tend to be non-curative salvage procedures that have potentially serious complications, especially in the case of elbow dysplasia (12–16). Additional treatment options, including analgesic drugs, anti-inflammatory and monoclonal antibody medications as well as nutritional supplements, have limited efficacy, can cause side effects and are not curative (17). In contrast, regenerative medicine (RM) utilizing mesenchymal stromal cells (MSCs), which have the capacity to self-renew and differentiate into multiple cell types, has increasingly emerged as an effective clinical treatment for MSD in both human and veterinary patients (18–22). In addition to their reparative potential, they possess anti-inflammatory and immune-modulating properties that allow them to control inflammation and pain (23–27). Furthermore, several canine RM studies have included platelet rich plasma (PRP) with MSCs, as the combination is considered to be synergistic in terms of regenerative effects (22, 28).

Veterinary clinical studies using intra-articular treatments of MSCs in osteoarthritic joints have demonstrated positive and effective outcomes in terms of reduced lameness and pain, and have been shown to be safe, see Voga et al. for a comprehensive review (19). However, long-term follow up, including diagnostic imaging of their disease modifying potential, is lacking in human and veterinary medicine (19).

Outcome measures for orthopedic studies include objective measures such as force plate and kinematic gait analysis, measures of weight distribution (stance analysis), range of joint motion (ROM) and pressure algometry in cases of lumbosacral disease (LSD). While force plate and gait analysis are most frequently used, a recent publication concluded that studies utilizing a weight distribution platform (stance analysis) to monitor response to treatment in dogs with orthopedic disease would be "clinically valuable and useful for establishing research standards" (29). Similarly, goniometry has been suggested

Abbreviations: A/C, Active and comfortable; BSA, Bovine serum albumin; CMI, Clinical metrology instrument; COMP, Canine outcome measures program; C/R, Calm and relaxed; CROM, Client reported outcome measures; DMEM, Dulbecco's Modified Eagles Medium; DPBS, Phosphate buffered saline; E/E, Energetic and enthusiastic; EM, Expansion medium; EMA, European Medicine Agency; EWB, Emotional wellbeing; FCS, Fetal calf serum; FDA, US Food and Drug Administration; GA, General anesthetic; H/C, Happy and content; HRQL, Health Related Quality of Life; IV, Intravenous; IVDD, Intervertebral disc disease; LS, Lumbosacral; LSD, Lumbosacral disease; LT, Laser Therapy; MID, Minimum important difference; MNT, Mechanical nociceptive testing; MSC, Mesenchymal stromal cell; MSK, Musculoskeletal; NRS, Numerical rating scale; NSAIDs, Non-steroidal anti-inflammatory drugs; OA, Osteoarthritis; PA, Pressure algometry; PBM, Photobiomodulation; PWB, Physical wellbeing; PRP, Platelet rich plasma; PSI, Pounds per square inch; QOL, Quality of Life; RCT, Randomized clinical trial; RM, Regenerative medicine; ROM, Range of motion; RWD, Real-world data; RWE, Real-world evidence; SD, Standard deviation; SS, Supraspinatus; US, Ultrasound (Diagnostic).

as a suitable technique for objective outcome assessment in orthopedic studies (30, 31). Pressure algometry (PA), or mechanical nociceptive testing (MNT), is an objective measure to quantify nociceptive thresholds and its use in animals has been described in a number of publications (32–37). Lane and Hill evaluated PA for measuring muscular pain at the thoracolumbar junction in dogs (36). They concluded that there was a positive increase in MNT, which related to improved muscular comfort in this region, over time in the two treatment groups but not in the control group. They propose that PA is a valid measure of MNT in the lumbar region in dogs and serves as an objective measure of muscular pain. Although clinically relevant change in PA readings has not been defined for specific anatomical locations in dogs, any increase following treatment would suggest a reduction in pain (38) which would be clinically significant even if that change was small. Various studies have shown increases in pressure pain threshold are associated with improved pain scores using clinical metrology instruments in humans with chronic lower back pain when compared in placebo-controlled trials (39, 40).

In addition to objective outcome measures which are useful for diagnosing the affected limb and measuring change, there are a number of subjective clinical metrology instruments (CMIs) in general use. These take the form of owner completed questionnaires designed to measure the functional limitation imposed by the disease and include the Canine Brief Pain Inventory (CBPI), Liverpool Osteoarthritis in Dogs (LOAD), Helsinki Chronic Pain Index (HCPI) and the Canine Orthopedic Index (COI) (41).

However, in 2006 the Canine Outcome Measures Program (COMP), formed with the intention of providing mechanisms and tools for improving the quality and impact of clinical studies in veterinary orthopedics, published guidelines which suggested that, in addition to at least one functional outcome, such as kinetics, kinematics, activity monitors, and/or an owner-reported CMI, all studies should include a validated health-related quality of life (HRQL) outcome measure (42).

Health-related quality of life instruments can be specific, focusing on particular conditions (disease specific), or they can be generic, designed for use in a variety of contexts. Disease specific instruments may be more sensitive to clinical change but generic instruments have been used successfully to quantify a range of impacts related to specific diseases including OA in people (43). Of the three currently available canine generic instruments (44–46), only VetMetrica™ (46) is validated for use in sick dogs. VetMetrica™ is an online behavior-based structured questionnaire instrument, designed to be completed on a computer or any mobile platform by the dog owner in around 5 min (46). It generates a HRQL profile for the dog with scores in four domains of QOL and has been used previously to measure the improvement in a group of dogs with OA treated with NSAIDs (47), and with RM (48).

While the majority of studies report a statistically significant change following treatment, responsiveness in a clinical measurement instrument is that property which ensures that the instrument can detect differences in health status that are important to the clinician and/or to the patient/dog owner and these need not be statistically significant (41). Responsiveness can be quantified by calculating a minimum important difference (MID) which is defined as "the smallest difference in score in the outcome of interest that informed patients or informed proxies perceive as important, either beneficial or harmful, and which would lead the patient or clinician to consider a change in the management" (49). The MID has been published for each domain of QOL in the VetMetrica™ instrument (50). In those measurement instruments where there is no MID published, clinical significance can be demonstrated by calculation of an effect size between control and treatment groups or between pre- and post-treatment groups (51).

Despite the extensive research and considerable promise shown by RM for treatment of MSD in canine and equine patients (19, 52), the origins, processing, and quality of stromal cells and PRP differ amongst the various treatment protocols, making it difficult to compare studies, a problem highlighted by Guest et al. (53). Additionally, there are no reports of large studies in which a variety of dog breeds with naturally occurring MSD were treated with RM. Data regarding protocols, duration of treatment responses and use in natural disease states such as OA in companion animals are also lacking (19). The present study addresses many of these concerns through its use of several validated outcome measures in a large sample of client-owned dogs with non-responsive chronic MSD recorded up to 4 years. The aim of this study was to investigate the efficacy of autologous MSC treatment for previously unresponsive chronic degenerative MSD in dogs, by retrospectively analyzing data from the clinical records of a single veterinary practice specializing in RM.[1] As such, this is an example of real-world data (RWD) which is defined by The Association of the British Pharmaceutical Industry as "data that are collected outside the controlled constraints of conventional randomized clinical trials (RCT) to evaluate what is happening in normal clinical practice" (54). While RCTs provide evidence of efficacy, studies using RWD have greater generalizability and give evidence of effectiveness in real-world settings (55). Following on from the US Food and Drug Administration (FDA) Real-world Evidence (RWE) program, RWD has become increasingly important in human healthcare to support a wide range of healthcare and regulatory decisions (56, 57). In addition to data generated by a selection of objective outcome measures, owner-reported HRQL data were obtained. Our hypothesis was that treatment with RM would produce both significant statistical and clinically relevant improvement in MSK function and QOL in affected dogs.

1 Greenside Veterinary Practice, Greenside Farm, St Boswells, UK.

2. Materials and methods

2.1. Ethical statement

This study was performed in line with the Mars scientific research and engagement policy (https://www.mars.com/about/policies-and-practices/scientific-engagement). All dog owners gave written informed consent for anonymised pet data to be used in the study. The RCVS Ethics Review Panel approved the study.

2.2. Case details and inclusion criteria

Medical records of client-owned dogs diagnosed with chronic MSD that were treated with RM from September 2017 to May 2021 were reviewed. Inclusion criteria for data collection were as follows: Dogs with MSD for which conventional therapy had been unsuccessful according to the referring veterinary surgeon; and whose owners had completed at least two sets of HRQL assessments; and at least one objective outcome measure. All cases were managed by a single clinician (author AA) who had extensive experience of RM having treated more than 600 dogs over 9 years with autologous MSCs, ensuring consistent clinical assessment, treatment and objective measurement outcomes. For each dog, all HRQL assessments were completed by the same owner.

On initial presentation all dogs underwent a full orthopedic and neurological physical examination including stance analysis and gait observation. Radiography and musculoskeletal ultrasound (MSK US), which was performed in paired joints allowing comparisons of measurements and echogenicity of anatomical structures between contralateral limbs, were undertaken to reach a definitive diagnosis. Confirmation that conventional therapy for the patients MSD had been unsuccessful was determined by reviewing the clinical history and demonstrating persistent pain, lameness or disability despite appropriate analgesic medications and previous interventions.

Osteoarthritis severity was graded on the basis of radiographic findings with additional clinical and ultrasound descriptions, using set criteria defined by author AA (Supplementary material 1). Where there was no radiographic evidence of OA, but ultrasound revealed a joint effusion and synovitis, and or cartilage defects, then these joints were classified as having Grade 1 OA.

Clinical and diagnostic findings were discussed with the owners and various treatment options including surgery, physical therapies, and altered pharmacological management, explained. Where a treatment plan was decided on that involved RM, the dog underwent fat harvest for stem cell extraction and culture. Patients whose treatment plan did not involve RM were returned to the referring veterinary surgeon for management.

For patients already receiving physical therapies (such as physiotherapy or hydrotherapy) this was discontinued after fat harvest and not resumed until after the post-treatment examinations at 12 weeks for single treatments and 18 weeks for two treatments. Physical therapies were not started until sufficient healing had been achieved in tendons and ligaments (as assessed by MSK US) and pain was determined to be under control.

2.3. MSC collection and preparation

2.3.1. Adipose tissue and blood collection

Dogs were anesthetized using a standard protocol and, following surgical preparation of the site, at least 5 g of adipose tissue was harvested from the falciform ligament *via* a cranial laparotomy incision cranial to the umbilicus. The adipose tissue was placed immediately into a sterile container with saline and sealed. An uncoagulated blood sample, the volume of which was determined by the quantity of stem cells required for culture and the patient's body weight and blood volume, was collected under aseptic conditions from the jugular vein. The adipose tissue and blood were packaged into cool boxes with chilled packs (4–10°C), sent to a specialized veterinary cell culture laboratory[2] and processed within 24 h of harvest.

2.3.2. Tissue processing and MSC culture

At the laboratory, MSCs were extracted from the adipose tissue samples as described by Smitzi et al. (58). Once in culture at passage 0 they were incubated at 37°C in a humidified incubator with 5% CO_2 in Expansion Medium (EM) (high glucose Dulbecco's Modified Eagles Medium (DMEM, ThermoFisher Scientific, Swindon, UK) with 10% Fetal Calf Serum (FCS, TCS Biosciences, Buckingham, UK) and 1% antibiotic and antimycotic (ABAM, ThermoFisher Scientific), which was changed every 2–3 days. The cultures were passaged until sufficient MSCs were present for treatment but were not passaged beyond passage 4. Twenty-four hours before the MSCs were due to be harvested, the flasks were washed twice with Phosphate Buffered Saline (DPBS, ThermoFisher Scientific) and incubated in a pre-treatment medium for 24 h as described above. For proprietary reasons, the constituents of the pre-treatment medium are not described.

Treatment vials were prepared by washing the attached cells with DPBS and then incubating for 5–10 min at 37°C in TrypLE^{TM} (ThermoFisher Scientific) until the cells were in suspension. The suspended cells were washed in DPBS by centrifugation at 1500 g. The final cell pellet was resuspended in Autologous serum with 10% saline and 10% Dimethyl Sulphoxide (DMSO, Sigma-Aldrich, Gillingham, UK) at a cell

2 Cell Therapy Sciences Ltd, Coventry, UK.

concentration of more than 2.5 million cells per ml for intra-articular treatment and 10 million cells per ml for epidural treatments. Intravenous doses were created at a concentration requested by the treating veterinary surgeon. Two milliliters of cell suspension were placed into a CellSeal^{TM} vial (Sexton Biotechnologies, Indianapolis, USA), sealed using a tube sealer, labeled and cryopreserved using a CoolCell^{TM} (Azenta Life Sciences, Manchester, UK) container in a −80°C freezer. Two 50 µl samples of the final MSC suspension were reserved for quality control. The cryopreserved treatment vials were maintained at −80°C during transportation and storage (for <4 weeks) at the clinic until they were required for injection. Internal quality control has confirmed that the cells remain viable for at least one month when stored at −80°C.

TABLE 1 Antibodies for immunophenotyping.

Primary antibodies	Isotope controls
CD44 Monoclonal Antibody (YKIX337.8), FITC	Rat IgG2a kappa Isotype Control (eBR2a), FITC
CD90 (Thy-1) Monoclonal Antibody (YKIX337.217), PE	Rat IgG2b kappa Isotype Control (eB149/10H5), PE
CD34 Monoclonal Antibody (1H6), PE	Mouse IgG1 kappa Isotype Control (P3.6.2.8.1), PE
CD45 Monoclonal Antibody (YKIX716.13), FITC	Rat IgG2b kappa Isotype Control (eB149/10H5), FITC
MHC Class II Monoclonal Antibody (YKIX334.2), APC	Rat IgG2a kappa Isotype Control (eBR2a), APC

Primary conjugated canine antibodies and their corresponding isotope controls. All antibodies were eBioscience^{TM} from Thermofisher.

2.3.3. MSC characterization and quality control

Trilineage differentiation was demonstrated based on the methods described by Russell et al. (59). For chondrogenic differentiation MSCs at passage 3 were seeded at 2 x 10^5 cells in 0.1 ml low glucose EM per well on a low adhesion Nunc u-bottomed 96 well plate (ThermoFisher Scientific) and left to settle in the incubator as described above. After 48 h the EM was removed, spheroids washed twice with PBS and then 0.1 ml StemPro Chondrogenesis Differentiation medium (ThermoFisher Scientific) was added per well. Control wells were maintained in low glucose EM throughout. Plates were maintained in the incubator for 21 days with medium changed every 2–3 days. Spheroids were stained with Alcian Blue (ThermoFisher Scientific) following fixation with paraformaldehyde, then washed with 0.1 N HCl (Sigma-Aldrich), neutralized with distilled water and visualized under light microscopy. The spheroids were then mounted on glass slides, compressed under a glass coverslip and imaged.

For osteogenic differentiation MSCs at passage 3 were seeded at 2 x 10^5 cells per well in 1 ml low glucose EM on a 24 well plate (Sarstedt, Leicester, UK) and incubated as described above with the medium changed every 2–3 days until they reached 80% confluence. The medium was removed, the cells washed with DPBS and then test wells were treated with 1 ml StemPro^{TM} Osteogenesis Differentiation medium (ThermoFisher Scientific) and control wells with low glucose EM for 14 days with medium changed every 2–3 days. The monolayer of cells was fixed with 10% Formalin (Sigma-Aldrich), washed with demineralised water and then 1 ml 40 nM Alizarin Red S (Sigma-Aldrich, UK) was added to each well and incubated at room temperature in the dark for 30 min. The stain was washed off with deionised water before visualization with an inverted microscope.

For adipogenic differentiation MSCs at passage 3 were seeded at 5 x 10^4/well onto a tissue culture coated 96 well plate (Sarstedt) in 0.1ml StemMACS AdipoDiff Media (Miltenyi Biotec, Bisley, UK), control wells were seeded at the same density in low glucose EM. The plate was incubated as described above and the medium changed every 2–3 days. After 14 days the cells were fixed with 4% paraformaldehyde, washed with DPBS and stained with Oil Red (Sigma-Aldrich) washed twice with deionized water and visualized with an inverted microscope.

Immunophenotyping was carried out based on the methods described by Krešić et al. (60) and Ivanovska et al. (61). Briefly, seven cell lines of MSCs (taken at random from the bank of MSCs stored at the lab) were cultured to passage 2 and when 80% confluent were trypsinised as described above. The cell pellet was resuspended in 1 ml of 4% paraformaldehyde (Sigma-Aldrich) for 15 min and washed with DPBS. For each antibody 1–2 x 10^5 MSCs for each cell line ($n = 7$) were transferred to conical Eppendorf tubes. The fixed MSCs were then resuspended in 1:100 diluted canine antibodies in 2% Bovine Serum Albumin (BSA, Sigma-Aldrich)/DPBS, incubated in the dark for 30 min at room temperature, washed twice with DPBS, resuspended in ice cold DPBS and read on the BD C6 flow cytometer (BD Biosciences, Wokingham, UK) with a 1 x 10^4 event limit (see Table 1 for the antibodies used for immunophenotyping). These data were analyzed using BD Accuri C6 Plus software (version 1.0.23.1; BD Biosciences). The samples were run with unstained controls and the corresponding isotope controls.

Release criteria for the MSC treatment vials required all batches (i.e., every individual MSC culture) to pass the final culture morphology check, a 4-day microbiology test and a post-cryo viability and cell count. The results of these tests were supplied to the treating veterinarian (AA) on a certificate of analysis. Quality control tests are detailed in Supplementary material 2.

2.4. PRP processing

Depending on body weight and amount of PRP required, 25 or 50 ml of anticoagulated blood was collected and total white blood cell (WBC), differential counts, red blood cell

(RBC) concentration and platelet concentration determined using an inhouse Idexx Procyte hematology analyser (Idexx Laboratories, Westbrook, ME, USA), calibrated according to the manufacturer's recommendations. The anticoagulated blood was processed, according to the manufacturer's instructions, using a canine validated system (PurePRP Kit, Companion Regenerative Therapies, Newark, DE, USA). One half to 1 ml of PRP was dispensed into 1 ml syringes for injection and a sample of the PRP was analyzed using an inhouse Idexx Procyte hematology analyser (Idexx Laboratories, Westbrook, ME, USA) as before. The PRP product composition was confirmed for each sample. The increased platelet cell count from whole blood was calculated by dividing the PRP platelet count by the whole blood platelet count to give a concentration factor specific to each patient.

2.5. Treatment protocol

At the clinic, MSC treatment vials were allowed to defrost at room temperature. The exact number of cells required for treatment was determined from the certificate of analysis which detailed the cell count in millions per milliliter, % viability post thaw, and release criteria passed.

Dogs were sedated with a combination of medetomidine (Sedator, Dechra Veterinary Products, Shrewsbury, UK) and methadone (Comfortan, Dechra Veterinary Products, Shrewsbury, UK) administered intravenously, or given a general anesthetic, as before, for treatment with a combination of stem cells and PRP, or MSCs alone in the case of LS epidural injection.

Treatment sites were aseptically prepared and joint injections performed using standard approaches. For intra-articular treatment, fluid was aspirated to ensure correct needle placement and to remove excessive fluid prior to injection of cells, and MSK US was used to guide treatments to target specific pathology in muscle, tendon or ligaments. LS epidural injections were performed with a spinal needle using a standard approach and, in those cases where spondylosis was present in the cervical and thoracic regions, IV stem cells were infused in addition to the epidural injection at the LS junction.

For each joint or tendon lesion, $>$ 2.5 million stem cells were injected at each location. In the case of LSD $>$ 10 million cells were injected in the epidural space at the LS junction and where IV treatments were administered, 1 million cells per kg bodyweight were given *via* slow IV infusion. MSCs and PRP were combined and mixed in a sterile manner immediately prior to injection for intra-articular and tendon treatments. MSCs alone were injected into the epidural space or when intravenous treatments were required. Adverse reaction to any treatment was recorded in the clinical record.

Treatment sites received Class IV laser therapy (Companion Therapy Laser CTC-15, LiteCure, LLC, DE. USA) directly after injection and a further five sessions were completed over the following 3–6 weeks. Laser therapy (LT) was applied using a laser-contact ball by continuously moving the head in a grid pattern over the entire treatment area as per the manufacturer's recommendations. Laser power and duration of treatment was tailored to each individual depending on body weight, body condition, hair length, hair color and skin color. The dose provided to each treatment area was 10 joules/cm^2.

All dogs were re-assessed clinically at approximately 6, 12, and 18 weeks following initial treatment and then every 3–6 months. At 12 weeks, in the case of severe pathology (i.e., Grade 3/5 OA or greater) or where dogs had received surgical arthroscopic intervention of the elbow prior to referral to author (AA), a second treatment of MSCs alone was administered. Similarly, at 12 weeks a repeat treatment with MSCs was administered where MSK US indicated that healing of treated soft tissue structures was incomplete. A single laser therapy treatment was provided at the time of injection to the treatment area when a second treatment was performed. In those dogs that received additional treatment more than 12 months after their previous treatment, the initial treatment protocol was followed. The treatment protocol has been summarized in Table 2.

2.6. Diagnostic imaging

Musculoskeletal US formed part of all clinical assessments and was used to evaluate muscles, tendons, ligaments, caudal lumbar intervertebral discs (IVD) and intraarticular structures including the joint capsule, volume of joint fluid, and changes to the synovium and articular surface integrity. Where pathological changes were unilateral, comparison was made with contralateral structures, using standard views. Tendons and their entheses were evaluated for enlargement by measuring their cross-sectional areas in specific anatomical locations and comparing to the contralateral structure. Elastography was used to image the elastic properties of tendons to confirm presence of fibrosis or scar tissue. Caudal lumbar IVD were evaluated by comparison with adjacent discs in order to measure thickness of the annulus fibrosus and echogenicity of the nucleus pulposus. Where there was extensive mineralization of soft tissue structures, in addition to MSK US, a repeat radiograph was taken of the affected area 12 weeks following initial treatment to determine the extent of any remaining abnormal mineralization. Where clinical assessment indicated the requirement for further treatment with RM, radiographs were taken and MSK US performed if appropriate, to establish if further or alternative pathology had developed.

2.7. Clinical outcome measurements

Objective outcome measures comprised part of the pre-treatment assessment and were repeated at all subsequent

TABLE 2 A summary of the treatment protocol used in all cases depending on the diagnosed pathology and severity in individual cases.

MSD diagnosed	Initial treatment with MSCs (>2.5 million cells) and PRP	Initial treatment with MSC alone	Follow-up MSC (>2.5 million cells) treatment 3 months after initial treatment	Epidural administration of MCSs (10 million MSCs)	IV administration of MSCs (1 million cells per kg bodyweight)	Laser therapy (10J/cm^2) at treatment site performed at time of each injection	3–6 week laser therapy course of five sessions on all treatment sites following initial treatment only
OA grade 1–2/5 with or without dysplasia	✓					✓	✓
OA grade 3–5/5 with or without dysplasia	✓		✓			✓	✓
ED with previous arthroscopic interventions and OA grade 1–5/5	✓		✓			✓	✓
Soft tissue pathology (including tendons and ligaments)	✓					✓	✓
Soft tissue with incomplete healing identified by MSK ultrasound at 3 months post initial treatment			✓			✓	
LSD		✓		✓		✓	✓
Spondylosis affecting the cervical, thoracic and lumbar spine				✓	✓	✓	✓

10.3389/fvets.2022.1014687

clinical assessments. Not all outcome measures were recorded for each patient where the clinical examination or diagnosis did not warrant it. For example, patients not suffering from LSD did not have PA performed and patients only suffering from LSD did not have joint goniometry performed.

2.7.1. Stance analysis

A weight distribution platform (Companion stance analyser, LiteCure LLC, Newark, Delaware, USA) was used according to the manufacturer's instructions to measure percentage of weight distribution through each of the four limbs. Normal (target) weight distribution was taken to be 30% for each thoracic limb and 20% for each pelvic limb (29). Since many dogs in the study had bilateral MSD, an overall deviation from normal weight bearing was calculated by summing the absolute deviations of recorded from target values for each limb. Thus, zero would represent normal weight bearing, and larger values increasing deviation from normal. This value not only gives a value of offloading but also compensatory overloading and gives a better measure where multiple limb MSDs are present.

2.7.2. Goniometry

The dog was positioned in lateral recumbency, and an appropriately sized universal plastic goniometer was used to measure full flexion and extension of the affected joint. The pivot point of the goniometer was placed over the center of motion of the joint and its arms aligned along the bone axes proximal and distal to the joint being measured. The proximal arm of the goniometer was held *in situ* whilst the joint was fully flexed and extended. The values were read in degrees from the goniometer and recorded in the clinical record. The ROM was calculated by subtracting the flexion angle from the extension angle. Further information regarding anatomical landmarks for goniometer placement are detailed in Supplementary material 3 and images of correct placement have been published previously (30).

2.7.3. Pressure algometry

When lumbosacral pain was detected during the physical examination by direct palpation, Lumbosacral flexion and on tail hyperextension, a pressure algometer (Force Ten FDX compact digital force gauge. Wagner instruments, Greenwich, CT, USA) was used to quantify the pressure pain threshold. The LS junction was identified by palpating the dorsal spinous processes of L7 and S1 vertebrae. Pressure was applied at a steady rate to the dorsal lumbosacral (LS) junction (L7-S1) at right angles to the skin and the peak force (PSI) applied in order to elicit a pain response (any one of the following—dropping away from the instrument, turning of the head, vocalization or lip licking) was recorded as an average of three measurements and rounded to the nearest whole number.

2.7.4. HRQL measurement (VetMetrica™)

The same owner for each dog included in this study was requested to complete VetMetrica™ assessments prior to treatment, then at 2, 6, 12, and 18 weeks post first treatment; then every 6 months thereafter. Except for the 2-week assessment, which did not coincide with a clinical examination, the owners completed their assessment before each clinical examination to minimize potential bias.

VetMetrica™ behavior-based structured questionnaire instrument contains 22 items (questions) for the owner. These items are simple descriptive terms, which are either positive (words associated with healthy conditions) or negative (words associated with unhealthy conditions). Each descriptor is associated with a 7-point (0–6) scale, which allows the owner to rate the extent to which the term depicts their dog. For example, for the term "playful", 0 represents "not at all playful and 6 represents "couldn't be more playful". Accordingly, in the case of a positive item like "playful" a score of 6 implies very good HRQL, but the same score implies very poor HRQL when the item is negative, for example "lethargic". A coded algorithm automatically transforms the owner responses to all 22 items into a HRQL profile for the dog which consists of raw scores (0-6) in 4 domains of QOL – Energetic/Enthusiastic (E/E), Happy/Content (H/C), Active/Comfortable (A/C), Calm/Relaxed (C/R). Summary scores in physical wellbeing (PWB) and emotional wellbeing (EWB) can be calculated by averaging the E/E and A/C scores (PWB) and H/C and C/R scores (EWB) (Author JR Personal Communication). To aid interpretation, these raw domain scores are optimized by normalizing them to the age-related healthy dog population, such that a score of 50 on a 0–100 scale represents the score for the age–related average healthy dog. Additionally, 70% of healthy dogs will score above a threshold set at 44.8 on the 0–100 scale (50).

In order to determine the clinical significance of improvements in HRQL domain scores, the difference in median values was calculated between pre–treatment and each successive post-treatment time window. A change equivalent or greater than the MID of 7 was considered clinically significant.

2.7.5. Vet clinical assessment

Timed to coincide with each owner HRQL assessment, other than the 2 weeks post initial treatment, a veterinary assessment (Supplementary material 4) was completed by author (AA) who was blinded to his previous scores by the fact that scores were entered directly into the VetMetrica™ database rather than the clinical record. The veterinary assessment comprised a list of common canine diseases which, when present, were graded as mild/moderate/severe/end stage. A freeform box was provided to accommodate any disease not specified in the list. Additional questions were as follows: "on a scale of 0–10, with 0 being no impact and 10 being the most impact, please assess how much

the dog's health status is reducing its quality of life (QOL)", and "on a scale of 0 to 10 with 0 being no pain and 10 being the pain could not be worse, please indicate what amount of pain you feel the dog is suffering".

2.7.6. Analgesic usage

Analgesic usage was compared at two time periods: pre-treatment up to 180 days (c.26 weeks) before the first treatment (but excluding the date of treatment) and 24–48 weeks post-treatment. Where multiple records existed, the latest in the pre-treatment period (closest to treatment date) and the earliest in the post-treatment period (closest to 6 months) was selected.

2.8. Data handling and analysis

2.8.1. Retrospective data collection

Patient data included signalment, history, diagnosis, prior treatments (including treatments at initial presentation), analgesic therapy, physical examination findings, diagnostic imaging results and objective outcome measurements (weight distribution at stance, joint angle goniometry measurements and pressure algometry readings) were extracted from the case record. Dogs were excluded from the analysis of each individual outcome measure if there were insufficient data recorded in the medical record pre- or post-treatment. Normalized scores in four domains of QOL calculated from the VetMetrica^{TM} owner-reported health related quality of life (HRQL) questionnaires, and vet pain and QOL impact scores, were extracted from the VetMetrica Database. Ideally HRQL assessments corresponded with clinic visits and vet assessments, except at 2 weeks when there was no clinic visit. However, individual owner circumstances often dictated that this was not possible. Consequently, a 14-day interval was considered a reasonable cutoff point to maximize the probability that the dog's health status had not changed between owner assessments and clinic visits, and so all assessment pairs that had >14 days between them were excluded from the HRQL analysis.

2.8.2. Statistical analysis

To determine if there was an improvement in objective outcome measures and owner reported health related quality of life following treatment with RM, data were divided into pre-treatment phase, and then into time windows 0–6 weeks, 7–12 weeks, 13–18 weeks, 19–24 weeks, 25–48 weeks, 49–78 weeks (18 months), and 79–104 weeks (24 months) post first treatment. Data beyond 104 weeks were not considered further because of low numbers.

Data were analyzed as a linear mixed model with time window as a fixed effect and dog within time window as a random effect. This analysis takes into consideration that there may be no, or multiple values per dog per time window. Significant effects ($p < 0.05$) were subsequently investigated using Tukey multiple comparisons. Data for LS pain were restricted to those dogs with LS disease. Likewise, joint ROM measurements were restricted to dogs receiving one or more treatments in that joint. For the analysis, the ROM values for right and left joints were averaged to provide a total ROM value for the joint. More limited data were available for the range of motion for stifle, hock, and carpi than for the other joints, so their analysis was supplemented by a further analysis just comparing pre-treatment with post-treatment (to 104 weeks) windows. Results are presented as boxplots of raw data for each time window.

To determine the relationship between change in stance and change in VetMetrica domain scores as well as Vet pain and QOL impact scores, deviation from perfect stance was matched to HRQL domain scores, vet pain and QOL impact scores if the interval between them was $\leq$ 14 days. For each HRQL, pain and QOL impact variable a linear mixed model was fitted with dog as a random effect and change in stance as a covariate.

The reduction in analgesic medication at two defined time points (pre- and post- treatment) was tested using Wilcoxon signed rank tests.

Cohen's effect size (d) was calculated for ROM and PA measures.

3. Results

3.1. MSC differentiation and immunophenotyping

Canine MSCs isolated and culture expanded for the dogs in this study conformed to International Society for Stem Cell Research standards (58) and the Position Statement for Veterinary MSCs (53) with respect to all criteria apart from Adipogenesis which did not occur under the conditions tested. Figure 1 shows that both the osteogenic and chondrogenic differentiation cultures stained positively compared with the corresponding controls but the adipogenic culture did not stain positively with Oil Red in comparison with the corresponding control. Figure 2 shows that the MSCs were positive for CD44 and CD90 whilst being negative for CD34, CD45 and MHCii.

3.2. PRP composition

On average the platelet concentration factor was found to be 6.3 times that of whole blood with a 98% reduction in RBCs and a 92% reduction in neutrophils when compared to whole blood from the same patient. This was consistent with findings of other investigators using the same system (62).

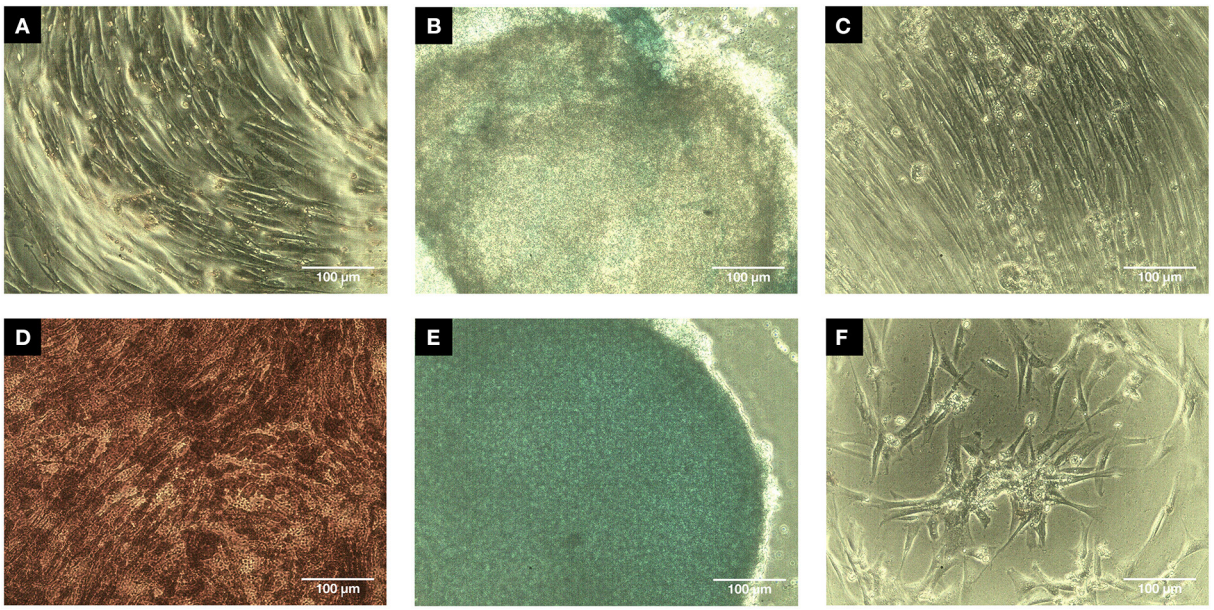

FIGURE 1
Trilineage assay micrographs (Scale bar = 100 µm). Passage 2 canine MSCs were successfully induced after 14 days into osteogenic differentiation **(D)** as mineralization was positively stained while the control **(A)** had no positive staining for Alizarin red. Similarly, chondrogenic differentiation was successfully induced after 21 days as indicated by intensity of positive Alcian blue staining **(E)** compared to the control **(B)** which only had partial positive staining. The adipogenic differentiation after 14 days was negative **(F)** with no Oil Red staining in comparison with the adipogenic differentiation control **(C)**.

3.3. Study population

Data were collected from 245 dogs, median age 6.3, range 6 months−14 years, 136 males and 109 females of which 72 and 76 respectively were neutered (Supplementary material 5). A wide range of breeds was represented, and these are detailed in Table 3. Dogs were referred for treatment with RM due to the severity and generalized nature of their MSD that was unresponsive to traditional treatments. On presentation dogs were receiving multiple analgesic medications including adjuvant drugs as well as NSAIDs but were still exhibiting pain and lameness. Twenty-four dogs had previous surgery related to cranial cruciate ligament rupture, 24 had previous surgical arthroscopic intervention for elbow developmental disorders, and 2 had surgical treatment for osteochondrosis (OCD) of the shoulder.

Two hundred and thirty-four dogs were diagnosed initially with OA. Grades of OA 1, 2, 3, and 4 were represented by 24, 99, 100, and 6 dogs respectively; a further five dogs were not graded on initial presentation. The remaining 11 dogs were suffering from tendinopathies and/or LSD in the absence of OA.

Dogs had between 1 and 8 treatments with RM. The frequency and percentage of dogs receiving treatment is shown in Table 4. Of the 106 dogs that received two treatments only, the second took place between 70 and 126 days (10–18 weeks) for 40 dogs and after 126 days for 66 dogs. The former group comprises patients receiving two treatments as part of the initial treatment protocol and for the latter group the mean (SD) of the days between treatments was 450.9 (321.4) with the second treatment being given due to clinical need. Supplementary material 6 indicates how many records/dogs were present in each time window for each analysis and includes tables of fitted means for each time window with letter codes from Tukey multiple comparisons such that means not sharing a common letter are significantly different ($p < 0.05$).

Figure 3 indicates the proportion of dogs that received treatment in each of the six joints on at least one occasion, and the proportion of dogs treated at the lumbosacral region at least once.

The different MSDs treated in the study group are listed in Supplementary material 7.

3.4. Musculoskeletal ultrasound

In the main, repeat evaluations of treated tendons and other soft tissue structures performed with MSK US at 12 weeks post-treatment demonstrated considerable improvements in tendon fiber patterns and a reduction or elimination of inflammatory change, fibrosis and mineralization, as shown in Figure 4B. Before treatment, the SS tendon and its enthesis were severely degenerated with a loss of linear fiber pattern,

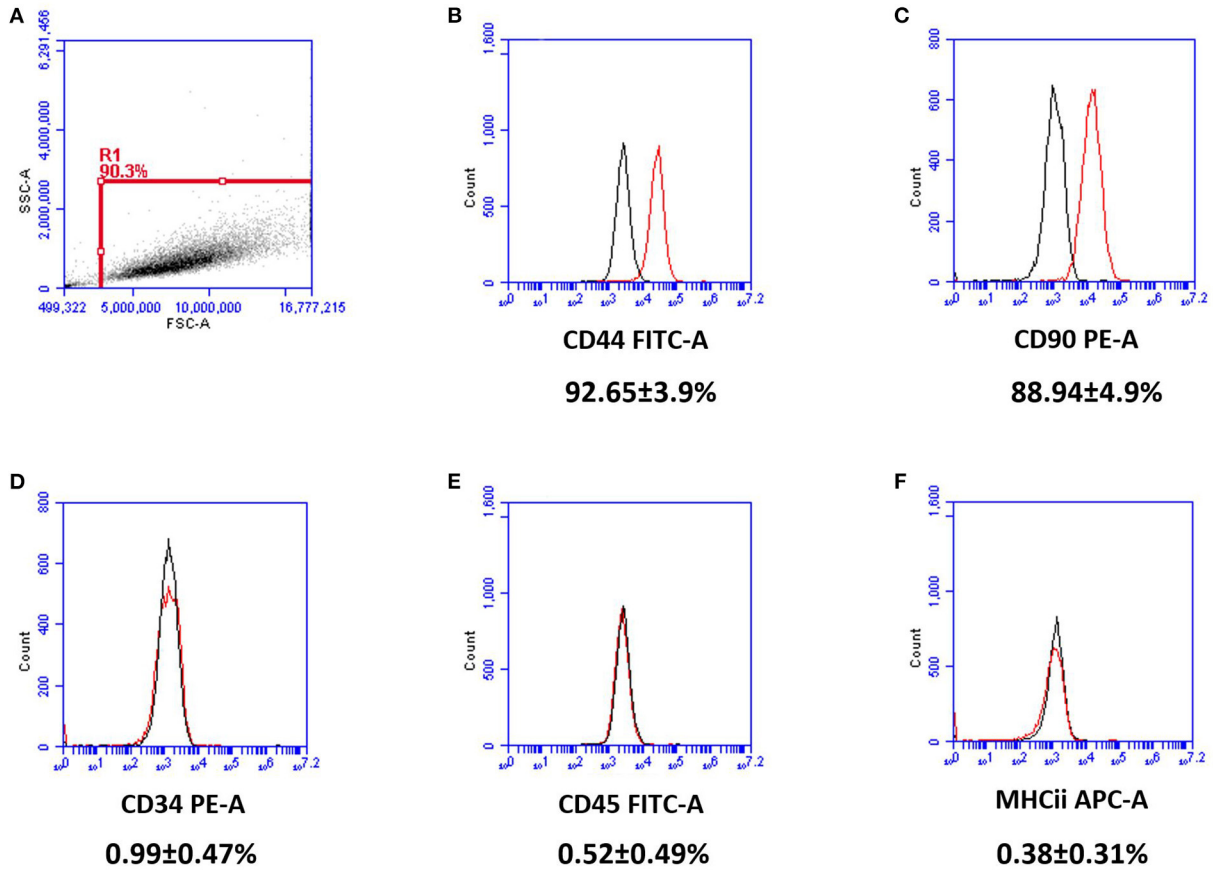

FIGURE 2
Flow cytometry results for passage 2 canine MSCs ($n = 7$). Cell surface markers were represented by the red histograms with isotope controls labeled black. Gating was set to R1 **(A)**. MSCs expressed CD44 **(B)** and CD90 **(C)**, while lacking expression of CD34 **(D)**, CD45 **(E),** and MHCii **(F)**. Percentages denote the intensity of positivity of the CD markers with standard deviations.

fibrotic infiltration, and areas of extensive mineralization, but at 12 weeks post-treatment the tendon had resumed a normal fiber pattern and the enthesis was remodeled to a normal "sharks' fin" appearance with resolution of the fibrotic and mineralised portions and normal echogenicity. Figure 4A shows radiographic evidence of resolution of abnormal mineralization in the SS tendon insertion in the same patient at the same time points. In contrast, Figure 5 is an example of incomplete healing following treatment in a 4-year-old Border Collie with a sports-related shoulder tendon injury. The image on the left shows a chronic biceps tendinopathy and a partial tear of the subscapularis tendon with complete disruption of the fibers. At 12 weeks post-treatment, there was a considerable improvement in the fiber pattern, fibrosis and echogenicity of the biceps tendon and its enthesis. The integrity of the subscapularis tendon had improved but there was incomplete healing. Following a second treatment the subscapularis tendon had healed completely with a normal fiber pattern, without fibrosis/scar tissue and no free-floating tendon fibers were visible in the medial shoulder compartment.

3.5. Outcome measures

3.5.1. Stance analysis

There were 855 records from 228 dogs up to week 104. The results are shown in Figure 6. Results of the mixed model analysis showed that there were significant time window effects ($p < 0.001$); all post-treatment means were significantly lower compared to pre-treatment.

3.5.2. Goniometry

There were 925 records from 234 dogs with a variable number of records/dogs for each measure, truncated at 104 weeks. Figure 7 represents the ROM in thoracic and pelvic limb joints, from pre-treatment to 104 weeks.

Analysis of individual joints indicated that there were significant time window effects ($p < 0.001$) with improvement at all time windows compared to the pre-treatment period for shoulder and hip; at all time windows except for 104 weeks for carpus and elbow ($p < 0.001$); and only at weeks 18 and

TABLE 3 Range of breeds represented in 245 dogs treated with regenerative medicine.

Breed	*n*
Labrador retriever	79
Border collie	39
Mixed breeds	20
English cocker spaniel	14
German shepherd / Alsatian	13
English springer spaniel	12
Golden retriever	10
Jack/Parson russell terrier	6
Bearded collie, Border terrier, Newfoundland, Rottweiler, Gordon setter, Staffordshire bull terrier	3
Bichon frise, Boxer, Hungarian vizsla, Lurcher, Weimaraner, Standard poodle	2
Airedale terrier, Alaskan malamute, Australian cattle dog, Australian kelpie, Australian shepherd, Cavalier King Charles spaniel, Smooth coated collie, French mastiff/Dogue de Bordeaux, Golden retriever, Greyhound, Italian spinone, Lakeland terrier, Miniature poodle, Patterdale terrier, Pug, Flat coated retriever, Rhodesian ridgeback, Samoyed, Scottish terrier, Slovakian rough haired pointer, Spanish water dog, and Toy poodle	1

TABLE 4 The number of dogs receiving between 1 and 8 treatments and their percentage of the study population ($n = 245$).

Number of treatments	Number of cases	% of study population
1	53	22%
2	106	43%
3	50	20%
4	19	8%
5	11	5%
6	4	2%
8	2	1%

104 for stifle ($p = 0.003$). Time window effects for the hock did not reach significance ($p = 0.062$). For those less well-recorded joints where pre/post-treatment analysis was carried out, all were significant; carpus and stifle both $p < 0.001$, hock $p = 0.020$. The maximum improvement in ROM was 12, 14, 20, and 22 degrees for the shoulder and stifle, hip, carpus and elbow respectively.

In terms of effect size, changes in ROM between pre-treatment and the first 6 weeks post-treatment had a Cohen's effect size (d) ranging from 1.05 to 2.14.

3.5.3. Pressure algometry

There were 568 records of LS pain from 171 dogs with LSD up to week 104. There were significant time window effects ($p < 0.001$) with all post-treatment means being significantly improved compared with pre-treatment (Figure 8). Cohen's effect size (d) was 2.20 for the same time period as ROM.

3.5.4. HRQL measurement (VetMetrica™)

A total of 954 owner Quality of Life (QoL) assessments in four domains were recorded from 212 dogs that had both QoL and treatment details up to week 104. Figure 9 shows the HRQL scores over time in all four domains. In E/E there were significant time window effects ($p < 0.001$) with all time window means after 6 weeks being significantly higher than pre-treatment. In H/C and C/R all post-treatment means were significantly higher than pre-treatment after 12 weeks ($p < 0.001$). In A/C all post-treatment means were significantly higher than pre-treatment ($p < 0.001$), with a slight reduction in later time windows.

From 13 to 78 weeks all improvements in median scores for E/E, H/C and A/C were considered clinically significant on the basis that they exceeded the MID of 7 (Supplementary material 8).

3.5.5. Vet clinical assessment

Vet pain and QOL impact scores were recorded 906 times from 223 dogs up to week 104. Figure 10 depicts the scores over time for vet pain and QOL impact. There were significant time window effects ($p < 0.001$) with all post-treatment means being significantly improved from pre-treatment, but with a deterioration in later time windows.

3.5.6. Relationships between change in stance and change in VetMetrica and vet assessment scores

There were change records from 123 dogs where the deviation from perfect stance was matched to HRQL domain scores within a 14-day period. These data showed that there was a significant relationship ($p < 0.001$) between the improvement in stance and the improvement in HRQL scores in all four domains. Similarly, the relationship between the improvement in stance and the decrease in vet-assessed pain (Figure 11) and QOL impact scores was significant ($p < 0.001$).

3.5.7. Analgesic usage

A total of 118 dogs had analgesic records in both pre- and post-treatment periods. Mean dates of records were 41 days

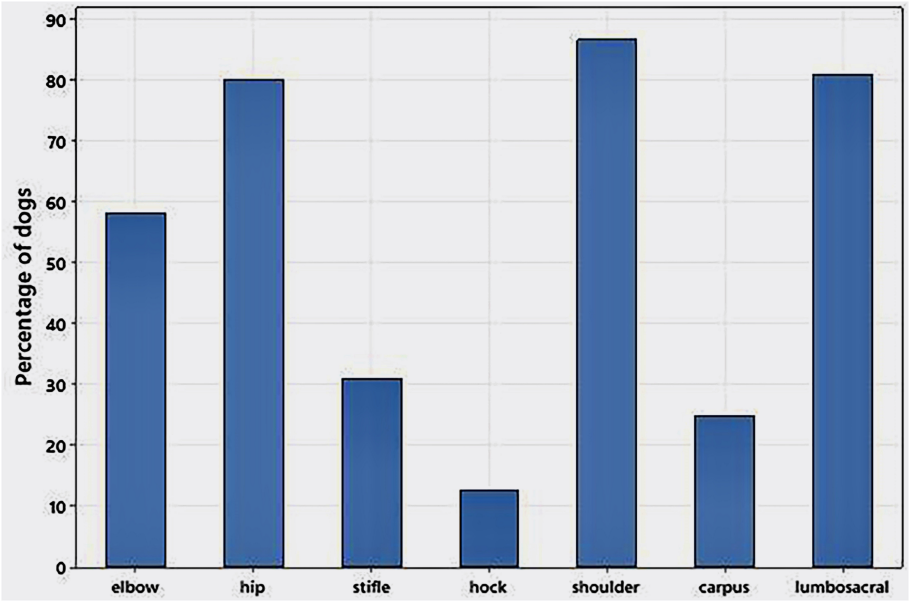

FIGURE 3
Proportion of 245 dogs with MSD treated with corresponding regenerative medicine to 104 weeks that received joint or lumbosacral treatments on at least one occasion. Multiple joints were treated in 89% of dogs and <1 % of dogs had only a single musculoskeletal disease treated.

pre-treatment (range 1–159 days before), and 225 days post-treatment (range 170–336). The proportion of dogs receiving NSAIDs declined from 74 to 50%, the change was significant ($p < 0.001$) based on a Wilcoxon signed rank test. The proportion of dogs receiving adjuvants (such as Paracetamol, Gabapentin, Codeine, Amantadine and Tramadol) declined from 80 to 35%, and the mean number of adjuvants per dog declined from 1.58 to 0.64. Both were significant ($p < 0.001$) using Wilcoxon signed rank tests.

3.6. Adverse events

A small number of mild adverse reactions, including skin irritations following clipping and surgical preparation of the skin were recorded. Transient short lived (<36 h) joint flares following intra-articular injection, were also reported in <1% of the study population.

4. Discussion

This paper is the first to report the duration of improvement that can be achieved with multiple applications of quality controlled, culture expanded autologous MSCs to treat widespread MSD affecting joints, tendons, ligaments and pathology of the LS region, in a large sample (245) dogs that were exhibiting pain and lameness despite receiving multiple analgesic medications, including adjuvant drugs as well as NSAIDs. In contrast, Sanghani-Kerai et al. reported the results of 25 dogs that received intra-articular injections of MSC and PRP on a single occasion as part of their OA management, and only three of the 25 dogs had more than one joint treated, with outcomes recorded for only 24 weeks (63). Furthermore, this study is the first to utilize a standardized therapeutic protocol that included LT in addition to MSCs and PRP. Compared with the standard approach of using objective outcome measures to define the functional impact of treatment, this study was enhanced by the addition of a validated HRQL assessment and by the use of Cohen's d effect size to quantify clinical significance in addition to statistical significance.

The authors consider RM to be a targeted treatment approach that requires a holistic MSD diagnosis to treat all areas of pathology concurrently in order to achieve the best outcomes. In addition to a complete orthopedic and neurological examination, diagnostic imaging was used to reach a definitive diagnosis in all cases. Radiographs were used to assess bone and joint changes and MSK US was used to evaluate soft tissue structures. Radiographs of the shoulder are not diagnostic for shoulder tendinopathies unless extensive mineralization is present, and so MSK US allowed for greater detection of tendinopathy than if radiography had been used alone. Furthermore, because MSK US provides a means to evaluate joint capsule pathology (hypertrophy and synovitis) as well as joint effusion and the articular surface it adds value to the grading of OA (64–73). Small osteophytes, which may be

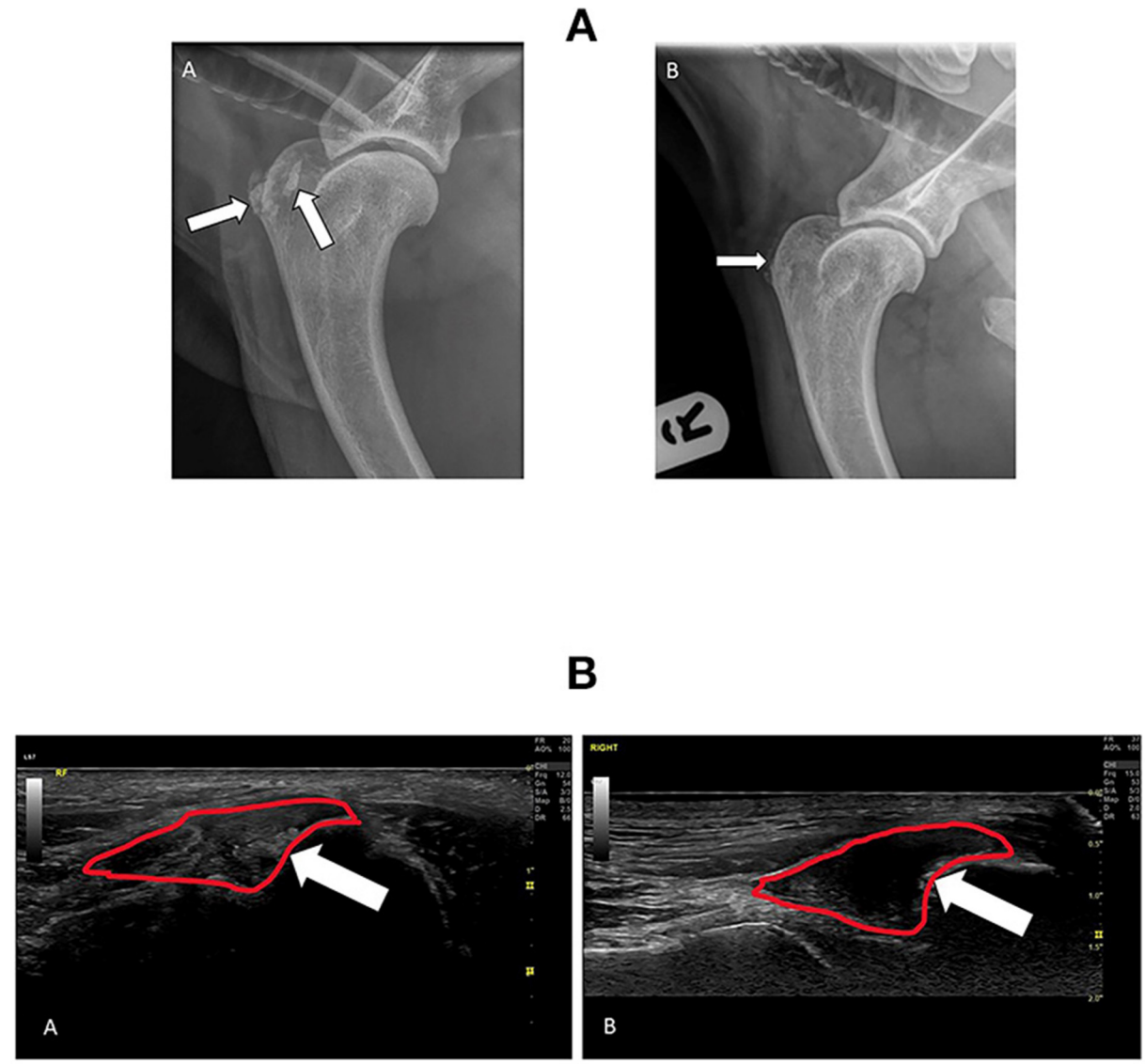

FIGURE 4
(A) Radiographs of the right shoulder from a 7-year-old male neutered Labrador with concurrent elbow dysplasia and OA showing extent of Supraspinatus (SS) tendon mineralization at the time of diagnosis (A) and 3 months following treatment with RM (B). The white arrows point to abnormal mineralization in the SS tendon and enthesis. Following treatment there has been a significant reduction in the extent of mineralization. **(B)** Ultrasound images of the right Supraspinatus (SS) tendon insertion before and after treatment in the same patient as in (A). The SS tendon enthesis is outlined in red and the white arrow points to areas of abnormal mineralization. (A), taken at the time of diagnosis, shows extensive mineralization of the enthesis and distal tendon with resultant acoustic shadowing. (B) was taken 3 months after treatment. This image shows a normal SS tendon and hypoechoic enthesis with only residual mineralization on the humeral attachment.

missed on plain radiographs, can be visualized within the joint, allowing for earlier detection of joint pathology. To the authors' knowledge, although it has been proposed as a useful tool in grading human OA (67), this is the first example of MSK US contributing to the grading of OA in dogs.

The majority of dogs had OA in multiple joints in more than one limb and there was a high prevalence of LSD. Indeed, this study is the first of its kind to evaluate treatment protocols encompassing multifocal MSD involving joints, soft tissue support structures and the spine. The most frequently treated joint was the shoulder, followed by hips then elbows with carpi, stifles and hocks less so. Labrador retrievers were over-represented in the study population, accounting for 32% of cases. Consequently, the high prevalence of hip and elbow developmental disease in this breed may have influenced the incidence of joints treated. Elbow dysplasia with secondary OA was also a common reason for presentation in this breed, with previous arthroscopic intervention being a regular feature. In

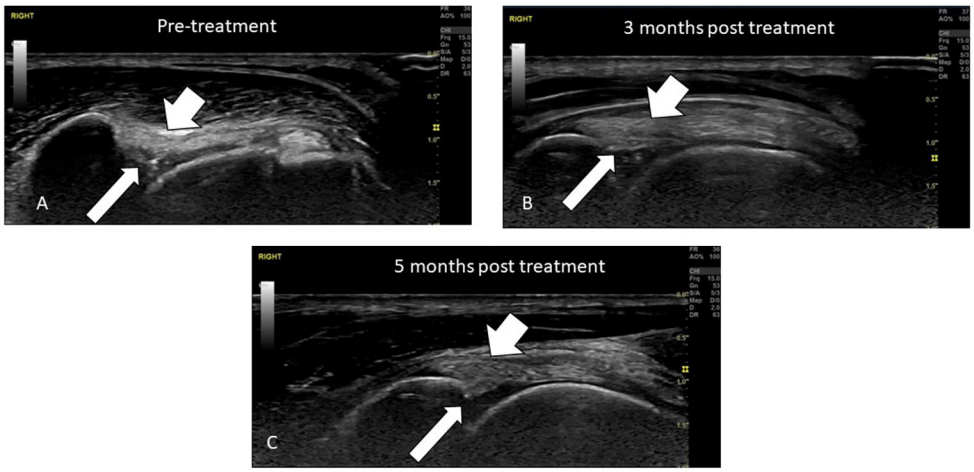

FIGURE 5
Ultrasound evaluation of a Biceps tendinopathy and partial Subscapularis tendon tear in 4-year-old agility dog before and after treatment with RM. The long arrows point to the position of the Subscapularis tendon and the short arrow the Biceps tendon. **(A)** Pre-treatment the Biceps tendon has extensive fibrosis and loss of a linear fiber pattern and enthesis and the Subscapularis tendon is partially torn with free floating fibers and fibrotic proliferation. **(B)** 3 months following treatment the Biceps tendon has shown extensive healing with a reduction in fibrosis and restoration of a more normal linear fiber pattern. The integrity of the Subscapularis tendon has improved but complete healing has not been achieved. A second treatment of MSCs was implanted. **(C)** 5 months following initial treatment and 2 months after the second treatment. The fiber patterns have improved with resolution of fibrotic infiltration, the biceps enthesis is normal and the integrity of the subscapularis has been restored.

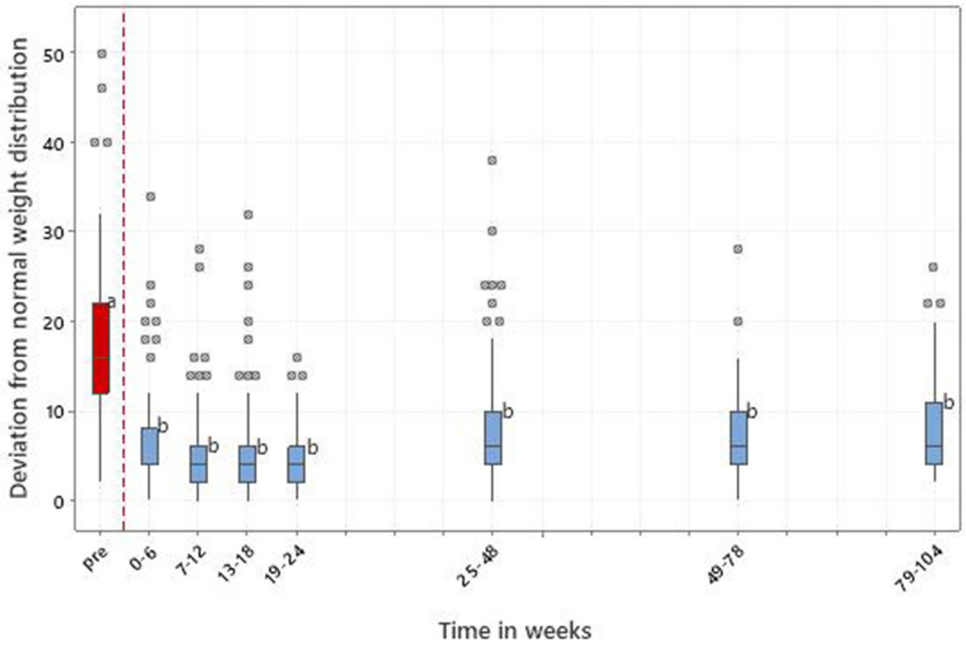

FIGURE 6
Results of stance analysis for 228 dogs with MSD treated with RM in time windows representing pretreatment (pre) and up to 104 weeks post initial treatment. 0 = perfect balance; > 0 = increasing imbalance. It should be noted that in this figure a single value of 78 in time window 7–12 weeks was removed in order to improve the use of the vertical space. This value related to a dog that had an acute traumatic incident resulting in non-weight bearing lameness, unrelated to its original diagnosed pathologies. The dog improved with rest and supplemental analgesia and its weight distribution normalized after 7 days. Letters adjacent to each bar indicate which time windows are significantly different (i.e., those not sharing a common letter).

10.3389/fvets.2022.1014687

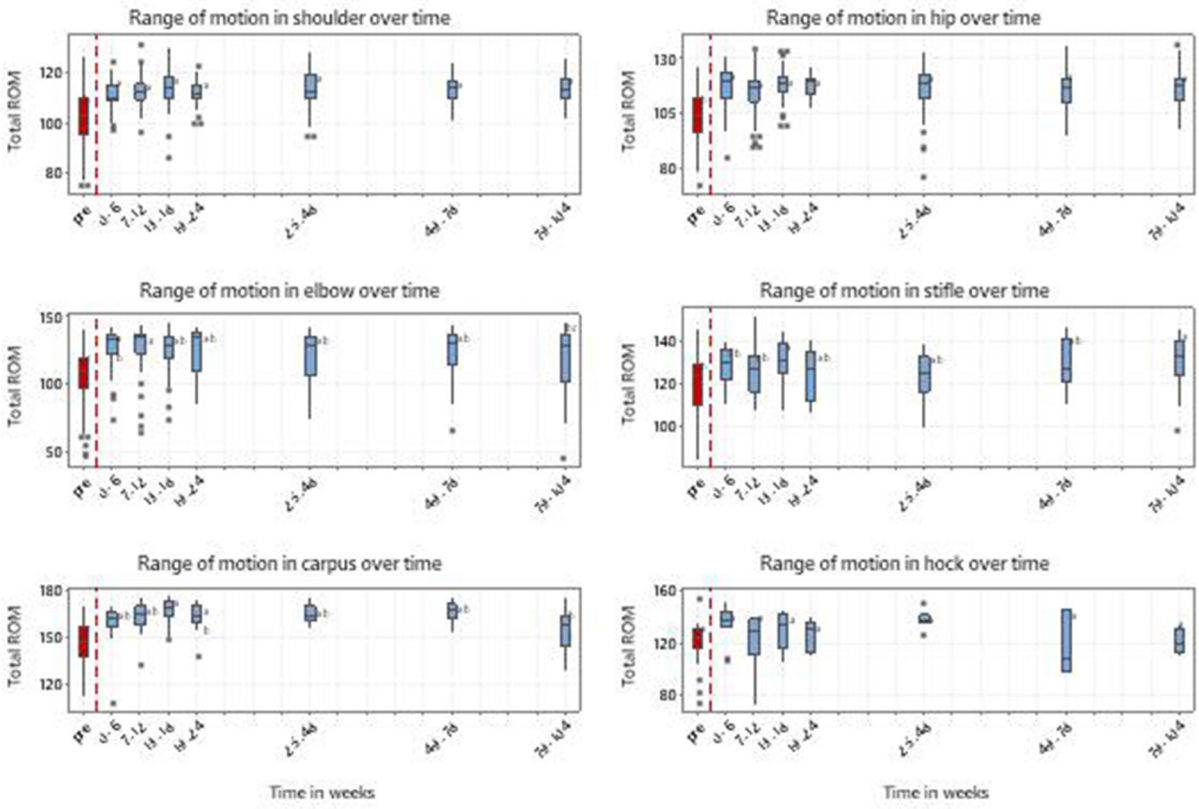

FIGURE 7
Range of motion in thoracic and pelvic limbs for 234 dogs with MSD treated with RM in time windows representing pretreatment (pre) and up to 104 weeks post initial treatment. Shoulder $n = 191$, Elbow $n = 123$, Carpi $n = 51$, Hip $n = 158$, Stifle $n = 60$ and Hock $n = 28$. Individual dogs may have received treatment to multiple joints. Letters adjacent to each bar indicate which time windows are significantly different (i.e., those not sharing a common letter).

these cases, clinical experience has shown that more aggressive treatment with RM was required and even then, the duration of effect appeared shorter than in patients without prior surgical intervention (AA personal communication). Accordingly, all dogs with elbow dysplasia that had previous arthroscopic surgery received a repeat treatment of MSCs at 12 weeks as a matter of routine.

It is interesting that the joint most often treated was the shoulder. Since intra-articular injections of MSCs and PRP will not affect structures outside the joint capsule, targeted ultrasound guided injection to extracapsular structures was undertaken, with the pathology first identified by MSK US. Consequently, shoulder treatments comprised intra-articular injection and/or ultrasound guided treatment of the shoulder tendons (commonly supraspinatus and biceps tendons), with tendon treatment predominating, indicating a very high prevalence of shoulder tendinopathies. This concurs with a recent study which reported that 55% of dogs with elbow developmental disease had concurrent shoulder tendinopathies (10). Where healing of a tendinopathy was incomplete by 12 weeks, a second treatment of MSCs was injected into the remaining lesions. This was most commonly required in the case of supraspinatus tendinopathy due to the severity, chronicity, and impermeable nature of the tendon enthesis where injection of therapeutics requires a fenestration technique. This, combined with areas of fibrosis and mineralization, limits the volume of MSCs and PRP that can be infused and increases the likelihood of a second treatment being required. However, resolution of mineralization of the supraspinatus tendon and restoration of a normal enthesis after one or two treatments, was an example of the regenerative capacity of MSC therapy in combination with PRP and LT.

According to the Position Statement published by Guest et al. (53), veterinary publications involving MSCs should describe the tissue source, preparation method, cultural method, passage number and method of banking the cells as well as the type of cells, antigenicity, cell dose, dosing schedule, delivery vehicle and method of delivery. The MSCs used here were autologous adipose derived MSCs, culture expanded using standardized protocols, release criteria and strict quality

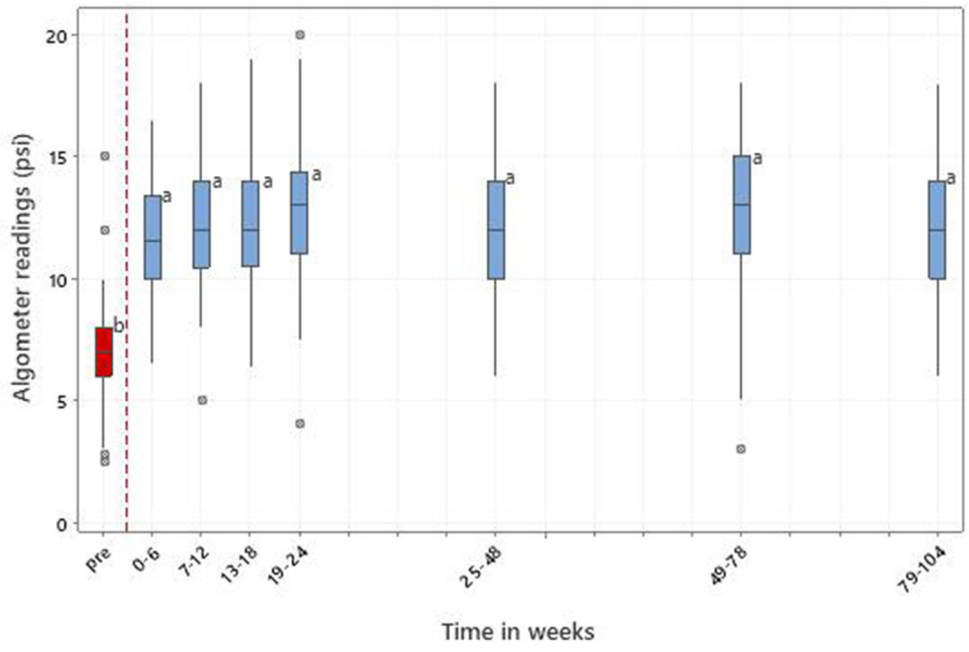

FIGURE 8
Pain threshold at the lumbosacral junction in 171 dogs with LSD treated with RM in time windows representing pretreatment (pre) and up to 104 weeks post initial treatment. Letters adjacent to each bar indicate which time windows are significantly different (i.e., those not sharing a common letter).

control in a cell culture laboratory authorized by the Veterinary Medicines Directorate, thus complying with the Position Statement (53). Additionally, subsequent recommendations by Ivanovska et al. in the manufacturing of MSCs for the treatment of OA in canine patients were also met (61). MSCs differentiated into chondrocytes and osteocytes but not into adipocytes, despite being derived from adipose tissue. However, according to Sasaki et al. (73) canine MSCs do not always differentiate into adipocytes when induced by a medium optimized for human MSC adipocyte differentiation and therefore this finding is not unusual (73–75). Whereas the efficacy of MSCs was initially considered to be due to their ability to differentiate into musculoskeletal lineages such as chondrocytes and osteocytes, more recently their immunomodulatory and paracrine actions, which influence the inflammatory environment through the release of growth factors and cytokines, are thought to be of more importance (25, 75–77). Despite this lack of clarity regarding the definitive mechanism of action of MSCs, this study has shown that dogs with severe, unresponsive MSD were substantially and rapidly improved by the RM protocol used and that this was sustained for up to 2 years in some dogs. The initial response to treatment can be attributed to the anti-inflammatory effects of the MSC and platelet secretome, but later effects of remodeling, healing and formation of new tissues occur over a more prolonged timeframe. Given that there is evidence that MSCs can persist at the site of injection for more than 10 weeks in OA joints (78) and more than 24 weeks in tendons (79), this could explain the extended sustained improvement following the initial anti-inflammatory effect.

This study looked at treatment responses in naturally occurring disease processes and provides impactful information regarding standardization of canine biological cell products and protocols. This is important for veterinary treatments and also confirms the potential for translational applications in human medicine. Both Ivanovska et al. and Webb et al. have advocated the use of naturally occurring canine disease, treated with standardized RM protocols, as an important area of research to bridge the gap between *in vitro* studies and human clinical trials (61, 80).

For all intra-articular and tendon treatments, MSC injections were accompanied by PRP and followed by a program of laser treatment. This protocol was designed to optimize the efficacy of the MSCs since they respond positively to growth factors released by platelets, and LT *via* PBM (81, 82). The PRP used here was optimal for anti-inflammatory treatments because it contained low numbers of neutrophils and erythrocytes and high concentrations of platelets compared with whole blood (62). Red blood cells and neutrophils have been shown to be deleterious in intra-articular environments through the production of pro-inflammatory mediators and causing synovite death (83). The mean platelet concentration in the prepared PRP was 6.3 times the whole blood concentration,

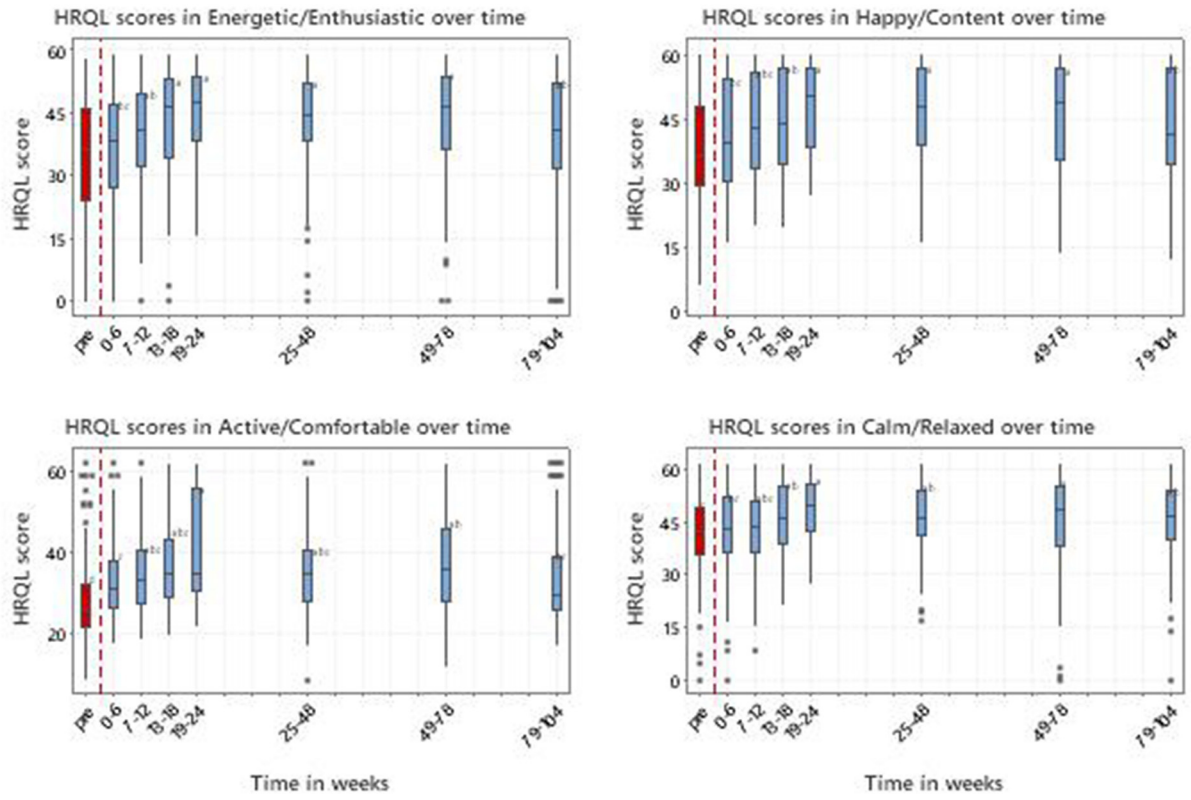

FIGURE 9
Scores in 4 domains of QOL (Energetic/Enthusiastic; Happy/Content; Active/Comfortable; Calm/Relaxed) for 212 dogs with MSD treated with RM in time windows representing pretreatment (pre) and up to 104 weeks post initial treatment. 50 represents the score for the average healthy dog and 70% of healthy dogs will score above 44.8. Letters adjacent to each bar indicate which time windows are significantly different (i.e., those not sharing a common letter).

but since the RM injections were a 1:1 mix of MSC suspension and PRP, the overall platelet concentration was approximately 3 times the physiological whole blood platelet concentration. This concentration is in line with the platelet doses reported to be most effective in human clinical studies and animal model studies (84–86). The injection of MSCs with PRP has been shown to be clinically effective in a range of inflammatory diseases (22, 28, 87). Growth factors released by platelets attract and stimulate MSCs to proliferate and to initiate wound healing responses (88). The authors suggest that these actions, together with the formation of a fibrin clot which acts as a scaffold for the MSCs within the injured, inflamed tissues, promoted the healing evident in the joints, and tendons reported in this study.

In order to treat LSD it was considered that MSCs should be injected without the addition of PRP to enable the cells to migrate to all areas of pathology (89). This migratory process, in theory, could be limited by fibrin clot formation and chemotactic cytokines produced by platelets directing MSCs to persist in the epidural space, thereby limiting more widespread effects in the LS region. MSCs have a potent anti-inflammatory effect but, more important in the case of LS stenosis, is their ability to reverse fibrosis, undo nerve compression and alleviate neuropathic pain (90, 91).

Illien-Junger et al. demonstrated homing of human bone marrow derived MSCs into degenerated bovine discs and a subsequent increase in proteoglycan synthesis within the disc demonstrating their migratory as well as regenerative capacity in intervertebral disc disease (IVDD) (92). In a review paper by Oehme et al. (93) four studies in dogs with experimentally induced lumbar IVDD treated with stem cell and progenitor cell transplantation demonstrated positive effects on intervertebral discs (93–99). While experimentally induced disease may differ markedly from that which occurs naturally, these studies are encouraging and support the clinical application described in this study.

Epidural implantation of MSCs at the LS junction provided a repeatable location for placement, allowing local migration in the posterior lumbar region. No adverse reactions were recorded in the clinical record for initial or subsequent treatments. This safety profile, combined with accessibility of the LS junction, makes repeat therapy and long-term management of LSD realistic. This is the first study to report significant improvement in pressure algometry readings together with a

very large Cohen's effect size (d) and it demonstrates that MSC epidural injection is a safe, minimally invasive and effective treatment for LSD. In contrast, Salmelin et al. report an incidence of 8.6% of side effects in 150 dogs treated with epidural steroids for LSD (100). Such medical management is not fully effective in controlling LS pain and furthermore surgical patients can develop clinical signs and pain following initial improvements (101).

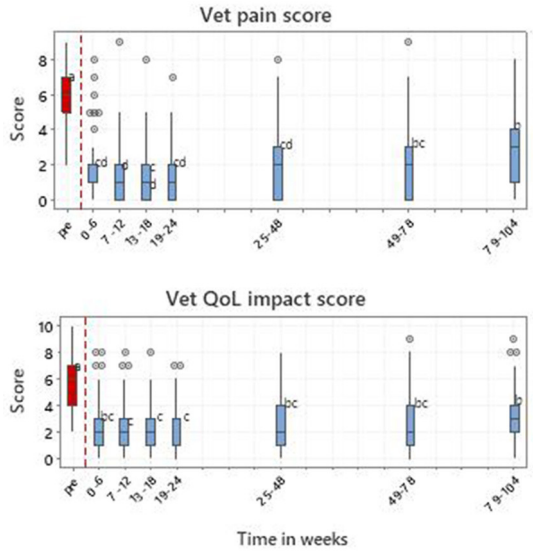

FIGURE 10
Vet-assessed pain and QOL impact scores for 223 dogs with MSD treated with RM in time windows representing pretreatment (pre) and up to 104 weeks post initial treatment. Letters adjacent to each bar indicate which time windows are significantly different (i.e., those not sharing a common letter).

In dogs with spinal disease such as intervertebral disc disease (IVDD) or spondylosis in the thoracic, cervical, and cranial lumbar regions, IV injection of MSCs was included in the protocol along with epidural MSCs. Stem cells administered intravenously can potentially reach structures where direct implantation is not possible or where epidural administration other than at the LS junction carries the risk of iatrogenic spinal cord injury. In a rodent model, IV stem cells have been shown to migrate to areas of spinal cord damage with positive therapeutic effects (94), including the treatment of neuropathic pain (91). Furthermore, IV MSC administration has been shown to be safe, even in high numbers (2.5 x 10^8 cells/kg body weight), in people and mammals (95). However, further study is required to evaluate the effects of combining epidural and IV MSCs and their potential synergistic effects on reducing spinal and neuropathic pain.

Laser therapy, an integral part of the treatment protocol, has been used extensively to treat soft tissue and orthopedic injury and pain in animals but there is little information to support its application in conjunction with MSCs (102). *In vitro* studies have shown LT to have beneficial effects on stem cell proliferation (103) and have also indicated that preconditioning of stem cells with photobiomodulation (PBM) can increase cell

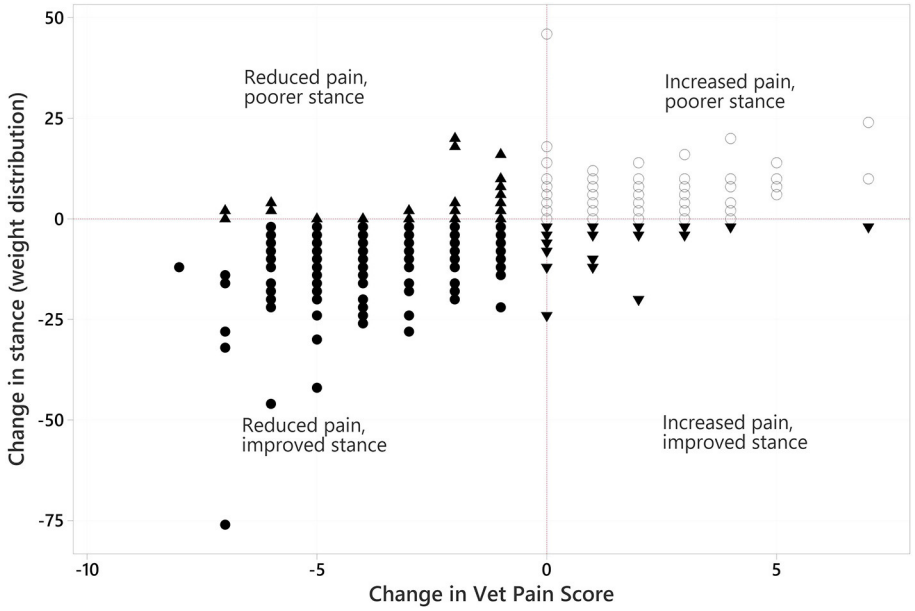

FIGURE 11
Scatter of changes in stance (weight distribution) plotted against changes in vet-assessed pain score. In each variable negative values reflect an overall improvement. Different symbols are used merely to indicate dogs in combinations of the improved/not improved categories of both variables.

function, leading to improved healing of wounds (104) and bone (105). Amaroli et al. have reviewed the effects of PBM on MSCs and have shown multiple examples of positive effects relating to their anti-inflammatory action, viability and proliferation and changing the cells lineage differentiation and secretome (106).

Experimental studies carried out *in vivo* have shown that combining PBM with stem cell therapy leads to improved outcomes and that, contrary to commonly held belief, there is no need for a time lapse between stem cell treatment and laser therapy (107–109). While these experimental studies have demonstrated the beneficial effects of combination therapy on soft tissue healing, the use of Class IV LT used simultaneously with injection of culture expanded canine MSCs in naturally occurring MSD has not been previously described, making this study the first to use this combined protocol. However, since all dogs received MSCs and PRP as well as LT any positive effects attributable to LT could not be defined. Nevertheless, Alves et al., using the same LT dose and time points as our study, demonstrated a positive effect on hip joint ROM and pain in dogs with OA, but found mean maximal increases in hip ROM of 8° compared to 14° described in our study (110). Upchurch et al. measured changes in hip ROM following treatment with MSC (stromal vascular fraction) and PRP alone and found a maximal mean increase in ROM of 11° in the 6 months following treatment (111). Although these studies are not directly comparable they suggest that the superior improvements in Hip ROM seen in our study could be due to a synergistic effect of combining MSCs, PRP, and LT but further study is required to substantiate this.

Published evidence to support electrotherapies and physical therapies in combination with RM is lacking and accordingly their use, apart from LT, was restricted in the initial treatment. Where dogs were receiving physical therapies at referral, these were discontinued at the time of diagnosis and fat harvest with physiotherapy or hydrotherapy resumed after the 12-week check demonstrated sufficient healing. For patients receiving a second RM treatment at 12 weeks, physical therapies were not resumed until 18 weeks after initial treatment. Therefore, the significant improvements in objective measures before 12 weeks post-treatment cannot be associated with physical therapies.

The outcome measures used in this study comprised part of patient evaluation aiding in the diagnosis of MSD and measuring clinical change. The information gained was used to inform further treatments where pain and functional parameters deteriorated following the initial treatment.

Although canine gait analysis using force plate data has been used extensively in studies involving orthopedic surgery outcomes, several variables such as walking velocity, head position, position of the handler, and changes in bodyweight between repeat measurements can affect kinematic and force plate data in normal dogs (112, 113). These can influence the reliability of these data and are compounded when a patient has multiple limb gait abnormalities as was the case in our study. Conversely, while the clinical relevance of static limb offloading has not been reported to the same extent, Clough et al., reported good sensitivity and specificity for the detection of both orthopedic disease and objective lameness, and suggested that stance analysis is clinically valuable for measuring response to treatment (29). Additionally, it has been shown that there was no difference in the sensitivity of ground reaction forces and static body weight distribution for measuring hip joint pain and evaluating limb use following treatment (114), hence our decision to use stance analysis in this study.

Stance analysis determines weight distribution whilst the dog is standing on a pressure plate, and it will offload a painful limb and redistribute its weight as a compensatory mechanism. Accordingly, any musculoskeletal pathology will be reflected in the stance making stance analysis an ideal measure of the global effects of MSD. However, there is little published evidence using stance analysis data when reporting treatment effects using RM. Skangals found beneficial, but not statistically significant changes, in weight distribution and joint ROM in 10 dogs with unilateral elbow OA treated with a single intra-articular injection of allogenic MSCs (115). The study found significant improvements in subjective owner reported outcome measures but not for the objective measures which is in marked contrast to the data reported here. Because patients had several limbs involved, often with multiple joint and spinal involvement, comparing affected to non-affected limbs was not possible. Instead, a measure of the absolute departure from a normal weight distribution was calculated. The improvement and normalization of weight distribution following treatment with RM was extremely rapid (from 6 weeks) and maintained to 104 weeks. The authors believe that the improvement resulted from a reduction in pain, with consequent decrease in offloading. Indeed, the fact that the improvement in stance correlated with the decrease in vet pain scores, as shown in Figure 11, lends weight to that hypothesis. A feature of this study was the reporting of clinical as well as statistical significance. In the case of VetMetrica (50) this was demonstrated when the MID of 7 was achieved in E/E, H/C and A/C at time points between 13 and 78 weeks. The demonstration of a significant relationship between change in stance and change in HRQL indicated that the change in stance was also clinically significant.

The ROM of treated joints was measured before and after intra-articular treatments with MSCs and PRP. Normal ROM has been published for a small number of breeds (30, 116–118) but a standard canine range of flexion and extension angles is not available. Nevertheless, following treatment, the increased ROM in this study was often dramatic with many joints regaining what was considered to be a clinically normal ROM by author AA. In the hip and shoulder joints all post-treatment measurements were statistically significantly higher than pre-treatment levels. The same was true for the carpi and elbows except for the 104-week time window. This shows that the ROM in the carpi and elbows starts to reduce approximately

2 years after initial treatment. In the stifle and hock unilateral disease was more common resulting in low sample numbers, and the authors consider that this may have contributed to the lack of statistically significant change in these joints. Also, total ROM measurements were averaged between contralateral paired joints at each time point resulting in a reduced average ROM reading in cases of unilateral treatment. Pre-treatment goniometry recordings were taken whilst the animal was under GA, negating the effect of pain limiting extension or flexion, but post-treatment angles were recorded in the conscious patient. Since Clark et al. found that the total ROM in the elbow increased by up to 11 degrees under sedation or GA compared with when the dog was conscious (119), the post-treatment results reported in this study may be an underestimation of the actual increase in total ROM. Nevertheless, the reported increases in total ROM were significant in most treated joints. These findings support the regenerative potential of MSCs since, for a joint to gain a greater total ROM, there must be some remodeling of the osteoarthritic new bone, changes in joint capsule thickness and elasticity or muscle-tendon length, which is restricting either flexion or extension.

A recent study investigated joint ROM in 20 working police dogs with hip OA before and after PBM therapy (110). This prospective, positive-controlled, double-blinded study showed that PBMT reduced pain levels and improved clinical findings in dogs with hip OA compared to the NSAID meloxicam for up to 90 days post-treatment (110). The increased total ROM in the treated group was less than that found in the present study following treatment with MSCs, PRP, and PBM therapy. Although the studies are not directly comparable and differ in timing of PBM treatments the therapeutic levels of LT (10 j/cm^2) were identical. This provides evidence to suggest that the improvements in hip total ROM are greater when MSCs and PRP are combined with PBM. Carr et al. found a mean increase in elbow ROM of 6° in dogs with elbow OA treated with PRP alone at 90 days post treatment compared with a 2° increase in the control group in a small cohort of Labradors (120). This is considerably less than the 22° increase in elbow ROM observed in a much larger number of dogs with elbow OA in this study suggesting that combining MSCs and LT with PRP has a greater effect on increasing ROM than PRP alone.

Pressure algometry has been used with success in numerus human studies (121–123), but this is the first study to use the technique to objectively measure changes in LS pain thresholds in dogs in a clinical setting. Over 80% of the treated dogs received injections of MSCs into the epidural space at the LS junction for the treatment of lower back pain associated with LSD in addition to concurrent appendicular pathologies. The prevalence of LSD suggests that changes in gait and weight distribution caused by appendicular MSD may predispose to accelerated degeneration at the LS junction, secondary to altered biodynamics of the spine. The PA results showed a statistically significant increase in pain threshold between pre-treatment measurements and all subsequent measurements up to 104 weeks following epidural injection of MSCs and this was supported by a significant reduction in analgesic and anti-inflammatory medication usage following treatment. The decrease in analgesic requirement was statistically significant up until 32 weeks on average, thus highlighting the pain-relieving properties of the RM treatment. It is noteworthy that the pre-treatment PA measurements were taken when the dogs were receiving analgesic medication whilst many of the post-treatment readings were recorded when analgesic medication had been discontinued or dramatically reduced, so the analgesic effect of MSC injection at the LS junction was likely to be underestimated.

The clinical significance of both ROM and PA was demonstrated by calculating the effect size between pre-treatment and the 6 weeks following treatment. Unlike statistical significance, effect size as measured by Cohen's (d) is independent of the sample size and is considered a good indication of clinical significance (124). An effect is considered large if $d > 0.8$ (125). In this study, Cohen's effect size (d) ranged from 1.05 to 2.14 for ROM and 2.2 for PA which would be considered as large to huge according to Sawilowsky (126).

This study measured LS pain following treatment with RM, however, physical changes to the LS junction were not investigated. It would be interesting to discover what regenerative changes, if any, coincide with the resolution of pain following treatment. Since there would be no requirement for anesthesia, MSK US could be a more economic non-invasive option than MRI to monitor change in hydration of the disc by determining its echogenicity and elastography. This technique has already shown the regenerative capacity of MSCs in tendons in this study by demonstrating reversal of scar tissue, fibrosis, and mineralization, resolution of inflammatory change, complete healing of partial tendon tears and restoration of normal entheses following treatment. Accordingly determining the regenerative potential of MSCs at the LS junction using MSK US will be the focus of further studies.

Many orthopedic specialists prefer objective outcome measures to client-reported outcome measures (CROMs), which include CMIs or HRQL measures, because they believe that the caregiver placebo effects, seen with subjective measures, could compromise the accuracy of their results. However, because CROMs are recognized as important by the FDA and the EMA, these have become an integral part of veterinary clinical trials. Even though Cook stipulated that, in orthopedic trials, CROMs should include a HRQL measure (42), there is still a tendency for researchers to rely on CMIs, perhaps because studies in dogs have shown that objective gait analysis and certain CMIs produce equivalent outcomes (53). It is interesting to note that, in their Position Statement Guest et al. use a low CMI score to indicate a "negligible identification of impact on quality of life" (53). While this inference may be true, it is an indirect association as CMIs are not measures of QOL. While CMIs

measure only the functional limitation imposed by the disease, VetMetrica™ HRQL instruments measure the emotional as well as the physical impact of the disease, and furthermore do so on a continuum from the worst to the best QOL (46).

VetMetrica assessments were completed by owners in accordance with the study protocol. In the domain A/C the improvement in all post-treatment time windows compared with pre-treatment was significant, with a similar result in E/E after 6 weeks and in H/C and C/R after 12 weeks. This indicated that the improvement in PWB preceded that of EWB by 6 weeks. This contrasts with treatment of OA with NSAIDs where an improvement in EWB is often seen before that of any improvement in PWB (47).

Currently studies showing a significant relationship between HRQL and objective measures are lacking, but the improvement in HRQL seen here mirrored that seen in all objective outcome measures. Indeed, formal analysis showed that there was a significant relationship between change in all HRQL domain scores and change in weight distribution, as measured by stance analysis, providing evidence of convergent construct validity for VetMetrica™. Of all the objective measures used, stance analysis was considered the most appropriate measure to correlate with HRQL measures since it is a global measure of musculoskeletal function. Similarly, the relationship between change in stance and change in vet assessments mirrored that of the change in stance and change in HRQL scores, with significant relationships for all three subjective measures, thus supporting the hypothesis that subjective and objective measures can produce equivalent outcomes in trials. However, it should be noted that if the pain and QOL impact assessments had been carried out by less experienced clinicians the relationship between these and stance may not have been as robust.

Importantly, in addition to the improvement in HRQL being statistically significant, clinical significance was demonstrated by the fact that the change in scores between pre- and post-treatment was equal to or greater than the MID in E/E, H/C, and A/C. Although this was not the case for C/R, the fact that this domain is affected by the temperament of the dog, may have been a contributing factor.

The veterinary assessments for pain and QOL impact as scored on a 0–10 numerical rating scale (NRS) provided additional subjective outcome measures in this study. The NRS is an ordinal scale and a major drawback to its use is inter-observer variability. However, the fact that a single observer completed all assessments removed that risk. Regarding assessing pain in non-verbal individuals, the FDA Guidance for Industry (127) states that an observer cannot validly attribute a pain score on behalf of another individual but can observe behaviors that indicate pain. Accordingly, in this study the pain assessment question was carefully worded to ensure that the score reflected the amount of pain the observer *felt* the dog was suffering. In this case, the observer (AA), a very experienced clinician dealing only with orthopedic conditions, was well placed to make that judgement. There is an argument that the same would not apply to judging QOL impact, since the clinician does not see the dog in its home environment, but the result of the analysis was remarkably similar with highly significant time window effects ($p < 0.001$) and all post-treatment means were significantly lower than pre-treatment. This may have reflected the close bond between author AA, the dog and its owner, formed over a considerable period and facilitated by an extensive consultation process supplemented by very regular updates on progress.

This study demonstrated a significant reduction in pain following treatment with RM, as measured by PA, stance analysis (offloading due to pain), vet pain scores and a significant reduction in analgesic requirement. Limitations of the study include the lack of a control group but the retrospective nature of the study made the reporting of a control group impossible. Had it been possible, the authors would have considered a control group inappropriate for the following reason: the study population consisted of client-owned dogs with MSD that was unresponsive to standard treatments at the time of referral, so continuing such treatment would be likely to prolong pain and suffering. Nevertheless, each dog was its own control, having been non-responsive to conventional treatments prior to the demonstration of significant improvements following targeted regenerative therapies. The authors consider a further limitation to be the fact that each objective outcome measure group size was different. This was due to the broad spectrum of pathologies present within the study population and omissions from the clinical record, however all dogs had at least two outcome measures recorded. Similarly, the number of HRQL assessments was reduced because the difference between these and the other outcome measurements had to be within 14 days of each other to be included in the analysis. However, since there were 954 assessments from 212 dogs up to week 104 this number was considered adequate for the study. Lack of blinding of author AA could be considered a limitation of the study in view of evidence of caregiver bias (128). This would be a serious consideration in a RCT but is not reported as such in RWD studies where data is collected from various sources including electronic patient records, as was the case in this study (129).

5. Conclusion

This study presents results of a longitudinal study being carried out in a veterinary practice specializing in RM, for the treatment of a large population of dogs with naturally occurring MSD that was unresponsive to conventional treatment. Importantly, the study complied with the minimal criteria for reporting MSCs in orthopedic applications published recently by Guest et al. (53). This, together with the use of several different validated outcome measures by a single, experienced, veterinary practitioner make this a uniquely important study of the efficacy

of RM in a clinical setting. Results have shown that using a standardized protocol of known numbers of autologous adipose derived MSCs, combined with leukocyte poor PRP where appropriate, injected into all areas of MSK pathology, resulted in rapid and profound positive effects in the patient's pain status (pressure algometry, vet score), function (stance analysis, goniometry) and QOL (VetMetrica™ HRQL assessment tool) for up to 2 years. Furthermore, this study endorses the use of VetMetrica™ in canine MSD by demonstrating a significant positive relationship with an objective measure of MSK function, providing evidence to support its value in orthopedic clinical trials.

The authors believe that this large scale, comprehensive study adds considerably to the evidence required to support the use of MSCs in canine orthopedic conditions and lays the foundations for further research regarding their regenerative potential. Furthermore, RM should be considered an important component in the multimodal approach to treatment of chronic degenerative MSK conditions in dogs, although care in selecting the most scientifically robust MSC and PRP products is imperative.

Data availability statement

The original contributions presented in the study are included in the article/Supplementary material, further inquiries can be directed to the corresponding author.

Ethics statement

The animal study was reviewed and approved by RCVS Ethics Review Panel. Written informed consent was obtained from the owners for the participation of their animals in this study.

Author contributions

AA, JM, and JR: conceptualization. TS: statistical analysis. All authors contributed to the article and approved the submitted version.

Funding

Linnaeus Veterinary Limited supported the costs of the Open Access Publication Charges.

Acknowledgments

We thank Luisa De Risio (Linnaeus Clinical Research and Excellence Director) and Christine Standen (Cell Therapy Sciences Clinical Director) for their help with preparation of the manuscript. The authors are grateful to all the dog owners who willingly provided data for this work.

Conflict of interest

JR is a director in NewMetrica Ltd, the company that develops the VetMetrica™ instruments. JM is a director in Cell Therapy Sciences that supplies the mesenchymal stromal cells.

The remaining authors declare that the research was conducted in the absence of any commercial or financial relationships that could be construed as a potential conflict of interest.

Publisher's note

Supplementary material

The Supplementary Material for this article can be found online at: https://www.frontiersin.org/articles/10.3389/fvets.2022.1014687/full#supplementary-material

References

1. O'Neill DG, Church DB, McGreevy PD, Thomson PC, Brodbelt DC. Longevity and mortality of owned dogs in England. *J Vet Med.* (2013) 198:638–43. doi: 10.1016/j.tvjl.2013.09.020

2. McGreevy PD, Wilson BJ, Mansfield CS, Brodbelt DC, Church DB, Dhand N, et al. Labrador retrievers under primary veterinary care in the UK: demography, mortality and disorders. *Canine* Med Genet. (2018) 5:1–3. doi: 10.1186/s40575-018-0064-x

3. Anderson KL, O'Neill DG, Brodbelt DC, Church DB, Meeson RL, Sargan D, et al. Prevalence, duration and risk factors for appendicular osteoarthritis in a UK dog population under primary veterinary care. *Sci Rep.* (2018) 8:1–2. doi: 10.1038/s41598-018-23940-z

4. Johnston SA. Osteoarthritis: joint anatomy, physiology, and pathobiology. *Vet Clin North Am Small Anim.* (1997) 27:699–723. doi: 10.1016/S0195-5616(97)50076-3

5. Fischer S, Anders A, Nolte I, Schilling N. Compensatory load redistribution in walking and trotting dogs with hind limb lameness. *J Vet Med.* (2013) 197:746–52. doi: 10.1016/j.tvjl.2013.04.009

6. Mündermann A, Dyrby CO, Andriacchi TP. Secondary gait changes in patients with medial compartment knee osteoarthritis: increased load at the ankle, knee, and hip during walking. *Arthritis Rheumatol.* 52.9 (2005):2835-2844. doi: 10.1002/art.21262

7. Fishkin Z, Miller D, Ritter C, Ziv I. Changes in human knee ligament stiffness secondary to osteoarthritis. *J Orthopaedic Res.* (2002) 20:204–7. doi: 10.1016/S0736-0266(01)00087-0

8. Merritt JL. Soft tissue mechanisms of pain in osteoarthritis. *Arthritis Rheumatol.* (1989) 18:4. doi: 10.1016/0049-0172(89)90016-4

9. Fink B, Egl M, Singer J, Fuerst M, Buenheim M, Jacob E. Morphologic changes in the vastus medialis muscle in patients with osteoarthritis of the knee. *Arthritis Rheumatol.* (2007) 56:3626–33. doi: 10.1002/art.22960

10. Canapp SO, Canapp DA, Carr BJ, Cox C, Barrett JG. Supraspinatus tendinopathy in 327 dogs: a retrospective study. *Vet Evid.* (2016) 1:3. doi: 10.18849/ve.v1i3.32

11. Johnson JA, Austin C, Breur GJ. Incidence of canine appendicular musculoskeletal disorders in 16 veterinary teaching hospitals from 1980 through (1989). *Vet Comp Orthop Traumatol.* (1994) 7:56–69. doi: 10.1055/s-0038-1633097

12. Cook JL, Payne JT. Surgical treatment of osteoarthritis. *Vet Clin North Am Small Anim.* (1997) 27:931–44. doi: 10.1016/S0195-5616(97)50087-8

13. Witte PG. Hip dysplasia: understanding the options (surgical management). *Companion Animal.* (2019) 24:249–56. doi: 10.12968/coan.2019.24.5.249

14. Bruecker KA, Benjamino K, Vezzoni A, Walls C, Wendelburg KL, Follette CM, et al. Canine elbow dysplasia: medial compartment disease and osteoarthritis. *Vet Clin North Am Small Anim Pract.* (2021) 51:475–515. doi: 10.1016/j.cvsm.2020.12.008

15. Corr S. Update on the management of canine cruciate disease. *In Pract.* (2022) 44:260–9. doi: 10.1002/inpr.135

16. Rehnblom E, Gordon-Evans WJ. Are dogs with hip dysplasia in less pain after total hip replacement than femoral head ostectomy? *Vet Evid.* (2022) 7:1. doi: 10.18849/ve.v7i1.388

17. Pye C, Bruniges N, Peffers M, Comerford E. Advances in the pharmaceutical treatment options for canine osteoarthritis. *J Small Anim Pract.* (2022) 63:721–38. doi: 10.1111/jsap.13495

18. Cui GH, Wang YY Li CJ, Shi CH, Wang WS. Efficacy of mesenchymal stem cells in treating patients with osteoarthritis of the knee: a meta-analysis. *Exp Ther Med.* (2016) 12:3390–400. doi: 10.3892/etm.2016.3791

19. Voga M, Adamic N, Vengust M, Majdic G. Stem cells in veterinary medicine—current state and treatment options. *Front Vet Sci.* (2020) 7:278. doi: 10.3389/fvets.2020.00278

20. Godwin EE, Young NJ, Dudhia J, Beamish IC, Smith RK. Implantation of bone marrow-derived mesenchymal stem cells demonstrates improved outcome in horses with overstrain injury of the superficial digital flexor tendon. *Equine Vet J.* (2012) 44:25–32. doi: 10.1111/j.2042-3306.2011.00363.x

21. Harman R, Carlson K, Gaynor J, Gustafson S, Dhupa S, Clement K, et al. prospective, randomized, masked, and placebo-controlled efficacy study of intraarticular allogeneic adipose stem cells for the treatment of osteoarthritis in dogs. *Front Vet Sci.* (2016) 3:81. doi: 10.3389/fvets.2016.00081

22. Vilar JM, Morales M, Santana A, Spinella G, Rubio M, Cuervo B, et al. Controlled, blinded force platform analysis of the effect of intraarticular injection of autologous adipose-derived mesenchymal stem cells associated to PRGF-Endoret in osteoarthritic dogs. *BMC Vet Res.* (2013) 9:1–6. doi: 10.1186/1746-6148-9-131

23. Bastos R, Mathias M, Andrade R, Amaral RJ, Schott V, Balduino A, et al. Intra-articular injection of culture-expanded mesenchymal stem cells with or without addition of platelet-rich plasma is effective in decreasing pain and symptoms in knee osteoarthritis: a controlled, double-blind clinical trial. *Knee Surg Sports Traumatol Arthrosc.* (2020) 28:1989–99. doi: 10.1007/s00167-019-05732-8

24. Cabon Q, Febre M, Gomez N, Cachon T, Pillard P, Carozzo C, et al. Long-term safety and efficacy of single or repeated intra-articular injection of allogeneic neonatal mesenchymal stromal cells for managing pain and lameness in moderate to severe canine osteoarthritis without anti-inflammatory pharmacological support: pilot clinical study. *Front Vet Sci.* (2019) 6:10. doi: 10.3389/fvets.2019.00010

25. Weiss AR, Dahlke MH. Immunomodulation by mesenchymal stem cells (MSCs): mechanisms of action of living, apoptotic, and dead MSCs. *Front Immunol.* (2019) 10:1191. doi: 10.3389/fimmu.2019.01191

26. Shi Y, Wang Y, Li Q, Liu K, Hou J, Shao C, et al. Immunoregulatory mechanisms of mesenchymal stem and stromal cells in inflammatory diseases. *Nat Rev Nephrol.* (2018) 14:493–507. doi: 10.1038/s41581-018-0023-5

27. Maki CB, Beck A, Wallis CB, Choo J, Ramos T, Tong R, Borjesson DL, Izadyar F. Intra-articular administration of allogeneic adipose derived MSCs reduces pain and lameness in dogs with hip osteoarthritis: a double blinded, randomized, placebo controlled pilot study. *Front Vet Sci.* (2020) 2020:570. doi: 10.3389/fvets.2020.00570

28. Tatsis D, Vasalou V, Kotidis E, Anestiadou E, Grivas I, Cheva A, et al. The combined use of platelet-rich plasma and adipose-derived mesenchymal stem cells promotes healing. A review of experimental models and future. *Perspect Biol Med.* (2021) 11:1403. doi: 10.3390/biom11101403

29. Clough WT, Canapp Jr SO, De Taboada L, Dycus DL, Leasure CS. Sensitivity and specificity of a weight distribution platform for the detection of objective lameness and orthopaedic disease. *Vet Comp Orthop Traumatol.* (2018) 31:391–5. doi: 10.1055/s-0038-1667063

30. Jaegger G, Marcellin-Little DJ, Levine D. Reliability of goniometry in Labrador Retrievers. *Am J Vet Res.* (2002) 63:979–86. doi: 10.2460/ajvr.2002.63.979

31. Hesbach AL. Techniques for objective outcome assessment. *Clin Tech Small Anim Pract.* (2007) 22:146–54. doi: 10.1053/j.ctsap.2007.09.002

32. Fischer AA. Algometry in diagnosis of musculoskeletal pain and evaluation of treatment outcome: an update. *J Musculoskelet Pain.* (1998) 6:5–32. doi: 10.1300/J094v06n01_02

33. Coleman KD, Schmiedt CW, Kirkby KA, Coleman AE, Robertson SA, Hash J, et al. Learning confounds algometric assessment of mechanical thresholds in normal dogs. *Vet Surg.* (2014) 43:361–7. doi: 10.1111/j.1532-950X.2014.12112.x

34. Briley JD, Williams MD, Freire M, Griffith EH, Lascelles BD. Feasibility and repeatability of cold and mechanical quantitative sensory testing in normal dogs. *J Vet Med.* (2014) 199:245–50. doi: 10.1016/j.tvjl.2013.10.025

35. Knazovicky D, Helgeson ES, Case B, Gruen ME, Maixner W, Lascelles BD. Widespread somatosensory sensitivity in naturally occurring canine model of osteoarthritis. *Pain.* (2016) 157:1325. doi: 10.1097/j.pain.0000000000000521

36. Lane DM, Hill SA. Pressure algometry measurement of canine muscular pain near the thoracolumbar junction: evaluation of a modified technique. *Vet Anaesth Analg.* (2016) 43:227–34. doi: 10.1111/vaa.12308

37. Hunt J, Knazovicky D, Lascelles BD. Murrell J. Quantitative sensory testing in dogs with painful disease: a window to pain mechanisms? *J Vet Med.* (2019) 243:33–41. doi: 10.1016/j.tvjl.2018.11.007

38. Haussler KK. Pressure algometry for the detection of mechanical nociceptive thresholds in horses. *Animals.* (2020) 10:2195. doi: 10.3390/ani10122195

39. Dias LV, Cordeiro MA, de Sales RS, Dos Santos MM, Korelo RI, Vojciechowski AS. Immediate analgesic effect of transcutaneous electrical nerve stimulation (TENS) and interferential current (IFC) on chronic low back pain: Randomised placebo-controlled trial. *J Bodyw Mov Ther.* (2021) 27:181–90. doi: 10.1016/j.jbmt.2021.03.005

40. Suzuki H, Tahara S, Mitsuda M, Izumi H, Ikeda S, Seki K, et al. Current concept of quantitative sensory testing and pressure pain threshold in neck/shoulder and low back pain. *InHealthcare.* (2022) 10:1485. doi: 10.3390/healthcare10081485

41. Reid J, Nolan AM, Scott EM. Measuring pain in dogs and cats using structured behavioural observation. *J Vet Med.* (2018) 236:72–9. doi: 10.1016/j.tvjl.2018.04.013

42. Cook JL. Canine orthopedic outcome measures program: where are we now? *Veterinary Surgery.* (2014) 43:229–31. doi: 10.1111/j.1532-950X.2014.12167.x

43. Hawker GA, Mian S, Kendzerska T, French M. Measures of adult pain: Visual analog scale for pain (vas pain), numeric rating scale for pain (nrs pain), mcgill pain questionnaire (mpq), short-form mcgill pain questionnaire (sf-mpq), chronic pain grade scale (cpgs), short form-36 bodily pain scale (sf-36 bps), and measure of intermittent and constant osteoarthritis pain (icoap). *Arthritis Care Res.* (2011) 63:S240–52. doi: 10.1002/acr.20543

44. Wojciechowska JI, Hewson CJ. Quality-of-life assessment in pet dogs. *J Am Vet Med Assoc.* (2005) 226:722–8. doi: 10.2460/javma.2005.226.722

45. Lavan RP. Development and validation of a survey for quality of life assessment by owners of healthy dogs. *J Vet Med.* (2013) 197:578–82. doi: 10.1016/j.tvjl.2013.03.021

46. Reid J, Wiseman-Orr L, Scott M. Shortening of an existing generic online health-related quality of life instrument for dogs. *J Small Animal Pract.* (2018) 59:334–42. doi: 10.1111/jsap.12772

47. Reid J, Wright A, Gober M, Nolan AM, Noble C, Scott EM. Measuring chronic pain in osteoarthritic dogs treated long-term with carprofen, through its impact on health-related quality of life. *Vet Comp Orthop Traumatol.* (2018) 31:A0015. doi: 10.1055/s-0038-1660890

48. Armitage A, Reid J. Measuring the impact of regenerative medicine (RM) on chronic degenerative conditions in dogs, using a validated owner-reported outcome measure (VetMetrica) which provides scores in 4 domains of health-related quality of life (HRQL). In: *BSAVA Congress Proceedings.* (2019). BSAVA Library. p. 515-516. doi: 10.22233/9781910443699.83.8

49. Schünemann HJ, Puhan M, Goldstein R, Jaeschke R, Guyatt GH. Measurement properties and interpretability of the Chronic respiratory disease questionnaire (CRQ). *COPD.* (2005) 2:81–9. doi: 10.1081/COPD-200050651

50. Davies V, Reid J, Wiseman-Orr ML, Scott EM. Optimising outputs from a validated online instrument to measure health-related quality of life (HRQL) in dogs. *PLoS ONE.* (2019) 14:e0221869. doi: 10.1371/journal.pone.0221869

51. McLeod SA. *What does effect size tell you? Simply psychology*. (2022). Available online at: https://wwwsimplypsychologyorg/effect-sizehtml (accessed September 30, 2022).

52. Mocchi M, Dotti S, Del Bue M, Villa R, Bari E, Perteghella S, et al. Veterinary regenerative medicine for musculoskeletal disorders: can mesenchymal stem/stromal cells and their secretome be the New Frontier? *Cells.* (2020) 9:1453. doi: 10.3390/cells9061453

53. Guest DJ, Dudhia J, Smith RK, Roberts SJ, Conzemius M, Innes JF, et al. Position statement: minimal criteria for reporting veterinary and animal medicine research for mesenchymal stromal/stem cells in orthopaedic applications. *Front Vet Sci.* (2022) 7:199. doi: 10.3389/fvets.2022.817041

54. Blonde L, Khunti K, Harris SB, Meizinger C, Skolnik NS. Interpretation and impact of real-world clinical data for the practicing clinician. *Adv Ther.* (2018) 35:1763–74. doi: 10.1007/s12325-018-0805-y

55. Luce BR, Drummond M, Jönsson B, Neumann PJ, Schwartz JS, Siebert UW, et al. HTA, and CER: clearing the confusion. *Milbank Q.* (2010) 88:256–76. doi: 10.1111/j.1468-0009.2010.00598.x

56. Conzemius MG, Evans RB. Caregiver placebo effect for dogs with lameness from osteoarthritis. *J Am Vet Med Assoc.* (2012) 241:1314–9. doi: 10.2460/javma.241.10.1314

57. Bian J, Lyu T, Loiacono A, Viramontes TM, Lipori G, Guo Y, et al. Assessing the practice of data quality evaluation in a national clinical data research network through a systematic scoping review in the era of real-world data. *J Am Med Inform Assoc.* (2020) 27:1999–2010. doi: 10.1093/jamia/ocaa245

58. Simitzi C, Vlahovic M, Georgiou A, Keskin-Erdogan Z, Miller J, Day RM. Modular orthopaedic tissue engineering with implantable microcarriers and canine adipose-derived mesenchymal stromal cells. *Front Bioeng Biotechnol.* (2020) 8:816. doi: 10.3389/fbioe.2020.00816

59. Russell KA, Gibson TW, Chong A, Co C, Koch TG. Canine platelet lysate is inferior to fetal bovine serum for the isolation and propagation of canine adipose tissue-and bone marrow-derived mesenchymal stromal cells. *PLoS ONE.* (2015) 10:e0136621. doi: 10.1371/journal.pone.0136621

60. Krešić N, Šimić I, Lojkić I, Bedeković T. Canine adipose derived mesenchymal stem cells transcriptome composition alterations: a step towards standardizing therapeutic. *Stem Cells Int.* (2017). 2017:4176292. doi: 10.1155/2017/4176292

61. Ivanovska A, Wang M, Arshaghi TE, Shaw G, Alves J, Byrne A, et al. Manufacturing mesenchymal stromal cells for the treatment of osteoarthritis in canine patients: challenges and recommendations. *Front Vet Sci.* (2022) 2022:587. doi: 10.3389/fvets.2022.897150

62. Carr BJ, Canapp Jr SO, Mason DR, Cox C, Hess T. Canine platelet-rich plasma systems: a prospective analysis. *Front Vet Sci.* (2016) 2:73. doi: 10.3389/fvets.2015.00073

63. Sanghani-Kerai A, Black C, Cheng SO, Collins L, Schneider N, Blunn G, et al. Clinical outcomes following intra-articular injection of autologous adipose-derived mesenchymal stem cells for the treatment of osteoarthritis in dogs characterized by weight-bearing asymmetry. *Bone Joint Res.* (2021) 10:650–8. doi: 10.1302/2046-3758.1010.BJR-2020-0540.R1

64. Naredo E, Acebes C, Möller I, Canillas F, de Agustín JJ, de Miguel E, et al. Ultrasound validity in the measurement of knee cartilage thickness. *Ann Rheum Dis.* (2009) 68:1322–7. doi: 10.1136/ard.2008.090738

65. Iagnocco A. Imaging the joint in osteoarthritis: a place for ultrasound? Best practice & research. *Clinical Rheumatology.* (2010) 24:27–38. doi: 10.1016/j.berh.2009.08.012

66. Möller I, Bong D, Naredo E, Filippucci E, Carrasco I, Moragues C, et al. Ultrasound in the study and monitoring of osteoarthritis. *Osteoarthr Cartil.* (2008) 16:S4–7. doi: 10.1016/j.joca.2008.06.005

67. Okano T, Mamoto K, Di Carlo M, Salaffi F. Clinical utility and potential of ultrasound in osteoarthritis. *Radiol Med.* (2019) 124:1101–11. doi: 10.1007/s11547-019-01013-z

68. Nelson AE. Turning the page in osteoarthritis assessment with the use of ultrasound. *Curr Rheumatol Rep.* (2020) 22:1–8. doi: 10.1007/s11926-020-00949-w

69. Oo WM, Bo MT. Role of ultrasonography in knee osteoarthritis. *JCR.* (2016) 22:324–9. doi: 10.1097/RHU.0000000000000436

70. Boonchaikitanan P, Choisunirachon N, Soontornvipart K. A feasibility of ultrasonographic assessment for femoral trochlear depth and articular cartilage thickness in canine cadavers. *Thai J Vet Med.* (2019) 49:257–64.

71. Sanghvi NT, Snoddy AM, Myers SL, Brandt KD, Reilly CR, Franklin TD. Characterization of normal and osteoarthritic cartilage using 25 MHz ultrasound. In: *IEEE Symposium on Ultrasonics.* (1990). New York, NY: IEEE. p. 1413–16

72. Kramer M, Gerwing M, Hach V, Schimke E. Sonography of the musculoskeletal system in dogs and cats. *Vet Radiol Ultrasound.* (1997) 38:139–49. doi: 10.1111/j.1740-8261.1997.tb00829.x

73. Sasaki A, Mizuno M, Mochizuki M, Sekiya I. Mesenchymal stem cells for cartilage regeneration in dogs. *World J Stem Cells.* (2019) 11:254. doi: 10.4252/wjsc.v11.i5.254

74. Humenik F, Maloveska M, Hudakova N, Petrouskova P, Hornakova L, Domaniza M, et al. Comparative study of canine mesenchymal stem cells isolated from different sources. *Animals.* (2022) 12:1502. doi: 10.3390/ani12121502

75. Kadiyala S, Young RG, Thiede MA, Bruder SP. Culture expanded canine mesenchymal stem cells possess osteochondrogenic potential in vivo and in vitro. *Cell Transplant.* (1997) 6:125–34. doi: 10.1177/096368979700600206

76. Galleu A, Riffo-Vasquez Y, Trento C, Lomas C, Dolcetti L, Cheung TS, et al. Apoptosis in mesenchymal stromal cells induces in vivo recipient-mediated immunomodulation. *Sci Translational Med.* (2017) 9:eaam7828. doi: 10.1126/scitranslmed.aam7828

77. García-Bernal D, García-Arranz M, Yáñez RM, Hervás-Salcedo R, Cortés A, Fernández-García M, et al. The current status of mesenchymal stromal cells: controversies, unresolved issues and some promising solutions to improve their therapeutic efficacy. *Front Cell Dev Biol.* (2021) 9:650664. doi: 10.3389/fcell.2021.650664

78. Li M, Luo X, Lv X, Liu V, Zhao G, Zhang X, et al. In vivo human adipose-derived mesenchymal stem cell tracking after intra-articular delivery in a rat osteoarthritis model. *Stem Cell Res Ther.* (2016) 7:1–13. doi: 10.1186/s13287-016-0420-2

79. Burk J, Berner D, Brehm W, Hillmann A, Horstmeier C, Josten C, et al. Long-term cell tracking following local injection of mesenchymal stromal cells in the equine model of induced tendon disease. *Cell Transplant.* (2016) 25:2199–211. doi: 10.3727/096368916X692104

80. Webb TL, Spaas JH, Guest DJ. One health and veterinary regenerative medicine: translational applications. *Front Vet Sci.* (2022) 2022:1016. doi: 10.3389/fvets.2022.959564

81. Wang K, Li Z, Li J, Liao W, Qin Y, Zhang N, et al. Optimization of the platelet-rich plasma concentration for mesenchymal stem cell applications. *Tissue Engineering Part A.* (2019) 25:333–51. doi: 10.1089/ten.tea.2018.0091

82. Moon JH, Rhee YH, Ahn JC, Kim B, Lee SJ, Chung PS. Enhanced survival of ischemic skin flap by combined treatment with bone marrow-derived stem cells and low-level light irradiation. *Lasers Med Sci.* (2018) 33:1–9. doi: 10.1007/s10103-017-2312-9

83. Braun HJ, Kim HJ, Chu CR, Dragoo JL. The effect of platelet-rich plasma formulations and blood products on human synoviocytes: implications for intra-articular injury and therapy. *Am J Sports Med.* (2014) 42:1204–10. doi: 10.1177/0363546514525593

84. Suchetha A, Lakshmi P, Bhat D, Mundinamane DB, Soorya KV, Bharwani GA. Platelet concentration in platelet concentrates and periodontal regeneration-unscrambling the ambiguity. *Contemp Clin Dent.* (2015) 6:510. doi: 10.4103/0976-237X.169850

85. Fleming BC, Proffen BL, Vavken P, Shalvoy MR, Machan JT, Murray MM. Increased platelet concentration does not improve functional graft healing in bio-enhanced ACL reconstruction. *Knee Surg Sports Traumatol Arthrosc.* (2015) 23:1161–70. doi: 10.1007/s00167-014-2932-6

86. Rappl LM. Effect of platelet rich plasma gel in a physiologically relevant platelet concentration on wounds in persons with spinal cord injury. *Int Wound J.* (2011) 8:187–95. doi: 10.1111/j.1742-481X.2011.00770.x

87. Han L, Fang WL, Jin B, Xu SC, Zheng X, Hu YG. Enhancement of tendon-bone healing after rotator cuff injuries using combined therapy with mesenchymal stem cells and platelet rich plasma. *Eur Rev Med Pharmacol Sci.* (2019) 23:9075–84.

88. Dos Santos RG, Santos GS, Alkass N, Chiesa TL, Azzini GO, da Fonseca LF, et al. The regenerative mechanisms of platelet-rich plasma: a review. *Cytokine.* (2021) 144:155560. doi: 10.1016/j.cyto.2021.155560

89. Kidd S, Spaeth E, Dembinski JL, Dietrich M, Watson K, Klopp A, et al. Direct evidence of mesenchymal stem cell tropism for tumor and wounding microenvironments using in vivo bioluminescent imaging. *Stem Cells.* (2009) 27:2614–23. doi: 10.1002/stem.187

90. Sheykhhasan M, Wong JK, Seifalian AM. Human adipose-derived stem cells with great therapeutic potential. *Curr Stem Cell Res Ther*. (2019) 14:532–48. doi: 10.2174/1574888X14666190411121528

91. Liu M, Li K, Wang Y, Zhao G, Jiang J. Stem cells in the treatment of neuropathic pain: research progress of mechanism. *Stem Cells Int*. (2020). 2020:8861251. doi: 10.1155/2020/8861251

92. Illien-Jünger S, Pattappa G, Peroglio M, Benneker LM, Stoddart MJ, Sakai D, et al. Homing of mesenchymal stem cells in induced degenerative intervertebral discs in a whole organ culture system. *Spine*. (2012) 37:1865–73. doi: 10.1097/BRS.0b013e3182544a8a

93. Oehme D, Goldschlager T, Ghosh P, Rosenfeld JV, Jenkin G. Cell-based therapies used to treat lumbar degenerative disc disease: a systematic review of animal studies and human clinical trials. *Stem cells Int*. (2015) 2015:946031. doi: 10.1155/2015/946031

94. Osaka M, Honmou O, Murakami T, Nonaka T, Houkin K, Hamada H, et al. Intravenous administration of mesenchymal stem cells derived from bone marrow after contusive spinal cord injury improves functional outcome. *Brain Res*. (2010) 1343:226–35. doi: 10.1016/j.brainres.2010.05.011

95. Ra JC, Shin IS, Kim SH, Kang SK, Kang BC, Lee HY, et al. Safety of intravenous infusion of human adipose tissue-derived mesenchymal stem cells in animals and humans. *Stem Cells Dev*. (2011) 20:1297–308. doi: 10.1089/scd.2010.0466

96. Serigano K, Sakai D, Hiyama A, Tamura F, Tanaka M, Mochida J. Effect of cell number on mesenchymal stem cell transplantation in a canine disc degeneration model. *J Orthop*. (2010) 28:1267–75. doi: 10.1002/jor.21147

97. Hohaus C, Ganey TM, Minkus Y, Meisel HJ. Cell transplantation in lumbar spine disc degeneration disease. *Eur Spine J*. (2008) 17:492–503. doi: 10.1007/s00586-008-0750-6

98. Hiyama A, Mochida J, Iwashina T, Omi H, Watanabe T, Serigano K, et al. Transplantation of mesenchymal stem cells in a canine disc degeneration model. *J Orthop*. (2008) 26:589–600. doi: 10.1002/jor.20584

99. Ganey T, Hutton WC, Moseley T, Hedrick M, Meisel HJ. Intervertebral disc repair using adipose tissue-derived stem and regenerative cells: experiments in a canine model. *Spine*. (2009) 34:2297–304. doi: 10.1097/BRS.0b013e3181a54157

100. Salmelin B, Fitzpatrick N, Rose J, Driver C. Safety profile of methylprednisolone acetate epidural injection in dogs treated for lumbosacral disease. In: *BSAVA Congress Proceedings*. (2019). Quedgeley: BSAVA Library. p. 546. doi: 10.22233/9781910443699.85.36

101. Worth A, Meij B, Jeffery N. Canine degenerative lumbosacral stenosis: prevalence, impact and management strategies. *Veterinary Medicine: research and reports*. (2019) 10:169. doi: 10.2147/VMRR.S180448

102. Pryor B, Millis DL. Therapeutic laser in veterinary medicine. *Vet Clin North Am Small Anim Pract*. (2015) 45:45–56. doi: 10.1016/j.cvsm.2014.09.003

103. Ginani F, Soares DM, Barboza CA. Effect of low-level laser therapy on mesenchymal stem cell proliferation: a systematic review. *Lasers Med Sci*. (2015) 30:2189–94. doi: 10.1007/s10103-015-1730-9

104. Ahmadi H, Amini A, Fadaei Fathabady F, Mostafavinia A, Zare F, Ebrahimpour-Malekshah R, et al. Transplantation of photobiomodulation-preconditioned diabetic stem cells accelerates ischemic wound healing in diabetic rats. *Stem Cell Res Ther*. (2020) 11:1–4. doi: 10.1186/s13287-020-01967-2

105. Khosravipour A, Amini A, Farahani RM, Zare F, Mostafavinia A, Fallahnezhad S, et al. Preconditioning adipose-derived stem cells with photobiomodulation significantly increased bone healing in a critical size femoral defect in rats. *Biochem Biophys Res Commun*. (2020) 531:105–11. doi: 10.1016/j.bbrc.2020.07.048

106. Amaroli A, Pasquale C, Zekiy A, Benedicenti S, Marchegiani A, Sabbieti MG, et al. Steering the multipotent mesenchymal cells towards an anti-inflammatory and osteogenic bias via photobiomodulation therapy: How to kill two birds with one stone. *J Tissue Eng*. (2022) 13:20417314221110192. doi: 10.1177/20417314221110192

107. Stancker TG, Vieira SS, Serra AJ. do Nascimento Lima R, dos Santos Feliciano R, Silva JA, et al. Can photobiomodulation associated with implantation of mesenchymal adipose-derived stem cells attenuate the expression of MMPs and decrease degradation of type II collagen in an experimental model of osteoarthritis? *Lasers Med Sci*. (2018) 33:1073–84. doi: 10.1007/s10103-018-2466-0

108. Kim H, Choi K, Kweon OK, Kim WH. Enhanced wound healing effect of canine adipose-derived mesenchymal stem cells with low-level laser therapy in athymic mice. *J Dermatol Sci*. (2012) 68:149–56. doi: 10.1016/j.jdermsci.2012.09.013

109. Lucke LD, Bortolazzo FO, Theodoro V, Fujii L, Bombeiro AL, Felonato M, et al. Low-level laser and adipose-derived stem cells altered remodelling genes expression and improved collagen reorganization during tendon repair. *Cell Prolif*. (2019) 52:e12580. doi: 10.1111/cpr.12580

110. Alves JC, Santos A, Jorge P, Carreira LM. A randomized double-blinded controlled trial on the effects of photobiomodulation therapy in dogs with osteoarthritis. *Am J Vet Res*. (2022) 83:8. doi: 10.2460/ajvr.22.03.0036

111. Upchurch DA, Renberg WC, Roush JK, Milliken GA, Weiss ML. Effects of administration of adipose-derived stromal vascular fraction and platelet-rich plasma to dogs with osteoarthritis of the hip joints. *Am J Vet Res*. (2016) 77:940–51. doi: 10.2460/ajvr.77.9.940

112. Adrian D, Brown D. Kinetic symmetry indices and standing gait analysis: A review of current methods and data. *J Vet Med*. (2022) 9:105814. doi: 10.1016/j.tvjl.2022.105814

113. Conzemius MG, Torres BT, Muir P, Evans R, Krotscheck U, Budsberg S. Best practices for measuring and reporting ground reaction forces in dogs. *Vet Surg*. (2022) 51:385–96. doi: 10.1111/vsu.13772

114. Seibert R, Marcellin-Little DJ, Roe SC, DePuy V, Lascelles BD. Comparison of body weight distribution, peak vertical force, and vertical impulse as measures of hip joint pain and efficacy of total hip replacement. *Vet Surg*. (2012) 41:443–7. doi: 10.1111/j.1532-950X.2012.00957.x

115. Skangals U. Stem cell therapy in the treatment of elbow joint osteoarthritis in dogs. *Eur J Vet Med*. (2022) 2:1–8. doi: 10.24018/ejvetmed.2022.2.3.30

116. Sabanci SS, Ocal MK. Comparison of goniometric measurements of the stifle joint in seven breeds of normal dogs. *Vet Comp Orthop Traumatol*. (2016) 29:214–9. doi: 10.3415/VCOT-15-05-0090

117. Thomovsky SA, Chen AV, Kiszonas AM, Lutskas LA. Goniometry and limb girth in miniature Dachshunds. *J Vet Med*. (2016). 2016:5846052. doi: 10.1155/2016/5846052

118. Formenton MR, De Lima LG, Vassalo FG, Joaquim JG, Rosseto LP, Fantoni DT. Goniometric assessment in French bulldogs. *Front Vet Sci*. (2019) 6:424. doi: 10.3389/fvets.2019.00424

119. Clarke E, Aulakh KS, Hudson C, Barnes K, Gines JA, Liu CC, et al. Effect of sedation or general anesthesia on elbow goniometry and thoracic limb circumference measurements in dogs with naturally occurring elbow osteoarthritis. *Vet Surg*. (2020) 49:1428–36. doi: 10.1111/vsu.13499

120. Carr BJ, Canapp Jr SO, Chun N, Gaver A. Clinical efficacy of platelet rich plasma for the treatment of elbow osteoarthritis in twenty dogs. *Vet Comp Orthop Traumatol*. (2018) 31:A3594. doi: 10.1055/s-0038-1668217

121. Hirayama J, Yamagata M, Ogata S, Shimizu K, Ikeda Y, Takahashi K. Relationship between low-back pain, muscle spasm and pressure pain thresholds in patients with lumbar disc herniation. *Eur Spine J*. (2006) 15:41–7. doi: 10.1007/s00586-004-0813-2

122. Giesbrecht RJ, Battié MC. A comparison of pressure pain detection thresholds in people with chronic low back pain and volunteers without pain. *Phys Ther*. (2005) 85:1085–92. doi: 10.1093/ptj/85.10.1085

123. Go JH, An HJ. The impact of joint mobilization and transcutaneous electrical nerve stimulation on pain in patients with lumbar spinal stenosis. *J Int Acad Phys Ther Res*. (2019) 10:1746–9. doi: 10.20540/JIAPTR.2019.10.1.1746

124. Cohen J. Quantitative methods in psychology: a power primer. In: *Psychological bulletin*. (1992). doi: 10.1037/0033-2909.112.1.155

125. Aarts S, Van Den Akker M, Winkens B. The importance of effect sizes. *Eur J Gen Pract*. (2014) 20:61–4. doi: 10.3109/13814788.2013.818655

126. Sawilowsky SS. New effect size rules of thumb. *J Mod Appl Stat Methods*. (2009) 8:26. doi: 10.22237/jmasm/1257035100

127. Guidance for Industry. Patient-reported outcome measures: use in medical product development to support labeling claims: draft guidance. *Health Qual Life Outcomes*. (2006) 4:79. doi: 10.1186/1477-7525-4-79

128. Sherman RE, Anderson SA, Dal Pan GJ, et al. Real-world evidence—what is it and what can it tell us? *N Engl J Med*. (2016) 375:2293–7. doi: 10.1056/NEJMsb1609216

129. US FDA. *Real-World Evidence*. (2020). Available online at: https://www.fda.gov/science-research/science-and-research-special-topics/real-world-evidence (accessed July 21, 2020).

frontiers | Frontiers in Veterinary Science

TYPE Case Report
PUBLISHED 19 January 2023
DOI 10.3389/fvets.2023.1003993

OPEN ACCESS

EDITED BY
Chavaunne T. Thorpe,
Royal Veterinary College (RVC),
United Kingdom

REVIEWED BY
Mohammed Zayed,
South Valley University, Egypt
Ana Ivanovska,
University of Galway, Ireland

*CORRESPONDENCE
Alessio Franini
✉ franinivet@gmail.com
Marco Patruno
✉ marco.pat@unipd.it

SPECIALTY SECTION
This article was submitted to Veterinary Regenerative Medicine, a section of the journal Frontiers in Veterinary Science

RECEIVED 26 July 2022
ACCEPTED 05 January 2023
PUBLISHED 19 January 2023

CITATION
Franini A, Entani MG, Colosio E, Melotti L and Patruno M (2023) Case report: Flexor carpi ulnaris tendinopathy in a lure-coursing dog treated with three platelet-rich plasma and platelet lysate injections.
Front. Vet. Sci. 10:1003993.
doi: 10.3389/fvets.2023.1003993

Case report: Flexor carpi ulnaris tendinopathy in a lure-coursing dog treated with three platelet-rich plasma and platelet lysate injections

Alessio Franini[1]*, Maria Grazia Entani[1], Elisa Colosio[1], Luca Melotti[2] and Marco Patruno[2]*

[1]Sporty Dog Veterinary Clinic, Brescia, Italy, [2]Department of Comparative Biomedicine and Food Science, University of Padua, Padua, Italy

In the present case report a 7-year-old male Whippet competing in lure-coursing presented with third-degree recurrent lameness of the right forelimb, pain on palpation of the caudal aspect of the carpus and swelling of the forearm proximally to the accessory carpal bone. Clinical, radiographic, and ultrasonographic evaluation diagnosed a flexor carpi ulnaris (FCU) chronic tendinopathy unresponsive to previously attempted conservative treatments such as oral non-steroidal anti-inflammatory drugs (NSAIDs) administration along with padded palmar splint application and rest. The dog was subjected to one injection of autologous platelet-rich plasma (PRP) obtained using a double centrifugation tube method, followed by two platelet lysate (PL) injections. Treatment was administered at three-week intervals. The healing process was assessed through clinical and ultrasonographic imaging (US) on the day of the first injection (T0), and at week three (T1), six (T2), twelve (T3), fifty-two (T4), and one-hundred-and-four (T5). Fiber alignment score (FAS) and echogenicity score (ES) were developed by modifying a previously published US assessment scale. At T1, ES, and FAS improvement was detected, and at T2, further improvements in ES and FAS were observed. Ultrasonographic results were clinically consistent with the improvement in lameness: lameness grade 3/4 was detected at T0 and grade 2/4 at T1. A lameness grade of 1/4 was detected at T2, and grade 0/4 was observed at T3, T4, and T5. Moreover, at T5, the dog returned to competition, and no history of re-injury was reported. Our results suggest that the treatment of FCU tendinopathy in lure-coursing dogs with a combination of consecutive injections of autologous PRP and PL could be feasible. Additionally, no adverse reactions were observed.

KEYWORDS

platelet-rich plasma (PRP), platelet lysate (PL), dog, tissue regeneration, regenerative medicine, canine orthopedics

1. Introduction

The flexor carpi ulnaris (FCU) muscle in dogs acts as a flexor and an abductor of the forepaw. It also has an antigravitational function. It consists of two bellies: the ulnar and humeral heads. Both end distally on the accessory carpal bone with two tendons. The ulnar head extends distally with a flat tendon laying lateral and palmar to the superficial digital flexor muscle, covering the humeral head. Progressing distally, it ends at the apex of the accessory carpal bone, which is separated from the humeral head tendon. The humeral head tendon is short, strong, and inserts into the apex of the accessory carpal bone (1).

Although only occasionally reported, lesions of the actual tendon itself have been described in Coursing dogs as typical sport-related injuries, and lesions of the insertion of the FCU tendon have been described in veterinary sports medicine as a consequence of strain followed by inadequate rest (2). A single case report on a Weimaraner was described in Kuan et al. (3) assuming that insertional tears of the FCU tendon have to be included in the differential diagnosis of thoracic limb lameness and peri-carpal swelling.

In human sports medicine, wrist and hand injuries reportedly affect a large part of the sporting population, and FCU tendinopathy is described as an overuse injury involving sports with a high potential of wrist and hand trauma such as tennis, handball, netball, or basketball (4).

The diagnosis of hand injuries in human medicine is considered challenging, and the importance of ultrasonographic evaluation of musculoskeletal diseases is increasing with applications in wrist injuries (5, 6). In veterinary medicine, ultrasound (US) is considered an affordable and available imaging technique that allows dynamic evaluation of anatomical structures, leading to subsequent examinations, thus providing an evaluation of the healing process of injured tendons and muscles. Although not considering the palmar face, carpal ultrasound has recently been described as a feasible imaging method for the assessment of tendinous structures of this highly complex joint (7).

The treatment of injuries caused by the insertion of the FCU tendon in humans has been reported to be conservative or surgical. The first consists of non-steroidal anti-inflammatory medications, splints, therapeutic strengthening, stretching programs, and steroidal injections. In contrast, surgical treatment is applied to patients who fail conservative management and has been reported as excision of the pathological tissue of the tendon (8).

In veterinary medicine, surgical treatment of injuries to the FCU tendon at its insertion has been reported in cases of avulsion from the accessory carpal bone providing suture of the damaged portion, splint in flexion of the carpus for 2 or 3 weeks, and restriction of activity for at least 6 weeks (2). Conservative management has been described as providing a padded splint for 3 weeks, oral administration of non-steroidal anti-inflammatory medications, and topical injections of steroids (3).

Although not described in the specific circumstances of FCU tendinopathy, the management of tendon lesions with regenerative medicine treatments appears to be a promising approach in human medicine. Among the regenerative strategies, the application of platelet-derived products, such as platelet-rich plasma (PRP) and platelet lysate (PL), has gained interest because of the concentrated content of bioactive factors, which is correlated to tissue healing properties. These factors include cytokines and growth factors, such as transforming growth factor-β (TGF-β), insulin-like growth factor 1 (IGF-1), platelet-derived growth factor (PDGF), vascular endothelial growth factor (VEGF), and basic fibroblast growth factor (bFGF), that by acting individually or in synergy can promote cell proliferation, cell migration, and recruitment along with angiogenesis, hence initiating a healing response within the damaged tissue (9–13). These products can be obtained with minimally invasive procedures and can be cryopreserved for multiple applications in a long-term perspective (9, 14). In Veterinary Medicine, the regenerative strategy to treat tendon injuries started to be studied in the nineties in the field of equine sports medicine, progressing during the years and gaining visibility in recent times also in the field of canine sports medicine, being described for the treatment of different orthopedic conditions in dogs (15, 16).

The canine flexor tendon has been studied as an animal model for flexor tendon healing and repair after different types of injuries for treatment in humans (17). Thus, the application of regenerative approaches for FCU tendinopathy in dogs may be a useful tool for providing preclinical data for future applications in human athletes.

In this study, a single case of FCU tendinopathy in a lure-coursing dog that was not responsive to conservative treatments and treated with multiple injections of autologous PRP and PL is described along with an ultrasonographic follow-up of the healing process 2 years after treatment.

2. Case description

2.1. Clinical history

A 7-year-old male Whippet competing in lure-coursing was referred to our hospital with a history of third-degree recurrent lameness to the right forearm. Symptoms were noticed 3 months before the clinical evaluation, and analog episodes were reported during the previous 3 years. Lameness was evident during walking, and it was worsening during sports activity as reported by the owner. No history of trauma was reported.

Conservative treatment with rest was previously suggested, and only a short leash walk was allowed. A padded palmar splint was administered and 4 mg/kg Carprofen was orally administered once a day for 2 weeks (18). No response to conservative treatment was achieved, and no improvements were observed at the time of the splint removal.

On clinical examination, the dog was found to be in good general health. Orthopedic examination showed third-degree right forelimb lameness, based on a previously reported orthopedic lameness evaluation system (19) (Table 1). Pain upon palpation of the caudal aspect of the right carpus and hyperextension of the same joint were detected. Swelling proximal to the accessory right carpal bone has also been previously reported. The range of motion of the carpal joint was bilaterally normal with mild pain reaction to right carpal hyperextension. The varus/valgus stress tests were non-pathologic in both thoracic limbs, with stable carpal joints.

2.2. Diagnostic imaging: Radiographic examination

Radiographic examination of both carpal joints on the mediolateral and craniocaudal standard views was performed without the need for anesthesia and showed soft tissue thickening

TABLE 1 Lameness evaluation system (19).

Grade	Degree of lameness
1	No lameness
2	Intermittent weight-bearing lameness
3	Permanent weight-bearing lameness
4	Non weight-bearing lameness

10.3389/fvets.2023.1003993

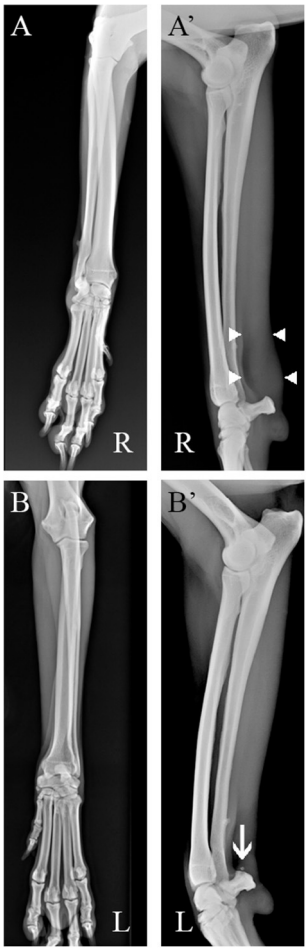

FIGURE 1
Radiographic assessment of the patient **(A)** Right side. Soft tissues thickening in the projection area of the FCU tendon, proximal to the accessory carpal bone [**(A')**, between white arrowheads] are detectable in the mediolateral standard view **(B, B')** Left side. Entensiophites are detectable at the proximal pole of the accessory carpal bone (white arrow). No changes were detected on both craniocaudal standard views.

in the projection area of the right FCU tendon, just proximal to the accessory carpal bone. Enthesophytes were detected at the proximal pole of the left accessory carpal. No changes were detected bilaterally on the craniocaudal standard view (Figure 1).

2.3. Diagnostic imaging: Ultrasonographic evaluation

Ultrasonographic evaluation of both carpal joints was performed using an 18 MHz linear transducer probe (MyLab SigmaVET, Esaote, Italy). For each assessment, a complete examination of the FCU tendon was performed using both longitudinal and transverse scans. The obtained images at each examination were evaluated and scored from 0 to 3 for two parameters, echogenicity score (ES) and fiber alignment score (FAS), modifying a previously published ultrasonographic assessment scale (20) (Table 2). The insertional portion of the right FCU tendon showed an ES of 3 compared to the contralateral one that had ES 1 without the presence of core lesions

TABLE 2 Ultrasound assessment system (20).

Parameter	Score system	Definition
Echogenicity	0	Normal echogenicity
	1	Mildly hypoechoic
	2	Moderate hypoechoicity
	3	Severe hypoechoicity
Fiber alignment	0	≥75% parallel fiber bundles at the insertion site
	1	50–74% parallel fiber bundles at the insertion site
	2	25–49% parallel fiber bundles at the insertion site
	3	≤25% parallel fiber bundles at the insertion site

and an FAS of 3 with <25% of parallel fiber bundles at the insertion on the accessory carpal bone. The contralateral group had FAS 1 with parallel fiber bundles at the insertion from 50 to 74%. Changes were detected in both the ulnar and humeral head of the tendon. Figure 2 shows the ultrasonographic appearance of the injured tendon at T0 and the evolution of the healing process during the PRP and PL administration program.

The clinical, radiographic, and ultrasonographic findings led to the presumptive diagnosis of FCU insertional tendinopathy. Because of the failure of conservative treatment, a regimen involving a PRP injection followed by two subsequent PL injections was suggested.

2.4. Treatment and follow-up

Blood samples (30 mL) were obtained from the jugular vein using an ACD-A 10% tube (BD Vacutainer®, BD, Italy). The treatment program consisted of three ultrasound-guided injections of autologous PRP prepared as previously described (21). Briefly, PRP was obtained following a double centrifugation tube method with first centrifugation at 2,800 rpm for 20 min and subsequently at 1,300 rpm for 15 min (TD4A-WS Desk Centrifuge, Drawell, China). All procedures were performed under sterile conditions. Three solutions of PRP (1 mL) were obtained at the end of the procedure. A blood count examination was performed on the first whole blood sample to assess the baseline platelet concentration of the dog, which was 165 K/μL. A subsequent blood count exam was made on the PRP sample having a platelet concentration of 1,029 K/μL assessing the achievement of a more than 5x platelet concentration for the final PRP preparation and a low concentration of white blood cells with 1,82 K/μL vs. 8,39 K/μL of the whole blood sample (BC-2800Vet, Mindray, China). Two of the three obtained PRP samples were frozen at −20°C and subsequently thawed for further administration of the PL (22).

On the day of the first injection (T0), an ultrasonographic examination was performed to assess the ultrasonographic appearance of the FCU tendons bilaterally. Before injection, no anesthesia was required, and the injection area, which was already clipped for ultrasonographic examination, was aseptically prepared. The treatment was inoculated in both heads of the right FCU tendon

10.3389/fvets.2023.1003993

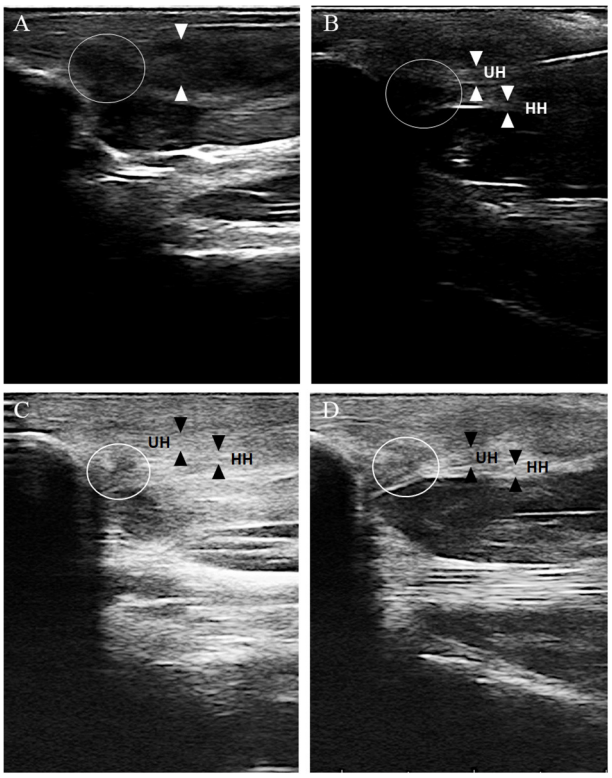

FIGURE 2
The ultrasonographic evolution of the healing process at different time points. **(A)** Ultrasonographic evaluation at T0, longitudinal scan. The ulnar and the humeral head of the right FCU tendon (between white arrowhead) can not be distinguished and shows ES 3 and FAS 3 (<25% parallel fiber bundles) at its insertional portion on the accessory carpal bone. A hypoechoic area with complete loss of fiber alignment is detected (white circle). **(B)** Ultrasonographic evaluation at T1, longitudinal scan. The ulnar (UH) and the humeral (HH) head of the right FCU tendon show at its insertional portion on the accessory carpal bone an ES 2 and a FAS 2 with parallel fiber bundles between 25 and 49%. The hypoechoic area with complete loss of fiber alignment is still visible (circle) and consistent with T0. **(C)** Ultrasonographic evaluation at T2, longitudinal scan. The ulnar (UH) and the humeral (HH) head of the right FCU tendon show at its insertional portion on the accessory carpal bone an ES 1 and a FAS 2 with parallel fiber bundles between 25 and 49%. The hypoechoic area with complete loss of fiber alignment is still visible but smaller in diameter (circle). **(D)** Ultrasonographic evaluation at T3, longitudinal scan. The ulnar (UH) and the humeral (HH) of the right FCU tendon show at is insertional portion on the accessory carpal bone an ES 1 and a FAS 1 with parallel fiber bundles between 50 and 75%. The hypoechoic area with complete loss of fiber alignment is still visible and consistent with T2 (white circle).

using a sterile 22G needle *via* ultrasonic guidance. Afterwards, only rest was prescribed, and short leash walks were allowed three times per day in the following 3 weeks.

The second and a third injection were performed at three (T1) and 6 weeks (T2), respectively, following the same protocol used for the first treatment and using the obtained PL (after freeze-thaw cycle) to continue the stimulation of the healing process.

3. Outcomes

The clinical and US outcome are summarized in Table 3.

TABLE 3 Clinical and US outcomes from T1 to T5.

Time	Clinical outcome	US outcome
T1	Decreased pain at palpation Decreased swelling of soft tissues Lameness score 2/4	ES 2 FAS 2
T2	No pain at palpation Mild swelling of soft tissues Lameness score 1/4	ES 1 FAS 1
T3	No pain at palpation No swelling of soft tissues Lameness score 0/4	ES 1 FAS 1
T4	No pain at palpation No swelling of soft tissues Lameness score 0/4	ES 1 FAS 1
T5	No pain at palpation No swelling of soft tissues Lameness score 0/4	ES 1 FAS 1

ES, Echogenicity score; FAS, Fiber alignment score; T1, week three; T2, week six; T3, week twelve; T4, week fifty-two, T5, week on-hundred and four; US, ultrasonographic imaging.

3.1. Clinical evaluation

Clinical assessments were performed every 3 weeks starting from the day of the first injection to the day of the last injection and every 12 weeks thereafter. In the present study, we report the clinical outcomes on the day of the first injection (T0), at three (T1), six (T2), twelve (T3), fifty-two (T4) and one-hundred-and-four (T5) weeks.

Before treatment, the dog presented with third-degree (3/4) right forelimb lameness, swelling of the palmar surface of the carpal joint, and pain on palpation of the affected region.

At T1, pain on palpation and swelling of the carpal region were slightly decreased; moreover, a reduction in the degree of lameness was observed (grade 2/4). The second injection was administered on the same day and it consisted of PL. At T2, the last PL injection was administered, and no pain on palpation was detected, with mild swelling of the carpal region. A grade 1/4 of lameness was recorded. At T3, 3 months after the first injection, no pain on palpation or swelling of soft tissues was detected, and grade 0/4 lameness was observed. T4 and T5 clinical examinations were consistent with T3 findings, with a complete restoration of forelimb function and return to sport. No reinjuries were reported.

3.2. Ultrasound evaluation

Ultrasound evaluation images are shown in Figure 2. At T0, before treatment, the US evaluation showed an ES 3 compared to the contralateral one that had ES 1 without detected core lesions and an FAS 3 with <25% of parallel fiber bundles at the insertion on the accessory carpal bone. The contralateral group had FAS 1 with parallel fiber bundles at the insertion from 50 to 74%. Changes were detected in both the ulnar and humeral head of the tendon.

At T1, the US examination was mildly improved with ES 2 and FAS 2 compared to the contralateral one, which was still consistent with T0. Doppler ultrasound examination revealed the presence of a small amount of neovascularization. At T2, the US examination showed additional improvement with ES 1 and FAS 1 compared to the contralateral limb: T3, T4, and T5. US evaluation showed ES 1

and FAS 1 with the same ultrasonographic appearance for the FCU tendons of both forelimbs.

4. Discussion

FCU tendinopathy is poorly described in veterinary literature and rarely reported as a cause of forelimb lameness in pet dogs but is listed among the typical injuries of lure-coursing dogs (2). Its diagnosis is and will remain challenging as long as the disease continues to be considered underestimated and underrepresented. Working and sporting dogs are prone to FCU tendon injuries due to the repeated stresses they undergo during performance, leading to chronic tendon strain injuries. The etiology of FCU tendinopathy is poorly described in veterinary sports medicine, whereas in human medicine, it is thought to be related to repeated strain activity and overuse due to chronic repetitive movements (23). Regarding other pathologies involving tendinous structures, misdiagnosis or unsuccessful treatments can lead to a greater chance of re-injury, thus, becoming potentially career ending for canine athletes.

In the One Health scenario, the investigation of the treatment of flexor tendon diseases in dogs can be useful for the collection of preclinical data. The flexor tendon system of dogs has often been studied as an animal model for the investigation of the flexor tendon healing process, and the results have already been applied in human medicine (24). Moreover, the regenerative approach seems to be promising for tendon pathology management in both veterinary and human medicine, since PRP is currently the most exploited strategy in human clinical practice to provide a regenerative stimulus for tendon healing. In veterinary medicine, especially in canine athletes, the administration of PRP in combination with intratendinous injection of mesenchymal stem cells has demonstrated clinical benefits in other tendinopathies with minimal invasiveness (25).

Nevertheless, the lack of standardization of PRP administration modality represents an important aspect to evaluate in both human and veterinary approaches (26).

In the present case report, an ultrasound-guided peritendinous injection of autologous PRP followed by two further injections of PL was administered for the treatment of chronic right FCU tendinopathy in a lure-coursing dog. The patient presented with chronic lameness and ultrasonographic signs of FCU tendinopathy that developed during sporting activity and was unresponsive to previously administered conservative standard treatments such as rest, splint immobilization, and NSAIDs oral administration. The lack of response to the conservative approach and the risk to develop gastro-intestinal tract problems with a long-term treatment with NSAIDs were the two pressing elements of the management of the injury. Thus, the peritendinous injection of 1 mL of autologous PRP, followed by two further administrations of 1 mL per injection of PL, was the novel approach of choice. Different studies have shown the beneficial effects of PRP and PL on tendon healing in veterinary medicine (27–33). The positive action has to be ascertained to the concentrated growth factors and cytokines present in PRP/PL, which contribute to tenocytes recruitment and proliferation; moreover, they stimulate injured tenocytes to secrete angiogenic factors (34, 35).

The results were beneficial for the dog, as the applied therapeutic program resulted in the disappearance of lameness and ultrasonographic improvement of fiber alignment along with echogenicity of the injured tendon. Moreover, during the treatment and follow-up period, the patient did not suffer from any re-injury episodes; after T4, the dog returned to the same competition level before injury. The ability to return to sports could suggest restoration of the biomechanical properties of the tendon after the injections to an adequate level that allowed the dog to return to competition. This might be related to the supposed capability of low WBC PRP to support the production of collagen type I (COL1) fibers during the tendon healing process. COL1 is the major component of fibrillar collagen in tendons and is responsible for linear fiber alignment. On the contrary collagen type III, that is synthetized during primary tendon healing process, leads to the formation of disorganized scar tissue, which is more prone to re-injury in cases of excess load (36). The subsequent administration of PL at an interval of 3 weeks might have prolonged the activation of the healing process, leading to a physiological grade of fiber alignment and a good improvement in symptoms. Finally, repeated injections of autologous PRP and PL for the treatment of FCU tendinopathy in dogs did not provoke any adverse or immune reaction to the patient, supporting the safety of the treatment of choice.

The US observations of the process are another important aspect of the present case report because, to our knowledge, no studies have been published on US evaluation of the healing process of FCU tendinopathy. Musculoskeletal ultrasonography is an imaging technique that has been used and validated for the diagnosis of several tendinopathies in both humans and dogs. It provides a non-invasive diagnosis and allows for feasible and cost-effective consecutive examinations to assess the response to treatment; moreover, it is useful for evaluating the changes in size, shape, and echogenicity of the tendon, avoiding patient sedation (37, 38). Ultrasonographic evaluation of the healing process and prolonged US follow-up over time led to a controlled progression of the fiber alignment, which is an important element in the return-to-play decision-making process. Thus, as in human and veterinary medicine, high-frequency ultrasound imaging can be considered a useful tool for planning a return-to-play evaluation protocol for FCU injury treatment.

To our knowledge, no studies on the successful treatment of a lure-coursing dog's FCU tendinopathy by multiple ultrasound-guided PRP and PL administration have previously been published. The feasibility of this therapeutic approach could be considered satisfactory and safe in this case, as the dog returned to competition without any adverse treatment reactions. The ultrasonographic evaluation of the healing process played a pivotal role in a return-to-play oriented approach, and our results might be considered encouraging for the study of a more standardized application protocol of PRP administration for canine athletes, helping to collect preclinical data for human research.

Data availability statement

The raw data supporting the conclusions of this article will be made available by the authors, without undue reservation.

Ethics statement

Ethical review and approval was not required for the animal study because the owner of the dog signed a written consent. Written

informed consent was obtained from the owners for the participation of their animals in this study.

Author contributions

AF and ME followed the clinical case and performed the PRP and PL injections. MP and LM contributed to study design and supervised the study. ME, EC, and LM wrote the original draft of the manuscript. AF, ME, EC, LM, and MP revised and edited the manuscript. All authors read and approved the final manuscript.

Acknowledgments

The authors want to thank Editage (www.editage.cn) for English language editing.

Conflict of interest

The authors declare that the research was conducted in the absence of any commercial or financial relationships that could be construed as a potential conflict of interest.

Publisher's note

All claims expressed in this article are solely those of the authors and do not necessarily represent those of their affiliated organizations, or those of the publisher, the editors and the reviewers. Any product that may be evaluated in this article, or claim that may be made by its manufacturer, is not guaranteed or endorsed by the publisher.

References

1. Hermanson JW. The muscular system. In: Evans HE, de Lahunta A, editors *Miller's Anatomy of the Dog*. 4th ed. St. Louis: Elsevier Saunders (2013). p. 250–1.

2. Gary Brown S. Unique veterinary problems of coursing dogs. In: Bloomberg MS, Dee JF, Taylor RA, editors Canine Sports Medicine and Surgery. Philadelphia: Saunders (1998). p. 432–3.

3. Kuan SY, Smith BA, Fearnside SM, Black AP, Allan GS. Flexor carpi ulnaris tendonopathy in a Weimaraner. *Aust Vet J.* (2007) 85:401–4. doi: 10.1111/j.1751-0813.2007.00187.x

4. Howse C. Wrist injuries in sport. *Sports Med.* (1994) 17:163–75. doi: 10.2165/00007256-199417030-00003

5. Olchowy C, Łasecki M, Zaleska-Dorobisz U. Wrist ultrasound examination - scanning technique and ultrasound anatomy. Part 1: dorsal wrist. *J Ultrason.* (2015) 15:172–88. doi: 10.15557/JoU.2015.0015

6. Olchowy C, Soliński D, Łasecki M, Dabrowski P, Urban S, Zaleska-Dorobisz U. Wrist ultrasound examination - scanning technique and ultrasound anatomy. Part 2: Ventral wrist. *J Ultrason.* (2017) 17:123–8. doi: 10.15557/JoU.2017.0018

7. González-Rellán S. Fdz-de-Trocóniz P, Barreiro A. Ultrasonographic anatomy of the dorsal region of the carpus of the dog. *Vet Radiol Ultrasound.* (2021) 62:591–601. doi: 10.1111/vru.13003

8. Budoff JE, Kraushaar BS, Ayala G. Flexor carpi ulnaris tendinopathy. *J Hand Surg Am.* (2005) 30:125–9. doi: 10.1016/j.jhsa.2004.07.018

9. Soares CS, Babo PS, Reis RL, Carvalho PP, Gomes ME. Platelet-derived products in Veterinary Medicine: a new trend or an effective therapy? *Trends Biotechnol.* (2021) 39:225–43. doi: 10.1016/j.tibtech.2020.07.011

10. Alves R, Grimalt R. A review of platelet-rich plasma: history, biology, mechanism of action, and classification. *Ski Appendage Disord.* (2018) 4:18–24. doi: 10.1159/000477353

11. Hudgens JL, Sugg KB, Grekin JA, Gumucio JP, Bedi A, Mendias CL. Platelet-rich plasma activates proinflammatory signaling pathways and induces oxidative stress in tendon fibroblasts. *Am J Sports Med.* (2016) 44:1931–40. doi: 10.1177/0363546516637176

12. Carr BJ. Platelet-rich plasma as an orthobiologic: clinically relevant considerations. *Vet Clin North Am - Small Anim Pract.* (2022) 52:977–95. doi: 10.1016/j.cvsm.2022.02.005

13. Andia I, Rubio-Azpeitia E, Maffulli N. Platelet-rich plasma modulates the secretion of inflammatory/angiogenic proteins by inflamed tenocytes. *Clin Orthop Relat Res.* (2015) 473:1624–34. doi: 10.1007/s11999-015-4179-z

14. Kaux JF, Libertiaux V, Dupont L, Colige A, Denoël V, Lecut C, et al. Platelet-rich plasma (PRP) and tendon healing: comparison between fresh and frozen-thawed PRP. *Platelets.* (2020) 31:221–5.

15. Camargo Garbin L, Lopez C, Carmona JU, A. critical overview of the use of platelet-rich plasma in equine medicine over the last decade. *Front Vet Sci.* (2021) 8:641818. doi: 10.3389/fvets.2021.641818

16. Canapp SO Jr, Leasure CS, Cox C, Ibrahim V, Carr BJ. Partial cranial cruciate ligament tears treated with stem cell and platelet-rich plasma combination therapy in 36 dogs: a retrospective study. *Front Vet Sci.* (2016) 3:112. doi: 10.3389/fvets.2016.00112

17. Shen H, Jayaram R, Yoneda S, Linderman SW, Sakiyama-Elbert SE, Xia Y, et al. The effect of adipose-derived stem cell sheets and CTGF on early flexor tendon healing in a canine model. *Sci Rep.* (2018) 8:11078. doi: 10.1038/s41598-018-29474-8

18. Borer LR, Peel JE, Seewald W, Schawalder P, Spreng DE. Effect of carprofen, etodolac, meloxicam, or butorphanol in dogs with induced scute synovitis. *Am J Vet Res.* (2003) 64:1429–37. doi: 10.2460/ajvr.2003.64.1429

19. Taroni M, Cabon Q, Fèbre M, Cachon T, Saulnier N, Carozzo C, et al. Evaluation of the effect of a single intra-articular injection of allogeneic neonatal mesenchymal stromal cells compared to oral non-steroidal anti-inflammatory treatment on the postoperative musculoskeletal status and gait of dogs over a 6-month period after tibial plateau leveling osteotomy: a pilot study. *Front Vet Sci.* (2017) 4:83. doi: 10.3389/fvets.2017.00083

20. Depuydt E, Broeckx SY, Van Hecke L, Chiers K, Van Brantegem L, Van Schie H, et al. The evaluation of equine allogeneic tenogenic primed mesenchymal stem cells in a surgically induced superficial digital flexor tendon lesion model. *Front Vet Sci.* (2021) 8:641441. doi: 10.3389/fvets.2021.641441

21. Perazzi A, Busetto R, Martinello T, Drigo M, Pasotto D, Cian F, et al. Description of a double centrifugation tube method for concentrating canine platelets. *BMC Vet Res.* (2013) 9:146. doi: 10.1186/1746-6148-9-146

22. Klatte-Schulz F, Schmidt T, Uckert M, Scheffler S, Kalus U, Rojewski M, et al. Comparative analysis of different platelet lysates and platelet rich preparations to stimulate tendon cell biology: in vitro study. *Int J Mol Sci.* (2018) 19:212. doi: 10.3390/ijms19010212

23. Knobloch K, Gohritz A, Spies M, Vogt PM. Neovascularisation in flexor carpi ulnaris tendinopathy: novel combined sclerosing therapy and eccentric training of the forearms in athletics' wrist pain. *BMJ Case Rep.* (2009) 2009:bcr08.2008.0714. doi: 10.1136/bcr.08.2008.0714

24. Zhang T, Lu CC, Reisdorf RL, Thoreson AR, Gingery A, Moran SL, et al. Revitalized and synovialized allograft for intrasynovial flexor tendon reconstruction in an in vivo canine model. *J Orthop Res.* (2018) 36:2218–27. doi: 10.1002/jor.23889

25. Dias IE, Cardoso DF, Soares CS, Barros LC, Viegas CA, Carvalho PP, et al. Clinical application of mesenchymal stem cells therapy in musculoskeletal injuries in dogs-a review of the scientific literature. *Open Vet J.* (2021) 11:188–202. doi: 10.5455/OVJ.2021.v11.i2.2

26. Filardo G, Di Matteo B, Kon E, Merli G, Marcacci M. Platelet-rich plasma in tendon-related disorders: results and indications. *Knee Surg Sports Traumatol Arthrosc.* (2018) 26:1984–99. doi: 10.1007/s00167-016-4261-4

27. Brossi PM, Moreira JJ, Machado TS, Baccarin RY. Platelet-rich plasma in orthopedic therapy: a comparative systematic review of clinical and experimental data in equine and human musculoskeletal lesions. *BMC Vet Res.* (2015) 11:98. doi: 10.1186/s12917-015-0403-z

28. Scala M, Lenarduzzi S, Spagnolo F, Trapasso M, Ottonello C, Muraglia A, et al. Regenerative medicine for the treatment of teno-desmic injuries of the equine. A series of 150 horses treated with platelet-derived growth factors *in vivo*. *Brooklyn.* (2014) 28:1119–24.

29. Bosch G, Van Schie HTM, De Groot MW, Cadby JA, Van De Lest CHA, Barneveld A, et al. Effects of platelet-rich plasma on the quality of repair of mechanically induced core lesions in equine superficial digital flexor tendons: a placebo-controlled experimental study. *J Orthop Res.* (2010) 28:211–7. doi: 10.1002/jor.20980

30. Geburek F, Gaus M, van Schie HTM, Rohn K, Stadler PM. Effect of intralesional platelet-rich plasma (PRP) treatment on clinical and ultrasonographic parameters in equine naturally occurring superficial digital flexor tendinopathies

- a randomized prospective controlled clinical trial. *BMC Vet Res.* (2016) 12:191. doi: 10.1186/s12917-016-0826-1

31. Schulz KS, Ash KJ, Cook JL. Clinical outcomes after common calcanean tendon rupture repair in dogs with a loop-suture tenorrhaphy technique and autogenous leuko-reduced platelet-rich plasma. *Vet Surg.* (2019) 48:1262–70. doi: 10.1111/vsu.13208

32. Garrett KS, Bramlage LR, Spike-Pierce DL, Cohen ND. Injection of platelet- and leukocyte-rich plasma at the junction of the proximal sesamoid bone and the suspensory ligament branch for treatment of yearling thoroughbreds with proximal sesamoid bone inflammation and associated suspensory ligament branch desmitis. *J Am Vet Med Assoc.* (2013) 243:120–5. doi: 10.2460/javma.243.1.120

33. Bonilla-Gutiérrez AF, López C, Carmona JU. Regenerative therapies for the treatment of tenodesmic injuries in horses. *J Equine Vet Sci.* (2019) 73:139–47. doi: 10.1016/j.jevs.2018.12.010

34. Zhou Y, Wang JH-C, PRP. Treatment efficacy for tendinopathy: a review of basic science studies. *Biomed Res Int.* (2016) 2016:1–8. doi: 10.1155/2016/9103792

35. Sundman EA, Cole BJ, Karas V, Della Valle C, Tetreault MW, Mohammed HO, et al. The anti-inflammatory and matrix restorative mechanisms of platelet-rich plasma in osteoarthritis. *Am J Sports Med.* (2014) 42:35–41. doi: 10.1177/0363546513507766

36. McCarrel TM, Minas T, Fortier LA. Optimization of leukocyte concentration in platelet-rich plasma for the treatment of tendinopathy. *J Bone Joint Surg Am.* (2012) 94:e143. doi: 10.2106/JBJS.L.00019

37. Delzell PB, Tritle BA, Bullen JA, Chiunda S, Forney MC. Clinical utility of high-frequency musculoskeletal ultrasonography in foot and ankle pathology: how ultrasound imaging influences diagnosis and management. *J Foot Ankle Surg.* (2017) 56:735–9. doi: 10.1053/j.jfas.2017.01.052

38. Canapp SO Jr, Canapp DA, Ibrahim V, Carr BJ, Cox C, Barrett JG. The use of adipose-derived progenitor cells and platelet-rich plasma combination for the treatment of supraspinatus tendinopathy in 55 dogs: a retrospective study. *Front Vet Sci.* (2016) 3:61. doi: 10.3389/fvets.2016.00061

frontiers | Frontiers in Veterinary Science

TYPE Review
PUBLISHED 17 March 2023
DOI 10.3389/fvets.2023.1032835

OPEN ACCESS

EDITED BY
Albert Earl Jergens,
Iowa State University, United States

REVIEWED BY
Jorge A. Piedrahita,
North Carolina State University, United States
Dipak Kumar Sahoo,
Iowa State University, United States

*CORRESPONDENCE
Louis C. Penning
✉ l.c.penning@uu.nl

SPECIALTY SECTION
This article was submitted to Veterinary Regenerative Medicine, a section of the journal Frontiers in Veterinary Science

RECEIVED 31 August 2022
ACCEPTED 28 February 2023
PUBLISHED 17 March 2023

CITATION
Penning LC and van den Boom R (2023) Companion animal organoid technology to advance veterinary regenerative medicine. *Front. Vet. Sci.* 10:1032835. doi: 10.3389/fvets.2023.1032835

Companion animal organoid technology to advance veterinary regenerative medicine

Louis C. Penning* and Robin van den Boom

Department of Clinical Sciences, Faculty of Veterinary Medicine, Utrecht University, Utrecht, Netherlands

First year medical and veterinary students are made very aware that drugs can have very different effects in various species or even in breeds of one specific species. On the other hand, the "One Medicine" concept implies that therapeutic and technical approaches are exchangeable between man and animals. These opposing views on the (dis)similarities between human and veterinary medicine are magnified in regenerative medicine. Regenerative medicine promises to stimulate the body's own regenerative capacity *via* activation of stem cells and/or the application of instructive biomaterials. Although the potential is enormous, so are the hurdles that need to be overcome before large scale clinical implementation is realistic. It is in the advancement of regenerative medicine that veterinary regenerative medicine can play an instrumental and crucial role. This review describes the discovery of (adult) stem cells in domesticated animals, mainly cats and dogs. The promise of cell-mediated regenerative veterinary medicine is compared to the actual achievements, and this will lead to a set of unanswered questions (controversies, research gaps, potential developments in relation to fundamental, pre-clinical, and clinical research). For veterinary regenerative medicine to have impact, either for human medicine and/or for domesticated animals, answering these questions is pivotal.

KEYWORDS

organoid, regenerative medicine, intestine, liver, disease modeling, companion animals, horse

Introduction

In ancient Egypt cats were considered to be sacred animals, demonstrated by the fact that mummified cats have been found near mummified people. When dogs became "man's best friend" is unclear but we know that the famous French philosopher Voltaire wrote "*c'est le meilleur ami que puisse avoir l'homme*," which translates as "the best friend man can possibly have" in the eighteenth century. The history of interactions between cats and dogs and man has some defining elements. Since the first genetic evidence for an Eastern Asian origin was published in 2002 the origin and timing of canine domestication has been heavily debated, as a result of novel analytical and archeological findings (1–13). In addition to domestication, two more recent factors have been the driving force behind feline and canine genetic research and high-quality medical care for pets. The first was the selective inbreeding of these animals, especially dogs, that started in the middle of the nineteenth century, seeking to optimize specific physical and behavioral traits needed to perform as working animals, as was common in those times (14). A second stimulus was the change in the appreciation of pets and horses, they became members of the family. Combined with a much-improved financial situation after the end of the Second World War, this led to an enormous boost in initiatives to bring veterinary medical care of pets to a very high level. Consequently, veterinary (medical) knowledge and technology available for diagnostics

and treatment specifically for pets, has become very comparable to that available for man. As a result, the "One Medicine" concept arose which implies that therapeutic and technical approaches are exchangeable between man and animals and can be used for their mutual benefit. Here we focus on adult stem cell-biology and organoid technology in veterinary Regenerative Medicine (RM) within the "One Medicine" concept. This review focuses on adult, organ-specific stem cells and the organoid cultures derived from them and the implications for disease modeling and potentially cell/organ replacement. For a recent review of farm and domestic animal organoids in food safety and public health (zoonotic diseases) readers are referred elsewhere (15).

Research strategy

The latest PubMed search was performed on Monday September 19th. Searching for organoid* AND (canine OR equine OR feline OR horse* OR dogs OR cats) revealed 457 hits (see Table 1). Inclusion of a time period from January 1st 2005, years before LGR5 was established as a hallmark of epithelial stem cells (16) and the creation of organoids from single LGR5+-cells (17) reduced the number to 91 hits and as such this Pubmed search revealed only organoids as defined by Lancaster and Knoblich (18). After individual analysis of these 91 papers, some were discarded for several reasons, most often the fact that the research had been conducted using the Madine Darby Canine Kidney cell line. This selection resulted in fewer than 50 papers, all of which are included in this review. To visualize the negative selection in this last round, the main reason for exclusion from this review is presented in Supplementary Table 1. A similar research strategy with (regenerative medicine) AND (canine OR equine OR feline OR horse* OR dogs OR cats) and further selection based on abstracts and content produced a very similar list of publications.

Furthermore, we restricted our selection to LGR5+ or Wnt-signaling dependent adult stem cell derived organoids because of the crucial role of LGR5 and Wnt in the culture of adult epithelial stem cells (19).

TABLE 1 Pubmed search strategy (latest search Monday September 19th, 2022) selection.

Organoid* AND (canine OR equine OR feline OR horse* OR dogs OR cats)	457 hits
# plus from January 1rts 2005 onwards	91 hits
Individual selection (see Supplementary Table 1)	38 hits

Is stem cell biology in veterinary medicine different from that in human medicine?

There does not appear to be an undisputed definition of "regenerative medicine" (RM) but, at the very least, it includes a process in which damaged or lost specialized tissue is artificially replaced by the proliferation of undamaged specialized cells. This definition is species independent and the inclusion of the word artificially discriminates RM from naturally occurring processes such as axial regeneration in amphibians, or antler regrowth in ungulates. In cell-mediated regenerative medicine stem cells, either pluripotent stem cells or adult stem cells (ASCs), are the workhorses of regeneration.

Adult (or organ specific) stem cells have a limited differentiation potential, restricted to (some) cell types of the organ in which they reside. Their activity is mediated by the so-called stem cell niche. The stem cell niche is a functional and organizational structure that provides signaling cues for cellular maintenance in a quiescent or toward an activation status. These stem cells are responsible for the replacement of cells during physiological cellular homeostasis, such as the rapid renewal of the intestinal lining (20). In addition, these cells become activated in case of severely hampered replacement of damaged cells, as is the case in chronic liver failure (21).

In vitro experiments require cells that resemble the physiology that one is interested in. One of the drawbacks of established cell lines is that these are often tumor-derived, and as such do not directly reflect physiological processes. On top of that, their oncogenic potential hampers applications in regenerative medicine. ASCs can overcome these limitations because ASCs can be harvested and cultured form healthy and diseased tissues. The culture of ASCs has skyrocketed since organoid cultures were developed (22). By definition, organoids are "*a collection of organ-specific cell types that develops from stem cells or organ progenitors and self-organizes through cell sorting and spatially restricted lineage commitment in a manner similar to in vivo*" (18). Three aspects of this definition deserve attention: (i) the cells of origin can be either pluripotent or ASC, (ii) not all cell types of the represented/donor organ need to be present or arranged as in the original architectural pattern within an organoid, (iii) no functional similarities with the represented/donor organ are mentioned. Organoid technology received a boost following the landmark discovery and subsequent identification of small intestine and colon stem cells which express the marker gene product LGR5 (16). Two years later single sorted LGR+ stem cells were shown to self- organize into crypt-villus like intestinal organoids (17). The transmembrane protein LGR5, involved in Wnt-signaling, turned out to be a classic adult stem cell marker for epithelial cells (18, 20).

Given that the regulatory signaling pathways in stem cell biology are highly evolutionary conserved it is expected that the creation of organoids from non-human or rodent species would be an easy task. However, the number of papers describing companion animal derived organoids is limited compared to mouse and human organoids [cfr ref. (22) with Table 1]. Tools to study species specific ASCs might be the culprit. The lack of convenient and validated tools to detect LGR5 expression in canine and feline tissues hampered the rapid extrapolation of data from man and mouse to veterinary biomedicine. Immunohistochemical staining of canine hair follicles showed immunopositive cells, but the specificity of the antibody was not confirmed with recombinant proteins (23). Rabbit polyclonal antibodies against LGR5 were used in a study on canine epithelial skin tumors (24), the overt cytoplasmic staining is in line with staining with validated antibodies in human cancers. This however is not sufficient selective to sort individual cells based

on plasmamembraneous LGR5-expression. Therefore, experiments with single cell sorted LGR5+ human and rodent ASCs cannot be repeated in pets and horses. This drawback forced researchers in veterinary medicine to use culture conditions in which the ASCs were specifically selected based on the presence or absence of (often human) growth factors. In order to advance veterinary regenerative medicine and its crucial role in the "One-Medicine" concept, knowledge, and appreciation of the (inter-)species differences are of utmost importance.

Organoids implemented in disease modeling and transplantation/replacement studies

Adult stem cells reside in an organ and can give rise to several of the cell types of that organ. The potential applications for adult stem cells in veterinary medicine include disease modeling and transplantation (Figure 1). These two applications come with their own specific points-of-concern, which can be partially addressed by means of organoid technology.

Disease modeling

The importance of organoids in disease modeling is based on the fact that disease specific organoids can be created from biopsies (or fresh cadavers) from individual patients.

Moreover, a potential disease-causing mutation can be corrected, allowing cause-effect studies. The artificial culture conditions, with excess growth factor(s), oxygen and other nutrients, and the lack of interaction with other cell types (stem cell niche), means that some caution should be exercised when *in vitro* results are compared to *in vivo* data.

Transplantation/replacement

Organ donation in veterinary medicine comes with ethical, logistical, and financial challenges. More realistic seems the application of organoid technology in veterinary medicine to provide predictive large animal models for human transplantations, given the similar size, environmental exposure, and life expectancy of pets and man, which are far more similar than rodents and man. This technology can be applied in a cross-species, intra-species or even autologous fashion (25, 26).

Feline and canine organoids derived from adult stem cells

Intestinal organoids

In 2009 a study was presented in which an ileal derived organoid transplantation was performed in six Beagle dogs (25). Little information was provided on the cellular composition of the transplanted organoids, and autologous transplantation did not lead to any neomucosa formation, irrespective of the location of the implant, in omentum or debrided intestine. In contrast, allogeneic organoids derived from fetal intestine resulted in mucosa formation only at the omentum implantation site. This positive result was found in three out of four dogs. It seems that no further investigations along these lines of research have been reported subsequently, although the search for canine intestinal organoids has continued.

A more detailed description of the establishment of intestinal organoids from domesticated animals was presented in 2017 (27). The long-term culture of intestinal organoids from various mammals, including cats, dogs, cows, horses, pigs and sheep was shown to depend on Wnt3a, R-spondin, and Noggin (27). This important observation confirmed the conservation of the signaling molecules needed for expansion of intestinal organoids. Quantitative RT-PCR results indicated *LGR5* mRNA expression, which confirms the importance of Wnt and R-spondin in the culture media. Unfortunately, the authors did not elaborate on the cellular differentiation of the stem cells toward other crypt and villus cell types.

Differentiation and more functional studies on canine intestinal organoids were centered along inflammatory bowel disease and intestinal (28–34). In line with the group's interest in understanding gastrointestinal diseases, intestinal organoids were cultured from healthy dogs, and dogs suffering from inflammatory bowel disease and intestinal adenocarcinomas. Crypt-villus structured organoids were derived from duodenal, jejunal, ileal, and colon regions, expressing markers for stem cells (*LGR5* mRNA in the bottom of the crypt), enteroendocrine cells, tuft cells and Paneth cells. Furthermore, the authors demonstrated the presence of a functional cystic fibrosis transmembrane conductance regulator (CFTR) and uptake of the parasite *Ascaris suum* derived vesicles (30). Inflammatory bowel disease was modeled in these canine colon organoids by means of LPS stimulation, which resulted in the differential expression of several tumor-associated genes, suggesting a mechanistic link between chronic inflammation and carcinogenesis (31).

Organoids derived from intestinal biopsies were used to investigate the differences in tight junction protein expression between dogs with protein losing enteropathy and healthy dogs (32). *In situ* hybridization (ISH), a way to measure mRNA expression in tissue slides, clearly showed enhanced *zonulin-1* mRNA levels in affected dogs compared to healthy dogs. As zonulin-1 negatively affects the cell-cell junctions, this observation explains the enhanced permeability (leakage) of the epithelial barrier which results in protein losing. From a stem cell marker perspective, this paper showed strongly elevated *LGR5* mRNA levels in enteropathic organoids. RNA-ISH circumvented the practical problem associated with the lack of validated anti LGR5-antibodies, by measuring mRNA levels rather than protein expression.

Together these in-depth molecular and functional descriptions of canine intestinal organoids pinpointed the important applications of organoid technology in disease modeling. The intestinal organoids form crypt-villus structures with the intestinal lumen on the inside. As such, this biologically relevant architecture hampers studies on transepithelial transport. To facilitate such

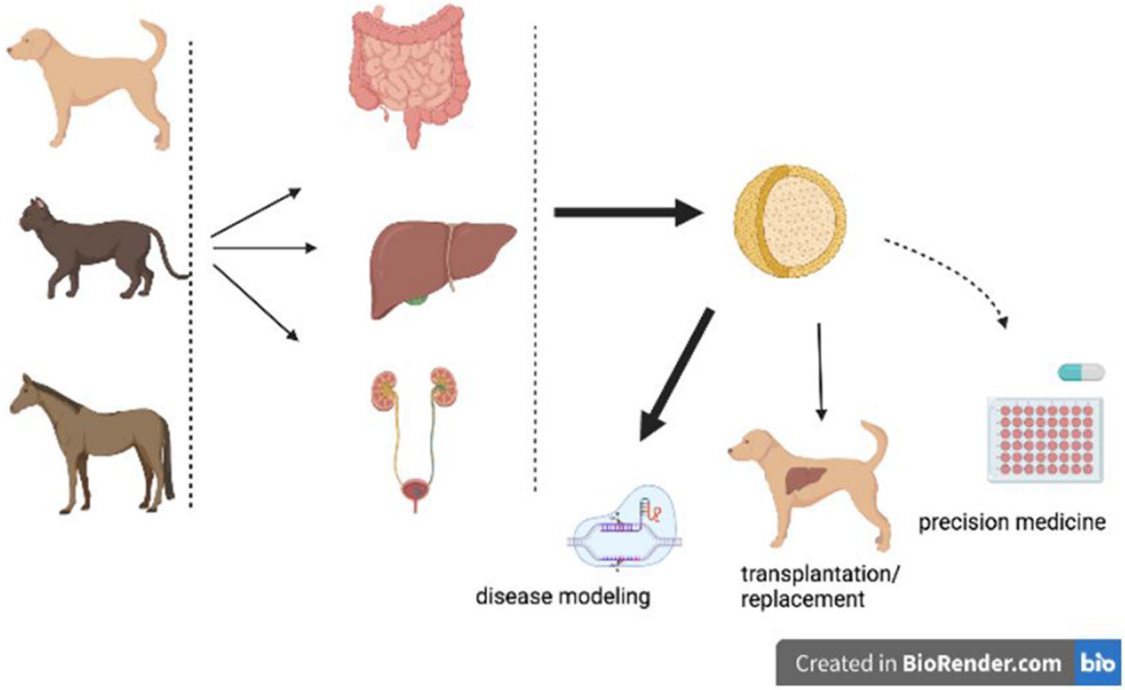

FIGURE 1
Potential and current applications of organoids in veterinary medicine. Organoids derived from various canine, feline, or equine organs can be used for disease modeling, precision medicine, or organ transplantations/replacement. Disease modeling is performed (fat black arrow), transplantations based on organoid technology is in a pre- clinical phase (thin black arrow), whereas precision medicine is on the horizon (dashed arrow).

studies and to measure microbial interactions the colon-derived organoids were cultured on a porous membrane in a polarized 2D-fashion (33). Cellular differentiation occurred, tight- and glycocalyx- junctions were formed, and the polarized cells expressed functional P-glycoprotein at the apical membrane. This adapted organoid system is deemed very well-suited for fundamental transport studies and disease modeling. A detailed protocol was presented on how to use canine organoids in a dual-chamber system permitting other researchers to create a similar experimental set-up for their own disease or species of interest (34).

Around the same time an international collaboration established and characterized long- term canine intestinal organoids derived from duodenum, jejunum, and colon (35). Although detailed gene expression analysis on cellular differentiation was described, and novel differentiation media compositions were provided, functional studies as presented by Allenspach's group were missing. This showed that small adaptations in the composition of organoid culture media need to be carefully described and species differences indicated.

Finally, one publication described feline intestinal organoids from ileum and colon aiming to study viral infections (36). Feline coronavirus infected only the colon-derived organoids, while the ileum-derived organoids remained uninfected.

All of the above studies investigated one or more aspects of the intestine using organoid technology. Little information is available to provide a more global analysis and comparison of gene expression levels and functional studies in relation to the most often used Caco-2 cell line (37). Both ATAC-Seq (open chromatin sequences) and RNA- Seq (expression analysis) was performed in human intestinal organoids and compared to Caco-2 cells. While the organoids' gene expression was enriched for transport systems and responses to oxidative stress, the Caco-2 cells highly expressed genes related to extracellular matrices. Interestingly, intestinal organoids reflected transport activity similar to the tissue of origin, even better then Caco-2 cells (38). Such in-depth molecular and functional studies are lacking in veterinary medicine, but the data from human intestinal organoids are promising. It remains to be seen how veterinary intestinal organoids can replace animals in pharmacological and toxicological studies related to intestinal tissue.

In summary (Table 2), canine and feline intestinal organoids can be created from most regions of the GI-tract and adaptation of the 3D-culture to a 2D system (cell polarization on a porous membrane) makes these cells ideally suited for disease modeling, especially because organoids can be created form biopsy material derived from animals with proven intestinal disorders.

Liver organoids

The first description of canine liver organoids was published in 2015 when hepatic stem cell derived organoids from COMMD1-deficient dogs were characterized (41). This paper reported the development of canine (liver) organoids and the authors presented

TABLE 2 Summary of publications on intestinal organoids from dogs, cats, or horses.

References	Species	Marker	Aim/disease	Remarks	Proliferation
Agopian et al. (25)	Dog	N/A	Transplantation	Neomucosal formation	N/A
Powell and Behnke (27)	Numerous	LGR5	Disease modeling	Proliferation not differentiation	Wnt3a, R-Spo-3, and Noggin
Mochel et al. (28)	Numerous	N/A	Are pets preclinical models?	Commentary paper	N/A
Kopper et al. (29)	Numerous	N/A	Model for IBD?	Review paper	N/A
Chandra et al. (30)	Dog	a.o. LGR5	Pre-clinical model	Functional swelling assay	Wnt3a, R-Spo-1, and Noggin
Sahoo et al. (31)	Dog	PROM1 and OLFM4	IBD model	Gene expression after LPS stimulus	Wnt3a, R-Spo-1, and Noggin
Allenspach and Iennarella-Servantez (32)	Dog	LGR5 and ZO-1	Protein-losing enteropathy	Overview	N/A
Ambrosini et al. (33)	Dog	Low LGR5 and high NEUROH3	Generating monolayer of organoids	Detailed description of polarized cells	Wnt3a, R-Spo-1, and Noggin
Gabriel et al. (34)	Dog	N/A	Generating monolayer of organoids	Methodology paper	Wnt3a, R-Spo-1, and Noggin
Kramer et al. (35)	Dog	a.o. LGR5, PROM1, and NEUROG3	Disease modeling	Proliferation and differentiation	Wnt3a, R-Spo-1, and Noggin
Tekes et al. (36)	Cat	Low LGR5 and high MUC2	Disease modeling (viral infections)	Viral infection possible	Wnt3a, R-Spo-1, and Noggin
Stewart et al. (39)	Horse	a.o. LGR5	Disease modeling	Proliferation and differentiation	Wnt3a, R-Spo-1, and Noggin
Hellman (40)	Horse	a.o. SOX9 and MUC2	Disease modeling	2D organoids	Wnt3a, R-Spo-1, and Noggin

N/A, not applicable, not described; IBD, Inflammatory Bowel Disease; LPS, LipoPolySaccharide.
Human recombinant growth factors (Wnt3a, R-Spo-1/3, and Noggin) are used.

evidence that the genetic defect leading to COMMD1-deficiency and subsequent hepatic copper accumulation was functionally restored by lentiviral transduction of the full coding sequence of the *COMMD1*-gene. These gene-corrected autologous hepatic stem cells were subsequently transplanted into recipient COMMD1-deficient dogs through the portal vein and survived for at least 2 years, but following engraftment in the liver hardly any proliferation of these cells was observed and no functional recovery with regard to copper accumulation and biliary copper excretion was observed (26). Of interest was the observation that organoids derived from healthy livers and liver from dogs with congenital portosystemic shunts (CPSS) were able to accumulate lipids if grown under conditions of excess free fatty acids in the medium, and as such resembled the steatosis as often observed in CPSS livers (42). As another example of disease modeling, canine liver organoids from healthy and COMMD1-defcient dogs and repaired COMMD1-deficient organoids were shown to have reduced FXR transcriptional activity, which is in line with observations in copper laden human livers (43–45).

Since cats, as obligate carnivores, may develop a peculiar hepatic lipid accumulation under stress (e.g., anorexia) and lipid-overload conditions, feline liver organoids were created and characterized in relation to feline lipidosis (46). Intra-cellular lipid droplets, both small and large, were formed if the organoids were cultured in high fat medium (0.4 mM oleic acid and 0.2 mM palmitic acid). This led to the establishment of rapidly growing feline liver organoids as an *in vitro* model for feline lipidosis, which was exploited to investigate the potential of several drugs to decrease hepatic lipid concentrations (47). Two candidate lipid lowering drugs were identified: T863 (a DGAT1-inhibitor that inhibits TAG synthesis) and AICAR, which seemed to mediate its lipid lowering effect by a decrease in *PLIN2* mRNA, a gene product responsible for lipid droplet formation [reviews on lipid droplet formation see Fader Kaiser et al. and Scorletti and Carr (48, 49)].

Given the gene expression and functions of some aspects of liver organoids, this system holds great promise for advancements in veterinary pharmacology as contributors to 3R (replace, reduce, and refine) policies. However, a cautionary mote was recently published on the hepatocytic phenotype of liver organoids (50). A comparison of numerous publications on transcriptome analysis and functional studies revealed that the hepatocyte-like cells in liver organoids derived from intrahepatic bile ducts or pluripotent stem cells (PSC) did not match the transcriptome of primary hepatocytes (gold standard). The intrahepatic bile duct or PSC-derived organoids more closely resembles cholangiocytes and HepG2 cells were actually more similar to primary hepatocytes. This would mean that the biotransformation potential of liver organoids might not be predictive for these activities *in vivo*. Although this study compared data from over 20 publications, canine, feline or equine liver organoids were not included. It is however conceivable that for these latter organoids the

transcriptome and hepatocyte functions will also differ from those of primary hepatocytes, at best mimicking the *in vivo* situation.

Together (Table 3), the work on canine and feline liver organoids has proven these organoids' potential as disease modeling systems and has provided important lessons for large animal models of autologous stem cell transplantations.

Skin organoids

The skin is probably the largest organ of the body, providing a barrier against external stressors and at the same time responsible for drug uptake. Moreover, scar tissue formation in the skin due to injury has social impact and affects quality of life (51). This has driven skin organoid research and the establishment of canine skin organoids (52, 53). Twelve dogs provided samples to establish and characterize canine skin organoids (51).

Immunohistochemistry and gene expression profiling confirmed that stem cell-based organoids were proliferative in expansion medium (Wnt stimulation and BMP inhibition) and in differentiation medium (i.e., neither R-spondin nor Noggin), with the typical cell types of the layered skin being expressed, as evidenced by a shift in keratin family member expression. An interesting observation was the differential mRNA expression of *lgr5* and its relative *lgr6*, viz lgr5 mRNA was only detected in hair follicle tissue and not in organoids, whereas *lgr6* was expressed both in hair follicles (HF) and intrafollicular epidermis (IFE) organoids at early passage. This is indicative of the different stem cell pools in HF isthmus, IFE and sebaceous glands in rodents (54).

To further optimize canine skin organoids representing the different epidermal cell layers culture media were adjusted (53). The most surprising finding was that IFE-derived organoids cultured in expansion medium (EM) resembled the layered skin architecture better than those cultured in differentiation medium (DM; addition of Wnt3a but not R- spondin or Noggin). Maybe the lack of Wnt proteins in the EM triggered some differentiation but further proof is needed to confirm this.

These EM-skin organoids are therefore suitable for disease modeling (e.g., atopic dermatitis) but when cultured on a porous membrane can be also used to study transepidermal drug uptake (33).

Neuronal organoids

Brain biopsies are not performed routinely, for obvious reasons. Therefore, most brain organoids are based on induced Pluripotent Stem Cells (iPSCs) differentiated into mini brains (55, 56). *Post-mortem* material from five dogs was dissected to harvest canine hippocampal neural precursors (57). The organoids, or more precisely neurospheres, as the cells grow as condensed 2D cultures, proliferated and upon differentiation expressed neuronal markers (beta-tubulin) and glial cell (glial fibrillary acid protein, GFAP) markers. Differentiation was dependent on the addition of brain derived growth factor (BNDF). Fetal spinal cords were dissected from canine embryos at 40 days of gestation and the neurospheres differentiated into GFAP+ and tubulin+ cells, indicative of neuronal stem and progenitor cell maturation (58). These models are important given that dogs can suffer spinal cord trauma and develop a plethora of neurological disorders, including epilepsy and narcolepsy (59, 60).

Cardiac organoids

The use of canine and feline models to stimulate "innovations" in cardiovascular research was recently strongly advocated (61) and extends beyond Doberman dogs with dilated cardiomyopathy or cats with cardiomyopathy (62, 63). Canine cardiosphere-derived cells (CDCs), cultured as 3-D organoids, differentiated into cardiomyocytes, smooth muscle cells, and endothelial cells *in vitro* (64). Moreover, canine CDCs injected intravenously in mice with doxorubicin-induced dilated cardiomyopathy engrafted in the heart, reduced fibrous tissue formation, and improved the cardiac capillary network.

Renal organoids

The most frequently used canine cell is probably the MDCK (Madine-Darby Canine Kidney) cell line. In contrast to this famous cell line, important in the study of cellular polarization, only one publication exists on canine kidney organoids (65). Multipotent cells from one canine kidney have Mesenchymal Stem Cell (MSC)-like properties (adipogenic, chondrogenic, and osteoblastic differentiation) and, once grown in Matrigel, formed tubule-like structures. Further differentiation toward several renal cell types was not reported and the MSC-like phenotype points more to an MSC than an adult kidney stem cell, although CD24 and CD133 expression is in line with characterized renal ASCs. Renal ASCs express, amongst others, CD24 and CD133 when cultured in medium with Wnt-stimulators but have no adipogenic, chondrogenic or osteoblastic differentiation potential (66, 67). This means that canine or feline renal SCS have not yet been unequivocally established.

Endometrial organoids

Lastly, feline endometrial organoids were polarized and expressed laminin in the basement membrane (68). Unfortunately, as this organoid was developed to assess plastic toxicity, little more information was provided on cellular differentiation or as a potential source of novel antibiotics, given the exposure of this organ to external microorganisms.

Prostate cancer organoids

Like humans, dogs can develop prostate cancer and in both species this disease carries a poor prognosis. In view of the One Medicine concept spontaneously formed canine prostate organoids can be used as a translational model. The surprising source of the cells used to develop prostate cancer organoids was urine

TABLE 3 Summary of publications on hepatic organoids from dogs or cats.

References	Species	Marker	Aim/disease	Remarks	Proliferation
Nantasanti et al. (41)	Dog	a.o. LGR5, PROM1, and SOX9	Copper storage disease modeling	Long term expansion, and bipotential differentiation	Wnt3a, R-Spo-1, and Noggin
Van den Bossche et al. (42)	Dog	a.o. LGR5, PROM1, and SOX9	Congenital portosystemic shunt modeling	Lipid profyling and intra-organoid lipid accumulation	Wnt3a, R-Spo-3, and Noggin
Wu et al. (43)	Dog	a.o. LGR5, PROM1, and SOX9	Copper storage disease modeling	COMMD1 -/- organoid and reconstituted functional COMMD1 organoids	Wnt3a, R-Spo-1, and Noggin
Kruitwagen et al. (46)	Cat	a.o. LGR5, PROM1, and BMI1	Disease modeling: lipidosis	Long term expansion, and bipotential differentiation	R-Spo-1 and Noggin
Haaker et al. (47)	Cat	LGR5	Drug screens for lipidosis	Lipid droplet formation cane be reduced by specific drugs	R-Spo-1 and Noggin
Kruitwagen et al. (26)	Dog	a.o. LGR5, PROM1, and SOX9	Copper storage disease stem cell transplantation	Autologous stem cell transplantation with COMMD1 -/- organoids where functional COMMD1 was reconstituted	Wnt3a, R-Spo-1, and Noggin

N/A, not applicable, not described. Human recombinant growth factors (Wnt3a, R-Spo-1/3, and Noggin) are used.

of 8 middle-aged to old dogs with various TNM classifications, which can be obtained non-invasively (69). Grown in Matrigel with medium composition as in man (including R-spondin and Noggin) the cells formed 3D luminal structures. The organoids expressed the epithelial marker E-cadherin, the myofibroblast marker alpha-SMA, basal cell marker CK5 and luminal cell marker CK8. When injected in immunodeficient mice these organoids formed tumors. All this indicated that the urine- derived prostate cancer cells behave like prostate cancer cells *in vivo*. Lastly, these cells were subjected to various chemotherapeutics in order to validate this system for disease modeling.

Mammary cancer organoids

Canine mammary organoids can be derived from mastectomy samples cultured in Matrigel in FBS-supplemented DMEM-Glutamax/Hams F12 medium (70). The expression of CK18 (epithelial and adenocarcinoma marker) and CK14 (myoepithelium) confirmed the cancerous phenotype of these tumor organoids. No further studies on chemotherapeutic sensitivity and tumor formation in nude mice have been reported. As neither FBS nor the defined organoid media with Wnt, R-spondin, and Noggin was used, a comparison with other organoid systems cannot be made.

Bladder cancer organoids

Four papers describe the establishment of canine bladder tumor organoids and the implications as models for drug response prediction (71–74). Typical epithelial and urogenital markers, such as E-cadherin, CK7 and CK20, were expressed. Moreover, the expression of vimentin and alpha-SMA indicated a more mesenchymal phenotype. Functional studies including the formation of tumors of injected organoids into NOD/SCID immunodeficient NOD/SCID mice, confirmed the cancerous phenotype of the bladder tumoroids. Finally, sensitivity to chemotherapeutics, specifically trametinib, was evaluated. All these data provided credence to the fact that these canine bladder tumor organoids resemble bladder tumors *in vivo* and might serve as *in vitro* models to evaluate drug responses on an individual level. As for the mammary tumors FBS was used as source of growth factors.

Thyroid cancer organoids

Follicular cell thyroid organoids were created form healthy and primary thyroid gland tumors (75). As for most 3D organoid cultures Noggin and R-spondin were needed for propagation of the organoids in Basement Membrane Extract (similar to Matrigel and also animal- derived). The expression of TSHR (TSH receptor), NIS (sodium iodide symporter), and TPO (thyroid peroxidase) was similar in the organoids and in the primary tumors. No other functional studies have been reported.

For canine bladder and prostate cancer, the organoid models seem to be representative of the tumor *in vivo*. Thyroid cancer organoids and mammary tumor organoids require more functional studies and comparisons with the behavior of the original tumor before these tumor organoids can be considered as One Medicine models. Although counterintuitive, culturing 3D organoids from tumor material is sometimes more complicated than culture from healthy adult stem cells. First, the advantage of growth factor independent growth of tumor cells is lost in the rich (yet defined)

culture media of 3D organoid cultures. In addition, the 3D structure inside the Matrigel, which is expensive and prone to batch-to-batch variations, requires long pre-culture processing and experienced handling. To overcome some of these limitations a so-called 2.5D organoid culture system was recently developed in which 3D organoids are cultured on top of (rather than as separate organoids) within a thick Matrigel layer (74). A further improvement in the tumor organoid field was the creation of these 2.5D structures without the need of 3D pre-culture (76). Applying this system, it seems possible to create tumor organoids and to study veterinary cancer biology, yet it is still dependent on Matrigel. A comparison with 2.5D organoids and similar tumors in DMEM showed enhanced proliferation in the organoid culture system. It remains to be seen how 2.5D on top of Matrigel organoids compare to 3D inside Matrigel organoids with regard to genetic stability (especially important for tumor-derived tissue), drug-sensitivity. For disease modeling this comparison must include differentiation potential to the required organ specific cell types.

Corneal organoids

Corneal blindness affects both man and dogs. Initial work on corneal epithelial cells established the expression of progenitor marker p63 (77). Cultured on murine 3T3 fibroblasts as feeder cells, the canine corneal epithelial cells proliferated but did not form tumors (78). True corneal organoids have recentlty been described, although only one dog and one cat were used as donors (79). Here, p63 expression was confirmed only in the canine organoid, but LGR5 expression was no detectable, neither in the dog or the cat. The low number of donors and the lack of LGR5 expression clearly indicate that this organoid system needs further evaluation with regard to stemness and differentiation potential of the corneal stem cells.

Equine adult stem cell derived organoids

Horses can be considered to be companion animals in many respects and are often treated by equine veterinary specialists. In large parts of the world horses, and other equids, are still used as working animals, whereas in the Western world *Equus caballus* is mainly used for sport and leisure. Horses are highly relevant large animal models for musculoskeletal disorders (osteoarthritis, tendinopathies) (80). Horses are frequently referred to veterinary clinics with gastro-intestinal disturbances, in particular colic, which refers to any cause of pain emanating from the gastro-intestinal tract (81, 82). Given the fact that *in vivo* studies in horses pose many logistical challenges related to the size (and cost) of the animals, but also related to standardization of conditions, one would anticipate an enormous commitment to establish equine organoids of various organ systems for *in vitro* research. Whatever the reason, only three papers describing the establishment and characterization of equine intestinal organoids have been published (27, 39, 40). Growth of these organoids, as in all intestinal organoid cultures, is Wnt dependent and upon differentiation various villus cell types, such as Goblet and Paneth cells, are formed. Important is the observation that these organoids can be cultured in a 2-D Transwell system permitting the study of microbial interactions with the luminal side of the epithelium. In 3-D organoid cultures the intestinal lumen is on the inside, which poses logistical hurdles when trying to expose these cells to microbials (82). Two papers describe equine oviductal and endometrial organoids to facilitate investigation of reproduction pathologies (83, 84). The creation of endometrial organoids from a Przewalski horse actually represents the first organoid of an endangered species (84, 85). This important observation proves the possibilities (and therefore novel opportunities) to investigate biological process in endangered species without the need to sacrifice these animals. Equine mammary organoids were functionally characterized and, importantly, prolactin induced the production of beta-casein (86). Although horses are not often used for their milk production, this large animal model might allow cross-species comparisons to better understand the mechanism of lactation.

At present, equine liver organoids have also been established, although editorial restrictions do not permit presentation of these (as yet) unpublished data. It thus remains a matter of time before an advanced *in vitro* model is available to study nutrient-related disorders in a standardized way with prognostic value for the *in vivo* situation (87).

Discussion and future perspectives

Most organoid cultures (except maybe the canine skin organoids) based on adult stem cells from epithelia are cultured in the presence of stimulators for canonical Wnt-signaling (Wnt and R-spondin proteins), EGF-signaling (epidermal growth factor), and BMP (bone morphogenic proteins) in-activation (Noggin or Gremlin-1). Often, differentiation is induced by the removal of proliferative signaling molecules (Wnt-, R-spondin proteins) and addition of BMP-proteins and Notch-inhibitors. In order to start investigations into novel organoid systems, the media composition as described above (27) can be used as a starting medium, from which by step-wise depletion of individual growth factor or signaling-modifiers an optimal culture medium can be deduced. Furthermore, this study showed that for a number of veterinary relevant species recombinant human Wnt3a, R-spondin-3, and Noggin in DMEM are crucial to establish organoid cultures. This defined medium seems to be a good start to evaluate proliferation and differentiation of organoids of interest (Figures 2A, B for canine pancreatic organoids and equine liver organoids).

The potential applications of organoid technology in the field of veterinary regenerative medicine are obvious (Figure 1), but also associated with a number of ethical dilemmas (Box 1). Although disease modeling is gaining momentum, the understanding of interactions between organoids from different organs is still in its infancy in veterinary medicine. Knowledge of cellular differentiation of organoids is not yet optimal, for instance regarding hepatocyte differentiation and the use of (multi-organ) organoids in a representative drug metabolism and safety platform. This leads to a set of open questions. Are validated antibodies to detect LGR5 expression in cats and horses available? Which cell membrane markers, other than LGR5, can be used to sort single cells and measure outgrowth into organoids based on this selection

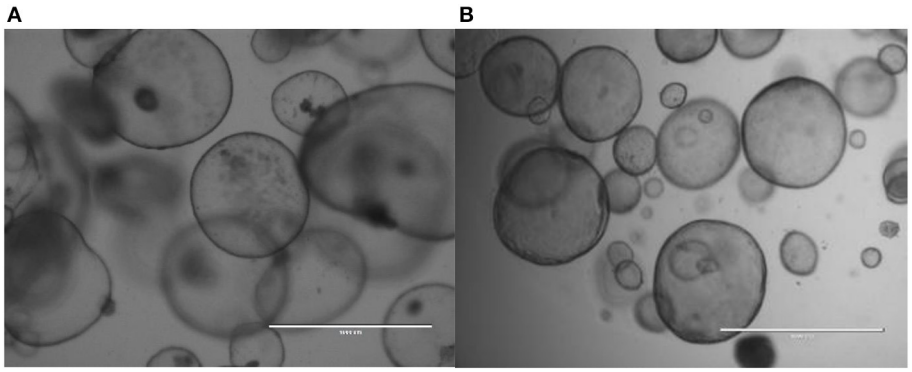

FIGURE 2
Canine pancreatic organdies **(A)** and equine liver organdies **(B)** in Matrigel. Freshly isolated cadaveric material was harvested and chopped into small pieces prior to culture. Although the initial cell cultures usually contain several cell types, the selective medium (aimed to simulate adult stem cells based on their high Wnt-signaling) after several days only stem cells survive and form these hollow structures.

BOX 1 Specific ethical issues related to Matrigel and organoid ownership.

The cell differentiation and sorting characteristics and spatially restricted lineage commitment can be addressed by a shift from 2-dimensional cultures on plastics to 3- dimensional cultures in hydrogels. These hydrogels provide structural support and possibly differentiation cues as well. The laminin-rich extracellular matrix from the Engelbreth-Holm- Swarm tumor (called Matrigel) is often used, but besides being of animal origin, and as such not FDA approved, the large batch-to-batch variation hampers experimental reproducibility (88). The search for animal-free alternatives to Matrigel is beyond the scope of this critical review, but definitely requires strong scientific input. This culture dilemma was nicely described for fetal bovine serum but is *mutatis mutandis* applicable to animal derived matrices too (89). In addition to these application limitations caused by Matrigel or animal derived alternatives, organoid technology comes with specific ethical questions, for instance related to the ownership of the cells and anonymization of patient derived material (90).

marker? How large is the variation in expression of cell markers and characteristics between organoids and even within organoids? How can we guide or improve cellular differentiation, and do we need species specific growth factors to achieve this? How cost-effective is precision medicine in veterinary medicine? Once functional cell replacement of transplants can be achieved in model systems, and the COMMD1-defcient dog transplantation studies showed that this in itself is not an easy task, what is the financial burden for the owners (26)?

Reviews highlight the potential and advocate the use of organoid technology in veterinary medicine for personalized medicine or toxicological studies (91, 92). In today's reality disease modeling and, to a lesser degree, the study of drug metabolism are being conducted with organoid technology in the field of veterinary medicine. The few studies on transplantations, the apex of stem-cell mediated regenerative medicine, are only in the pre-clinical phase for human trials, at best. No long-term cure has been achieved but the choices of the large animal models (pigs and dogs) permit size-based extrapolation to pediatric patients. As such, the model animals are the true heroes of the one medicine concept, bridging the gap between veterinary medicine and human medicine as was recently advocated in Nature Medicine for dogs in particular (93).

Author contributions

Both authors listed have made a substantial, direct, and intellectual contribution to the work and approved it for publication.

Conflict of interest

The authors declare that the research was conducted in the absence of any commercial or financial relationships that could be construed as a potential conflict of interest.

Publisher's note

Supplementary material

The Supplementary Material for this article can be found online at: https://www.frontiersin.org/articles/10.3389/fvets.2023.1032835/full#supplementary-material

References

1. Savolainen P, Zhang YP, Luo J, Lundeberg J, Leitner T. Genetic evidence for an East Asian origin of domestic dogs. *Science.* (2002) 298:1610–3. doi: 10.1126/science.1073906

2. Pang JF, Kluetsch C, Zou XJ, Zhang AB, Luo LY, Angleby H, et al. mtDNA data indicate a single origin for dogs south of Yangtze River, less than 16,300 years ago, from numerous wolves. *Mol Biol Evol.* (2009) 26:2849–64. doi: 10.1093/molbev/msp195

3. vonHoldt BM, Pollinger JP, Earl DA, Knowles JC, Boyko AR, Parker H, et al. A genome-wide perspective on the evolutionary history of enigmatic wolf-like canids. *Genome Res.* (2011) 21:1294–305. doi: 10.1101/gr.116301.110

4. Axelsson E, Ratnakumar A, Arendt ML, Maqbool K, Webster MT, Perloski M, et al. The genomic signature of dog domestication reveals adaptation to a starch-rich diet. *Nature.* (2013) 495:360–4. doi: 10.1038/nature11837

5. Thalmann O, Shapiro B, Cui P, Schuenemann VJ, Sawyer SK, Greenfield DL, et al. Complete mitochondrial genomes of ancient canids suggest a European origin of domestic dogs. *Science.* (2013) 342:871–4. doi: 10.1126/science.1243650

6. Wang GD, Zhai W, Yang HC, Fan RX, Cao X, Zhong L, et al. The genomics of selection in dogs and the parallel evolution between dogs and humans. *Nature Commun.* (2013) 4:860. doi: 10.1038/ncomms2814

7. Freedman AH, Gronau I, Schweizer RM, Ortega-Del Vecchyo D, Han E, Silva PM, et al. Ge nome sequencing highlights the dynamic early history of dogs. *PLoS Genet.* (2014) 10:e1004016. doi: 10.1371/journal.pgen.1004016

8. Shannon LM, Boyko RH, Castelhano M, Corey E, Hayward JJ, McLean C, et al. Genetic structure in village dogs reveals a Central Asian domestication origin. *Proc natl Acad Sci USA.* (2015) 112:13639–44. doi: 10.1073/pnas.1516215112

9. Wang GD, Zhai W, Yang HC, Wang L, Zhong L, Liu YH, et al. Out of southern East Asia: The natural history of domestic dogs across the world. *Cell Res.* (2016) 26:21–33. doi: 10.1038/cr.2015.147

10. Freedman AH, Wayne RK. Deciphering the origin of dogs: From fossils to genomes. *Annu Rev Anim Biosci.* (2017) 5:281–307. doi: 10.1146/annurev-animal-022114-110937

11. Serpell JA. Commensalism or cross-species adoption? A critical review of theories of wolf domestication. *Front Vet Sci.* (2021) 8:662370. doi: 10.3389/fvets.2021.662370

12. Losey RJ, Nomokonova T, Guiry E, Fleming LS, Garvie-Lok SJ, Waters-Rist AL, et al. The evolution of dog diet and foraging: Insights from archaeological canids in Siberia. *Sci Adv.* (2022) 8:eabo6493. doi: 10.1126/sciadv.abo6493

13. Bergström A, Stanton DWG, Taron UH, Frantz L, Sinding MS, Ersmark E, et al. Grey wolf genomic history reveals a dual ancestry of dogs. *Nature.* (2022) 607:313–20. doi: 10.1038/s41586-022-04824-9

14. van Steenbeek FG, Hytönen MK, Leegwater PA, Lohi H. The canine era: The rise of a biomedical model. *Anim Genet.* (2016) 47:519–27. doi: 10.1111/age.12460

15. Kawasaki M, Goyama T, Tachibana Y, Nagao I, Ambrosini YM. Farm and companion animal organoid models in translational research: A powerful tool to bridge the gap between mice and humans. *Front Med Technol.* (2022) 4:89579. doi: 10.3389/fmedt.2022.895379

16. Barker N, van Es JH, Kuipers J, Kujala P, van den Born M, Cozijnsen M, et al. Identification of stem cells in small intestine and colon by marker gene Lgr5. *Nature.* (2007) 449:1003–7. doi: 10.1038/nature06196

17. Sato T, Vries RG, Snippert HJ, van de Wetering M, Barker N, Stange DE, et al. Single Lgr5 stem cells build crypt-villus structures *in vitro* without a mesenchymal niche. *Nature.* (2009) 459:262–5. doi: 10.1038/nature07935

18. Lancaster MA, Knoblich JA. Organogenesis in a dish: Modeling development and disease using organoid technologies. *Science.* (2014) 345:1247125. doi: 10.1126/science.1247125

19. Leung C, Tan SH, Barker N. Recent advances in Lgr5+ stem cell research. *Trends in Cell Biol.* (2018) 28:380–91. doi: 10.1016/j.tcb.2018.01.010

20. Beumer J, Clevers H. Cell fate specification and differentiation in the adult mammalian intestine. *Nat Rev Mol Cell Biol.* (2021) 22:39–53. doi: 10.1038/s41580-020-0278-0

21. Campana L, Esser H, Huch M, Forbes S. Liver regeneration and inflammation: From fundamental science to clinical applications. *Nat Rev Cell Biol.* (2021) 22:608–24. doi: 10.1038/s41580-021-00373-7

22. Jalan-Sakrikar N, Brevini T, Huebert RC, Sampaziotis F. Organoids and regenerative hepatology. *Hepatology.* (2022) 2022:1–18. doi: 10.1002/hep.32583

23. Gerhards NM, Sayar BS, Origgi FC, Gaichet A, Mueller EJ, Welle MM, et al. Stem cell-associated marker expression in canine hair follicles. *J Histochem Cytochem.* (2016) 64:190–4. doi: 10.1369/0022155415627679

24. Bongiovanni L, Brachelente C, Moreno E, Welle MM. Canine epithelial skin tumours: Expression of the stem cell markers Lgr5, Lgr6 and Sox9 in light of new cancer stem cell theories. *Vet Sci.* (2020) 7:62. doi: 10.3390/vetsci7020062

25. Agopian VG, Chen DC, Avansino JR, Stelzner M. Intestinal stem cell organoids transplantation generates neomucosa in dogs. *J Gastrointest Surg.* (2009) 13:971–82. doi: 10.1007/s11605-009-0806-x

26. Kruitwagen HS, Oosterhoff LA, van Wolferen ME, Chen C, Nantasanti Assawarachan S, Schneeberger K, et al. Long- term survival of transplanted autologous canine liver organoids in a COMMD1- deficient dog model of metabolic liver disease. *Cells.* (2020) 9:410. doi: 10.3390/cells9020410

27. Powell RH, Behnke MS. WRN conditioned media is sufficient for *in vitro* propagation of intestinal organoids from large farm and small companion animals. *Biol Open.* (2017) 6:698–705. doi: 10.1242/bio.021717

28. Mochel JP, Jergens AE, Kingsbury D, Kim HJ, Martin MG, Allenspach K. Intestinal stem cells to advance drug development, precision, and regenerative medicine: A paradigm shift in translational research. *AAPS J.* (2017) 20:17. doi: 10.1208/s12248-017-0178-1

29. Kopper JJ, Iennarella-Servantez C, Jergens AE, Sahoo DK, Guillot E, Bourgois-Mochel A, et al. Disease pathogenesis and accelerate drug discovery: A one health approach. *Front Toxicol.* (2021) 3:773953. doi: 10.3389/ftox.2021.773953

30. Chandra L, Borcherding DC, Kingsbury D, Atherly T, Ambrosini YM, Bourgois-Mochel A, et al. Derivation of adult canine intestinal organoids for translational research in gastroenterology. *BMC Biol.* (2019) 17:33. doi: 10.1186/s12915-019-0652-6

31. Sahoo DK, Borcherding DC, Chandra L, Jergens AE, Atherly T, Bourgois-Mochel A, et al. Differential transcriptomic profiles following stimulation with lipopolysaccharide in intestinal organoids from dogs with inflammatory bowel disease and intestinal mast cell tumor. *Cancers.* (2022) 14:3525. doi: 10.3390/cancers14143525

32. Allenspach K, Iennarella-Servantez C. Canine protein losing enteropathies and systemic complications. *Vet Clin North Am Small Pract.* (2021) 51:111–22. doi: 10.1016/j.cvsm.2020.09.010

33. Ambrosini YM, Park Y, Jergens AE, Shin W, Min S, Atherly T, et al. Recapitulation of the accessible interface of biopsy- derived canine intestinal organoids to study epithelial-luminal interactions. *PLoS ONE.* (2020) 15:e0231423. doi: 10.1371/journal.pone.0231423

34. Gabriel V, Zdyrski C, Sahoo DK, Dao K, Bourgois-Mochel A, Atherly T, et al. Canine intestinal organoids in a dual- chamber permeable support system. *J Vis Exp.* (2022) 2:181. doi: 10.3791/63612-v

35. Kramer N, Pratscher B, Meneses AMC, Tschulenk W, Walter I, Swoboda A, et al. Generation of differentiating and long-living intestinal organoids reflecting the cellular diversity of canine intestine. *Cells.* (2020) 9:822. doi: 10.3390/cells9040822

36. Tekes G, Ehmann R, Boulant S, Stanifer ML. Development of feline ileum- and colon- derived organoids and their potential use to support feline coronavirus infection. *Cells.* (2020) 9:2085. doi: 10.3390/cells9092085

37. Yin S, Ray G, Kerschner JL, Hao S, Perz S, Drumm ML, et al. Functional genomics analysis of human colon organoids identifies key transcription factors. *Physiol Genomics.* (2020) 52:234–44. doi: 10.1152/physiolgenomics.00113.2019

38. Weiss F, Holthaus D, Kraft M, Klotz C, Schneeman M, Schulzke JD, et al. Human duodenal organoid-derived monolayers serve as a suitable barrier model for duodenal tissue. *Ann Ny Acad Sci.* (2022) 1515:155–67. doi: 10.1111/nyas.14804

39. Stewart AS, Freund JM, Gonzalez LM. Advanced three-dimensional culture of equine intestinal epithelial stem cells. *Equine Vet J.* (2018) 50:241–8. doi: 10.1111/evj.12734

40. Hellman S. Generation of equine enteroids and enteroid-derived 2D monolayers that are responsive to microbial mimics. *Vet Res.* (2021) 52:108. doi: 10.1186/s13567-021-00976-0

41. Nantasanti S, Spee B, Kruitwagen HS, Chen C, Geijsen N, Oosterhoff LA, et al. Disease modeling and gene therapy of copper storage disease in canine hepatic organoids. *Stem Cell Rep.* (2015) 5:895–907. doi: 10.1016/j.stemcr.2015.09.002

42. Van den Bossche L, Schoonenberg VAC, Burgener IA, Penning LC, Schrall IM, Kruitwagen HS, et al. Aberrant hepatic lipid storage and metabolism in canine portosystemic shunts. *PLoS ONE.* (2017) 12:e0186491. doi: 10.1371/journal.pone.0186491

43. Wu X, Chien H, van Wolferen ME, Kruitwagen HS, Oosterhoff LA, Penning LC. Reduced FXR target gene expression in copper-laden livers of COMMD1-deficient dogs. *Vet Sci.* (2019) 6:78. doi: 10.3390/vetsci6040078

44. Wooton-Kee CR, Jain AK, Wagner M, Grusak MA, Finegold MJ, Lutsenko S, et al. Elevated copper impairs hepatic nuclear receptor function in Wilson's disease. *J Clin Invest.* (2015) 125:3449–60. doi: 10.1172/JCI78991

45. Hamilton JP, Koganti L, Muchenditsi A, Pendyala VS, Huso D, Hankin J, et al. Activation of liver X receptor/retinoid X receptor pathway ameliorates liver disease in Atp7B(-/-) (Wilson disease) mice. *Hepatology.* (2016) 63:1828–41. doi: 10.1002/hep.28406

46. Kruitwagen HS, Oosterhoff LA, Vernooij IGWH, Schrall IM, van Wolferen ME, Bannink F, et al. Long-term adult feline liver organoid cultures for disease modeling

of hepatic steatosis. *Stem Cell Rep.* (2017) 8:822–30. doi: 10.1016/j.stemcr.2017.02.015

47. Haaker MW, Kruitwagen HS, Vaandrager AB, Houweling M, Penning LC, Molenaar MR, et al. Identification of potential drugs for treatment of hepatic lipidosis in cats using an *in vitro* feline liver organoid system. *J Vet Intern Med.* (2020) 34:132–8. doi: 10.1111/jvim.15670

48. Fader Kaiser CM, Romano PS, Vanrell MC, Pocognoni CA, Jacob J, Caruso B, et al. Biogenesis and breakdown of lipid droplets in pathological conditions. *Front Cell Dev Biol.* (2022) 9:826248. doi: 10.3389/fcell.2021.826248

49. Scorletti E, Carr RM. A new perspective on NAFLD: Focusing on lipid droplets. *J Hepatol.* (2022) 76:934–45. doi: 10.1016/j.jhep.2021.11.009

50. Ardisasmita AI, Schene IF, Joore IP, Kok G, Hendriks D, Artegiani B, et al. A comprehensive transcriptomic comparison of hepatocyte model systems improves selection of models for experimental use. *Comm Biol.* (2022) 5:1094. doi: 10.1038/s42003-022-04046-9

51. Sun H, Zhang YX, Li YM. Generation of skin organoids: Potential opportunities and challenges. *Front Cell Dev Biol.* (2021) 9:709824. doi: 10.3389/fcell.2021.709824

52. Wiener DJ, Basak O, Asra P, Boonekamp KE, Kretzschmar K, Papaspyropoulos A, et al. Establishment and characterization of a canine keratinocyte organoid culture system. *Vet Dermatol.* (2018) 29:375–e126. doi: 10.1111/vde.12541

53. Wiener DJ, Studer IC, Brunner MAT, Hermann A, Vincenti S, Zhang M, et al. Characterization of canine epidermal organoid cultures by immunohistochemical analysis and quantitative PCR. *Vet Dermatol.* (2021) 32:179–e44. doi: 10.1111/vde.12914

54. Füllgrabe A, Joost S, Are A, Jacob T, Sivan U, Haegebarth A, et al. Dynamics of Lgr6? progenitor cells in the hair follicle, sebaceous gland, and interfollicular epidermis. *Stem Cell Reports.* (2015) 5:843–55. doi: 10.1016/j.stemcr.2015.09.013

55. Sidhaye J, Knoblich JA. Brain organoids: An ensemble of bioassays to investigate human neurodevelopment and disease. *Cell Death Differ.* (2021) 28:52–67. doi: 10.1038/s41418-020-0566-4

56. Lancaster MA, Corsini NS, Wolfinger S, Gustafson EH, Phillips AW, Burkard TR, et al. Guided self-organization and cortical plate formation in human brain organoids. *Nat Biotechnol.* (2017) 35:659–66. doi: 10.1038/nbt.3906

57. Lowe A, Dalton M, Sidhu K, Sachdev P, Reynolds B, Valenzuela M. Neurogenesis and precursor cell differences in the dorsal and ventral adult canine hippocampus. *Neurosci Lett.* (2015) 593:107–13. doi: 10.1016/j.neulet.2015.03.017

58. Santos SIP, de Oliveira VC, Pieri NCG, Bressan FF, Ambrósio CE, Feitosa MLT. Isolation and characterization of neural stem cells from fetal canine spinal cord. *Neurosci Lett.* (2021) 765:136293. doi: 10.1016/j.neulet.2021.136293

59. Löscher W. Dogs as a natural animal model of epilepsy. *Front Vet Sci.* (2022) 9:928009. doi: 10.3389/fvets.2022.928009

60. Tonokura M, Fujita K, Nishino S. Review of pathophysiology and clinical management of narcolepsy in dogs. *Vet Rec.* (2007) 161:375–80. doi: 10.1136/vr.161.11.375

61. van der Velden J, Asselbergs FW, Bakkers J, Batkai S, Bertrand L, Bezzina CR, et al. Animal models and animal-free innovations for cardiovascular research: Current status and routes to be explored. Consensus document of the ESC working group on myocardial function and the ESC Working Group on Cellular Biology of the Heart. *Cardiovasc Res.* (2022) 6:cvab370. doi: 10.1093/cvr/cvab370

62. Wess G, Domenech O, Dukes-McEwan J, Häggström J, Gordon S. European Society of Veterinary Cardiology screening guidelines for dilated cardiomyopathy in Doberman Pinchers. *J Vet Cardiol.* (2017) 19:405–15. doi: 10.1016/j.jvc.2017.08.006

63. Kittleson MD, Meurs KM, Harris SP. The genetic basis of hypertrophic cardiomyopathy in cats and humans. *J Vet Cardiol.* (2015) 1(Suppl.):S53–73. doi: 10.1016/j.jvc.2015.03.001

64. Hensley MT, de Andrade J, Keene B, Meurs K, Tang J, Wang Z, et al. Cardiac regenerative potential of cardiosphere- derived cells from adult dog hearts. *J Cell Mol Med.* (2015) 19:1805–13. doi: 10.1111/jcmm.12585

65. Chen TC, Neupane M, Chien SJ, Chuang FR, Crawford RB, Kaminski NE, et al. Characterization of adult canine kidney epithelial stem cells that give rise to dome-forming tubular cells. *Stem Cells Dev.* (2019) 28:1424–33. doi: 10.1089/scd.2019.0049

66. Yengej FA, Jansen J, Rookmaaker MB, Verhaar MC, Clevers H. Kidney organoids and tubuloids. *Cells.* (2020) 9:1326. doi: 10.3390/cells9061326

67. Schutgens F, Rookmaaker MB, Margaritis T, Rios A, Ammerlaan C, Jansen J, et al. Tubuloids derived from human adult kidney and urine for personalized disease modeling. *Nat Biotechnol.* (2019) 37:303–13. doi: 10.1038/s41587-019-0048-8

68. Dundon M, Madden O, Comizzoli P. Three-dimensional culture of endometrial cells from domestic cats: A new *in vitro* platform for assessing plastic toxicity. *PLoS ONE.* (2019) 14:e0217365. doi: 10.1371/journal.pone.0217365

69. Usui T, Sakurai M, Nishikawa S, Umata K, Nemoto Y, Haraguchi T, et al. Establishment of a dog primary prostate cancer organoid using the urine cancer stem cells. *Cancer Sci.* (2017) 108:2383–92. doi: 10.1111/cas.13418

70. Cocola C, Molgora S, Piscitelli E, Veronesi MC, Greco M, Bragato C, et al. FGF2 and EGF are required for self-renewal and organoid formation of canine normal and tumor breast stem cells. *J Cell Biochem.* (2017) 118:570–84. doi: 10.1002/jcb.25737

71. Elbadawy M, Usui T, Mori T, Tsunedomi R, Hazama S, Nabeta R, et al. Establishment of a novel experimental model for muscle- invasive bladder cancer using a dog bladder cancer organoid culture. *Cancer Sci.* (2019) 110:2806–21. doi: 10.1111/cas.14118

72. Elbadawy M, Sato Y, Mori T, Goto Y, Hayashi K, Yamanaka M, et al. Anti-tumor effect of trametinib in bladder cancer organoid and the underlying mechanism. *Cancer Biol Ther.* (2021) 22:357–71. doi: 10.1080/15384047.2021.1919004

73. Elbadawy M, Fujisaka K, Yamamoto H, Tsunedomi R, Nagano H, Ayame H, et al. Establishment of an experimental model of normal dog bladder organoid using a three-dimensional culture method. *Biomed Pharmacother.* (2022) 151:113105. doi: 10.1016/j.biopha.2022.113105

74. Abugomaa A, Elbadawy M, Yamanaka M, Goto Y, Hayashi K, Mori T, et al. Establishment of 25D organoid culture model using 3D bladder cancer organoid culture. *Sci Rep.* (2020) 10:9393. doi: 10.1038/s41598-020-66229-w

75. Jankovic J, Dettwiler M, Fernández MG, Tièche E, Hahn K, April-Monn S, et al. Validation of immunohistochemistry for canine proteins involved in thyroid iodine uptake and their expression in canine follicular cell thyroid carcinomas (FTCs) and FTC-derived organoids. *Vet Pathol.* (2021) 58:1172–80. doi: 10.1177/03009858211018813

76. Morita M, Fujita N, Takahashi A, Nam ER, Yui S, Chung CS, et al. Evaluation of ABCG2 and p63 expression in canine cornea and cultivated corneal epithelial cells. *Vet Oppthalmol.* (2015) 18:59 doi: 10.1111/vop.12147

77. Morita M, Fujita N, Abe M, Hayashimoo K, Nakagawa T, Nishimura R, et al. Canine corneal epithelial cells possess a sustained proliferative capacity and generate a spontaneously derived cell line. *Exp Cell Res.* (2018) 171:155–63. doi: 10.1016/j.exer.2018.03.003

78. Bedos L, Wickham H, Gabriel V, Zdyrski C, Allbauigh RA, Sahoo DK, et al. Culture and characterization of canine and feline corneal epithelial organoids: A new tool for the study and treatment of corneal diseases. *Front Vet Sci.* (2022) 9:1050467. doi: 10.3389/fvets.2022.1050467

79. Abugomaa A, Elbadawy M, Yamamoto H, Ayame H, Ishihara Y, Sato Y, et al. Establisment of a direct 25D organoid culture model using companion animal cancer tissues. *Biomed Pharmacother.* (2022) 154:113597. doi: 10.1016/j.biopha.2022.113597

80. Ribitsch I, Baptista PM, Lange-Consiglio A, Melotti L, Patruno M, Jenner F, et al. Large animal models in regenerative medicine and tissue engineering: To do or not to do. *Front Bioeng Biotechnol.* (2020) 8:972. doi: 10.3389/fbioe.2020.00972

81. Van den Boom R, van der Velden MA. Short- and long-term evaluation of surgical treatment of strangulating obstructions of the small intestine in horses: A review of 224 cases. *Vet Q.* (2001) 23:109–15. doi: 10.1080/01652176.2001.9695095

82. Bowden A, England GCW, Brennan ML, Mair TS, Furness WA, Freeman SL, et al. Indicators of critical outcomes in 941 horses seen "out-of-hours" for colic. *Vet Rec.* (2020) 187:492. doi: 10.1136/vr.105881

83. Thompson RE, Johnson AK, Dini P, Turco MY, Prado TM, Premanandan C, et al. Hormone-responsive organoids form domestic mare and endangered Przewalski's horse endometrium. *Reproduction.* (2020) 160:819–31. doi: 10.1530/REP-20-0266

84. Thompson RE, Meyers MA, Veeramachaneni DNR, Pukazhenthi BS, Hollinshead FK. Equine oviductal organoid generation and cryopreservation. *Methods Protoc.* (2022) 5:51. doi: 10.3390/mps5030051

85. Thompson RE, Meyers MA, Pukazhenthi BS, Hollinshead FK. Evaluation of growth, viability, and structural integrity of equine endometrial organoids following cryopreservation. *Cryobiology.* (2022) 104:56–62. doi: 10.1016/j.cryobiol.2021.11.003

86. Bartlett AP, Harman RM, Weiss JR, Van de Walle GR. Establishment and characterization of equine mammary organoids using a method translatable to other non-traditional model species. *Development.* (2022) 149:dev200412. doi: 10.1242/dev.200412

87. Beaumont M, Blanc F, Cherbuy C, Egidy G, Giuffra E, Lacroix-Lamandé S, et al. Intestinal organoids in farm animals. *Vet Res.* (2021) 52:33. doi: 10.1186/s13567-021-00909-x

88. Li ML, Aggeler J, Farson DA, Hatier C, Hassell J, Bissell MJ. Influence of a reconstituted basement membrane and its components on casein gene expression and secretion in mouse mammary epithelial cells. *Proc Natl Acad USA.* (1987) 84:136–40. doi: 10.1073/pnas.84.1.136

89. Valk J. Fetal Bovine serum-a cell culture dilemma. *Science.* (2022) 375:143–4. doi: 10.1126/science.abm1317

90. Bredenoord AL, Clevers H, Knoblich JA. Human tissues in a dish: The research and ethical implications of organoid technology. *Science.* (2017) 355:eaaf9414. doi: 10.1126/science.aaf9414

91. Nantasanti S, de Bruin A, Rothuizen J, Penning LC, Schotanus BA. Concise review: Organoids are a powerful tool for the study of liver disease and personalized treatment design in humans and animals. *Stem Cells Transl Med.* (2016) 5:325–30. doi: 10.5966/sctm.2015-0152

92. Augustyniak J, Bertero A, Coccini T, Baderna D, Buzanska L, Caloni F. Organoids are promising tools for species-specific *in vitro* toxicologic al studies. *J Appl Toxicol.* (2019) 39:1610–22. doi: 10.1002/jat.3815

93. Arnold C. Sick as a dog: How understanding canine diseases will save human lives. *Nature Med.* (2022) 28:1970–3. doi: 10.1038/s41591-022-02025-5

Frontiers in Veterinary Science

Transforms how we investigate and improve animal health

The third most-cited veterinary science journal, bridging animal and human health with a comparative approach to medical challenges. It explores innovative biotechnology and therapy for improved health outcomes.

Discover the latest Research Topics

See more →

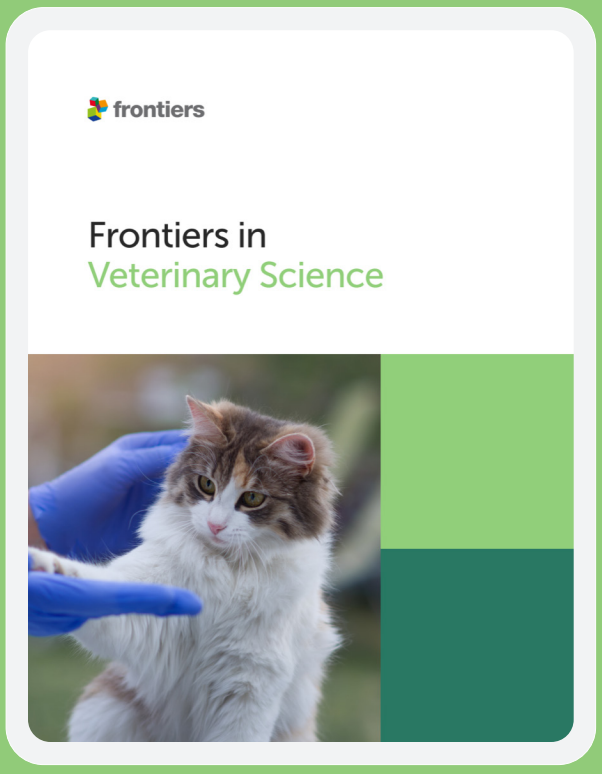

Frontiers

Avenue du Tribunal-Fédéral 34
1005 Lausanne, Switzerland
frontiersin.org

Contact us

+41 (0)21 510 17 00
frontiersin.org/about/contact